UNIVERSIDADE DO ALGARVE

Coastal Responses to sea-level rise on centennial to millennial time scales: development of hybrid model-based forecasting for the Guadiana Estuary

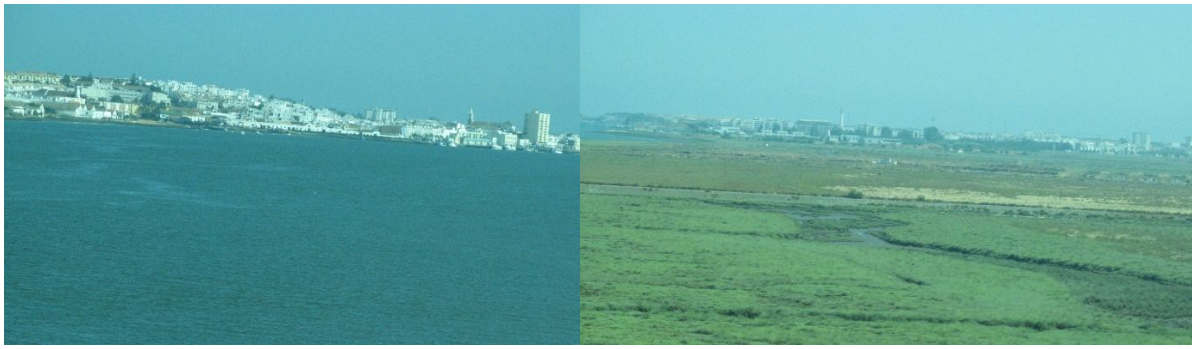

Dissanayake Mudiyanselage Ruwan Sampath

Doutoramento em Ciências do Mar, da Terra e do Ambiente, Ramo de Geociências, Especialidade em Dinâmica Litoral

2015

UNIVERSIDADE DO ALGARVE

Coastal Responses to sea-level rise on centennial to millennial time scales: development of hybrid model-based forecasting for the Guadiana Estuary

Dissanayake Mudiyanselage Ruwan Sampath

Doutoramento em Ciências do Mar, da Terra e do Ambiente, Ramo de Geociências, Especialidade em Dinâmica Litoral

Tese Orientada por:

Doutor Tomasz Boski (Universidade do Algarve)

Dedicated to all rivers, estuaries and great oceans that provide plenty of resources and joy to the mankind, unfortunately, whose relentless exploitations of the Mother Nature due to their selfish greediness have been endangered not only the survival of themselves but the very existence of the whole world.

To my parents, Sirisena and Ramani,

My wife Nadeesha

My sister Ruwani,

For supporting me unconditionally,

Even when I do nothing but my studies.

"The cold remote islands

And the blue estuaries

Where what breathes, breathes

The restless wind of the inlets,

And what drinks, drinks

The incoming tide."

The Blue Estuaries - By Louise Bogan

“Solving a problem for which you know there’s an answer is like climbing a mountain with a guide, along a trail someone else has laid…..

The truth is somewhere out there in a place no one knows, beyond all the beaten paths.

And it’s not always at the top of the mountain.

It might be in a crack on the smoothest cliff or somewhere deep in the valley.”

— *Yōko Ogawa*

ACKNOWLEDGEMENTS

Since bachelors years, I had a dream of doing a doctoral degree and then to engage in my own research carrier to explore a few things to my interest in the environmental engineering and science field. Sometimes I was distracted a bit, but I was able to realign my focus. Now I think I have reached very near to that goal. It was not a smooth or direct path, but decorated with numerous hardships and sacrifices. Despite all these obstacles, I was able to move forward inch by inch along this path due to generous helps, encouragement, and continuous guidance by a few people who are with me altogether.

The first name that I remember with a lot of gratitude and respect is my supervisor Prof. Tomasz Boski, at the University of Algarve. First, I would like to express my sincere appreciation to him, for his continuous guidance and unwavering support. He even supervised me during my Erasmus Mundus Master's degree in Water and Coastal Management. I discussed with him so many ideas to improve the scope of the thesis. Sometimes some of them have to be abandoned due to logistical and practical reasons. Yet, I could always count on his help to carry out this doctoral study. Many times he gave me a good opportunity to explore my own ideas. Prof. Tomasz´s attention to all aspects of a student life, in particular of a foreign student is very remarkable. I was able to solve not only the academic problems, but also the personal issues arisen due to lots of reasons. I can remember forever, how he helped me to overcome financial issues when my father was required to undergo a bypass surgery. He also helped me in a lot of ways when I suffered from a disease for a long time. If I did not have those assistance, I may not be able to do this study successfully. Thus, I would like to thank for him for everything. I also would like to thank Prof. Alice Newton during this study. She sent me important research papers for my study whenever she comes across one. She gave me valuable guides whenever I met her at the University of Algarve or at the University of Cadiz. She is also a mentor to me in numerous ways during this study period.

During this journey in Portugal, Carlos Loureiro, a friend since I started my studies here from 2007. He helped me to work with models, ARCGIS and other academic activities. I was always able to count on him for whatever assistance that I required during these 8 years. Carlos Sousa too helped me in numerous ways to solve issues with ARCGIS, creating graphics and for field work. Erwan Garel and Carlos Sousa helped me to carry out the bathymetric surveying, finding data from various Portuguese sources. Ana Gomes helped me to sort out some of the academic issues related to the Academic Service of the University of Algarve. Carlos Loureiro, Carlos Sousa and Ana Gomes helped me to get some of the sections translated into Portuguese. Laura Ferreira and Bruno Fragoso also helped me in many ways. I was so very warmly welcome by everyone in the Centro de Investigação Marinha e Ambiental (CIMA) at the University of Algarve. It didn't take long to feel like I was a member of the family of CIMA. The atmosphere in the CIMA group was great and I would like to thank everyone including Zélia Coelho.

Since my childhood, I received a strong support and encouragement for academic activities from my parents Sirisena and Ramani and sister. They avoid me from a lot of distractions. The encouragements by my wife Nadeesha and her parents and siblings to focus strictly on my academic work have been fundamental. She always reminds me that I have to forget all the other things, but to spend time for study. I would like to thank especially my sister for looking after our parents, which is my obligation. Finally, I would like to thank everyone at the University of Algarve for their kind attention and helps when a need arise.

This research was possible through the financial support of:

- Ph.D grant by Fundação para a Ciência e Tecnologia (SFRH/BD/70747/2010)
- Research grant by Centro de Investigação Marinha e Ambiental (UID/MAR/ 00350/2013)

ABSTRACT

In the context of hybrid approach, this study was focused on formalizing and application of a simple and idealized model using a set of theoretical framework based on rule-based morphological expressions. Main objectives were: *(1)* to simulate the sedimentary infilling of the Guadiana Estuary palaeovalley due to eustatic sea-level rise during the Holocene, against previous geomorphological and post-glacial palaeoenvironmental reconstructions based on facies interpretation and ^{14}C dating; *(2)* to assess potential morphological impacts and risk of habitat shift by simulating the morphological evolution of the Guadiana estuary and its intertidal zone for the worst case of sea level rise and sedimentation scenarios predicted for the 21st century; *(3)* to assess the sensitivity of bed friction coefficient, power index of the current velocity in the erosion rate function, river discharge, and sea-level rise rate in determining the decadal scale morphological evolution in the Guadiana estuary; and *(4)* To understand the effect of dam construction along the Guadiana river on the estuarine morphology.

According to the results, the long-term modelling of the morphological evolution in the estuary due to sea-level rise during the Holocene complemented previous reconstructions, based on interpretations of the experimental data. The intermediate hybrid approach that was followed in this study appears to be a useful tool for simulating the morphological evolution of an estuarine system during the period of postglacial sea-level rise. It seems particularly suited to the more sheltered environments of an estuarine system where vertical aggradation dominates the sedimentary infilling of the palaeovalley. However, the direct application of Estuarine Sedimentation Model and the intermediate hybrid model, are very much applicable to a system where there is net accretion throughout the estuarine system. These constraints were compensated to a certain extent using the fully developed hybrid model as it was able to produce elevation change distribution from 2000 to 2014 in the Guadiana estuary, approximately similar to the observed normal probability distribution for the same period. This

improved model was able to produce spatial variability of eroding and accreting regions, enabling the coupling of decadal scale model to centennial scale model. Furthermore, results indicate the deficiencies of defining the environmental flow as a percentage of dry season flow and the risk of habitat loss from the intertidal zone. Thus, a multi-dimensional approach has to be adopted to mitigate their consequences of sea-level rise and drastic flow regulations on the ecosystem of the Guadiana estuary.

Keywords: Estuaries, Sea-level rise, Long-term morphological evolution, Behaviour-oriented models, Hybrid models Hindcasting and forecasting

RESUMO

No contexto de uma abordagem híbrida, este estudo focou-se na formalização e aplicação de um modelo simples e idealizado baseado no enquadramento teórico resultante de expressões geomorfológicas. Os objetivos principais foram: (1) simular o preenchimento sedimentar do palaeovale do estuário do Guadiana devido à subida eustática do nível do mar durante o Holocénico, considerando reconstruções geomorfológicas e pós-glaciais palaeoembientais por sua vez baseadas em interpretação de fácies e datações por Carbono-14; (2) avaliar os potenciais impactos morfológicos e de risco de mudança de habitats através da simulação fa evolução morfológica do estuário do Guadiana e respetiva zona intertidal de acordo com o pior cenário de subida do nível do mar e de sedimentação projetado para o século XXI; (3) avaliar a sensibilidade do coeficiente de fricção de fundo, índice de potência da velocidade de corrente na função de taxa de erosão, e taxa de subida de nível do mar na determinação da evolução morfológica do estuário do Guadiana numa escala temporal de décadas; e (4) perceber qual o efeito na morfologia estuarina da construção de barragens ao longo do rio Guadiana.

De acordo com os resultados obtidos, a modelação a longo prazo da evolução morfológica do estuário devido â subida do nível do mar durante o Holocénico complementou reconstruções prévias baseadas em interpretações de dados experimentais. A abordagem intermédia híbrida seguida neste estudo apresenta-se como uma ferramenta útil para simulação da evolução morfológica de um sistema estuarino durante o período de subida do nível do mar pós-glacial. Torna-se ainda particularmente aplicável a ambientes mais abrigados de um sistema estuarino onde a agradação vertical domina o processo de preenchimento sedimentar do palaeovale. Porém, a aplicação direta do Modelo de Sedimentação Estuarina e do modelo intermédio híbrido é igualmente aplicável a um sistema onde exista acreção generalizada por todo o sistema estuarino. As limitações encontradas foram relativamente compensadas através

da utilização do modelo hibrido totalmente desenvolvido. Este permitiu estimar a variação de elevação do estuário do Guadiana entre 2000 e 2014 de forma aproximadamente semelhante à distribuição normal de probabilidade observada para o mesmo período. Este modelo melhorado permitiu a produção de variabilidade espacial de regiões em acreção e erosão, possibilitando a união entre o modelo operante à escala de décadas com o modelo operante à escala de séculos. Ainda, os resultados obtidos apontam para as limitações na definição de um caudal ecológico como um percentagem do caudal em época seca, e o risco de perda de habitats da zona intertidal. Assim, uma abordagem multi-dimensional deverá ser adotada de forma a mitigar as consequências da subida do nível do mar e da regulação drástica do caudal no ecossistema do estuário do Guadiana.

Palavras-chave: Estuários, Subida do nível do mar; Evolução morfológica a longo prazo; Modelos orientados por comportamento; Modelos híbridos; Reconstrução retrospetiva e preditiv

RESUMO ALARGADO

A Humanidade enfrenta grandes desafios no que diz respeito à mitigação e adaptação aos impactos das alterações climáticas globais, incluindo os decorrentes da subida do nível do mar em ambientes estuarinos durante o século XXI. Consequentemente, as autoridades têm que tomar decisões de gestão e implementar políticas que minimizem os riscos de inundação, bem como as ameaças para os habitats estuarinos e costeiros, devido aos cenários que projetam uma subida do nível do mar. Tais impactos negativos podem ser exacerbados devido às atividades humanas intensivas que se desenvolvem nestas regiões. Em contraponto com a abordagem dominante do século XX de mitigar os problemas de erosão costeira com recurso a intervenções intrusivas de engenharia dita "pesada", que falharam em muitos casos, as aplicações de estratégias de engenharia ditas "ligeiras" têm vindo a ser identificadas como uma abordagem mais sustentável a ser adotada no presente século. Para tal é necessária uma boa compreensão dos processos físicos e biológicos de longo termo, os quais controlam a dinâmica de sistemas estuarinos na sua globalidade. Uma abordagem robusta de modelação terá então que ser considerada para compreender o grau de resposta e sensibilidade de sistemas estuarinos a alterações nos processos dominantes, tais como dinâmica de marés, subida do nível do mar, descarga fluvial e abastecimento sedimentar fluvial. Contudo, a dinâmica sedimentar e, especialmente, as alterações morfológicas de longo-termo são difíceis de modelar, uma vez que a maioria dos modelos de previsão são baseados na simulação de eventos discretos e num insuficiente conhecimento de processos estocásticos.

Apesar de as condições ambientais serem naturalmente diferentes, compreender e simular a evolução estuaria Holocénica em resposta à subida eustática do nível do mar deverá servir como base para prever a sua evolução morfológica durante o século XXI. É ainda importante compreender a incerteza e sensibilidade dos parâmetros de controlo na evolução morfológica durante este século. Existem algumas desvantagens nas abordagens de modelação

baseadas em processos explícitos e baseadas em comportamentos. Em comparação, os modelos híbridos, apesar de estarem ainda numa fase inicial de desenvolvimento, podem combinar o rigor dinâmico de modelos baseados em processos com o conhecimento observacional incorporado em modelos assentes em relações geomorfológicas empíricas ou modelos baseados em comportamentos. Prandle (2004; 2009) desenvolveu uma conceptualização teórica baseada em expressões obtidas a partir de relações morfológicas empíricas, recorrendo à simplificação da equação unidimensional de propagação de momento axial em águas pouco profundas e da equação de continuidade. As teorias daí resultantes fornecem formulações explícitas para as velocidades de corrente, séries temporais de concentração do sedimento em suspensão em função da elevação, alturas de maré, descarga fluvial, dimensão do sedimento, atrito de fundo, erodibilidade e porosidade do sedimento. Desta forma, o modelo híbrido de evolução morfológica está assente nos desenvolvimentos apresentados em Prandle (2004; 2009) e outras relações empíricas obtidas em vários estudos desenvolvidos no sistema estuarino do rio Guadiana.

Para complementar investigações de campo que descreveram a história geomorfológica e a variação do nível do mar ao longo dos últimos 13.000 anos no estuário do Guadiana, localizado no sudoeste da Península Ibérica, foi, no presente estudo, inicialmente aplicado o Modelo de Sedimentação Estuarina de forma a compreender a capacidade e aplicabilidade de uma abordagem de modelação baseada em comportamentos para realizar simulações de longo-termo da evolução morfológica do estuário do Guadiana em resposta às projeções de subida do nível do mar e cenários de défice sedimentar (Capítulo 2). Em segundo lugar, no contexto de uma abordagem híbrida, formalizou-se um modelo simples e idealizado, o qual foi programado em ambiente MATLAB com recurso à conceptualização teórica baseada em expressões morfológicas empíricas obtidas por Prandle (2004; 2009) de forma a:

(i) Simular o preenchimento sedimentar do paleovale do estuário do Guadiana devido à subida eustática no nível do mar durante o Holocénico (Capítulo 3);

(ii) Avaliar os resultados da modelação em comparação com reconstruções geomorfológicas e paleoambientais pós-glaciais baseadas em interpretação de fácies e datação por radiocarbono – ^{14}C (Capítulo 3);

(iii) Simular a evolução morfológica do estuário do Guadiana e as suas zonas entre marés para os cenários mais gravosos em termos de subida do nível médio do mar e sedimentação previstos para o século XXI (Capítulo 4);

(iv) Analisar os impactos morfológicos potenciais e os riscos de deslocação de habitats por forma a permitir a formulação de políticas de gestão de longo-termo para a totalidade do sistema estuarino (Capítulo 4);

(v) Avaliar a sensibilidade ao coeficiente de atrito de fundo e exponenciação da velocidade da corrente na função da taxa de erosão, bem como a taxa de subida do nível do mar na determinação da evolução morfológica do estuário do Guadiana à escala da década (Capítulo 5);

(vi) Compreender qual o efeito das barragens construídas no longo do Rio Guadiana na morfologia estuarina (Capítulo 5);

(vii) Comparar a taxa de denudação da bacia hidrográfica do Rio Guadiana com recurso ao método isotópico Berílio 10 (^{10}Be) e o método do balanço sedimentar (Capítulo 6);

(viii) Avaliar a sensibilidade da descarga fluvial (fluxo ambiental) na evolução morfológica de longo-termo após a conclusão da barragem de Alqueva em 2002 (Capítulo 7);

Os objetivos 1 a 4 e 7 foram alcançados através da estimação dos coeficientes adimensionais de acreção líquida para um transepto hipotético, compreendido entre o nível máximo de maré alta e a máxima profundidade no estuário do Guadiana, recorrendo-se às expressões

matemáticas do modelo híbrido de Prandle (2004; 2009). Os coeficientes daí resultantes foram utilizados para simular a evolução morfológica do estuário do Guadiana usando o Modelo de Sedimentação Estuarina (ESM), o qual representa uma abordagem de modelação numérica orientada por comportamentos morfológicos. Consequentemente, a abordagem implementada no presente trabalho é considerada como uma abordagem híbrida intermédia. As simulações do modelo para os objetivos 5, 6 e 8 foram baseadas no modelo híbrido aperfeiçoado (completamente desenvolvido), o qual estima diretamente a evolução morfológica do estuário do Guadiana de forma a compreender a sensibilidade dos parâmetros de controlo na alteração da elevação em resposta à subida do nível do mar e redução do fornecimento sedimentar. O objetivo 8 servirá para o desenvolvimento de estratégias de gestão de forma a minimizar o impacto da subida do nível do mar e a redução drástica da descarga fluvial devido à construção da barragem de Alqueva.

De acordo com os resultados da aplicação direta do Modelo de Sedimentação Estuarina, durante o século XXI a evolução morfológica do estuário do Guadiana e a sua zona entre marés adjacente são provavelmente melhor representadas pelas projeções que combinam o cenário de subida do nível do mar A1F1 (59 cm) com o cenário de intervenção humana da sedimentação (0.65 mm/ano). Esta combinação de cenários fornece uma percepção ampla do grau de vulnerabilidade do estuário em condições de carência sedimentar. Nestas condições, verificar-se-á um aumento significativo na profundidade efetiva do canal principal. A sedimentação acima do nível médio do mar atingirá apenas 37% do total da sedimentação potencial, o que se deve à exclusividade do forçamento de maré nesta secção. Este valor aumentará até 50, 53 e 57% quando considerado um acréscimo no espaço de acomodação em função de projeções de subida do nível do mar de 38, 48 e 58 cm, respectivamente. A translação horizontal (para terra) do limite superior da zona entre marés do estuário será mais significativa na margem Portuguesa, quando comparada com a mesma translação na margem Espanhola. Nesta última,

em função de uma translação limitada dos limites superiores da zona entre marés, haverá um maior risco de desaparecimento de sapais em função do aumento da submergência resultante da subida do nível do mar. Adicionalmente, a translação para terra do nível médio do mar será mais significativa na margem Espanhola, onde os sapais deverão sofrer maior pressão devido à aceleração da subida do nível do mar; este fenómeno deverá ser menos significativo na margem Portuguesa. Em termos gerais, a zona entre marés do estuário do Guadiana deverá aumentar entre 3 a 5% por cada aumento de 10 cm no nível do mar até ao final do século XXI, o que representará uma perda efetiva de terra emersa devido à subida do nível do mar.

Contudo, o modelo em causa é bastante simples e não considera a erosão induzida pelas marés, bem como a variação na descarga fluvial. Consequentemente, este tipo de modelo é muito mais aplicável a sistemas onde se verifica uma acreção efetiva em todo o sistema estuarino. Assim, os constrangimentos na investigação observados em abordagens de modelação orientadas por comportamentos podem ser compensados com a utilização de abordagens híbridas (comportamento-processos), as quais poderão auxiliar na exploração de algumas das vantagens de modelos baseados em processos. Mesmo considerando que este modelo é extremamente idealizado e que os resultados podem conter grandes incertezas, os resultados obtidos podem, pelo menos, indicar a ordem de magnitude dos impactos morfológicos potenciais no sistema estuarino do Guadiana resultantes dos cenários de subida do nível do mar e sedimentação para o século XXI.

Para melhorar a compreensão atual da resposta de sistemas estuarinos a forçamentos naturais, a evolução morfológica do estuário do Guadiana durante o Holocénico, devida à subida eustática do nível do mar, foi simulada com recurso a uma abordagem híbrida intermédia. A modelação de longo termo da evolução morfológica no estuário serviu para complementar reconstruções anteriores, baseadas na interpretação de dados experimentais. As simulações foram realizadas através da estimação dos coeficientes adimensionais de acreção

líquida para um transepto hipotético desde o nível máximo de maré alta até à profundidade máxima do estuário do Guadiana, utilizando as expressões matemáticas híbridas de Prandle (2004; 2009). Os coeficientes obtidos foram utilizados para simular a evolução morfológica do estuário do Guadiana utilizando o Modelo de Sedimentação Estuarina (ESM), o qual corresponde a uma abordagem de modelação numérica orientada por comportamentos, e recorrendo-se a uma representação temporal estabelecida com base na determinação de 26 idades radiocarbono. Para além disso, a evolução morfológica nas zona entre marés foi graduada em termos da frequência de inundação pela maré e os coeficientes adimensionais de acreção líquida relativamente ao referencial hidrográfico Português (2 m abaixo do nível médio do mar).

De acordo com os resultados obtidos, seis dos nove perfis topográficos da superfície extraídos dos resultados das simulações reproduzem com precisão os perfis topográficos reais. As simulações demonstraram realismo quando aplicadas aos ambientes mais protegidos do estuário, nos quais a agradação sedimentar vertical é o mecanismo dominante do processo de preenchimento. As melhores reconstruções da morfologia atual baseadas no modelo, obtidas em quatro simulações diferentes, apresentaram erros médios quadráticos da ordem dos ±4.8 m. Este valor é comparável com o erro associado à estimativa do nível médio do mar em 11.500 anos Cal. BP e com as incertezas na reconstrução da superfície do paleovale para 11.500 anos Cal. BP. O erro médio na simulação da elevação da superfície obtida por acreção sedimentar em relação à elevação da superfície de acreção real é de 27.5%, o que é considerado aceitável para a escala temporal milenar adoptada. A abordagem híbrida intermédia que foi implementada neste estudo demonstrou utilidade para a simulação da evolução morfológica de um sistema estuarino durante o período de subida do nível do mar pós-glacial. Esta abordagem demonstrou ser particularmente adequada para os ambientes mais protegidos de um sistema

estuarino, onde a agradação vertical controla o processo de preenchimento sedimentar do paleovale.

Este erro é comparável com o associado à estimativa do nível médio do mar há 11 500 anos Cal. BP e com as incertezas na recriação da superfície do paleovale há 11 500 anos Cal. BP. O erro médio da simulação da elevação da superfície do sedimento acrecionado relativamente à atual altura média de acreção foi de 27,5%, valor que é considerado aceitável para a escala de tempo milenar que foi adoptada. A abordagem híbrida intermediária que foi seguida neste estudo parece ser uma ferramenta útil para simular a evolução morfológica de um sistema estuarino durante o período pós-glacial de súbida do nível médio do mar. Esta parece particularmente apropriada para ambientes mais confinados de um sistema estuarino onde a agradação vertical domina o preenchimento sedimentar do paleovale.

Descobertas como a função de erodibilidade e os coeficientes da acreção líquida não dimensional da simulação otimizada do preenchimento do estuário do Guadiana, devido à subida do nível médio do mar durante o período do Holocénico, foram utilizados para prever a evolução morfológica à escala da decada. Os resultados da previsão do modelo indicaram que, se as propriedades biogeoquímicas do sistema estuarino do Guadiana forem as ideais para a migração no sentido do continente e adaptação dos sapais com as súbidas dos níveis do mar, o único risco seria a redução de 0,05 e 0,6 km^2 dos habitats de alto sapal na margem portuguesa em resposta, respetivamente, aos cenários de limite inferior e superior de súbida do nível médio do mar e sedimentação. Se a capacidade de adaptação da vegetação de sapal das zonas recentemente migradas é muito fraca, as comunidades de baixo e médio sapal serão ameaçadas de extinção sobre o cenário do limite superior, tanto na margem portuguesa como na espanhola. Esta vegetação será substituída por planícies lodosas ou arenosas ou novos baixos sapais com uma baíxa riqueza de espécies. Sobre as piores condições ambientais e de súbida do nível médio do mar, a terra do sistema estuarino disponível para os altos sapais será de cerca de 1,4 km^2 no

final do século XXI. A área total recém inundada, devido às marés e à súbida do nível do mar será de 3,2 e 11,8 km^2, respetivamente, para os limites inferior e superior. Embora nós reconheçamos que há espaço para melhorias adicionais da abordagem híbrida intermediária, os presentes resultados de previsão podem produzir uma visão ampla dos impactos relacionados com a súbida do nível médio do mar para fíns de gestão holísticos.

A taxa de desnudamento da bacia do Guadiana foi estimado para quantificar as taxas de evolução da paisagem numa escala de tempo milenar. Tal servirá para compreender os controlos e eficiências de processos geomórficos relevantes e para estabelecer a relação entre as alterações climáticas e a resposta da paisagem. As estimativas podem ser usadas para alcançar os objetivos de gestão de sedimento de toda a bacia, em particular para os rios transfronteiriços. Assim, o principal objetivo foi estimar e comparar a taxa de desnudamento da bacia do rio Guadiana utilizando o método do isótopo ^{10}Be e o método do balanço sedimentar.

De acordo com a abordagem do balanço sedimentar, a taxa média de desnudamento da bacia do rio Guadiana seria de $1,58*10^{-3}$ cm/ano**.** A taxa média de desnudamento do estuário do Guadiana derivada da média anual do fluxo do isótopo foi de $1,3 \pm 0,2x10^{-2}$ cm/ano, enquanto que a mesma derivada usando as médias mensais foi de $0,79 \pm 0,62 \ x10^{-2}$ cm/ano. Isto é uma ordem de magnitude superior à mesma deridada usando o método do balanço sedimentar. Contudo, se aplicarmos 90% do factor de retenção (para contar com a retenção do sedimento pelas barragens) para o valor estimado utilizando a abordagem do balanço sedimentar, os resultados seriam comparáveis com o limite superior da taxa de desnudamento estimada usando o método do isótopo ^{10}Be. O factor de correção de 85% estaria de acordo com o limite inferior da taxa de desnudamento medida através do método do isótopo, enquanto que 80% iria representar aproximadamente o valor estimado usando a média mensal das concentrações do isótopo ^{10}Be. Consequentemente, as taxas de desnudamento da bacia do rio

Guadiana que foram derivadas do método do isótopo ^{10}Be podem ser comparáveis com as obtidas através do método do balanço sedimentar, apenas se os resultados desta última abordagem forem corrigidos para a atenuação da descarga sólida pela barragem. Por outro lado, a estimativa da taxa de desnudação utilizando o método do balanço sedimentar e o método do isótopo ^{10}Be podem ser usadas como uma nova abordagem para estimar o factor de retenção sedimentar pelas barragens. Isto irá servir como uma validação da força e capacidades do modelo. Contudo, é necessário efetuar mais estudos para melhorar as estimativas.

A sensibilidade do coeficiente de fricção do leito, o índice de poder da velocidade da corrente em função da taxa de erosão e da taxa de súbida do nível do mar para a determinação da evolução morfológica do estuário do Guadiana à escala da decada, foram avaliados utilizando puramente um modelo híbrido baseado num guião com linguagem de programação de MATLAB. A evolução hidrodinâmica e morfológica à escala da década foram simuladas utilizando soluções analitícas generalizadas de um enquadramento teórico, no qual a propagação da maré no estuário foi representada pelas médias unidimensional e transversais das equações das ondas de água rasas enquanto que as condições de fricção foram linearizadas num canal estuarino de forma triangular e síncrona. Os principais objectivos deste estudo foram validar o modelo de evolução morfológical de curta prazo e encontrar as suas sensibilidades a efeitos combinados de formas de fricção de superfície e do leito, poder da velocidade da corrente residual, taxa de súbida do nível do mar e tempo.

O sub-modelo à escala da decada foi aplicado no estuário do Guadiana localizada na fronteira a sul entre Portugal e Espanha. Os registos da descarga do rio de 2000 a 2014 na estação do Pulo do Lobo do rio Guadiana foram utilizadas para derivar uma média aproximada da descarga do rio numa série temporal. A batimetria de entrada foi derivada de um mapa do ano 2000 e o diâmetro do sedimento do leito do rio foi obtido a partir de estudos anteriores. Foi realizado um levantamento batimétrico em maio de 2014 usando uma sonda de feixe único. As marés foram

modeladas usando os constituintes de maré M2; M4; S2; O1; K1; MSf; N2; K2; MS4 e M6. A inclinação do leito do rio foi assumida como constante. A função do coeficiente de erodibilidade do sedimento foi obtida da simulação do preenchimento sedimentar Holocénico (capítulo 3). A concentração de sedimento suspenso foi derivada usando uma formula empírica e a SSC no pico das discargas foram derivadas ampliando as estimativas por forma a serem compativeis com estudos anteriores em situações de grandes descargas no rio.

De acordo com os resultados de simulação do modelo para diferentes poderes de velocidade de corrente da função da taxa de erosão (n) e alteração no coeficiente de fricção (f), existe uma boa compatibilidade entre a batimetria observada em 2014 e quatro batimetrias simuladas. Concluindo, o modelo à escala da decada foi capaz de produzir alterações da distribuição da elevação de 2000 a 2014 no estuário do Guadiana, aproximadamente semelhantes à distribuição de probabilidade normal observada para o mesmo período. A variação da média das alterações da elevação ($\overline{\Delta Z}$) e o desvio padrão (σ) exibem uma relação logaritmica para os poderes da velocidade da corrente da função da taxa de erosão (n) desde 1,5 até 3 e depois não há alterações significativas em $\overline{\Delta Z}$ e σ para aumentos adicionais de n. Um efeito combinado no $\overline{\Delta Z}$ e σ é identificada entre n e o factor de fricção para a velocidade de corrente modelada inferior a 1 m/sec. As distribuições normais das alterações de elevações modeladas, aproximou-se da distribuição normal observada para a alteração de elevação para n = 1,8; 2; 2,5 e 3, enquanto a fricção é alterada -20 %, (0,8f), 0 %, (f), +50 %, (1,5f), e 107 % (2,07f), respetivamente. O f dá os valores estimados da fricção de cada célula utilizando uma expressão empirica. $\overline{\Delta Z}$ e σ das simulações ótimas acima referidas são altamente comparável aos valores observados correspondentes de 0,369 e 0,766 m, respetivamente. As diferenças entre $\overline{\Delta Z}$ com ou sem súbida do nível do mar relativamente ao aumento da taxa de espaço de acomodação convergem para o valor zero com um aumento da taxa de súbida do nível do mar acima da presente taxa média global de súbida do nível do mar, assim

o aceleramento da súbida do nível do mar causaria uma destruição significante ao sensível ecosistema do estuário do Guadiana.

As observações de campo sugerem que um aumento da erosão e transporte do sedimento para o oceano, a combinação com maior aplicabilidade seria dada por n = 1,8 e 0,8f ou n = 2 e f. O modelo foi capaz de produzir variabilidade espacial das regiões de erosão e acreção, assim poderá haver uma discrepância em magnitude. De acordo com as simulações, haveria uma aumento da acreção nos canais mais profundos que não é continua no caso observado que pode dever-se a perturbações da sedimentação resultantes de atividades humanas como a navegação frequente de grande navios ao longo do canal profundo. A erosão teve lugar principalmente nas planícies lodosas rasas. Tal implica que a planície lodosa irá aprofundar-se com a súbida do nível do mar. Estas áreas podem ser preenchidas por sedimentos marinhos, mas isto irá também causar um efeito deletério à sobrevivência do sistema se sapal, como observamos nesta área de estudo. Finalmente, embora o modelo completo tenha sido formulado para simular uma evolução morfológica do estuário a longo prazo, o módulo do modelo à escala da década seria útil para simular as batimetrias a curto prazo dos canais do estuário e para estimar o volume da dragagem do canal para a navegação. Contudo, é importante estabelecer a distribuição normal do ΔZ nos estuários através da realização de vários levantamentos batimétricos, pelo menos anualmente.

Há evidências que provam a inadequação do fluxo ambiental que é para ser mantido no rio Guadiana para sustentar condições minímas para o funcionamento do rio. Os métodos para estimar o fluxo ambiental não reconhecem a descarga fluvial requerida para manter os habitats de sapal e não considera a ameaça da súbida do nível do mar. Portanto, o presente estudo foi focado sobre a avaliação da sensibilidade da descarga do rio na evolução morfológica no estuário em resposta ao pior caso de súbida do nível do mar e aos cenários de sedimentação. A avaliação foi principalmente baseada na abordagem híbrida explicada no capítulo 5. Os dados para esta avaliação foram obtidos de estudos empíricos levados a cabo no rio Guadiana e no seu estuário. As simulações foram

efetuadas para três casos em termos do fluxo base do rio. O primeiro foi a função de fluxo de base modelada que é aproximadamente equivalente ao fluxo observado e que foi aumentada por factores de 1,5 e 2 nos outros dois casos. Através do aumento o fluxo de base da descarga do rio por uma factor de 1,5 e 2, o volume líquido de sedimento erodido pode ser reduzido cerca de 25 e 40% com respeito ao volume líquido de sedimento erodido dado pela descarga do rio modelada no primeiro caso. Contudo, os resultados indicam que mesmo que o fluxo de base fosse aumentado, o risco de perda de habitat incapaz de recuperer efetivamente. Tal poderá sugerir as deficiências da definição do fluxo ambiental como uma percentagem de fluxo de estação seca. Assim, uma abordagem multi-dimensional tem de ser adotada para mitigar as suas consequências de súbida do nível do mar e regulações dr´sticas do fluxo no ecossistema do estuário do Guadiana.

TABLE OF CONTENTS

LIST OF FIGURES

LIST OF TABLES

Chapter 1

Introduction

1.1 GENERAL INTRODUCTION

1.1.1 WHAT IS AN ESTUARY AND HOW IT IS FORMED AND EVOLVE?

An estuary is the seaward portion of a drowned river valley (Dalrymple et al., 1992) and it is a semi-enclosed transitional water body (Potter et al., 2010) that extends from landward tidal limits to the seaward limit of coastal influence (Cameron and Pritchard, 1963; Nichols and Biggs, 1985). Thus, in chemical terms the salinity range in an estuary extends from 0.5 to 30-35 ‰ (Pritchard (1967). River valleys incised due to erosion in response to a fall in sea-level during low stands (Fagherazzi et al., 2004). Then they were drowned forming the present morphology of estuaries by the subsequent postglacial sea-level rise during the Holocene (Roy et al., 1994). Estuaries have since infilled with marine and fluvial sediment to varying degrees depending on the global forcing like sea-level rise rate (Bridge, 2003) and local controls including wave climate, the availability of riverine and coastal sediment, and the river and tidal hydrodynamics (Wright and Coleman, 1973).

In meso-tidal regimes (tidal range 2 - 4m), fluvial discharge controls the geomorphologic evolution of the estuary (Wolanski, 2006). However the observed high variability in valley morphologies may be due to other controlling factors including hydrodynamics, sediment supply, geomorphology, climate and human activities (Chaumillon

et al., 2011). The life span of an estuary extends over a millennial time scale passing through several stages of life from youth to maturity and old or terminal age (Roy, 1984; Roy, 1994; Roy et al., 2001). According to Wolanski, 2006, at the first stage the river valleys are flooded due to sea-level rise and during the second stage, tidal inundation fosters the growth of salinity resisting vegetation and finally, during the terminal stage, freshwater vegetation will dominate the habitat as the plains become higher in elevation than high tide limits due to various forms sedimentation.

1.1.2 CLASSIFICATION OF ESTUARINE SYSTEMS

In terms of management and modelling perspectives, setting the right typology of estuaries is important because it defines the dominant processes in the long term evolution of the estuarine morphology. According to geomorphological features of estuaries, Pritchard, (1967) proposed a four type classification: (1) drowned river valleys, (2) fjord type estuaries, (3) bar-built estuaries and (4) estuaries produced by tectonic processes. Based on geomorphology and topography, Davidson *et al.*, (1991) classified estuaries into nine categories: (i) fjord, (ii) fjard, (iii) ria, (iv) coastal plain, (v) bar built, (vi) complex, (vii) barrier beach, (viii) linear shore and (ix) embayment. According to the primary process that shaped the underlying palaeovalley before the sedimentation during the Holocene, Hume and Herdendorf (1988) divided estuaries in to five classes with sixteen sub-classes based on the geomorphology and oceanographic characteristics of the estuary, and catchment hydrology (Fig. 1.1). Hume et al., (2007) presented a new classification of estuaries based on a hierarchical view of the abiotic components that define estuarine environments. Accordingly, estuaries are grouped into four levels: (1) global scale variation based on differences in climatic and oceanic processes (Solar radiation, heating and cooling, precipitation, evaporation), which are discriminated by the factors: latitude, oceanic basins and large landmasses; (2) variation in

estuary hydrodynamic processes (mixing, circulation, stratification, sedimentation, and flushing), which are discriminated by estuary basin morphometry, river and oceanic forcing; (3) variation among estuaries that are due to catchment processes (Supply of fresh water, sediment and water chemistry constituents), which are discriminated by catchment geology and catchment land cover; and (4) variation among estuaries that are due to local hydrodynamic processes Sediment deposition and erosion, which are discriminated by ocean swell, tidal currents, wind waves and depth.

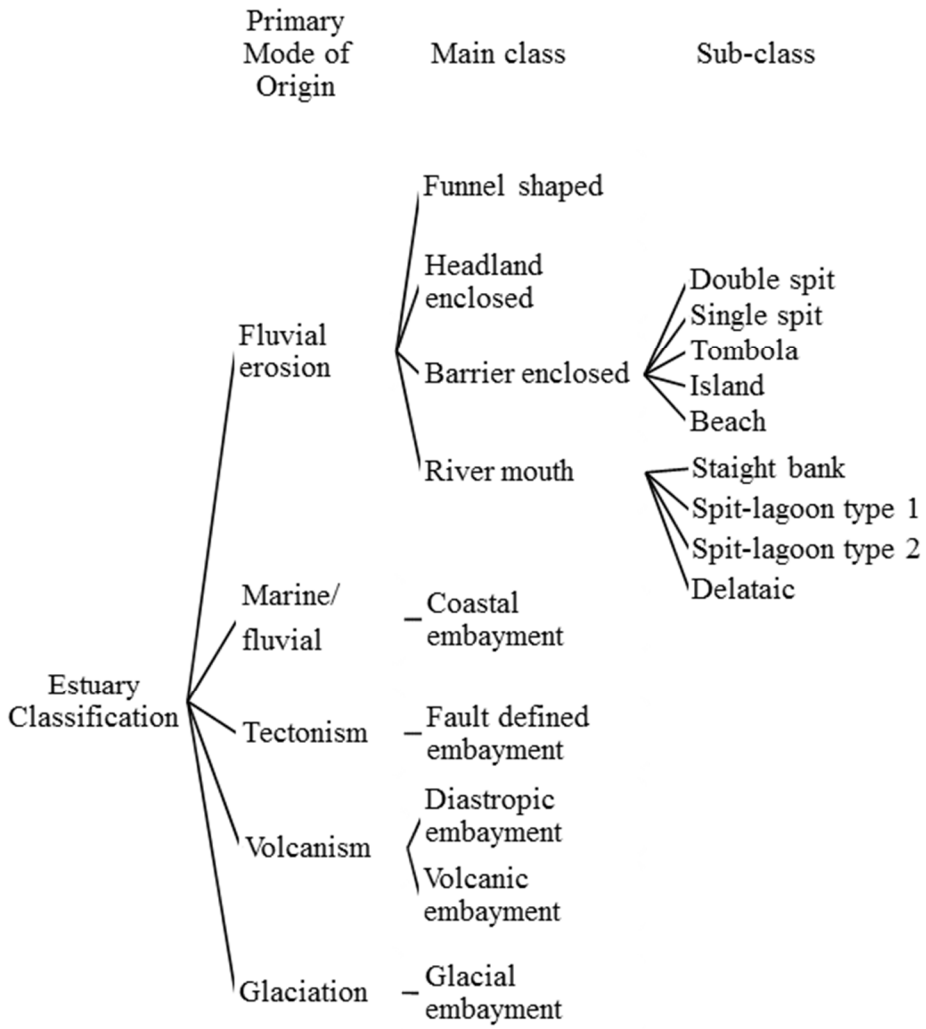

Figure 1.1 Classification of estuaries according to the primary process that shaped the underlying palaeovalley before the sedimentation during the Holocene, and based on the geomorphology and oceanographic characteristics, tides, and catchment hydrology (based on Hume and Herdendorf, 1988).

It was recognized that the tidal range (Dyer, 1996) increases upstream with the convergence of the estuarine margins while friction reduces the tidal range. Thus, according to the dominance of the friction and convergence over the tidal range, estuaries also can be classified as hypersynchronous, synchronous and hyposynchronous (Nichols and Biggs, 1985). If the convergence forcing exceeds friction, they are called hypersynchronous estuaries, in which tidal range and current increase towards the head of these funnel shaped estuaries and in the riverine section, tidal range reduces as the friction increases (Dyer, 1996). The opposite is true for hyposynchronous estuaries. In synchronous estuaries, the effect of friction and convergence of margins on tidal range is equal and the sea surface slope due to axial gradient in phase of tidal elevation significantly exceeds the gradient from changes in tidal amplitude (Prandle, 2009).

In the context of facies distribution of estuaries, Dalrymple et al., (1992) grouped them according to the dominance of tides and waves. Accordingly, in a wave dominated estuary, its mouth experiences high wave energy and the sediment eroded in the adjacent coastline will be deposited to form a subaerial barrier/spit or submerged bars. As the mouth is constricted with increased deposition, currents will increase so as to have balance in sediment deposition and erosion (Dyer, 1996). In tide dominated estuaries, tidal currents play the dominant role in transporting the fluvial sediments, resulting in significant upstream transport of bedload sediment (Wells, 1995). In such estuaries, mouth area will be flanked by sandbanks aligned with the dominant direction of the current flow (Dyer, 1996). Interestingly, Chaumillon et al., (2011) identified a mixed system which can be classified as neither tide nor wave dominated. However, they cannot be defined solely according to the magnitudes of tidal range (Wells, 1995). If the rising-tide time is shorter than the falling-tide time, such estuaries are flood-dominant while the opposite is true for ebb dominant systems (Wang et al., 2002). Chaumillon

et al., (2011) defined a schematic representative cross sections showing the variability of French valley fills related to their energetic and morphologic classification.

On the basis of vertical structure of salinity, estuaries can be further classified as salt wedge, strongly stratified (salt-wedge or Fjord type), weakly stratified (partially mixed) or vertically mixed (laterally homogeneous or inhomogeneous) (Cameron and Pritchard, 1963; Dyer, 1996). The estuarine circulation will be controlled by the balance between the pressure gradient induced by the outer estuary surface slope, the baroclinic pressure gradient due to the along-estuary salinity gradient, and the stress associated with the estuarine circulation (Geyer et al., 2000). Therefore, this classification considers the balance between buoyancy forcing from river discharge and mixing from tidal forcing, which determines the volume of oceanic water entering the estuary during each tidal cycle (Valle-Levinson, 2010). In vertically stratified estuaries, there would be no mixing of salt and freshwater (Dyer, 1996), which can be observed in large river discharge combined with weak tidal forcing particularly during the flood tide (Valle-Levinson, 2010). In partially mixed estuaries, there is a significant vertical density gradient (Fischer, et al., 1979) resulting from moderate to strong tidal forcing and weak to moderate river discharge (Valle-Levinson, 2010). In a vertically homogeneous estuary, there is sufficient mixing so that the salt-water and fresh water interface disappears at high tidal current velocities (Biggs, 2012) and weak river discharge (Dyer, 1996). Consequently, mean salinity profiles in mixed estuaries are practically uniform and mean flows are unidirectional with depth (Valle-Levinson, 2010).

However, it is important to note that defining a mutually exclusive classes of estuaries may not be practical, given that some estuaries may belong to more than one class as there is a range of properties and processes (Wells, 1995). Many estuarine systems may change from one class to another in subsequent tidal cycles, or from month to month, or from season to season (dry or wet), or from one location to another within the same estuary (Valle-Levinson, 2010).

1.1.3. IMPORTANCE OF ESTUARINE SYSTEMS AND THREATS ON THEIR SURVIVAL

Many estuaries around the world serve as economically important links between land and sea, as navigational channels providing access to harbours and inland waterways, and at the same time, they act as valuable natural environments, providing shelter, feeding and breeding grounds and nurseries to a wide variety of species (De Vriend, 2003). Human activities associated with estuarine systems have been carried out over many centuries (Kolahdoozan and Falconer, 2003). But human involvement with these systems has now widen at an ever larger scale and many estuarine ecosystems are stressed to the extreme (De Vriend, 2003). There is growing concern about sustainable management of estuarine resources, in the context of balancing the economic exploitations and healthy functionality of natural systems in the face of increasingly larger scale developments and higher demands on navigability for ever larger ships (Prandle, 2004; (De Vriend, 2003).

Natural functionality of estuarine systems, may be further affected by renewable energy extraction, cooling water abstraction, aggregate mining, fishing, habitats, agriculture, waste disposal, and leisure activities. Estuarine environments are facing increasing rates of change due to raising temperature, changing freshwater runoff, changes in sea level, likely increases in flooding events (Huthnance et al., 2008). As predicted in series of reports by the Intergovernmental Panel on Climate Change (IPCC, 2007; 2013) the observed global climate change is expected to significantly affect mean sea levels, storminess and river flows, which will in turn impact on estuarine systems (Norton et al., 2007). However, the response of an estuary to above forcings will be modified by natural concurrent morphological adjustments and past and present human interventions (Prandle, et al., 2005). Extensive land clearing for agriculture and human settlements within the mountainous part of the catchments may accelerate the sediment supply from rivers into the estuary (Milliman and Meade, 1983;

Milliman and Syvitski, 1992). On the other hand, large dams may reduce river discharge significantly and thereby, the fluvial sediment supply (Wolanski et al., 2001, 2004).

1.2 MODELLING LONG-TERM EVOLUTION OF ESTUARINE SYSTEMS

1.2.1. ESTUARINE MORPHODYNAMIC PROCESSES

An estuary consists of complex physical systems that are subject to the influences of waves, tides, river flow and human interventions (Karunarathna et al., 2008). The morphology of estuaries is a result of complex nonlinear interplay between water and sediment motion and bed topography (Hibma et al., 2004). The exact form and its magnitude of the response of estuarine morphology to hydrodynamic factors and global climate forcing like sea-level rise will depend on the dominance of those forcing factors and other controls such as sediment characteristics and local geology at a particular estuary (Karunarathna et al., 2008). On the other hand, the dominant hydrodynamic processes of an estuary will have a feedback effect from the tidal asymmetry, wave-driven currents and wave-induced stirring effects, which are all affected by the local seabed bathymetry (Luo, et al., 2013).

The steady supply of energy by the tidal currents, sediment moves in and out of the estuary (Bell et al., 2000), hence tidal motion is the principal shaping factor of meso- and macroscale features in estuaries to which wind waves add (Prandle, 2004). The interaction between tide and basin morphology is partly responsible for the deformation of the tidal wave creating asymmetry in tidal currents changing the flow pattern, and thus the sediment transport, (van der Spek, 1997). For instance, tidal waves distort over low intertidal areas and along shallow channels with decreasing depth landwards resulting in faster wave propagation at high tide than low tide (Dronkers 1986). In deep channels and over the intertidal areas above the mean tide level, tidal waves are distorted in such a way that the fine sediment is exported into

the sea (Towned et al., 2007). In short estuaries, the mean depth of the basin and the relative volume and height of inter-tidal shoals are the principal morphologic features affecting the tidal asymmetry. Thus, the net sediment transport direction at the estuarine mouth depends on the relative strength of two processes, namely: 1) landwards transport in the shallow water depths due to tidal asymmetry and 2) seawards sediment transport within the estuary's deep channels (Luo, et al., 2013). The sediment movement changes the morphology of the estuary by completing the feedback loop as described by Wang et al. (2002).

Tidal flats tend to equilibrium if the maximum bottom shear stress, resulting from tidal currents and wind waves, is spatially uniform (Hibma, et al., 2004). Wind and swell waves, in particularly during storms can rework large amounts of sediment at the entrances to estuaries, which can then be moved into the estuary by the incoming tide while smaller waves can erode sediments off the shallow intertidal banks inside the estuary basin (Bell, et al., 2000). If the tidal flat surface area in an estuary was strongly reduced while increasing the channel depth, tidal current velocity will increase in estuaries (van der Spek, 1997). Inter-tidal flats in proximity to deep channels may impact on the overall flood/ebb-dominance of an estuary and hence the resultant estuary infilling or transporting of sediment into the sea (Speer and Aubrey 1985; Friedrichs and Madsen 1992; Kang and Jun 2003). The enhancement of sediment infilling in estuaries during stormy situations due to increase in wave-induced currents is shown in sediment model studies (Rainford, 1997). Therefore, changes in storminess can contribute to changes in the rate of infilling in estuaries (van der Wal et al., 2002). Neal (1993) illustrated the positive feedback mechanism between estuarine infilling and a decrease in wave energy, for a variety of wave conditions. However, these sediments will only have a residual effect on long term (Hanson et al., 2003).

In the context of the long-term evolution of estuaries, the rate of sediment infilling will determine by the balance between the sediment accommodation space, created by a rise in relative sea level, and sediment supply (van der Spek, 1997). Changes to the tidal asymmetry in response to sea-level rise depend on the geometry of the estuary. Friedrichs and Aubrey (1996) correlate these forcings with the hypsometry of basins, i.e., the distribution of horizontal surface area with respect to elevation. Convex profiles (from a bottom point-of-view) are associated with tide dominance resulting in large tidal amplitudes and minor wave activity, while concave profiles are correlated with wave-dominated basins (Hibma et al., 2004). If the intertidal flats are relatively low in the tidal frame sea-level rise will favour import of sediment leading to channel infilling to maintain its equilibrium volume with respect to the tidal volume (Towned, et al., 2007). Flood-dominant estuaries are shallow systems with large inter-tidal basin storage and enhance landward near-bed transport, while ebb-dominant basins are deep systems with small inter-tidal basin storage (Wang et al., 2002). However, increase or decrease of the flood or ebb dominance in a particular system depends on the initial state at the onset of sea level rise (Towned, et al., 2007). According to many studies (e.g. O'Brien 1931; Townend 2005), the tidal volume and cross-sectional area are proportionate. If this relationship is to be maintained as the tidal volume changes with sea-level rise, the estuary volume must self-adjust by giving rise to channel enlargement (Towned, et al., 2007).

The essential characteristics of tidal dynamics in estuaries are almost entirely determined by tidal range, estuarine bathymetry with some modulation by bed roughness and river flows (Prandle, 2004). According to van Rijin, (2011), the tidal range in estuaries is affected by four principal processes: (a) inertia related to acceleration an deceleration effects, (b) amplification (or shoaling) due to the decrease of the width and depth (convergence) in landward direction and (c) damping due to bottom friction, and (d) partial reflection at landward end of the estuary, whereas bathymetric convergence produces continuous reflection

along the entire length of the channel. The response of estuaries to tidal forcing is primarily governed by continuity (mass) and the axial momentum balance since lateral velocities are often smaller than axial velocities (Winant and Velasco, 2003). According to a Grace 1936; Bowden and Fairbairn 1952; Geyer et al. 2000, acceleration, pressure gradients, and bottom friction are the dominant terms of the axial momentum balance. The relative phase between fluctuations in water level and axial velocity depends on the length of the estuary and the importance of friction (Winant and Velasco, 2003). Accordingly, in a long or shallow estuary, the tidal wave progresses from the ocean into the estuary and decays with distance while maintaining water level and axial velocity in phase.

Though estuaries show a great diversity of size, shape, depth, and shaping factors, the horizontal salinity gradient and the resulting density gradient is a general characteristic of estuaries (Geyer and MacCready, 2014), conditioning the estuarine circulation due to mixing of salt and fresh water (Leeder, 2009). The estuarine circulation and sediment transport can result in convergences that deposit sediment in quiescent zones and change the bed surface elevation (George, et al., 2012). The lateral circulation enhance the sediment export from the estuary into the sea (Cheng, 2007). The density-induced flow can affect the landward sediment transport of fine sand in suspension at the mouth of an estuary (Thomas et al., 2002). Generally, constant vertical mixing is assumed in case of the residual estuarine circulation and its temporal and spatial variations were neglected (MacCready, 2004; Talke et al., 2009). Prandle, (2004) derived a rule-based morphological expressions including explicit formulations for tidal intrusion length by simplifying the one-dimensional equation of axial momentum propagation. Waves increase mixing of fresh and saline water masses at the interface of river and sea, resulting in a decrease in outflow velocities and lateral expansion of the river outflow, thus encouraging sediment deposition close to the river mouth (van Maren, 2005).

1.2.2 CLASSIFICATION OF MODELLING APPROACHES OF LONG-TERM MORPHOLOGICAL EVOLUTION IN ESTUARINE SYSTEMS.

Prediction of the long term morphological behaviour of estuaries generally follows three approaches: 1) Behaviour-oriented models, 2) process-based models, and 3) Hybrid models.

1.2.2.1 BEHAVIOUR ORIENTED MODELS:

The behaviour oriented or top down models depend on observations of long-term geological and geomorphological evolution in estuaries (Karunarathna et al., 2008). Behaviour oriented models can be further classified into two groups: 1) geomorphologically-based models, in which empirical formulations based on statistical analysis of observed long-term morphological evolution (e.g. Bruce et al; 2003; Stopper, 1996; Stolper , 2002; Sampath et al., 2011) and 2) rule-based models derived from whole-estuary regime concept such as volume (Huthnance, et al., 2008). ASMITA is a rule based behaviour-oriented model that describes morphological interaction between a tidal basin and its adjacent coastal environment (Stive et al. 1998). In terms of volume (Kragtwijk et al. 2004), the model formulates the interaction among tidal system with the major morphological elements being viewed at an aggregated scale (Rossington *and* Spearman, 2009). Under constant hydrodynamic forcing, each element of the system is assumed to approach towards a morphological equilibrium that can be defined as a function of hydrodynamic forcing and basin volume (van Goor et al. 2003). This approach is suitable for simulating morphological evolution in centennial scale (Dissanayake et al., 2009). However, due to the very reason that the morphological evolution is represented in terms of volume, spatial evolution of inlet elements cannot be investigated using the ASMITA model (Dissnayake et al., 2011) and therefore visualization of the evolution of the topobathymetry of the basin is not possible. That would be disadvantageous in terms of management aspects. Furthermore, there are behaviour oriented models based on concepts of trend analysis, form

characterization, regime relationships, translation or “rollover” with rising sea level, accommodation space, sediment budgeting, tidal asymmetry and equilibrium along-axis profile (Huthnance, et al., 2008). This type of models are more effective in predicting long term and estuary-wide evolution of estuarine morphology but the major drawback is the lack of detailed physics (Karunarathna et al., 2008).

1.2.2.2 PROCESS-BASED MODELS

Process-based or bottom-up models are based on the basic principles that describe the underlying physical processes (De Vriend and Ribberink, 1996; Friedrichs and Aubrey, 1996; Dronkers, 1998; Hibma 2004; Dissnayake et al., 2011). Therefore, evolution of the estuary morphology derived from solving two- or three-dimensional hydrodynamic models combined with sediment transport and morphodynamic modules (Karunarathna, et al., 2008). The time step of hydrodynamic modules are few seconds, therefore, it demands high computing capacity and time. The efficiency of these models has significantly improved by the introduction of the morphological acceleration factor (MORFAC) (LESSER *et al.*, 2004; ROELVINK, 2006), permitting to simulate long-term evolution of estuaries using models like DELFT3D (Dissnayake, et al., 2011). In this approach, efficiency can be increased by schematizing the input parameters and only considering the most dominant physical processes (Dastgheib, 2012.). Notwithstanding we are unaware of any attempt to simulate the morphological evolution of estuaries in millennial time-scale. However process-based models may be more suitable for assessing local and short term morphodynamic changes in an estuary, due to limitation of insufficient mathematical knowledge of sediment transport processes and their linkage to hydrodynamics (Karunarathna et al., 2008).

1.2.2.3 HYBRID MODELS

Hybrid approach is developed by combining the entities and advance in both behaviour-oriented and process based models. The top-down model concept of an equilibrium state constrains the form of evolution and rates and spatial distributions will be given by bottom-up models (Huthnance, et al., 2008). Spearman et al. (1995) and Van De Kreeke (1996) linked hydrodynamic models with regime relationships for estuaries. Wang et al. (1998) developed combined the advection-diffusion equation with empirical equilibrium relationship of estuaries. An Inverse approach proposed by Karunarathna et al., (2008) is a hybrid model, which uses a sequence of bathymetries to infer an effective source distribution for bed evolution according to a bottom-up based diffusion-type equation.

Many countries experience difficulties in sustainable long-term management of resources in estuarine systems due to various local constraints and due to lack of confidence or capacity to use commercially available trustworthy modelling tools (Prandle, 2006). This issue can be addressed by developing hybrid models by combining the numerical models that based on the idealized and simplified first principles and observational experience encapsulated in rule-based geomorphological models (Woodroffe, 2003). Prandle, (2004; 2006) developed an Analytical Emulator based on the simplification of the one dimensional equation of axial momentum propagation. The results include a number of general rule-based morphological explicit expressions relating the estuarine depth with the parameters of river flow and channel side slope (Norton et al.,.2007). These results has successfully been used to explain how estuarine bathymetries evolved in response to tidal and riverine processes (Prandle et al., 2006).

1.2.3. TIME SCALE OF COASTAL EVOLUTION MODELS

At a wide range of special and temporal scales, the morphology of a tidal basin evolves due to complex and dynamic interactions among sedimentary features of the system and

hydrodynamic and morphodynamic processes controlled by the global and local factors (Karunarathna at al., 2008; Hibma et al., 2004, A Dastgheib, 2012). A differentiation of morphological features in temporal and spatial scales were introduced by De Vriend (1996). Accordingly, ripples and dunes formed on the bed are the smallest morphological phenomena. Those are categorized as microscale features in the time scale of seconds to minutes and in the spatial scale of a few millimetres to a few centimetres (Kraus et al., 1991). Changes of these features are instantaneous (Cowell and Thom, 1997). Alternating ebb- and flood-channels and shoals are mesoscale features (Hibma, et al., 2004). Features such as ebb tidal deltas, tidal flats and inlet channel are the macro-scale sedimentary environments (Karunarathna et al., 2008). The entire estuarine system and its adjacent coast including the shoreface can be considered as a megascale feature (Hibma et al., 2004). According to Karunarathna et al., (2008), time scales of estuary morphology evolution may vary from hours to days (short term), months to few years (medium term), decades to few hundred years (long-term) and several millennia (geological scale).

Due this highly complex nature of the system , de Vriend (1996) consented that all-purpose model for predicting the evolution of tidal system morphodynamics does not exist and it is not likely to emerge in near future. Therefore, a range of evaluation and prediction tools are required to address the estuarine morphological evolution at different special and temporal scales (Blott et al., 2006). Due to cyclic and seasonal nature of short-term processes governed by time-varying phenomena including waves and tides, morphological changes in such time frame may average out in the long run, as the longer-time evolution is determined by much weaker residual effects, which are often disregarded in short -term models (Hanson et al., 2003). Process-based modelling approaches to long term coastal evolution can severely limited by theoretical and practical limitations (Karunarathna et al., 2008) as the large scale evolution

of the coastal systems are controlled by large-scale processes like erosion caused by sea level rise over centennial to millennium time scale (Hanson et al., 2003).

1.3 CLIMATE CHANGE AND SEA-LEVEL RISE

1.3.1 GLOBAL CLIMATE CHANGE AND SEA-LEVEL RISE

Coastal zones, throughout the world, can be considered as a man-dominated ecosystems with increasing vulnerability to catastrophic or extreme events and long termm processes due to natural causes like sea-level changes operating on different timescales and widespread human interventions including human settlements, land reclamations, construction of coastal defence structures and river flow regulations (Messerli et al., 2000). The phenomenon of the esustatic sea-level rise is an inevitable consequence of thermal expansion of water and melting of glaciers due to increasing temperatures, directly linked to the growing emission of greenhouse gases (Neves et al., 2013).Likewise the severity of the hazards and the vulnerability of the coastal low lands due to the flooding by the combined action of tides and storm surges may increase in the event of the climatically induced sea level rise and storminess (Fortunato, et al., 2014).

According to IPCC, 2013, the projected rate of global mean sea-level rise during the 21st century is expected to exceed the rate observed during 1971–2010 for all “Representative Concentration Pathway” (RCP) scenarios due to increases in ocean warming and loss of mass from glaciers and ice sheets. Projections of sea level rise are larger than that of in the IPCC (2007), primarily because of improved modelling of land-ice contributions. The lower (5%) and upper limits (95%) of projections of global mean sea-level rise in 2100 compared to 1986–2005 would be 0.28 to 0.61 m for RCP2.6, 0.36 to 0.71 m for RCP4.5, 0.38 to 0.73 m for RCP6.0, and 0.52 to 0.98 m for RCP8.5. The corresponding rates during 2081–2100 are

estimated to be 2 to 7 mm yr^{-1} for RCP2.6, 4 to 9 mm yr^{-1} for RCP4.5, 5 to 10 mm yr^{-1} for RCP6.0, and 8 to 16 mm yr^{-1} for RCP8.5, (IPCC, 2013). However, if the collapse of marine-based sectors of the West Antarctic ice sheet is initiated, the global mean sea-level would rise substantially above the likely range during the 21st century (Fretwell et al., 2013). Even though, this potential additional contribution was not precisely quantified but there is a moderate confidence that it would not exceed some decimetres of sea level rise during the 21st century. Hence there would be serious challenges to human occupancy of coastal regions worldwide imposed by the emerging natural system forcings that have been studied less comprehensively to date.

1.3.2 CLIMATE INDUCED SEA-LEVEL RISE IN THE CONTEXT OF PORTUGAL

Numerous studies have been carried out on the sea-level rise and its impacts along Portuguese coast during the last century and some of these studies are the based on analysis of tide gauge records (Dias and Taborda 1992; Santos et al., 2002; Antunes and Taborda, 2009; Sampath, et al., 2011; 2015; Mendes et al., 2013). According to Meyssignac and Cazenave (2012), the sea-level rise rate along the Portuguese coastline was 3.2 mm/yr in the last two decades, ensuring a direct relation with the global mean sea-level rise as suggested by Dias and Taborda, (1992). Lopes *et al.* (2011) has predicted that the mean sea level rise for this coast ranging between 0.28 m and 0.42 m, for the period 2091–2100 relative to 1980–1999. The sea-level rise in turn will affect the tidal range in estuarine systems as a feedback effect (Mendes et al., 2013). The sea level rise results in increase of amplitude and decrease of phase of the main tidal constituents and subsequently the intensification of the tidal asymmetry in the confined water bodies, which will increase the erosion as the velocity increase within the tidal basin (Picardo et al., 2012). This study further reveals an intensification of the tidal prism and a higher tendency for the salinization of the adjacent lands as per the projected sea level rise of

0.42 m by the end of 21st century. There would be increase of tidal prism resulting considerable increase of volume of salt water flowing through the mouth tidal basin during the tidal flood will for sea level rise scenarios considered by Lopes et al. (2011).

Estuarine margins which accommodate marsh syatems and tidal flats are at high risk in the case of Tagus estuary in Portugal for the scenarios considered by Rilo et al. (2013). According to a case study carried out in Lisbon, over a total area of 8550 ha, if sea-level rises 2.5 metres by 2100 as per the selected scenario, about 67 ha of local coastal areas may be affected by inundation (Neves et al., 2013). However, vulnerability of sea level rise cannot be isolated because the combined effect of both storm surges and high tides also have to be considered for assessing the cumulative impact of coastal hazard due to three factors. Model hindcasts and statistical analysis of the data (from 1979 to 2010) reveal the growth of extreme sea levels from south to north along the Portuguese coast, where the difference between the extreme sea level at the southernmost station (South of Tangier, Morocco) and the northernmost (East of Gijon, Spain) is about 0.6 m (Fortunato, et al., 2014).

The SIAM project (Climate Change in Portugal: Scenarios, Impacts, and Adaptation Measures), established in its final report in 2002 climate change and socioeconomic scenarios for the 21st century, which included an integrated and multisectorial assessment of the impacts of climate change on water resources and coastal zones (Santos, et al., 2002; Carvalho et al., 2014). Despite, policies framework oriented on mitigation introduced in Portugal at the end of the 1990s, greenhouse gas emissions continued to rise beyond its Kyoto target for 2012, and the country had to resort to the Kyoto Flexibility Mechanisms in order to comply (Carvalho et al., 2014). However, a study undertaken by Fereira et al., 2008, underscores lack of specific mitigation policies to face sea-level rise impacts in Portugal but suggested that the strict implementation of existing laws can be used to prevent and/or reduce socio-economic impacts of sea-level rise. In such a context, prediction of morphological evolution in estuarine systems

are utmost important to tackle some of the mitigating and adaptation issues in planning and implementation stages of policy framewors intended to holistic management of coastal resources.

1.4. AIMS AND OBJECTIVES

As explained in the section 1.1.3, the mankind faces serious challenges to mitigate and adopt to the impacts of global climate change including sea level rise in estuarine environments in the 21st century. Corresponding and line authorities have to take management policy decisions to minimise flood risk and threats to habitats due to projected sea-level rise scenarios as the impacts may be aggravated due to intensive human activities associated with these regions. In contrast to the 20th century approach of mitigating coastal erosion problems with intrusive engineering applications, which fails in many instances, soft engineering applications have to be implemented in this century. That requires a good understanding of the long term physical and biological processes that governs the estuarine system as a whole.

A robust model approaches come to play an increasing role in understanding the degree of response and sensitivity of estuarine systems to changes in dominant processes like tidal dynamics, sea-level rise, river discharge and fluvial sediment supply. However, sediment dynamics and especially longer-term changes in morphology are escaping the trustworthy predictions as most of the predictive models are case based without a proper accommodation of stochastic processes themselves (Huthnance et al., 2008).

Despite obvious differences in environmental conditions from the present day , understanding and hindcasting the Holocene estuarine evolution in response to eustatic sea-level rise seems appropriate as a basis for forecasting the morphological evolution in the 21st century. It is also important to understand the uncertainty and sensitivity of controlling parameters on morphological evolution during this century. There are some disadvantages in

process-based and behaviour-oriented model approaches as described in the section 1.2.3. In contrast, hybrid models, though in its infancy, can combine the dynamical rigour of process-based models alongside the observational experience encapsulated in rule-based geomorphological or behaviour-oriented models (Woodroffe, 2003). Prandle (2004) derived a set analytical solutions (a theoretical framework based on rule-based morphological expressions) by simplification of the one-dimensional equation of axial momentum propagation for shallow water and the continuity equation. They provide explicit formulations of the residual current velocities, time series of suspended sediment concentration as a function of elevation, tidal heights, river discharge, sediment grain-size, bed friction, erodibility of sediment, porosity and roughness of sediment. Consequently an attempt will be made to develop in this study a hybrid morphological evolution model based on the works of Prandle (2004; 2009) and other observational/interpretational studies carried out in the Guadiana estuarine system (e.g. Boski et al, 2002; 2008; Garel et al; 2009; 2014; Morales et al., 2006; Delgado et al., 2012).

To complement field investigations that have described geomorphological history and sea-level change over the last 13,000 years in the Guadiana Estuary of southwestern Iberia (Boski et. al., 2008, 2002; Delgado et al., 2012), in the present study we will first apply Estuarine Sedimentation Model to understand the skills and applicability of the behaviour-oriented approach for long-term simulations of the morphological evolution of the Guadiana estuary in response to the projected sea-level rise and sediment deficiency scenarios described in the Chapter 2.

Secondly, in the context of hybrid approach, a simple and idealized model was formalised by means of MATLAB tool using a set of theoretical framework based on rule-based morphological expressions derived by Prandle (2004; 2009):

(i) To simulate the sedimentary infilling of the Guadiana Estuary palaeovalley due to eustatic sea-level rise during the Holocene (Chapter 3);

(ii) To evaluate model outputs against previous geomorphological and post-glacial palaeoenvironmental reconstructions based on facies interpretation and ^{14}C dating (Chapter 3);

(iii) To simulate the morphological evolution of the Guadiana estuary and its intertidal zone for the worst case of sea level rise and sedimentation scenarios predicted for the 21st century (Chapter 4);

(iv) To assess potential morphological impacts and risk of habitat shift to enable formulation of long-term management policies for the entire estuarine system (Chapter 4);

(v) To assess the sensitivity of bed friction coefficient, strength of the residual current, and sea-level rise rate on determining the decadal scale morphological evolution in the Guadiana estuary (Chapter 5);

(vi) To understand daming impact along the Guadiana river on the estuarine morphology (Chapter 5);

(vii) To compare the denudation rate of the Guadiana river catchment using the 10 Be isotope method and the sediment budget method (Chapter 6); and

(viii) To assess the sensitivity of river discharge on morphological evolution, which gives insight into required minimum river discharge (environmental flow) to offset the impact of the Alqueva dam (Chapter 7).

The objectives from 1 to 4 and 7 were achieved by estimating the non-dimensional net accretion coefficients for a hypothetical transect from the maximum high tide to the maximum depth in the Guadiana estuary using the hybrid mathematical expressions of Prandle (2004; 2009). Then resulting coefficients were used to simulate the morphological evolution of the

Guadiana estuary using Estuarine Sedimentation Model (ESM), which follows a behaviour-oriented numerical modelling approach (Bruce et al., 2003). The model simulations for objectives 5, 6 and 8 were based on the further improved hybrid model, which directly used to simulate the morphological evolution of the Guadiana estuary to understand the sensitivity of the controlling parameters on elevation change in response to sea-level rise and sediment supply reductions. The objective 8 will serve for mitigating the impact of sea-level rise and drastic reduction of river discharge due to the construction of the Alqueva dam to certain extent.

1.5 REFERENCES

ANTUNES, C. and TABORDA, R., 2009. Sea level at Cascais tide gauge: data, analysis and results. Journal of Coastal Research, SI 56 (Proceedings of the 10th International Coastal Symposium), Lisbon, Portugal, 218 – 222.

Bell, R., Green M., Hume, T., Gorman, R., 2000. Estuaries what regulates sedimentation in estuaries? NIWA, Water and Atmosphere. 4, 1-4.

Biggs, R.B., 2012. Coastal bays.. In: Davis Jr., R.A. (Ed.), Coastal Sedimentary Environments. Springer-Verlag, New York, pp. 69-100. 716p

Blott, SJ., Pye, K., van der Wal D., Neal, A., 2006. Long-term morphological change and its causes in the Mersey Estuary, NW England Geomorphology 81, 185–206.

Boski, T., Moura, D., Veiga-Pires, C., Camacho, S., Duarte, D., Scott, D.B., Fernandes S.G., 2002. Postglacial sea-level rise and sedimentary response in the Guadiana Estuary, Portugal/Spain border. Sedimentary Geology. 150, 103–122.

Boski, T., Camacho, S., Moura, D., Fletcher, W., Wilamowski, A., Veiga-Pires, C., Correia, V., Loureiro, C., Santana, P., 2008. Chronology of post-glacial sea-level rise in two estuaries of the Algarve coast, S. Portugal. Estuarine, Coastal and Shelf Science. 77, 230–244.

Bowden, K. F., and L. A. Fairbairn (1952), A determination of the frictional forces in a tidal current, Proc. R. Soc. London, Ser. A, 214, 371– 392, doi:10.1098/rspa.1952.0175.

Bridge, JS., 2003. Rivers and Floodplains: Forms, Processes, and Sedimentary Record. John Wiley & Sons, Blackwell Science, Oxford. p491.

Bruce E, Cowell P, Stolper D. 2003. Development of a GIS-based estuarine sedimentation model. In Woodruffe, CD Furness FA. (eds.) Coastal GIS 2003 – Wollongong University, Australia, papers on Maritime Policy 14: 271-285.

Cameron WM., Pritchard DW, 1963, Estuaries, In: The Sea (Ed. MN Hill), Vol. 2, Wiley, New York, 306-324.

Carvalho, A., Schmidt, L., Santos, FD., Delicado, A., 2014. Climate change research and policy in Portugal. Wiley Interdisciplinary Reviews: Climate Change 5(2), 161-290.

Chaumillon, E., Tessier, B., Reynaud, J.-Y., 2011. Variability of incised valleys and estuaries along French Coasts: an analog to oil reservoirs where topography influence preservation potential? Recovery—CSPG CSEG CWLS Convention.

Cheng, P., 2007. Modeling Sediment Transport in Estuarine Environment: Effects of Tidal Asymmetry, Lateral Circulation and Sediment-induced Stratification. PhD thesis.

Cowell PJ. and Thom BG., 1997. Morphodynamics of coastal evolution. In: R.W.G. Carter and C.D. Woodroffe, Coastal evolution, Late Quaternary shoreline morphodynamics, Cambrich University Press, 33-86.

DALRYMPLE, R.W., ZAITLIN, B.A., AND BOYD, R., 1992, Estuarine facies models: Conceptual basis and stratigraphic implications: Journal of Sedimentary Petrology, v. 62, p. 1130–1146.

Dastgheib, A., 2012. LONG-TERM PROCESS-BASED MORPHOLOGICAL MODELING OF LARGE TIDAL BASINS, PhD Thesis. CRC Press/Balkema, Taylor & Francis.

Davidson NC, Laffoley Dd, Doody JP, Way LS, Gordon J, Key R, Drake CM, Pienkowski MW, Mitchell R, Duff KL, 1991, Nature conservation and estuaries in Great Britain, Nature Conservancy Council, Peterborough, UK.

Delgado, J., Boski, T., Nieto, J.M., Pereira, L., Moura, D., Gomes, A., Sousa, C., García-Tenorio, R., 2012. Sea-level rise and anthropogenic activities recorded in the late Pleistocene/Holocene sedimentary infill of the Guadiana Estuary (SW Iberia). Quaternary Science Reviews. 33, 121–141. DOI: 10.1016/j.quascirev.2011.12.002.

De Vriend, H., Ribberink, J.S., 1996. Mathematical modelling of meso-tidal barrier island coasts, Part II: process based simulation models. In: Liu, P.L.F. (Ed.), Advances in Coastal and Ocean Engineering, vol. 2, pp. 151-197.

De Vriend, H.J., 1996. Mathematical modelling of meso-tidal barrier island coasts: Part I. Empirical and semi-empiricalmodels. In: Liu, P.L.-F., (Ed.), Advances in Coastal and Ocean Engineering, vol. 2, pp. 115– 149.

De Vriend, HJ., 2003. Advances in morphordynamics of tidal rivers and estuaries. International Conference on Estuaries and Coasts November 9-11, 2003, Hangzhou, China

DIAS, J.A. and TABORDA, R., 1992. Tidal gauge in deducing secular trends of relative sea level and crustal movements in Portugal, Journal of Coastal Research, 8(3), 655-659.

Dissanayake, D.M.P.K., Ranasinghe. R., and Roelvink, J.A., 2009. Effect of sea level rise in inlet evolution: a numerical modelling approach, Journal of Coastal Research, SI 56, Proc. of the 10th International Coastal Symposium, Lisbon, Portugal, pp. 942- 946.

Dissanayake, D.M.P.K., Ranasinghe. R., and Roelvink, J.A., Wang, ZB., 2011. Process-based and semi-empirical modelling approaches on tidal inlet Evolution, Journal of Coastal Research ICS2011 (Proceedings of the 11th International Coastal Symposium, Seczzecn Poland SI 64, 1013 – 1017.

Dronkers, J. 1986 Tidal asymmetry and estuarine morphology. Neth. J. Sea Res. 20, 117–131. (doi:10.1016/0077-7579(86)90036-0)

Dronkers, J., 1998. Morphodynamics of the Dutch Delta. In: Dronkers, J., Scheffer, M. (Eds.), Physics of Estuaries and Coastal Seas. Balkema, Rotterdam, pp. 297e304.

Dyer, K. R. 1996 The definition of the Severn estuary. *Proceedings of the Bristol Naturalists' Society* **56,** 53–66.

Fagherazzi S, Howard AD, Wiberg PL. 2004. Modeling fluvial erosion and deposition on continental shelves during sea level cycles. *J. Geophys. Res. Earth Surf.* 109(F3):F03010

Ferreira, O´., Dias,J.A.,Taborda,R., 2008.Implicationsofsea-levelrisefor continental Portugal.JournalofCoastalResearch24(2),317–324.

FISCHER, H. B., E.J. LIST, H. C. Y. KoH,J. IMBERGER, AND N. A. BROOKS. 1979. Mixing in inland and coastal waters. Acaclemic'Press, Inc., New York. 483p.

Fortunato, AB., Li, K., Bertin, X., Rodrigues M.,, 2014. Determination of Extreme Sea Levels along the Portuguese Coast. 3rd Jornadas de Engenharia Hidrográfica Lisboa, 24 -26 de Junho de 2014, 151-154.

Friedrichs, C.T., Madsen, O.S., 1992. Nonlinear diffusion of the tidal signal in frictionally dominated embayment. Journal of Geophysical Research 97, 5637–5650.

Friedrichs, C.T., Aubrey, D.G., 1996. Uniform bottom shear stress and inter tidal hypsometry of intertidal flats. In: Pattiarachchi, C. (Ed.), Mixing Processes in Estuaries and Coastal Seas, Coastal and Estuarine Studies Series. American Geophysical Union, Washington, pp. 405-429.

Fretwell, P., et al., 2013: Bedmap2: Improved ice bed, surface and thickness datasets for Antarctica. Cryosphere, **7**, 375–393.

George, DA., Gelfenbaum, G., Stevens, AW., 2012. Modeling the Hydrodynamic and Morphologic Response of an Estuary Restoration. Estuaries and Coasts, 35, 1510–1529.

Garel, E., Sousa, C., Ferreira, Ó. Morales, J.A., 2014. Decadal morphological response of an ebb-tidal delta and down-drift beach to artificial breaching and inlet stabilisation. Geomorphology. 216, 13–25.

Garel, E., Pinto, L., Santos, A., Ferreira, ó., 2009. Tidal and river discharge forcing upon water and sediment circulation at a rock-bound estuary (Guadiana Estuary, Portugal). Estuarine, Coastal and Shelf Science. 84, 269–281. DOI 10.1016/j.ecss.2009.07.002.

Geyer, W.R., and P. MacCready. 2014. The estuarine circulation. Annual Review of Fluid Mechanics 46: 175–197

Geyer, W. R., J. H. Trowbridge, and M. M. Bowen, 2000: The dynamics of a partially mixed estuary. *J. Phys. Oceanogr.*, **30,** 2035–2048.

Grace, S. (1936), Friction in the tidal currents of the Bristol Channel, Mon. Not. R. Astron. Soc., 3, 388–395.

Hanson, H., Aarninkhof, S., Capobianco, M., Jime´nez, J.A., Larson, M., Nicholls, R.J., Plant, N.G., Southgate, H.N., Steetzel, H.J., Stive, M.J.F., De Vriend, H.J., 2003. Modelling of coastal evolution on yearly to decadal time scales. Journal of Coastal Research 19 (4), 790–811.

Hibma, A., Stive, M.J.F., Wang, Z.B., 2004. Estuarine morphodynamics. Coastal Engineering 51, 765– 778.

Hume TM, Herdendorf CE, 1988, A geomorphic classification of estuaries and its application to coastal resource management, Journal of Ocean and Shoreline Management, 11, 249-274.

Hume, T.M., Snelder, T., Weatherhead, M., Liefting, R., 2007. A controlling factor approach to estuary classification. Ocean and Coastal Management 50, 905-929.

Huthnance, J.M., Karunarathna, H., Lane, A., Manning, A.J., Norton, P., Reeve, D.E., Spearman, J., Soulsby, R.L., Townend, I.H., Wolf, J., Wright, A., 2008. Development of estuary morphological Models. R&D Technical Report FD2107/TR, Joint Defra/EA Flood and Coastal Erosion Risk Management R&D Programme p67.

IPCC 2007. Climate Change 2007: The Physical Science Basis. Contribution of Working Group I to the Fourth Assessment Report of the Intergovernmental Panel on Climate Change, In: Solomon, S., Qin, D., Manning, M., Chen, Z., Marquis, M., Averyt, K.B., Tignor, M., Miller, H.L. (Eds.), Cambridge University Press, Cambridge, United Kingdom and New York, NY, USA.

IPCC, 2013. Climate Change 2013: The Physical Science Basis. Contribution of Working Group I to the Fifth Assessment Report of the Intergovernmental Panel on Climate Change [Stocker, T.F., D. Qin, G.-K. Plattner, M. Tignor, S.K. Allen, J. Boschung, A. Nauels, Y. Xia, V. Bex and P.M. Midgley (eds.)]. Cambridge University Press, Cambridge, United Kingdom and New York, NY, USA, 1535 pp.

Kang, W., Jun, K.S., 2003. Flood and ebb dominance in estuaries in Korea. Estuarine, Coastal and Shelf Science, Ocean Dynamics 56 (C4), 178–198.

Karunarathna H, Reeve D, Spivack M. 2008. Long-term morphodynamic evolution of estuaries: An inverse problem, *Estuarine, Coastal and Shelf Science* 77: 385-395

KOLAHDOOZAN M. and FALCONER R. A. 2003. Three-dimensional geomorphological modelling of estuarine waters. International Journal of Sediment Research, IRTCES, 18 (1), 1–16.

Kraus N.C., Larson M., Kriebel D.L, 1991. Evaluation of beach erosion and accretion predictors. Proc. Co. Sediments'91, ASCE, Seattle, pp.527-587.

Kragtwijk NG, Zitman TJ, Stive MJF, Wang ZB (2004) Morphological response of tidal basins to human interventions. Coast Eng 51:207–221

Leeder, MR., 2009. Sedimentology and Sedimentary Basins: From Turbulence to Tectonics. John Wiley & Sons, Apr 1, 2009 – 608p

LESSER, G.R.; ROELVINK, J.A.; VAN KESTER, J.A.T.M., and STELLING, G.S., 2004. Development and validation of a threedimensional morphological model, *Journal of Coastal Engineering*, 51, 883-915.

Lopes, C.L., Silva, P.A., Dias, J.M., Rocha, A., Picado, A., Plecha, S. and Fortunato, A.B., 2011. Local sea level change scenarios for the end of the 21st century and potential physical impacts in the lower Ria de Aveiro (Portugal). Continental Shelf Research, 31, 1515-1526.

Luo, J., Li, M., Sun, Z., O'Connor, BA., 2013. Numerical modelling of hydrodynamics and sand transport in the tide-dominated coastal-to-estuarine region. Marine Geology 342, 14–27.

MacCready, P. 2004. Toward a unified theory of tidally averaged estuarine salinity structure, Estuaries, 27(4), 561–570, doi:10.1007/BF02907644.

Mendes, R., Vaz, N., Dias, J.M., 2013. Potential impacts of the mean sea level rise on the hydrodynamics of the Douro river estuary In: Conley, D.C., Masselink, G., Russell, P.E. and O'Hare, T.J. (eds.), Proceedings 12th International Coastal Symposium (Plymouth, England), Journal of Coastal Research, Special Issue No. 65, pp. 1951-1956,

Messerli, B., Grosjean, M., Hofer, T., Núñez, L., Pfister, C., 2000. From nature-dominated to human-dominated environmental changes, Quaternary Science Reviews. 19, 459-479.

Meyssignac, B., Cazenave, A., 2012. Sea level: A review of present-day and recent-past changes and variability. Journal of Geodynamics 58, 96–109,

Milliman, J.D., Meade, R.H., 1983. World-wide delivery of river sediment to the oceans. Journal of Geology 91, 1e21.

Milliman, J.D., Syvitski, J.P.M., 1992. Geomorphic/tectonic control of sediment discharge to the ocean: the importance of small mountainous rivers. Journal of Geology 100, 525-544.

Morales, J.A., Delgado, I., Gutierrez-Mas, J.M., 2006. Sedimentary characterization of bed types along the Guadiana Estuary (SW Europe) before the construction of the Alqueva dam. Estuarine, Coastal and Shelf Science. 70, 117–131.

Neal, A., 1993. Sedimentology and Morphodynamics of a Holocene Coastal Dune Barrier Complex, Northwest England. Ph.D. Thesis, Reading University.

Neves, B., Rebelo, C., Rodrigues, A.M., 2013. Modelling Sea-Level rise in the Lisbon city coastal area, using Free and Open Source Technologies. VII Jornadas de SIG Libre, 3-6 March 2013, Girona, Catalonia, Spain. 1-11.

Nichols, M.M. and Biggs, R.B., 1985. Estuaries. In: R.A. Davis Jr. (Editor), Coastal Sedimentary Environments. Springer, New York, pp.77-187.

NORTON, P., MANNING, AJ., TOWNEND, I., LANE, A., KARUNARATHNA, H., 2007. APPLICATION AND INTER-COMPARISON OF ESTUARY MORPHOLOGICAL MODELS. 42nd Defra Flood and Coastal Management Conference, University of York from 3rd to 5th July 2007

O'Brien, M. P. 1931 Estuary tidal prism related to entrance areas. Civil Eng. 1, 738–739.

Picado, A., Mendes, R., Vaz, N., Dias, J.M., 2012. Impact of sea level rise in coastal systems – Ria de Aveiro case study. Geophysical Research Abstracts, Vol. 14, EGU2012-4864, 2012.

Prandle, D., 2004. How tides and river flows determine estuarine bathymetries Progress in Oceanography 61, 1–26

Prandle, D., 2006. Dynamical controls on estuarine bathymetry: Assessment against UK database. Estuarine, Coastal and Shelf Science 68, 282-288.

Prandle, D., 2009. Estuaries: Dynamics, Mixing, Sedimentation and Morphology. Cambridge University Press, New York, pp. 236.

Prandle, D., Lane, A. and Manning, A.J., 2005. Estuaries are not so unique. *Geophysical Research Letters*, Vol. 32, doi:10.1029/2005GL024797.

Prandle, D., Lane, A. and Manning, A.J., 2006. New typologies for estuarine morphology. *Geomorphology*, 81, 309-315

Pritchard, DW., 1967. What is an estuary? Physical viewpoint, *in* Lauff, G.H., ed., Estuaries: American Association for the Advancement of Science, Publication 83, p. 3-5.

Potter IC, Chuwen BM, Hoeksema SD, Elliott M (2010) The concept of an estuary: A definition that incorporates systems which can become closed to the ocean and hypersaline. Estuar Coast Shelf Sci 87: 497-500.

Rainford, W.M., 1997. The Sustainability of Sand Winning near Horse Bank in the Ribble Estuary. Report William Rainford (Holdings) Ltd and Shoreline Management Partnership, Liverpool.

Rilo, A., Freire, P., Guerreiro, M., Fortunato, A.B., Taborda, R. 2013. Estuarine margins vulnerability to floods for different sea level rise and human occupation scenarios. *In:* Conley, D.C., Masselink, G., Russell, P.E. and O'Hare, T.J. (eds.), *Proceedings 12th International Coastal Symposium* (Plymouth, England), *Journal of Coastal Research*, Special Issue No. 65, pp. 820-825.

ROELVINK, J.A., 2006. Coastal morphodynamic evolution techniques, *Journal of Coastal Engineering*, 53, 277- 287.

Roy, P.S., 1984. New South Wales estuaries: their origin and evolution. In: Thom, B.G. (Ed.), Coastal Geomorphology in Australia. Academic Press, New York, pp. 99e121.

Roy, P.S.; Cowell, P.J.; Ferland, M.A. and Thom, B.G., 1994. Wave dominated coasts. In: Carter, R.W.G. and Woodroffe, C.D. (eds), Coastal Evolution: Late Quaternary shoreline morphodynamics, Cambridge University Press, Cambridge, 121–86.

Roy, P.S., 1994. Holocene estuary evolution e stratigraphic studies from southeastern Australia. In: Dalrymple, R.W., Boyd, R., Zaitlin, B.A. (Eds.), Incised-Valley Systems: Origin and Sedimentary Sequences. Society for Sedimentary Petrology, pp. 241-264. Special Publication 51.

Roy, P.S., Williams, R.J., Jones, A.R., Yassini, I., Gibbs, P.J., Coates, B., West, R.J., Scanes, P.R., Hudson, J.P., Nichol, S.L., 2001. Structure and function of south-east Australian estuaries. Estuarine, Coastal and Shelf Science 53, 351-384.

Rossington, K. and Spearman, J., 2009. Past and future evolution in the Thames Estuary. Ocean Dynamics (2009) 59:709–718 DOI 10.1007/s10236-009-0207-4

Sampath, D.M.R., Boski , T., Silva P.L., Martins F.A., 2011. Morphological evolution of the lower Guadiana estuary and its intertidal zone in response to the projected sea level rise and sediment supply reduction scenarios. J*ournal of Quaternary Science* 26(2) 156–170. DOI: 10.1002/jqs.1434

Sampath, D.M.R., Loureiro, C., Boski, T., Martins, F., Sousa, C., 2015. Modelling of estuarine response to sea-level rise during the Holocene: Application to the Guadiana Estuary - SW Iberia. Geomorphology. 232, 47-64**.**

Santos FD, Forbes K, Moita R., 2002 Climate Change in Portugal. Scenarios, Impacts and Adaptation Measures—SIAM Project. Lisbon: Gradiva. p454.

Spearman, J.R., Dearnaley, M.P., Dennis, J.M., 1995. A simulation of estuary response to training wall construction using a regime approach. Coastal Engineering 33 (2e3), 71e90.

Speer, P.E., Aubrey, D.G., 1985. A study of non-linear tidal propagation in shallow inlet estuarine system, Part II: a theory. Estuarine, Coastal and Shelf Science 21,

Stive MJF, Wang ZB, Capobianco M, Ruol P, Buijsman MC (1998) Morphodynamics of a tidal lagoon and the adjacent coast. In:Dronkers (ed) Physics of estuaries and coastal seas. Balkema, Rotterdam, pp 397–407

Stolper, D. (1996). The Impact of sea-level rise on estuarine mangroves: Development and Application of a Simulation Model. Honours Thesis, University of Sydney, Sydney; 1-90.

Stolper D. 2002. Modelling the Evolution of Estuaries and Their Intertidal Zones. Ph.D. Thesis, University of Sydney, Sydney; 1-189.

Talke, S. A., H. E. de Swart, and H. M. Schuttelaars (2009), Feedback between residual circulations and sediment distribution in highly turbid estuaries: An analytical model, Cont. Shelf Res., 29(1), 119–135, doi:10.1016/j.csr.2007.09.002.

Thomas, C., Spearman, J., Turnbull, M., 2002. Historical morphological change in the Mersey Estuary. Continental Shelf Research 22 (11–13), 1775–1794.

Townend, I. H. 2005 An examination of empirical stability relationships for UK estuaries. J. Coast. Res. 21, 1042–1053. (doi:10.2112/03-0066R.1)

TOWNEND, I.H., WANG Z. B., REES, J. G., 2007. Millennial to annual volume changes in the Humber Estuary. Proc. R. Soc. A (2007) 463, 837–854 doi:10.1098/rspa.2006.1798

Valle-Levinson, A. (Ed.), 2010. Definition and classification of estuaries. In: Contemporary Issues in Estuarine Physics. Cambridge University Press, Cambridge, pp. 1–11.

Van De Kreeke, J., 1996. Morphological changes on a decadal time scale in tidal inlets: modelling approaches. Journal of Coastal Research SI 23, 73e82.

Van Goor MA, Zitman TJ, Wang ZB, Stive MJF (2003) Impact of sealevel rise on the morphological equilibrium state of tidal inlets. Mar Geol 202:211–227

Van Maren, D.S., 2005. Barrier formation on an actively prograding delta system: The Red River Delta, Vietnam. Marine Geology. 224, 123– 143.

Van Rijn, LC., 2011. Analytical and numerical analysis of tides and salinities in estuaries; part I: tidal wave propagation in convergent estuaries. Ocean Dynamics (2011) 61:1719–1741. DOI 10.1007/s10236-011-0453-0

Van der Spek, A.J.F., 1997. Tidal asymmetry and long-term evolution of Holocene tidal basins in The Netherlands: simulation of palaeo-tides in the Schelde estuary. Marine Geology 141, 71-90.

Van der Wal, D., Pye, K., Neal, A., 2002. Long-term morphological change in the Ribble Estuary, northwest England Marine Geology 189, 249-266

Wang, Z.B., Karssen, B., Fokkink, R.J., Langerak, A., 1998. A dynamical/empirical model for long-term morphological development of estuaries. In: Dronkers, J., Scheffers, M.B.A.M. (Eds.), Physics of Estuaries and Coastal Seas.

Wang, Z.B., Jeuken, M.C.J.L., Gerritsen, H., de Vriend, H.J., Kornman, B.A., 2002. Morphology and asymmetry of the vertical tide in the Westerschelde estuary. Continental Shelf Research 22, 2599–2609.

Wells, J.T., 1995. Tide-dominated estuaries and tidal rivers. In: Perillo, G.M.E. (Ed.), Geomorphology and Sedimentology of Estuaries, Developments in Sedimentology, Vol. 53. Amsterdam, Elsevier, pp. 179–206.

Winant, CD., De VELASCO, GG., 2003. Tidal Dynamics and Residual Circulation in a Well-Mixed Inverse Estuary. Journal of Physical Ocenaography. 33, 1365-1379.

Wolanski, E., Moore, K., Spagnol, S., D'Adamo, N., Pattiaratchi, C., 2001. Rapid, human-induced siltation of the macro-tidal Ord River estuary, western Australia. Estuarine, Coastal and Shelf Science 53, 717e732.

Wolanski, E., Spagnol, S., Williams, D., 2004. The impact of damming the Ord River on the fine sediment budget in Cambridge Gulf, northwestern Australia. Journal of Coastal Research 20, 801-807.

Wolanski, E., 2006.The evolution time scale of macro-tidal estuaries: Examples from the Pacific Rim. Estuarine, Coastal and Shelf Science 66, 544-549.

Woodroffe, C.D., 2003. Coasts: Form, Process and Evolution. Cambridge University Press, 623 pp.

Wright, L.D., Coleman, J.M., 1973. Variations in morphology of major river deltas as a function of ocean waves and river discharge regimes. American Association of Petroleum Geology Bulletin 57, 177-205.

Chapter 2

Morphological evolution of the Guadiana estuary and intertidal zone in response to projected sea level rise and sediment supply scenarios

Sampath, D.M.R., Boski , T., Silva P.L., Martins F.A., 2011. Morphological evolution of the lower Guadiana estuary and its intertidal zone in response to the projected sea level rise and sediment supply reduction scenarios. J*ournal of Quaternary Science* 26(2) 156–170. DOI: 10.1002/jqs.1434

ABSTRACT

Analysis of Holocene sediment accumulation in the Guadiana estuary (southern Portugal) during sea level rise since ca 13 000 cal yr BP was used to simulate the long-term morphological evolution of the lower Guadiana estuary and the associated intertidal zone for 21st Century predicted sea level rises. Three sea level rise scenarios given by the IPCC (2007) were used in the simulations of morphology using a large-scale behaviour-oriented modelling approach. Sedimentation rate scenarios were derived both from the Holocene evolution of the estuary and from a semi-empirical estimation of present day sediment aggradation. Our results show that the net lateral expansion of the intertidal zone area would be about 3% to 5% of the present intertidal zone area for each 10 cm rise in sea level. Under constraints imposed by the lack of fluvial sediment supply, the lateral expansion of the landward boundary of the intertidal zone will occur mainly in the Portuguese margin of the Guadiana estuary while submergence of the salt marshes will occur in the Spanish margin. Therefore, the Spanish margin is highly vulnerable to both sea level rise and lack of sediment supply.

Key words

Morphological evolution, sea level rise, behaviour-oriented modelling, estuarine systems, human pressures

2.1 INTRODUCTION

Over the last several decades, the demands on estuaries by humans have increased rapidly, resulting in the overall deterioration of these systems. The morphology of estuaries is naturally determined by progressive infilling dependent on the accommodation space and on the supply of suspended sediment, sourced from either catchments or marine sources. As the infilling continues, the tidal asymmetry diminishes, which in turn results in a deceleration of the estuary infilling. Eventually, the estuary will reach a state of dynamic equilibrium where further sediment deposition is balanced by equivalent erosion released from the estuary (Dronkers, 1986).

Any change in tidal regime, sea level, river discharge, or sediment supply will lead to a perturbation of the dynamic equilibrium and subsequently a new equilibrium state will be achieved (Pethick, 1994). The response to a given perturbation will depend on the characteristics of individual units of the estuarine system and will tend to involve a lag period before the system moves into a new dynamic equilibrium (Jeuken, *et al.,* 2003). The pathway of attaining a new equilibrium in estuarine systems impacted either by natural perturbations or by human interventions will be governed by the hydrodynamic, morphodynamic, and

biological processes operating in them. Consequently, changes in the architecture of the system can affect the system partly or as a whole. For instance, if the aggradation of sediment does not keep pace with the increasing accommodation space in response to sea level rise, salt marshes would be drowned and would disappear from the system. The equilibrium of these processes and their interactions under human or naturally imposed constraints will determine whether a particular estuarine system exhibits resilient behaviour or whether it will be drowned with a rise in sea level (French, 2006; Kirwan and Murray, 2008).

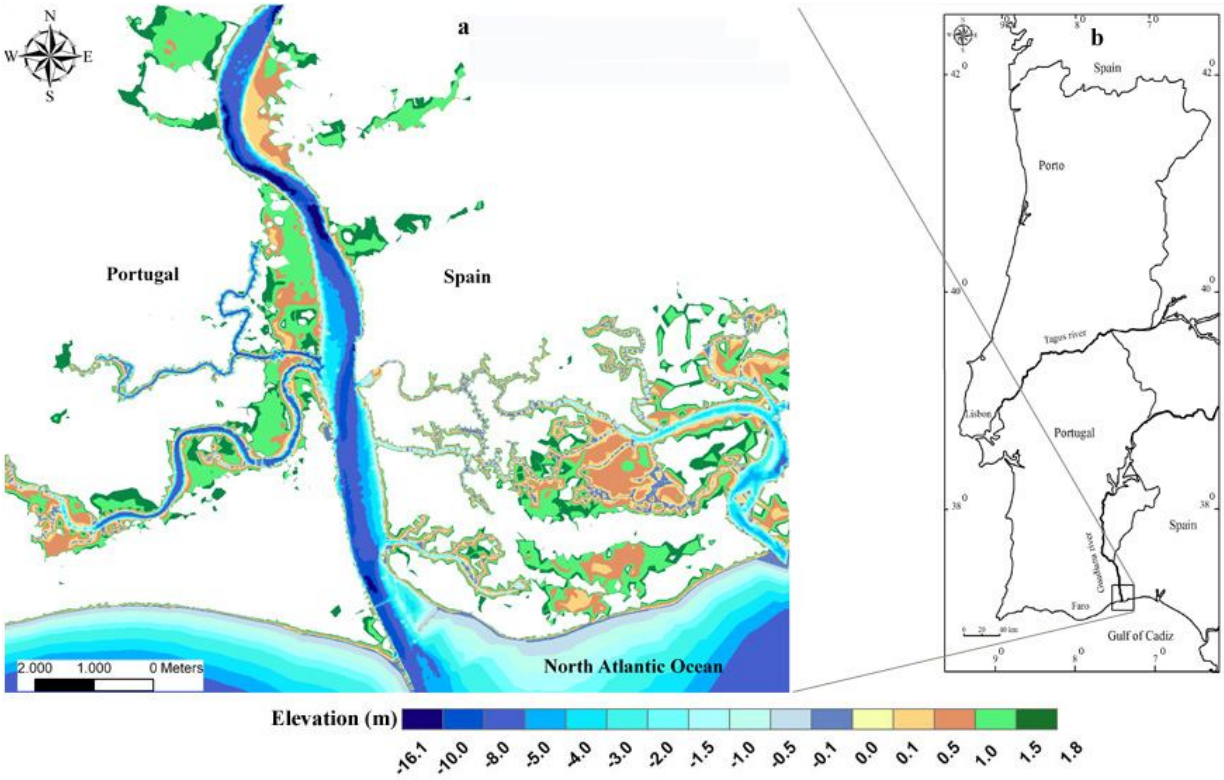

Figure 2.1 Study area and digital elevation model of the Guadiana estuary derived using bathymetric maps for year 2000.

The Guadiana estuary (Fig. 2.1) is a good example of an estuarine system with a long history of impacts caused by human activities. At present, the estuary is subject to a drastic reduction of river flow and sediment discharge due to the construction of more than 40 dams

along the Guadiana River. The usual peak flood events observed in winter have disappeared since the construction of the Alqueva dam, which created the largest artificial lake ($4150*10^6$ m^3) in Europe (Machado et al., 2007). Due to the consequent shortage of silt supplied by the river, there has been a rapid decrease in the area of salt marshes. In addition, the construction of jetties at the mouth of the Guadiana River has almost completely cut off the longshore sediment transportation from west to east. This has resulted in a reduction of marine sediment supplied to the estuary over the last 35 years (Gonzalez et al., 2004). The effects of this construction are clearly manifest on the Spanish side of the estuary, where rapid erosion at an average rate of 3 m/yr has occurred (Gonzalez, et al., 2001a), with a maximum 4.8 m/yr from 1996 to 2005 (Sampath, 2008).

A better understanding of the sensitivity of the Guadiana estuarine system to forcing from sea level rise or from human interference is required if the sustainable management of the estuary is to be achieved. Therefore, the main objectives of this study are two-fold: i) to simulate the morphological evolution of the Guadiana estuary and its intertidal zone for different sea level rise and sedimentation scenarios predicted for the 21st Century; and ii) to assess potential morphological impacts to enable formulation of long-term management policies for the entire estuarine system. In this paper, we explain the morphological evolution of the Guadiana estuary using an idealized behaviour-oriented numerical approach. Simulation was performed for three IPCC (2007) sea level rise scenarios. Under each sea level rise scenario, four simulations were carried out for four locally derived sedimentation rates. The study can be considered as a simple conceptual model for estimating the impacts of sea level rise under sediment supply reductions into an estuarine system due to human interventions in the catchment.

2.2. STUDY AREA

2.2.1 HYDRODYNAMIC SETTING OF THE GUADIANA ESTUARY

The Guadiana estuary is a narrow, deeply incised bedrock controlled estuary experiencing the final stages of sediment infilling along with initial coastal progradation (Boski et al., 2008). The estuary, which is located at the southern border between Spain and Portugal, is 60 km long; it has a maximum width of 550 m; and the maximum depth varies between 5 and 17 m (Wolanski et al., 2006). However, our main focus is the lower Guadiana estuary (11.6 km).

The Guadiana River drainage basin is the fourth largest on the Iberian Peninsula, with a length of 810 km and an area of 66,960 km^2 (Garel et al., 2009); it traverses extensive rural areas from Spain to Portugal and includes the Iberian Pyritic Belt (Morales, 1995). The regional climate is classified as semi-arid, but July and August are arid months while November to January can be considered as temperate-humid (Morales, 1995). Before the first impoundment of the dam, low flows in summer and episodic flooding events in winter characterized the hydrographic regime of the Guadiana River. However, the peak flood events recorded in winter have now virtually disappeared (Machado et al., 2007) and discharge has approached a quasi-steady state (Wolanski et al., 2006).

The estuary exhibits a semidiurnal, meso-tidal regime with a mean range of approximately 2.5 m. The mean neap tidal range is 1.22 m and the mean spring tidal range is 2.82 m (Morales, 1997), with the maximum spring tidal range being 3.88 m (Gonzalez, et al., 2001b). Tidal wave propagation in the estuary generates currents with velocities exceeding 0.5 m/s (Morales, 1997). Tidal currents at the river mouth are about 0.6 m/s during the peak flood tide and 1.2 m/s during the peak ebb tide (Instituto Hidrogrphico, 1998). Flood and ebb currents in the estuary can reach 0.8 and 0.9 m/s, respectively, during a mean spring tide (Morales, et

al., 2006). Ebb currents last for 6 hours 50 minutes while flood currents prevail for 5 hours 35 minutes at the mouth (Morales, 1997).

The waves in this coastal region can be classified as medium to low energy waves, and in terms of frequency of occurrence, 49% of the waves represent Atlantic swells and 51%, local sea waves.The mean annual offshore significant wave height is about 0.92 m with an average period of 4.6 s (Costa, 1994). Dominant offshore waves are mainly from the southwest (frequency 50%) while southeast waves represent 25% of occurrences (Costa, 1994).

2.2.2 PAST AND PRESENT SEA LEVEL RISE TRENDS

Understanding of past and present trends in sea-level rise is particularly important for simulating morphological evolution using a behavior-oriented modeling approach. The average rate of sea level rise as deduced from borehole data from the Guadiana estuary is about 7 mm/yr for the period 13000 to 7000 cal BP. Since then, the rate has been about 1.3 mm/yr (Boski et al., 2002; 2008). However, there is no existing analysis of the recent trends in sea-level rise for the coastline adjacent to the Guadiana estuary in terms of either tide-gauge data or satellite altimetry data. It is not possible to estimate it using tide gauge data because there is no continuous data set for the Guadiana estuarine area.

On the other hand, recent analysis of satellite altimetry data has shown that there has been a significant increase in the global mean rate of sea-level rise (Bindoff et al., 2007). Therefore, the recent rate of sea-level rise along the coastline of the Guadiana estuary was approximated from coarsely graduated colour maps of Fenoglio-Marc and Groten (2004) and Milne et al. (2009).The values for the south Portugal coastline are 2-4 and 2-3 mm/yr, respectively, where the former was deduced from multi-satellite data for European seas for the period 1995 to 2001 and without applying the inverse-barometer correction, while the latter

value was deduced from the global satellite altimetry data set with the inverse-barometric correction.

2.3. METHODOLOGY

2.3.1 ESTUARINE SEDIMENTATION MODEL

We adopted the estuarine sedimentation model (ESM), which involves a behaviour-oriented approach, to predict the long-term morphological evolution of the Guadiana estuary and the associated intertidal zone in response to the rise in sea level and reduction in sediment supply. This model was initially developed by Stolper (1996; 2002) and takes into account 3 factors: (1) changes in the rate of sea-level rise; (2) elevation-dependent accommodation space available for the deposition of sediment; and (3) inundation-dependent vertical accretion rate of sediment (Bruce et al., 2003). Behaviour-oriented numerical models are relatively more effective than process-based models in simulating long-term evolution of estuaries because the former are based on empirical rules or expert analysis (Karunarathne et al., 2008). As the model does not explicitly take into account the estuarine physical processes, including tidal hydrodynamics, channel-shoal sediment exchange, and gravitational circulation, it is not possible to represent dynamic interactions and feedback that leads to morphological change. The main difficulty is the lack of understanding of such processes in centennial time scale and the stochastic nature of these processes. This would have been considered as a drawback of the present approach. However, we overcame this limitation to some extent by representing the net deposition behavior due to estuarine processes using net long-term sedimentation rate scenarios derived from borehole data analysis.

Moreover, the Guadiana estuary lies within a sheltered environment because of the 2 jetties and the Óbril sandbank located close to the river mouth. Therefore, the height of the wind waves is significantly attenuated within the estuary. The sediment grain size across the

lower estuary bed is almost uniform, except in the intertidal zone (Morales et al., 2006). The grain size distribution in an estuary is possibly related to the energy levels of the estuary (Hamilton, 1979); therefore, the distribution of the energy levels across the lower Guadiana estuary should be uniform. The near uniform distribution of sediment accretion rates observed across the Guadiana estuary (Boski et al., 2002; 2008) may be due to the above reason. In the Guadiana estuary, deep subsidence is negligible (Lobo et al., 2003). Long-term accumulation of organic matter is insignificant due to anaerobic respiration within the organic sediment (Boski et al., 2008). Therefore, in the centennial time scale we assume that shallow compaction is also negligible. Therefore, from a coastal zone management perspective, in order to understand the order of magnitude of potential morphological impacts, it is justifiable to use a simple idealized model for predicting the long-term morphological changes in estuarine systems due to natural and anthropogenic forcing.

In this extremely simplified model, we represent the net sediment deposition rate (dS/dt) at a given location below the high-tide level of the estuary as a function of the maximum net deposition rate (S^{max}) observed in the estuary and the tidal inundation frequency (Eq. 2.1). This assumption has been used in a number of previous aggradation models (e.g. Allen, 1995; Morris et al., 2002; Kirwan and Murray, 2008). Even though the mass balance approach is zero-dimensional, we represent the spatial distribution of the net aggradation by defining the net sedimentation rate as function of the tidal inundation frequency, which is a function of depth below the maximum spring high tide (Eq. 2.2). It is assumed that the tidal inundation frequency increases with the sea-level rise by ΔH (Eq. 2.3):

$$\frac{dS}{dt} = S^{max} \times \text{Tidal inundation frequency} \quad (2.1)$$

$$\text{Tidal inundation frequency} = f(h) \quad (2.2)$$

$$\text{Tidal inundation frequency} = f(h - \Delta H) \quad (2.3)$$

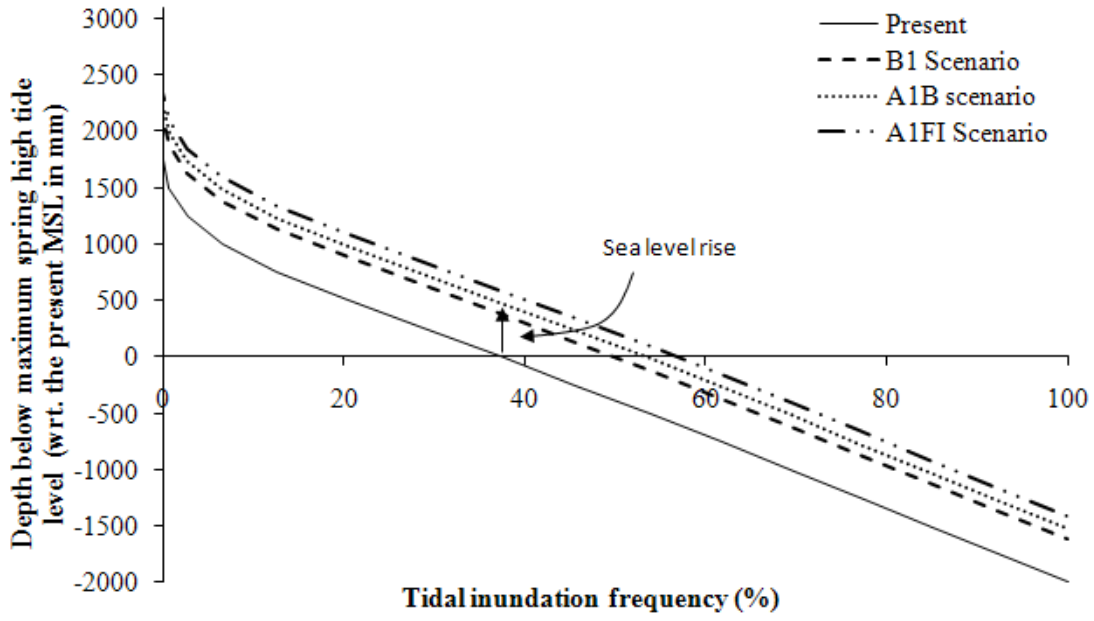

Figure 2.2 Relationship between the tidal inundation frequency and the depth below maximum spring high tide level for the present mean sea level and the IPCC (2007) sea level rise scenarios B1, A1B, and A1FI.

The relationship between the tidal inundation frequency and depth below maximum spring high tide (relative to mean sea level) was derived for the meso-tidal regimes observed along the Portuguese coastline (Fig. 2.2). We used the high frequency tide gauge data from nearby tide gauge stations (Vila Real St Antonio, Huelva) to calculate the duration for which the water level exists below the maximum spring high tide level for each tidal cycle and at a given location. The tidal inundation frequency at a particular depth was then calculated using the corresponding total duration of water remaining above the ground (depth interval is 0.25 m) for all the tidal cycles from 1991 to 1995. We represent the tidal inundation frequency as a percentage of the maximum inundation frequency. It appears that the non-dimensional tidal inundation frequency depends strongly on the tidal range, decreasing in a linear fashion with an increase in intertidal zone depth from -2.0 to +1.0 m but converging slowly to 0% from +1.0 m to a maximum spring high tide of +3.88 m.

2.3.2 SEA LEVEL RISE SCENARIOS

Simulation was performed for 3 IPCC (2007) sea-level rise scenarios and 4 sedimentation scenarios. The sea-level rise scenarios selected in this study were: (1) the global sustainability scenario (B1); (2) balanced use of fossil fuel under the globalized economy scenario (A1B); and (3) intensive use of fossil fuel under the globalized economy scenario (A1FI).

Linear regression analysis of tide gauge data sets from Cascais and Lagos shows that the sea-level rise along the Portuguese coastline will be 14–57 cm by the end of 21st century (Dias and Taborda, 1992). This value is comparable with the upper limit projection (59 cm) of sea-level rise under the A1FI sea-level rise scenario of IPCC, 2007. Furthermore, an analysis of long-term tide gauge data from the same stations for the 20th century shows that the average rate of sea-level rise is 1.3 ± 0.1 and 1.5 ± 0.2 mm/yr, respectively (Dias and Taborda, 1992). As these values are comparable with the global mean rate of sea-level rise for the 20th century (e.g. Barnett, 1984; Gornitz and Lebedeff, 1987), Dias and Taborda (1992) concluded that most of the signals indicating sea-level rise detected at these stations are of global origin. Thus, it seems reasonable to assume that the rate of sea-level rise along the Portuguese coast in future will be comparable with the projections of the global mean rate mentioned in the IPCC 2007 report. As tectonic subsidence is known to be negligible in the Guadiana estuary area (Lobo et al., 2003), the above assumption is further justified. The upper bound values under the A1B and B1 scenarios are approximately 10 and 20 cm less, respectively, than the A1FI scenario.

Simulations were performed for 11 percentile values (P = 5, 15, 25, 35, 45, 50, 55, 65, 75, 85, and 95%).The envelope for sea level rise scenarios consist of the lower bound (5%) and upper bound curve (95%). For intermediate sea level rise curves for other P values (between 5 and 95%), Cowell and Zeng (2003) assumed a normal distribution for the range of rises in sea level. Their method yields a characteristic elongated *S*-shape cumulative probability sea level

rise curve. Due to the large uncertainties involving other parameters and the sea level projections themselves, we approximated the sea level rise cumulative probability curve as a linear function for intermediate P values between 5 and 95% for a given year. Thus, eleven sea-level rise time series (corresponding to the 11 percentile values) were produced for the period 2010 to 2100 for each sea level rise scenario, to each of which four sediment accumulation rate scenarios were applied as derived using Equations 4, 5, 6, and 11. Altogether, 44 simulations were carried out to predict the morphological evolution of the Guadiana estuary for each sea level rise and sedimentation scenarios. However, in this paper, we present in detail the simulated morphology by the end of 21st century only for the upper bound values (P = 95%) of 3 sea-level rise scenarios (Table 1). The decadal behaviour of the morphological evolution of the estuary is described only for the A1B scenario in terms of the cumulative sediment volume deposited in the estuary (Fig. 2.3).

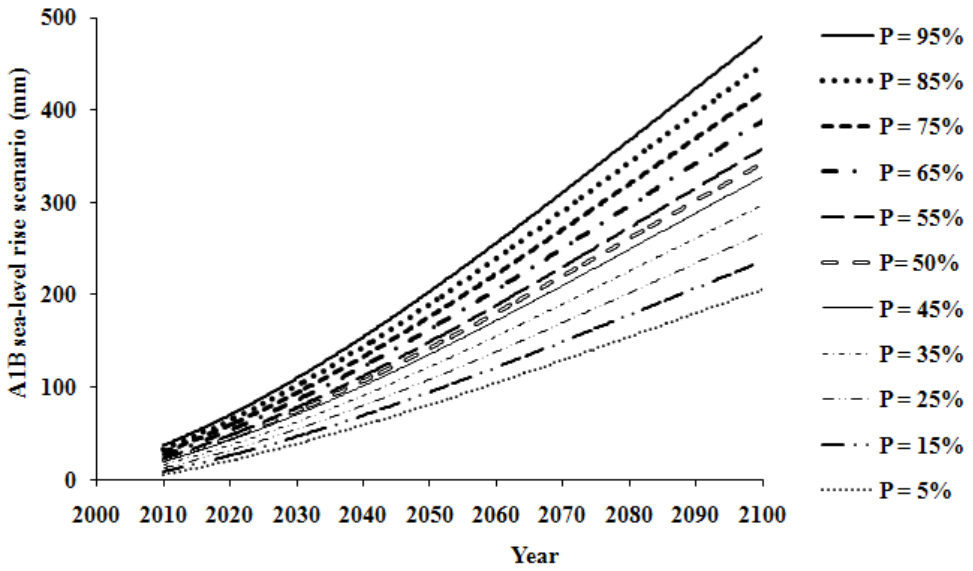

Figure 2.3 Envelope of IPCC (2007) sea level rise scenario A1B (balanced use of fossil fuel). The 5% and 95 % curves are the lower and upper limits respectively of the A1B sea level rise scenario, and intermediate sea level rise curves represent intermediate percentile confidence limits (P) as denoted.

2.3.3 SEDIMENTATION SCENARIOS

The time-averaged maximum net sedimentation rate (S^{max}) was represented using local sedimentation scenarios that were based on the behaviour of the Guadiana estuary since 13000 cal BP. The infilling of the Guadiana estuary has kept pace with sea level rise since 13000 cal BP (Boski et al., 2002; 2008). This observation was used as the basis for a sedimentation scenario in which the sedimentation rate is equal to the rate of sea level rise (Eq. 2.4), named the maximum (Max) sedimentation scenario. The values of the Max sedimentation scenario corresponding to the three sea level rise scenarios are given in Table 1.

$$S_{\text{Max}}^{\text{max}} = \frac{\Delta(\text{SLR})}{\Delta T} \qquad (2.4)$$

Where Δ(SLR) is the change in sea level over the time interval ΔT.

Table 2.1 Sea level rise and sedimentation scenarios used in the simulations.

Case	Sea Level Rise Scenario (IPCC, 2007)	Sea Level Rise (m) (IPCC, 2007)	Sea Level Rise Rate (mm/yr) (IPCC, 2007)	Maximum sedimentation rate (S^{max})	
				Scenario	Rate (mm/yr)
B1HI	B1 (Global sustainability)	0.38	3.9	Human Intervention (HI)	0.65
B1Min				Minimum (Min)	1.30
B1Avg				Average (Avg)	2.10
B1Max				Maximum (Max)	3.90
A1BHI	A1B (Balanced use of fossil fuel)	0.48	6	Human Intervention (HI)	0.65
A1BMin				Minimum (Min)	1.30
A1BAvg				Average (Avg)	3.70
A1BMax				Maximum (Max)	6.00
A1FIHI	A1FI (Intensive use of fossil fuel)	0.59	9.7	Human Intervention (HI)	0.65
A1FIMin				Minimum (Min)	1.30
A1FIAvg				Average (Avg)	5.50
A1FIMax				Maximum (Max)	9.70

The second sedimentation scenario used was 1.3 mm/yr (Eq. 2.5), which is the estimated sedimentation rate for the period 7000 cal BP to present (Boski et al., 2002; 2008).

Thus, it is the minimum (Min) sedimentation scenario over the geological time scale. Such a scenario would be possible if the estuary response to the rapid sea level rise was characterized by a phase lag as observed elsewhere. For instance, the phase lag in the morphological response in the case of a linear trend in sea level rise in the Humber estuary represents a time-lag of ca 35 years (Townend et al., 2007) and the phase lag in the Westerschelde estuary is much larger, with the order of magnitude being a century (Jeuken et al., 2003).

$$S_{\text{Min}}^{\text{max}} = 1.3 \tag{2.5}$$

An intermediate sedimentation rate scenario was derived using the average of the above two scenarios, termed the Avg scenario (Eq. 2.6). The values of the average sedimentation scenario corresponding to the three sea level rise scenarios are reported in Table 1.

$$S_{\text{Avg}}^{\text{max}} = 0.5[S_{\text{Min}}^{\text{max}} + S_{\text{Max}}^{\text{max}}] \tag{2.6}$$

However, it appears that the future sediment supply to the Guadiana estuary will be strongly influenced by dam construction and by groyne construction along the west bank of the river mouth. Since the construction of the Alqueva dam, a drastic reduction in the river discharge and a consequent decrease in the supply of fluvial sediment have been observed. Due to the shortage of silt supplied by the river, the area of salt marshes is currently in rapid decline. Sediment deposition is dependent on the suspended sediment available in the estuary, which is determined by the balance between sediment transported out of the estuary by river discharge and the sediment brought into the estuary by saline water intrusion. The latter process occurs mainly in the bottom water layer. If there were a net import of sediment, it would be, initially, trapped in the main estuary channel. This process is characterized by the sediment trapping

efficiency of an estuary. The net sediment flux (Q_{ST}) into the Guadiana estuary across its mouth was calculated using Eq. 2.7, derived by Schubel and Carter (1984).

$$Q_{ST} = Q_W \bar{C}_b \left[1 - \frac{(\Delta C/\bar{C}_b)(1+\upsilon^*)-\upsilon^*}{(\Delta S/\bar{S}_b)(1+\upsilon)-\upsilon}\right] \quad (2.7)$$

Where: Q_W is the river discharge; $\bar{S}_b$ and $\bar{C}_b$ are, respectively, the average concentration of suspended sediment and the salinity in the lower layer; ΔC and ΔS are, respectively, the differences in the concentration of suspended sediment and salinity between the surface and bottom layers; υ and υ* are the fractions of the total seaward flux of salt and suspended sediment that are balanced by dispersion.

If Q_{ST} is greater than zero, that quantity of sediment flux would be imported into the estuary. The river discharge was calculated using the data of Instituto da Água (INAG) for Pulo do Lobo station where the average discharge from 2003 to May 2009 was 31.85 m^3/s. Morales (1995) has shown empirically that the suspended sediment flux ($\bar{C}$) transported by the Guadiana River can be estimated in terms of river discharge (Eq. 2.8). The average suspended sediment concentration of the bottom layer ($\bar{C}_b$) (Eq. 2.9) was approximated using Eq. 2.8 and data given by Machado et al. (2007).

$$\bar{C} = \left(\frac{Q_W}{0.03}\right)^{0.5} \quad (2.8)$$

$$\bar{C}_b = 6 \times Q_W^{0.5} \quad (2.9)$$

The overall component within the square brackets of Eq. 2.7 was taken as a constant to overcome the lack of a comprehensive data set. The value of this constant (1.38) was calculated using data given by Machado et al. (2007) and Caetano et al. (2006). Thus, a relationship (Eq.

2.10) was able to be derived to estimate the sediment trapped (Q_{ST}) by the lower estuary in terms of river discharge (Q_W).

$$Q_{ST} = 1.38Q_w^{1.5} \quad (2.10)$$

If the sediment trapped were initially distributed uniformly in the lower estuary (an approximate area of 6.5 km^2), the maximum sediment deposition rate (S^{max}) would be approximately 0.65 mm/yr. This value is 50% of the sediment deposition rate over the last 7000 years as provided by Boski et al. (2008). These conditions were termed the human intervention (HI) scenario (Eq. 2.11).

$$S_{HI}^{max} \approx 0.65 \quad (2.11)$$

As the ESM model is coupled to the ESRI ARCGIS Geographic Information Systems platform, the visualization and analysis of the simulated morphological evolution of the estuary were carried out using GIS geoprocessing techniques for the different sea level rise and sedimentation scenarios investigated.

2.4 RESULTS:

2.4.1 MORPHOLOGICAL EVOLUTION DUE TO PROJECTED SEA LEVEL RISE AND SEDIMENTATION SCENARIOS

On the whole, under changing sea level and sedimentation conditions, the morphological evolution in the intertidal zone occurs mainly adjacent to the secondary channels of the Guadiana estuary. Salt marshes represent a large part of the intertidal zone above the mean sea level. There may not be significant morphological changes along the banks

of the main river because they are controlled with artificial structures such as jetties and groynes. In all simulated sedimentation and sea level cases, the landward boundary of the intertidal zone will gradually retreat landward with sea level rise during the 21st Century, while the river boundary delimited by the mean sea level will also retreat landward but at a slower rate. The morphological evolution of the Guadiana estuary shows distinct variations in behaviour according to the four sedimentation scenarios and three sea level rise scenarios used in the modelling, as discussed immediately below.

2.4.1.1 Human intervention sedimentation scenario

Under the HI sedimentation scenario, there would be a net increase in water depth throughout the estuary relative to the mean sea level defined for each sea level rise scenario (Figs. 2.4*a*-i, 2.5a-i, and 2.6a-i). The present bathymetry and simulated bathymetries for the 3 sea-level rise scenarios are approximately equal, indicating that bathymetric changes are probably relatively small (Figs 2.4*a*-ii, 2.5a-ii, and 2.6a-ii). However, the cumulative sediment volume deposited over the estuary bed is different in each scenario (1846285, 1913147, and 1887810 m^3, respectively). The net accretion of the deeper zones of the estuary is approximately 0.1 m in response to each sea-level rise scenario under the H1 sedimentation scenario. The sediment deposition along the main channel shows longitudinal bar formation that is 3-4 km in length. Furthermore, the net increase in the effective water depth (i.e. relative to rising mean sea levels defined for the respective sea level rise scenarios) under these conditions can be clearly identified along the central longitudinal axis of the river (Figs. 2.7*a*, 2.7*b* and 2.7*c*). The resulting bed profile along the central axis relative to the present mean sea level is shown in figures 2.7*d*, 2.7*e*, and 2.7*f*, respectively. The reduction of sediment supply would result in comparative expansion of the sand bypassing channel with time. This behaviour can be seen clearly under the A1FI sea level rise scenario (Fig. 2.6a-i).

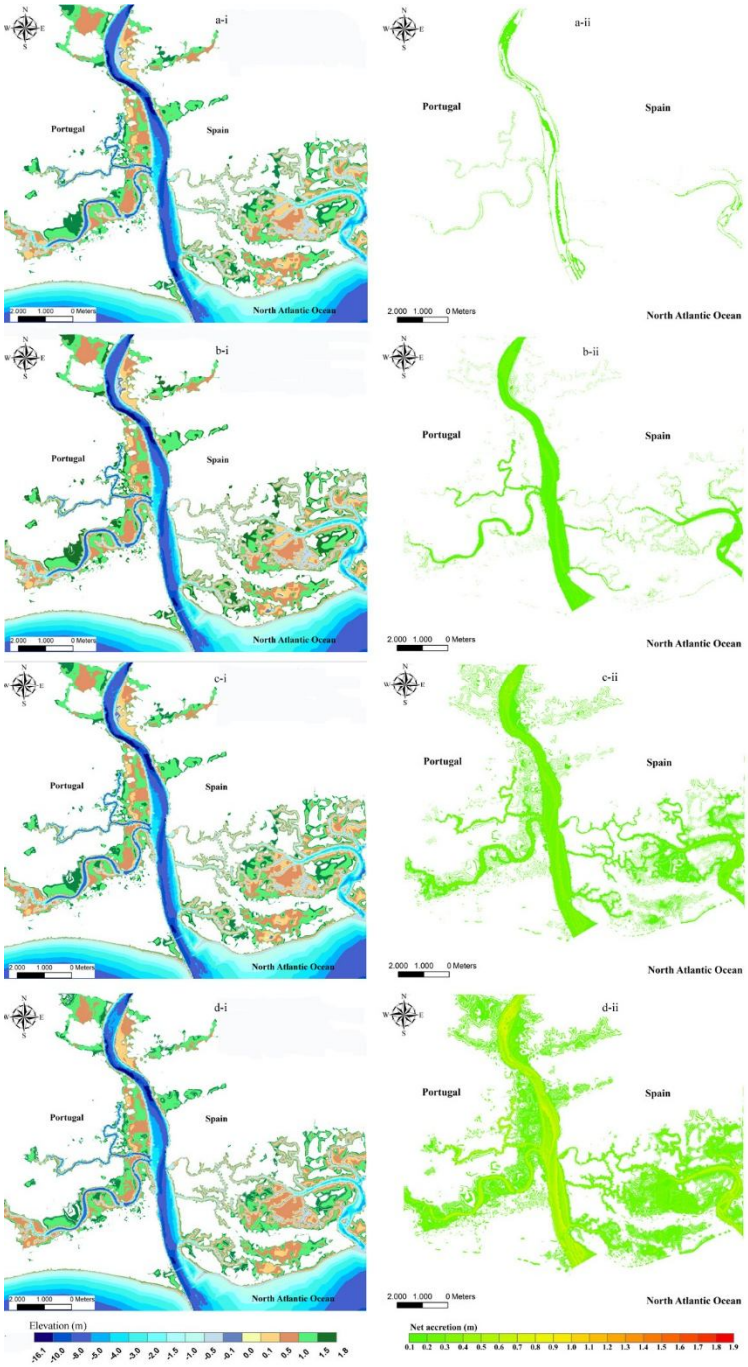

Figure 2.4 Simulated morphological evolution: (i) depth below the maximum spring high-tide level relative to the mean sea level and (ii) net accretion of the Guadiana estuary by the end of the 21st century for B1 sea-level rise scenario and for sedimentation scenarios: (a) HI (0.65 mm/yr); (b) Min (1.3 mm/yr); (c) Avg (2.1 mm/yr); and (d) Max (3.9 mm/yr) and the expansion of the intertidal zone area relative to the area in year 2000 is 6.1, 5.9, 5.4, and 4.1 km^2, respectively.

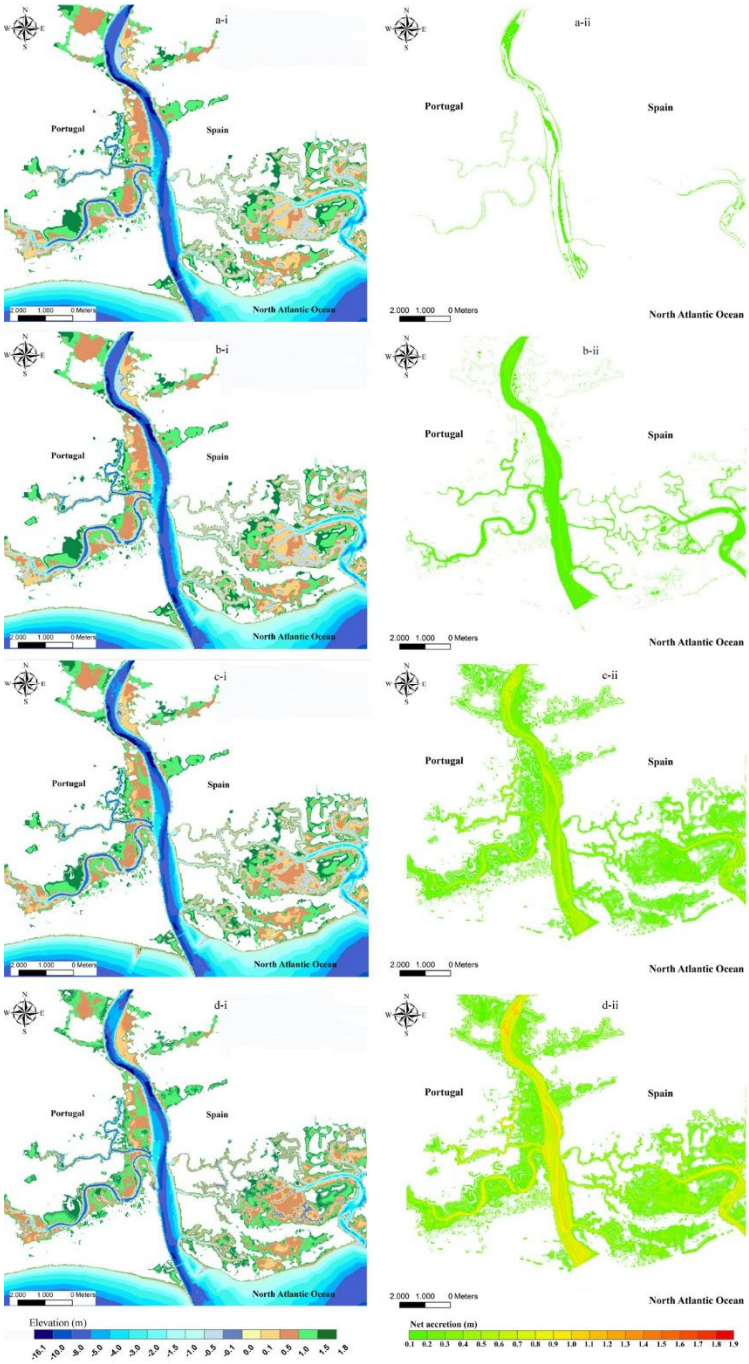

Figure 2.5 Simulated morphological evolution: (i) depth below the maximum spring high-tide level relative to the mean sea level and (ii) net accretion of the Guadiana estuary by the end of the 21st century for A1B sea-level rise scenario and for sedimentation scenarios: (a) HI (0.65 mm/yr); (b) Min (1.3 mm/yr); (c) Avg (3.7 mm/yr); and (d) Max (6.0 mm/yr) and the expansion of the intertidal zone area relative to in the area in year 2000 is 7.7, 7.6, 6.8, and 5.5 km^2, respectively.

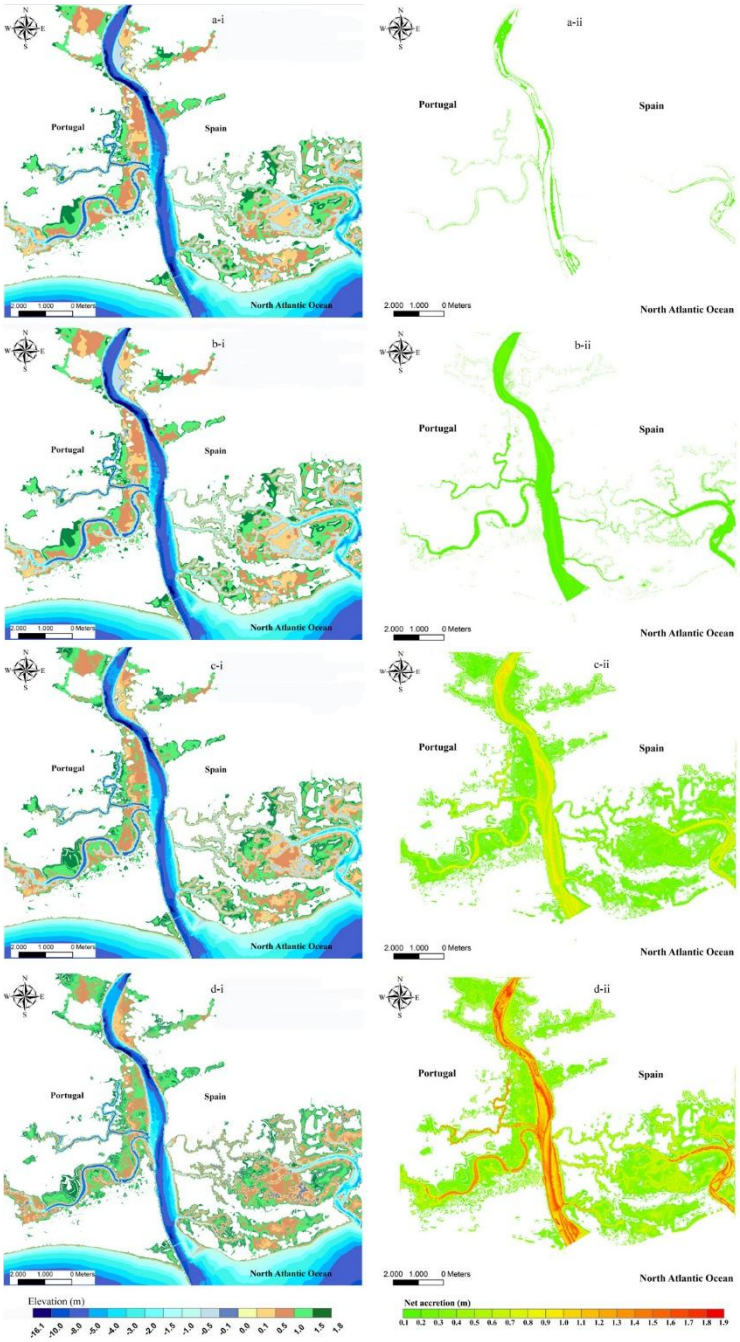

Figure 2.6 Simulated morphological evolution: (i) depth below the maximum spring high-tide level relative to the mean sea level and (ii) net accretion of the Guadiana estuary by the end of the 21st century for A1FI sea-level rise scenario and for sedimentation scenarios: (a) HI (0.65 mm/yr); (b) Min (1.3 mm/yr); (c) Avg (5.5 mm/yr); and (d) Max (9.7 mm/yr) and the expansion of the intertidal zone area relative to the area in year 2000 is 9.4, 9.3, 8.1, and 6.4 km^2, respectively.

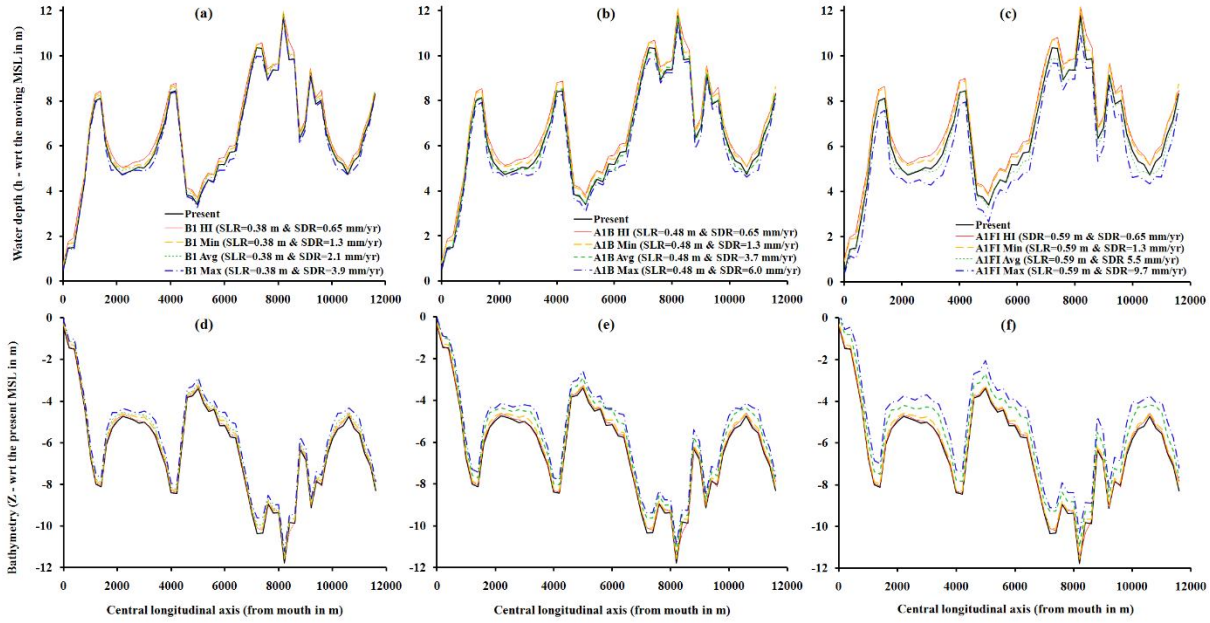

Figure 2.7 Depth variations along the central longitudinal axis of the Guadiana estuary for sea level rise scenarios B1 (0.38 m), A1B (0.48 m), and A1FI (0.59 m) and corresponding sedimentation scenarios (a, b, and c are the mean depth variation; and d, e, and f are the bed profile relative to present mean sea level).

The salt marshes would be completely submerged due to the projected rise under any of the three sea level rise scenarios. The maximum submergence would be experienced when the projected sea level rise is 59 cm. Under these conditions, salt marshes would deteriorate resulting in a reduction in the area covered by salt marshes in the Spanish margin and in particular around Beliche bend located 10 km upstream from the river mouth.

2.4.1.2 MINIMUM (GEOLOGICAL TIME SCALE) SEDIMENTATION SCENARIO

The morphological evolution of the Guadiana estuary under the minimum sedimentation (Min) scenario (1.3 mm/yr) for each sea level rise scenario shows similar behaviour to that described above for the HI sedimentation scenario. If the sedimentation rate were the same as the average value observed since 7000 cal BP, the net increase in effective

water depth would be lower due to the increase in sediment deposition (Figs. 2.4b-i, 2.5b-i, and 2.6b-i). The net accretion along the estuary will probably increase but the fluctuations along the axis may be minimal (Figs. 2.4b-ii, 2.5b-ii, and 2.6b-ii). The average accretion height is 0.2 m for the three sea level rise scenarios. The deeper zones show a similar pattern of morphological evolution under each sea level rise scenario. Under the Min sedimentation scenario, salt marshes would be completely submerged due to the projected sea level rises. However, the submergence will not be as severe as the submergence under the HI sedimentation scenario (0.65 mm/yr). Hence, salt marsh deterioration in the Spanish margin would be reduced in the Min sedimentation scenario compared with the HI scenario.

2.4.1.3 AVERAGE SEDIMENTATION SCENARIO

Since the sedimentation rate under the average sedimentation scenario (0.5*Sea Level Rise Rate +1.3*0.5 in mm/yr) is not constant because of its dependence on the rate of sea level rise, the morphological evolution of the estuary is expected to be different to that under the human intervention and minimum sedimentation scenarios. The Avg scenario would enhance sedimentation in the Guadiana estuary in sympathy with the sea level rise. Thus, under the B1 and A1B sea level rise scenarios, the effective water depth in the main channel would be approximately equal to the present effective water depth (Figs. 2.4c-i. and 2.5c-i). However, there would be an overall decrease of effective water depth for the A1FI sea level rise scenario and in some localities it would be well below the present effective water depth (Fig. 2.6c-i). This enhancement of sedimentation would be apparent along the longitudinal axis of the main channel (Figs. 2.7*a*, 2.7*b*, and 2.7*c*). The average heights of sediment deposition along the main channel will be approximately 0.3, 0.5, and 0.7 m in the case of the B1, A1B, and A1FI sea-level rise scenarios, respectively (Figs. 2.4c-ii, 2.5c-ii, and 2.6c-ii). The expansion of the sand

bypassing channel would be retarded under the enhanced sedimentation condition. Intertidal zone submergence also would reduce significantly under these circumstances.

2.4.1.4 Maximum sedimentation scenario

Under the maximum sedimentation (Max) scenario, the morphology of the Guadiana estuary and its intertidal zone may evolve as it has done during the Holocene for each sea level rise scenario (i.e., there may not be a significant effective water depth variation irrespective of the changes in sea level). In fact, the sediment deposition under the Max scenario conditions would result in a reduction of the effective water depth compared to the present water depth of the main channel (Figs. 2.4d-i, 2.5d-i, and 2.6d-i). The average heights of deposition along the main channel would be 0.5, 0.8, and 1.4 m for the B1, A1B, and A1FI sea level rise projections, respectively (Figs. 2.4d-ii, 2.5d-ii, and 2.6d-ii). The increased accommodation space in the main channel would be offset by the sediment deposition maintaining a stable system. Under the Avg and Max sedimentation scenarios, the bypassing channel would contract compared to its present dimensions. If the sedimentation further increased, longitudinal bars developed along the main channel resulting in the formation of at least 2 channels (Fig 2.6d-ii). It is clear that the present sediment discharge is insufficient to maintain a stable effective water depth within the lower Guadiana estuary. Therefore, the Max sedimentation scenario only provides the possible morphological evolution under undisturbed conditions or conditions similar to the pre-anthropogenic period. The expected behaviour of the effective depth variation under the maximum sedimentation rate can be considered as an indirect assessment of the accuracy of the modelling approach.

2.5. IMPACT ASSESSMENT DUE TO SLR AND SEDIMENT SUPPLY REDUCTION

2.5.1 REGRESSION OF THE MEAN SEA LEVEL CONTOUR OF THE ESTUARY

There is a significant lateral translation of the landward boundary of the intertidal zone for each sea-level rise scenario. However, there is no significant horizontal translation of the mean sea level (0 m) contour of the Guadiana River under these scenarios (Fig 2.8). Therefore, there will be a significant expansion of the intertidal zone area by the end of the 21st century. The average landward translation of the 0 m contour is about 7.6 m and the maximum translation is 60 m in the western margin. A comparatively large translation of the 0 m contour, on average 27 m, is expected in the eastern margin. At the Spanish margin of the estuary, there is a significant local lateral expansion in the vicinity of the bend located 10 km upstream of the mouth of the estuary, due to the flatness of the terrain compared to the other parts of the estuary. If the secondary currents (cross-currents) around the estuary bend were high, there would be a lowering of the water level around the bend in the Spanish margin while creating greater elevation in the Portuguese margin. A reduction in the amount of submergence in the Spanish margin due to this phenomenon would be minimal as the secondary currents in the Guadiana estuary are weak. On the whole, the 0 m contour retreats landward for all sea level rise and sedimentation scenarios except under the conditions of the A1FI sea level rise scenario with the Max sedimentation scenario (a highly improbable case according to the present conditions). For 59 cm rise of sea level and S^{max} equal to the corresponding rate of sea level rise, several segments of the 0 m contour line could be translated into the estuary channel, causing progradation of the Spanish margin of the Guadiana River.

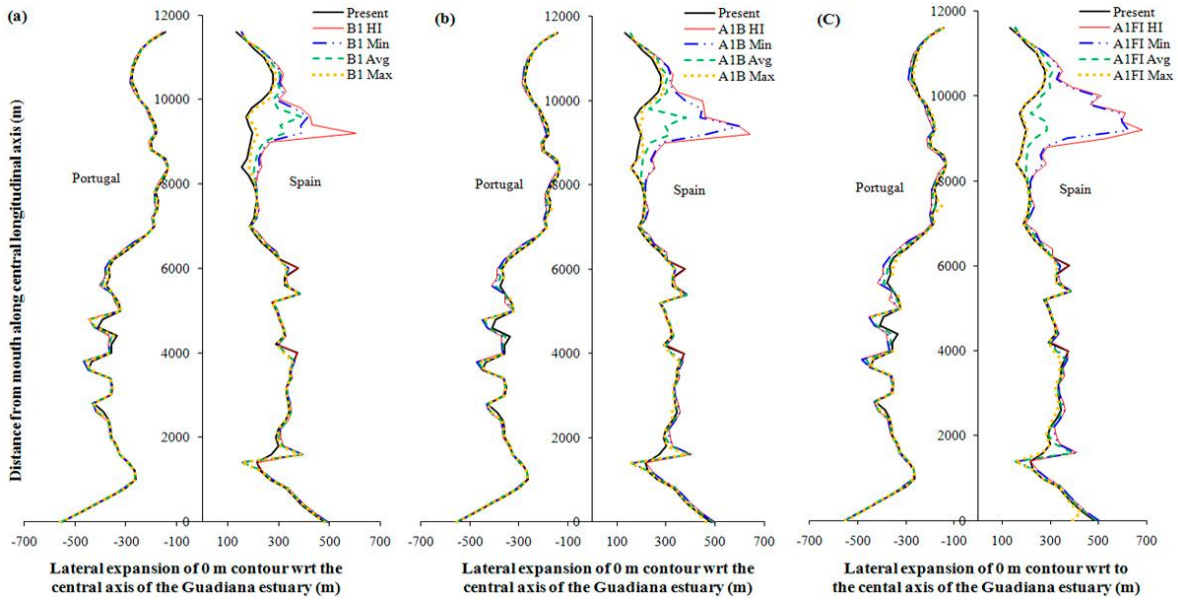

Figure 2.8 Lateral movement of the 0 m contour of the Guadiana estuary in response to sea level rise scenarios (a) B1 0.38 m; (b) A1B 0.48 m; and (c) A1FI 0.59 m for each of four sedimentation rate scenarios (Max = sea level rise rate; Min = 1.3 mm/yr; Avg = 0.5(1.3 + sea level rise rate) mm/yr; and HI = 0.65 mm/yr, an approximation to account for the reduction in sediment supply due to human interventions such as dam construction).

2.5.2 CORRELATION OF IMPACTS WITH SLRR AND OF SEDIMENTATION

In quantifying the overall morphological evolution of the Guadiana estuary, it is important to find correlations among parameters of morphological changes and sea level rise and sedimentation rates. Results indicate that, irrespective of the sedimentation scenario, the intertidal zone area of the Guadiana estuary would increase for all three sea level rise scenarios (Figure 9*a*). Although the maximum sedimentation rate was maintained as equal to the sea level rise rate, there would be a net increase in the area of the intertidal zone by the end of 21st century.

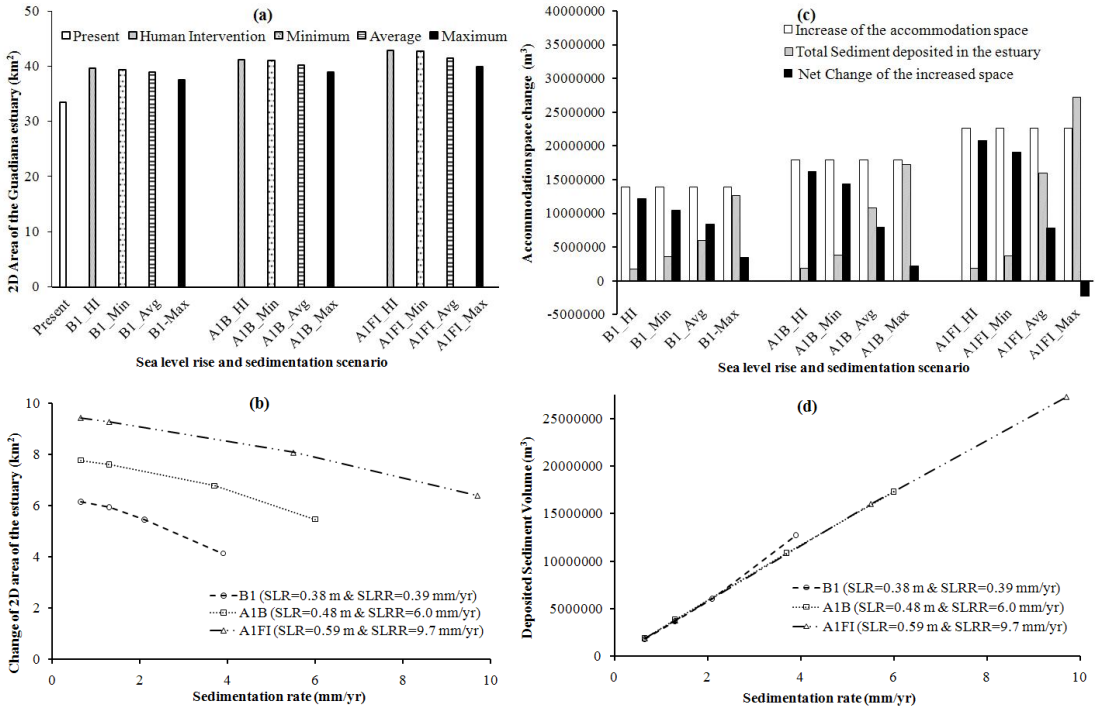

Figure 2.9 Morphological response of the Guadiana estuary to sea level rise and sedimentation scenarios: (a) Variation of the intertidal zone area; (b) Variation of the change of the intertidal zone area with sedimentation rate; c) Accommodation volume change of the estuary; d) Variation of sediment volume added with respect to change in sedimentation rate.

This is mainly due to two reasons: 1) there is a significant horizontal translation of the landward boundary of the intertidal zone for rise in sea level but the landward translation of mean sea level contour is insignificant, thereby, there is a net increase of the intertidal zone area of the estuary for each scenario; and 2) this can be attributed to reduced sedimentation above mean sea level due to the low tidal inundation frequency for the upper intertidal zone. For instance, the present potential sedimentation above mean sea level is only 37% of the total potential sedimentation in the intertidal zone. This may increase up to 50, 53, and 57% due to the increased accommodation space resulting from the projected sea level rise of 38, 48 and 59 cm, respectively (Fig. 2.2). The potential sedimentation was defined for a unit S^{max} value (1 mm/yr) and constant bed slope below the maximum spring high-tide level. If the sea level were

to rise by 59 cm, potential sedimentation above a height of 1.0 m would increase only from 5 to 25%. We assume the tidal range will be constant during the 21st Century. But it is not possible to predict that the increase of the intertidal zone area will result in increase of salt-marsh area because it depends on the soil characteristics of that area.

The maximum increase in the area of the intertidal zone occurs for the A1FI sea level rise scenario (59 cm) under the HI sedimentation scenario. Even though the HI scenario represents a 50% reduction in sedimentation relative to the Min scenario, under both sedimentation scenarios the lateral expansion of the intertidal zone is almost equal for the three sea level rise scenarios (Fig. 2.9a). Generally, the expansion of the intertidal zone for each 10 cm rise of the sea level is about 3-5% of the present intertidal zone area for the 12 cases. According to Fig. 2.9b, the net change in the intertidal zone area decreases linearly with an increase in sedimentation rate, and the rate of decrease is very similar for the three sea level rise scenarios. The net change in accommodation volume decreases markedly with an increase in the sedimentation rate (Fig. 2.9c). In one case, under the A1FI sea level rise scenario and with a sedimentation rate equal to the rate of sea level rise (A1FI-Max scenario), the net change in accommodation volume becomes negative; that is, the increase in accommodation volume due to sea level rise is offset (or more than offset) by the sediment added into the estuary. However, for all other scenarios, there would be a net increase in accommodation volume and therefore most parts of the Guadiana estuary would be drowned due to the sea level rise. The volume of sediment added into the estuary is a linear function of the sedimentation rate (Fig. 2.9d).

2.5.3 DECADAL BEHAVIOUR OF MORPHOLOGICAL EVOLUTION

The behaviour of the morphological evolution of the estuary was further assessed in terms of the cumulative sediment volume deposited in the estuary for the A1B sea level rise

scenario and for four sedimentation scenarios, using a 5-year input and 10-year step output. The cumulative sediment volume deposited in the estuary through the 21st Century is a function of the sediment deposition rate which is controlled by the supply of sediment into the estuary.

2.5.3.1 MAXIMUM AND AVERAGE SEDIMENTATION SCENARIOS

If the rate of sediment deposition kept in pace with the rate of sea level rise (Max scenario), there would be an exponential increase in cumulative sediment addition over time for the sea level rises given by the corresponding percentile values (Fig. 2.10*a*). The Avg scenario also shows an exponential increase in cumulative sediment addition but the rate of increase is small (Fig. 2.10*c*).

2.5.3.2 MINIMUM AND HUMAN INTERVENTION SEDIMENTATION SCENARIOS

As shown in Figs. 2.10*b* and 2.10*d*, if the sediment deposition rate became constant (0.65 and 1.3 mm/yr), the cumulative sediment addition would not show any significant variation for rises in sea level as given by the corresponding percentile values. There is a linear increase in cumulative sediment addition with time. However, the cumulative sediment volume deposited in the estuary over the 100-year time period has no correlation with percentile value. For instance, for the Min sedimentation scenario, the curve of the cumulative sediment volume deposited corresponding to the 35% percentile value represents the upper limit of the envelope until 2070, after which the 5% curve becomes the upper limit.

The lower limit of this envelope corresponds to the 5% percentile limit until 2060, after which the 55% curve becomes the lower limit. However, the envelope is very narrow and the fluctuations are not significant relative to the cumulative sediment volume deposited by a given year. Similar behaviour is found for the HI scenario. The average gradient of the cumulative

sediment addition curves for a S^{max} value of 0.65 mm/yr (HI scenario) is approximately 50% of that for the 1.3 mm/yr sedimentation rate of the Min scenario.

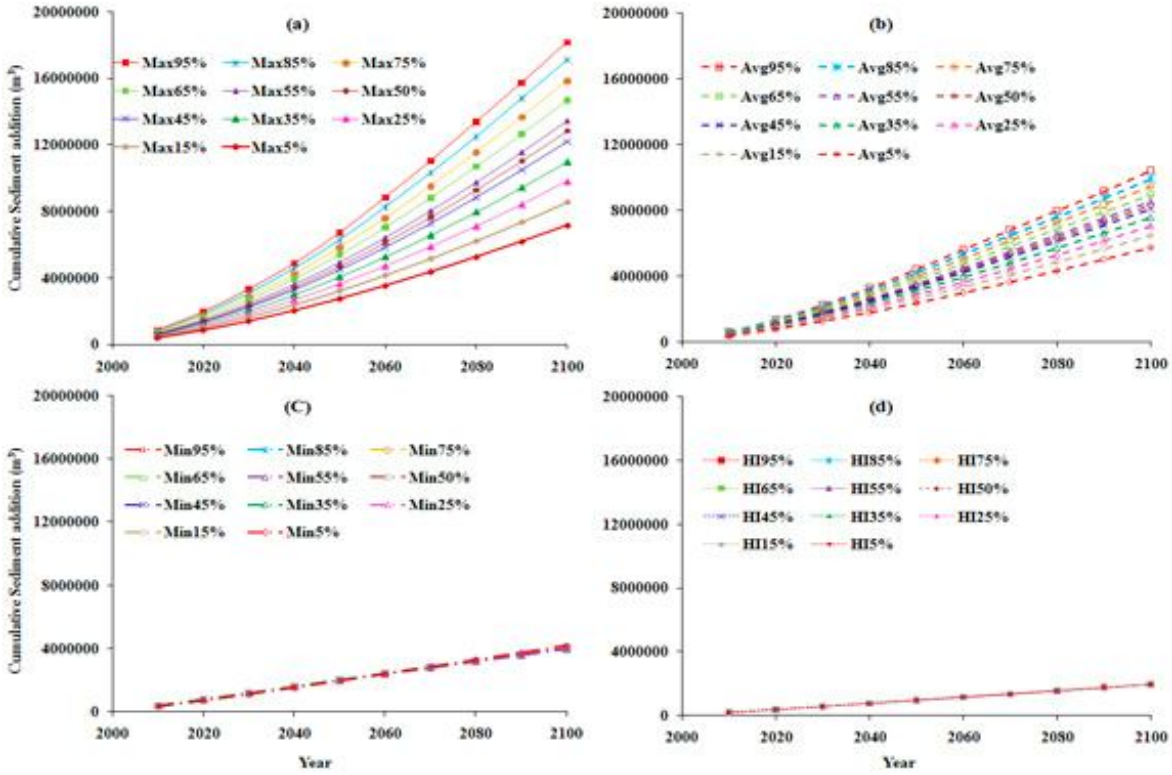

Figure 2.10 Cumulative sediment volume added into the Guadiana estuary for different percentile values of the A1B sea level rise scenario during the 21st Century for sedimentation rate scenarios: (a) Max = sea level rise rate; (b) Min = 1.3 mm/yr; (c) Avg = 0.5(1.3 + sea level rise rate); (d) HI = 0.65 mm/yr).

The variation in cumulative sediment addition with sedimentation rate is linear and shows strong dependence on time compared to the P values (Fig. 2.11). That is, the gradient of cumulative sediment addition (V_{SD}^{C}) with maximum sedimentation rate (S^{max}) for a given year does not vary much with sea level rises corresponding to higher P values. This behaviour is mathematically expressed in eq. 2.12.1, in which the coefficients a and b depend only on time (T). The influence of the P value is absorbed into the sea level rise which is dependent on both

P and T (Eq. 2.12.4). However, the prominence of P in the gradient term of eq. 2.12.4 is lower than that of T. As the magnitudes of sea level rise projections are less than 1 m, a negative sign resulted from Eq. 2.12.4 when taking the natural logarithm of projected sea level rise. The logarithmic nature of Eq. 2.12.4 may not represent any physical significance other than being a consistently high value for the coefficient of determination in the regression analysis.

$$V_{SD}^{C} = [aLn(SLR) + b]S^{max} \quad (2.12.1)$$

$$a = 0.04\,\mathrm{Ln}(T) - 76 \quad (2.12.2)$$

$$b = 31632T - 6 \times 10^{7} \quad (2.12.3)$$

$$Ln(SLR) = -e^{(25+0.09P-0.012T-0.00005PT)} \quad (2.12.4)$$

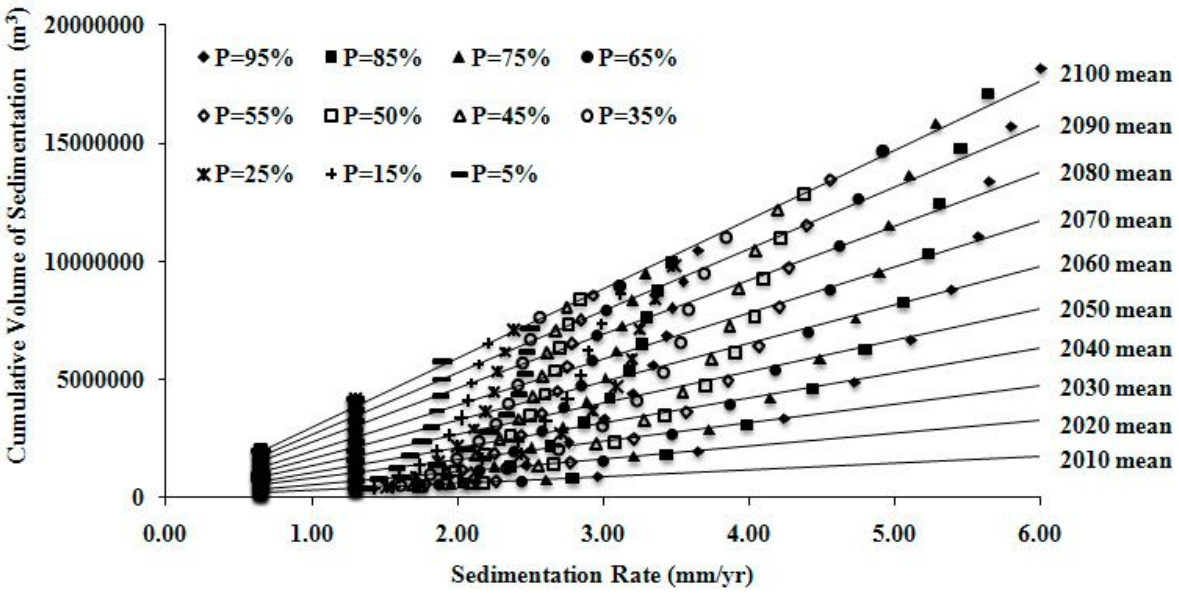

Figure 2.11 Variation of cumulative sediment volume added with respect to sedimentation rate for the period 2010 to 2100 with a 10-year output time step and for percentile (P) values of 5, 15, 25, 35, 45, 50, 55, 65, 75, 85 and 95%. A percentile value is an expression of the uncertainty in the sea level rise predictions for a given year (2010 to 2100). Straight lines are the linear best fit for the total data set belonging to each year.

2.6. DISCUSSION

2.6.1 IMPLICATIONS FOR ESTUARINE EVOLUTION AND MANAGEMENT

As the present sediment discharge is insufficient to maintain a stable effective water depth within the lower Guadiana estuary, the morphological evolution of the estuary and its associated intertidal zone during the 21st Century is probably best represented under the scenario that combines the A1FI sea level rise scenario (59 cm) and the human intervention sedimentation scenario (0.65 mm/yr). Under the conditions of this scenario, there is a significant net increase in the effective water depth of the main channel. The landward horizontal translation of the landward limits of the intertidal zone would be significant in the Portuguese margin of the estuary compared to that in the Spanish margin. This means that although there may be a loss of salt marsh habitats in the western margin, there is likely to be a landward shift in the entire system. Such processes may occur only if the soil characteristics are suitable for growth of salt-marsh vegetation. Even though such a submergence of land may considered as a loss in terms of restricting the type of economic activities able to take place, from an environmental point of view it is recommended that the process should be allowed to occur. A managed retreat would be a better option for particular economic activities such as salt production. Thus, we may identify a buffer zone for the estuary.

In the Spanish margin, due to the limited landward translation of the landward limits of the intertidal zone, there is likely to be a high risk of salt marsh habitats disappearing as a result of increased submergence from sea level rise. In addition, the landward translation of mean sea level will be significant in the Spanish margin, and its salt marshes will experience more pressure due to accelerated sea level rise than will be the case in the Portuguese margin. Thus, salt marsh habitats in the eastern margin would be further squeezed. Therefore, mitigation measures should be taken to improve the natural adaptability of this region; for instance, the removal of hard defence structures. If the environmental flow regulated by the Alqueva dam

could be increased, the lower estuary would receive more fine sediment, which would help to sustain the marsh vegetation.

2.6.2 LIMITATIONS OF THE ESTUARINE SEDIMENTATION MODEL

The application of the Estuarine Sedimentation Model to predict the morphological evolution of the Guadiana estuary and its intertidal zone can be considered as an initial step in developing a robust management tool for sustainable use of the resources produced by the estuary. In this context, the results of this study are provisional because the model is highly simplified. However, the use of fewer parameters and the simplification of processes may be useful for minimizing the uncertainties involved in the long-term forecasting of such parameters (Cowell et al., 1995).

The degree of influence of these processes on estuarine morphological evolution is different in intertidal and subtidal regions. Allochthonous (mineral) and autochthonous (organic) sedimentation and shallow compaction are dominant processes in the saltmarsh areas. Erosion and sediment resuspension due to tidal and wave activities are minimal in salt marshes, while these processes would be important in tidal flats and subtidal channels. This is due mainly to the high wave attenuation within the vegetation canopy in marsh environments. In the context of long-term predictions of morphological evolution, neglecting resuspension due to wave activities for an initial modelling exercise can be reasonably justified because the incident wave heights and secondary currents within the Guadiana estuary are almost insignificant. This is due primarily to the sheltered nature of the area, resulting in the low energy environment of the Guadiana estuary (Boski, et al., 2008).

Furthermore, the sedimentation scenarios were defined based on the maximum sediment deposition rate (S^{max}) in the estuary. In the modelling, we substituted the net maximum sedimentation rates estimated from borehole data for the Guadiana estuary, being

the difference between accretion and erosion over a geological time scale. Thus, the total sedimentation and erosion processes have been represented implicitly in our model. This strategy was used to overcome the limitations of the behaviour modelling approach. It should also be noted that the parameter S^{max} is only a representative value for the entire estuary, derived from borehole data analysis, and therefore the present model does not accommodate its possible spatial variation over the area of the estuary.

Shallow compaction is negligible in estuaries dominated by mineral sediment deposition (Temmerman, et al., 2004). As the Guadiana estuary has become affected by a drastic reduction in fluvial sediment supply, the overall supply of silt and fine sediments into the estuary has reduced significantly. The main source of sediment supply into the estuary is now of marine origin, from where the largely coarse sand will be imported into the estuary. Therefore, shallow compaction in the Guadiana estuary can be neglected for simulating its morphological evolution. In the estuary, organic sedimentation may be excluded in the long term modelling of its morphological evolution because the long term accumulation of organic matter in the form of peat is likely to be insignificant due to the intense anaerobic respiration of organic matter via sulphate reduction (Boski, 2008). This process also results in a low amount of autocompaction of the accumulated sediment. If this approach is to be used in different geographical regions, sedimentation due to organic matter, shallow compaction due to pore pressure dissipation, and deep subsidence may have to be taken into account. In northern Europe, organic matter deposition helps to maintain a stable water depth for salt marsh habitats, and as a result salt marshes will not be so vulnerable to pressure from sea level rise.

As the long-term sediment accretion has been assumed as a function of tidal inundation frequency (Allen, 1995), it is important to derive this function using a high frequency tide gauge data over a sufficient observation period. However, the data set available at Vila Real St Antonio tide gauge station, which is the closest station to the lower Guadiana estuary area, is

not continuous. The derived function shows that it is highly dependent on the tidal range. The linearity of this function will be lost only around the high tide region (above 1.0 m MSL). Therefore, in the Guadiana estuarine area, the uncertainty of this function will be greatest in the upper region of the intertidal zone. Furthermore, it is important to incorporate temporal variation in the suspended sediment flux due to meteorological forcing in mesotidal estuarine systems (French et al., 2008). However, as the river run-off is highly regulated in the Guadiana River, the variability in suspended sediment flux would be insignificant.

The evolution time scale of an estuarine feature (e.g. channel) of length L and depth H is HL/K, where K is the effective diffusivity ($K = 2\pi C_d U^3/g\ (1-p) \tan \phi$; U is the current velocity; p, porosity; g, gravitational acceleration; ϕ, angle of repose of sand; and C_d, drag coefficient) (EA and Defra, 2007). The range of the evolution time scale for the Guadiana estuary channel is approximately 30 to 10 years for the typical range of drag coefficient, i.e. 0.001 to 0.005 (typical parameter values: H = 10 m, L = 35 km, U = 0.6 m/s, p = 0.4 and ϕ = 35°). Therefore, the use of a 5-year input time step for simulating the morphological evolution of the Guadiana estuary is justified.

As process-based approaches are effective for simulating the evolution of individual features (e.g. tidal inlets and mudflats) of estuarine systems (Hibma et al., 2003; 2004), developing a hybrid approach may overcome some of the deficiencies of the present approach. With a hybrid approach, it may be possible to incorporate tidal hydrodynamics, channel-shoal sediment exchange, and gravitational circulation as well as represent dynamic feedback between sedimentation and tidal currents and between sediment transport and morphological change. In addition, it would be interesting to carry out further studies on sedimentation rates that exceed the sea level-rise rate.

2.7 CONCLUSIONS

The morphological evolution of the Guadiana estuary and its associated intertidal zone during the 21st Century are probably best represented under the scenario that combines the A1FI sea level rise scenario (59 cm) and the human intervention sedimentation scenario (0.65 mm/yr). This scenario gives a broad insight into the degree of vulnerability of the estuary under sediment starvation conditions. There would be a significant net increase in the effective water depth of the main channel for these conditions. The potential sedimentation above present mean sea level attains just 37% of the total potential sedimentation due only to tidal forcing in the intertidal zone. This value increases up to 50, 53, and 57% when an additional accommodation space is created in response to projected sea level rises of 38, 48, and 59 cm, respectively. The landward horizontal translation of the landward limit of the intertidal zone would be significant in the Portuguese margin of the estuary compared to that in the Spanish margin. In the Spanish margin, due to the limited translation of the landward limits of the intertidal zone area, there would be high risk of salt marsh habitats disappearing due to increased submergence resulting from sea level rise. In addition, the landward translation of mean sea level would be significant in the Spanish margin, where salt marshes will experience more pressure due to accelerated sea level rise; this phenomenon would be less significant in the Portuguese margin. On the whole, the intertidal zone area would increase by 3-5% for each 10 cm rise of sea level by the end of the 21st Century, representing a loss of land area due to sea level rise.

The morphological evolution of the Guadiana estuary in response to predicted sea level rise under the maximum sedimentation scenario resembles the actual post-glacial behaviour of the estuary. That is, the estuary has kept up with the pace of sea level rise, irrespective of the sea level rise rate. The maximum sedimentation scenario indicates sediment accumulation but without any significant lateral progradation in the tidal flats and marshes bounded by high density tidal channel system in the Spanish margin. However, such sediment supply conditions

are very unlikely to occur during the 21st Century, given the deficit in fluvial sediment supply resulting from the drastic reduction of river water discharge following the construction of a large number of dams. Thus, the obtained results under the maximum sedimentation scenario are of more theoretical interest than practical.

The approach taken should be considered as an initial conceptual framework able to be improved in the future. Constraints in the behaviour-oriented modelling approach used may be compensated in future studies by using a hybrid (behaviour-process) approach, which would help to exploit some of the advantages of process-based methods. Even though this model is extremely idealized and the results may have large uncertainties, it may provide at least the order of magnitude of potential morphological impacts on the Guadiana estuarine system due to the rise in sea level and sedimentation scenarios of the 21st century.

ACKNOWLEDGMENTS: This work has been carried out in the framework of FCT PTDC/CLI/68488/2006 project EVEDUS and EU 6th FP-SPICOSA project. The authors acknowledge Dr. David Stolper, Vivira Cadungog, Dr. Peter Cowell and Dr. Eleanor Bruce, School of Geosciences, University of Sydney, and the Sydney Olympic Park Authority for development and access to the ESM.

2.8 REFERENCES

Allen, JRL., 1995. Salt marsh growth and Flandrian sea level: implication of a simulation model for Flandrian coastal stratigraphy and peat-based sea-level curves. *Sedimentary Geology* 100: 21–45.

Barnett, TP., 1984. The estimation of global sea level change: A problem of uniqueness. *Journal of Geophysical Research* 89: 7980-7988.

Bindoff N., Willebrand J., Artale V., Cazenave A., Gregory J., Gulev S., Hanawa K., Le Quéré C., Levitus S., Nojiri Y., Shum CK., Talley L., Unnikrishnan A., 2007. Observations: oceanic climate and sea level. In: Solomon S, Qin D, Manning M, Chen Z, Marquis M, Averyt KB, Tignor M, Miller HL. (Eds.), Climate change 2007: the physical science basis. Contribution of Working Group I to the Fourth Assessment report of the Intergovernmental Panel on Climate Change. Cambridge University Press, Cambridge, UK.

Boski, T., Moura, D., Veiga-Pires, C., Camacho, S., Duarte, D., Scott, DB., Fernandes, SG., 2002. Postglacial sea-level rise and sedimentary response in the Guadiana Estuary, Portugal/Spain border. *Sedimentary Geology* 150: 103–122.

Boski, T., Camacho, S., Moura, D., Fletcher, W., Wilamowski, A., Veiga-Pires, C., Correia, V., Loureiro, C., Santana P., 2008. Chronology of post-glacial sea-level rise in two estuaries of the Algarve coast, S. Portugal. *Estuarine, Coastal and Shelf Science* 77: 230-244.

Bruce, E., Cowell, P., Stolper, D., 2003. Development of a GIS-based estuarine sedimentation model. *In* Woodruffe, CD Furness FA. (eds.) *Coastal GIS 2003* – Wollongong University, Australia, *papers on Maritime Policy* 14: 271-285.

Caetano, M., Vale, C, Falc~ao, M., 2006. Particulate metal distribution in Guadiana estuary punctuated by flood episodes. *Estuarine, Coastal and Shelf Science* 70: 109-116.

Costa C. 1994. Final Report of Sub-Project A. Wind Wave Climatology of the Portuguese Coast. Technical Report POWAVES 6/94-A, IH/LNEC.

Cowell PJ, Roy PS, Jones RA. 1995. Simulation of large-scale coastal change using a morphological-behaviour model. *Marine Geology* 126: 45- 61.

Cowell PJ, Zeng TQ. 2003. Integrating Uncertainty Theories with GIS for Modelling Coastal Hazards of Climate Change. *Marine Geodesy* 26(1): 5-18.

Dias J, Taborda R. 1992. Tidal gauge data in deducing secular trends of relative sea-level and crustal movements in Portugal. *Journal of Coastal Research* 8 (3): 655- 659.

Dronkers J. 1986. Tidal asymmetry and estuarine morphology, Netherlands. *Journal of Sea Research* 20(2/3): 117-131.

EA, Defra, 2007. Development of Estuary Morphological Models, Annex A: Guidelines for application of Bottom-Up estuarine models to assess impacts of Global Climate Change and interventions on flood risks and sediment regimes. *Joint Defra/EA Flood and Coastal Erosion Risk Management R&D Programme,* R&D Project Record FD2107/PR, 1-78.

Fenoglio-Marc L, Groten E. 2004. Long-term sea level variability from multi-satellite altimetry in the European seas. Proc. of the 2004 Envisat & ERS Symposium, Salzburg, Austria 6-10 September 2004 (ESA SP-572, April 2005): 1-6.

French J. 2006. Tidal marsh sedimentation and resilience to environmental change: Exploratory modelling of tidal, sea-level and sediment supply forcing in predominantly allochthonous systems. *Marine Geology* 235: 119-136.

French JR, Burningham H, Benson T. 2008. Tidal and Meteorological Forcing of Suspended Sediment Flux in a Muddy Mesotidal Estuary. *Estuaries and Coasts* 31:843-859. DOI 10.1007/s12237-008-9072-5.

Ganju NK, Schoellhamer DH. 2010. Decadal-Timescale Estuarine Geomorphic Change Under Future Scenarios of Climate and Sediment Supply. *Estuaries and Coasts* 33:15-29. DOI 10.1007/s12237-009-9244-y.

Garel E, Pinto L, Santos A, Ferreira ó. 2009. Tidal and river discharge forcing upon water and sediment circulation at a rock-bound estuary (Guadiana estuary, Portugal). *Estuarine, Coastal and Shelf Science* 84: 269-281. DOI 10.1016/j.ecss.2009.07.002.

Gonzalez R, Dias JMA, Ferreira O. 2001a. Recent Rapid Evolution of the Guadiana Estuary Mouth (Southwestern Iberian Peninsula). *In*: Healy TR. (ed.), *ICS 2000 (Proceedings), Journal of Coastal Research* Special Issue, 34: 516-527.

Gonzalez R, Dias JMA, Ferreira O. 2001b. Factors influencing sediment balance in estuarine systems: The example of the Guadiana Delta and Estuary (SW Iberia), *(Proceedings)*, V REQUI/ I CQPLI Lisboa, Portugal.

Gonzalez R, Dias JMA. Lobo F, Mendes I. 2004. Sedimentological and paleoenvironmental characterisation of transgressive sediments on the Guadiana Shelf (Northern Gulf of Cadiz, SW Iberia) *Quaternary International* 120: 133-144.

Gornitz V, Lebedeff S. 1987. Global sea level changes during the past century. In Nummedal D, Pilkey OH, Howard JD. (eds.), Sea level fluctuations and coastal evolution, Society of Economic Paleontologists and Mineralogists; 3-16.

Hamilton D. 1979. The high energy, sand and mud regime of the Severn Estuary, south-west Britain. In: Severn RT, Dineley D, Hawker LE. (Eds.), Tidal Power and Estuary Management. Colston Papers No. 30, Scientechnica, Bristol, 162–172.

Hibma A, De Vriend, HJ, Stive MJF. 2003. Numerical modelling of shoal pattern formation in well-mixed elongated estuaries. *Estuarine, Coastal and Shelf Science* 57(5-6): 981-991.

Hibma A, Stive, MJF, Wang ZB. 2004. Estuarine morphodynamics. *Coastal Engineering* 51: 765-778.

Instituto Hidrogr"afico, 1998. Portugal Continental Costa Oeste e Sul Cabo de Sao Vicente "a Foz do Guadiana. Bathymetric Chart, 1st Edition. Scale 1:150’000, Projection Mercator, International Ellipsoid, European Datum (Potsdam).

IPCC 2007. Climate Change 2007: The Physical Science Basis. Contribution of Working Group I to the Fourth Assessment Report of the Intergovernmental Panel on Climate Change, In Solomon S, Qin D, Manning M, Chen Z, Marquis M, Averyt KB, Tignor M, Miller HL. (eds.). Cambridge University Press, Cambridge, United Kingdom and New York, NY, USA.

Jeuken MCJL, Wang ZB, Keiller D, Townend IH, Liek GA. 2003. Morphological response of estuaries to nodal tide variation, In: International Conference on Estuaries & Coasts (ICEC-2003): 167-173.

Karunarathna H, Reeve D, Spivack M. 2008. Long-term morphodynamic evolution of estuaries: An inverse problem, *Estuarine, Coastal and Shelf Science* 77: 385-395

Kirwan ML, Murray AB. 2008. Ecological and morphological response of brackish tidal marshland to the next century of sea level rise. Westham Island, British Columbia. *Global and Planetary Change* 60: 471-486.

Lobo FJ, Dias JMA, González R, Hernández-Molina FJ, Morales JA. Díaz del Río V. 2003. High-resolution seismic stratigraphy of a narrow, bedrock-controlled estuary: the Guadiana estuarine system, SW Iberia. *Journal of Sedimentary Research* 73: 973-86.

Machado A, Rocha F, Gomes C, Dias J. 2007. Distribution and Composition of Suspended Particulate Matter in Guadiana Estuary (Southwestern Iberian Peninsula), Journal *of Coastal Research***,** Special Issue 50: 1040-1045.

Milne GA, Gehrels WR, Hughes CW, Tamisiea ME. 2009. Identifying the causes of sea-level change, *Nature Geoscience* 2: 471-478.

Morales JA. 1995. Sedimentologı´a del estuario del Rı´o Guadiana (S.W. Espan˜a-Portugal), Servicio de Publicaciones, Huelva University; 1-322.

Morales JA. 1997. Evolution and facies architecture of the mesotidal Guadiana River delta (S.W. Spain–Portugal). *Marine. Geology* 138: 127-148.

Morales JA, Delgado I, Gutierrez-Mas JM. 2006. Sedimentary characterization of bed types along the Guadiana estuary (SW Europe) before the construction of the Alqueva dam. *Estuarine, Coastal and Shelf Science* 70: 117-131

Morris JT, Sundareshwar PV, Nietch CT, Kjerfve B, Cahoon DR. 2002. Responses of coastal wetlands to rising sea level. *Ecology* 83: 2869-2877.

Pethick JS. 1994. Estuaries and wetlands: function and form. In: Thomas T. *Wetland Management*, London; 75-87.

Sampath DMR. 2008. Impact of Shoreline Retreat and Inundation due to Sea Level rise along the Coastline adjacent to the Guadiana Estuary, Portugal/Spain Border, MSc. thesis, University of Alagarve, Portugal; 1-93

Scubel JR, Carter HH. 1984. The estuary as a filter for fine-grained suspended sediment. In: V.S. Kennedy (Ed.) The estuary as a filter. Academic Press, NY; 81-105.

Stolper, D., 1996. *The Impact of sea-level rise on estuarine mangroves: Development and Application of a Simulation Model*. Honours Thesis, University of Sydney, Sydney; 1-90.

Stolper D., 2002. Modelling the Evolution of Estuaries and Their Intertidal Zones. Ph.D. Thesis, University of Sydney, Sydney; 1-189.

Temmerman S., Govers G., Wartel, S., Meire, P., 2004. Modelling estuarine variations in tidal marsh sedimentation: response to changing sea level and suspended sediment concentrations. *Marine Geology* 212: 1-19.

Townend IH., Wang ZB., Rees J., 2007. Millennial to annual volume changes in the Humber Estuary. *Proceedings of the Royal Society* 463: 837-854. DOI 10.1098/rspa.2006.1798.

Wolanski E., Chicharo L., Chicharo MA., Morais P., 2006. An ecohydrology model of the Guadiana Estuary (South Portugal) *Estuarine. Coastal and Shelf Science* 70: 132-143.

Chapter 3

Modelling of estuarine response to sea-level rise during the Holocene: Application to the Guadiana Estuary - SW Iberia

Sampath, D.M.R., Loureiro, C., Boski, T., Martins, F., Sousa, C., 2015. Modelling of estuarine response to sea-level rise during the Holocene: Application to the Guadiana Estuary - SW Iberia. Geomorphology. 232, 47-64**.**

ABSTRACT

This paper focuses on simulations of the morphological evolution of an estuary during sedimentary infilling that accompanied Holocene sea-level rise. The simulations were conducted using the Estuarine Sedimentation Model, which uses a behaviour-oriented approach, supported by the chronostratigraphy of the estuary's sedimentary sequence. Behaviour curves were computed to represent the relationship between the estuarine channel depth below maximum high tide and the net accretion at a given location relative to the average sedimentation rate of the estuary during the Holocene. The model was validated by comparing the observed present-day bathymetry of the Guadiana River Estuary, southeastern Portugal, with the corresponding simulated bathymetries for nine control sections across the estuary. The best fit between simulated and actual sediment surface elevations was obtained along the cross-sections in the sheltered, low-energy environments of the estuary. The accuracy of the sedimentary stratigraphy of the best-fit model was further established using 16 radiocarbon ages obtained from five boreholes in the estuary. The present approach is particularly suitable for simulating long-term morphological evolution in sheltered estuarine environments where tidally driven vertical aggradation dominates at centennial to millennium timescales. However, the accuracy of simulated sediment surface elevations and consequently the robustness of behaviour-type models based on Geographical Information System platforms can be enhanced by incorporating (i) the impacts of nearshore hydrodynamic processes and episodic flood events in highly energetic channels, and (ii) the impacts of cross-currents in meandering channel sections.

Keywords: Guadiana estuary; Hindcasting; Morphological evolution; Sea-level rise; Behaviour-oriented models

3.1 INTRODUCTION

An estuary is a semi-enclosed water body that is associated with a complex mosaic of ecosystems linking terrestrial and aquatic environments, including the subtidal, intertidal, and surrounding terrestrial habitats. These highly complex and diverse systems are sensitive to natural forcing, as generated by sea-level rise, and to human activities such as the development of harbours, shipping channels and recreational facilities (Lanzoni and Seminara, 2002). Estuaries are ephemeral features that during the eustatic sea-level rise of the last 15,000 years progressed along drowned fluvial valleys (Schubel, 1971; Perillo, 1995). Under natural sediment supply conditions, these estuaries have gradually adapted to the prevailing hydrodynamic conditions during the period of sea-level stabilization (Lanzoni and Seminara, 2002). According to Cooper et al., 2012, some evidence suggests that incised valley estuarine systems exhibit an adaptive capacity in response to sea-level rise (e.g. “keep-up” and “catch up” estuaries) while tending towards equilibrium conditions in which the local sea-level rise is balanced by the sediment accumulation (Stevenson et al., 1986; Nichols, 1989).

The morphological evolution of an estuary is the result of non-linear interactions between water, sedimentary processes, and bathymetry during both fluvial and marine flooding, which occur over a wide range of temporal and spatial scales (Hibma et al., 2004). According to Friedrichs et al. (1990), an increase in sea level in an estuarine system where the banks have curved profiles initially results in channel deepening and the expansion of accommodation space, thereby enhancing ebb and flood asymmetry (i.e., the difference between peak ebb and flood tidal currents). Consequently, more sediment from marine and/or fluvial sources enters the estuary, resulting in an increase in sediment deposition rates and a decrease in depth, thereby reducing the marine influence (Pethick, 1994; Anthony et al., 2002). If the sediment supply is unhindered, this feedback process will lead the estuary to achieve a new equilibrium state. Throughout the Holocene, estuarine systems migrated landwards in

response to sea-level rise in a two-stage feedback process (Townend and Pethick, 2002): (1) horizontal retreat of the seaward margins of salt marshes and upper mudflats, and (2) vertical accretion on the newly submerged surfaces because of increased accommodation space. If there is a decrease in sediment supply and/or rapid increase in sea-level rise above the adaptive capacity of the system, the feedback mechanisms may not be sufficient to maintain stable water depths in an estuary. Thus, according to the classification of Cooper et al. (2012), an estuary can turn into a 'give-up' estuary from its original behaviour of either a 'keep-up' or 'catch-up' estuary.

The coastal zone occupies 18% of the world's land surface and stretches over 842,000 km (Smith, 2005). Coastal plains and lowland river valleys have always been the most populated areas (Wolanski et al., 2004) in which human activities and associated infrastructure have increased steadily over the last several centuries (McGranahan et al., 2007). Dams that control the world's major rivers have reduced sediment supply to the shoreline by up to 90% (Syvitski et al., 2005), and shorelines have been further impacted by the construction of coastal defences and by land reclamation (Townend and Pethick, 2002).

Global vulnerability analyses by Nicholls et al. (2007) and IPCC (2007) have predicted an increased vulnerability of the coastal zone to sea-level rise, increased storminess, and climate change. Indeed, the assembled records of altimetric data from the TOPEX/Poseidon, Jason-1, and Jason-2 satellite missions indicate that the average rate of sea-level rise during the period 1993–2009 was 3.4 ± 0.4 mm/yr (Nerem et al., 2010), which is double the 1.7 mm/yr rate of the twentieth century.

The cumulative result of human activities and natural pressures is enhanced erosion, habitat loss, and increased flood risk to the coastal environment (Valiela, 2006). A substantial reduction in the amount of sediment supplied to estuaries reduces vertical accretion and decreases their capacity to keep pace with sea-level rise (Ganju and Schoellhamer, 2010). Such

constraints on the adaptive capacity of estuaries to sea-level rise will likely provoke a decrease in the area of wetlands and will affect their habitats in the near future. Many estuarine ecosystems have already lost part of their ability to adapt horizontally (Townend and Pethick, 2002) and vertically (Ganju and Schoellhamer, 2010) in response to sea-level rise. To accommodate these trends in coastal planning and territorial management, a better understanding of the long-term behaviour of an estuarine system is required. Adaptation strategies depend on the ability to integrate information about the geomorphology of the system, knowledge of Holocene estuarine evolution, and information about the forcing conditions such as sea-level rise and tidal conditions across a range of spatial and temporal scales (Townend, 2010). In particular, the early to mid-Holocene may be useful to understanding future sea-level change (PALSEA, 2010), because rates of eustatic sea-level rise during this period were in the order of 6 mm/yr or more (Stanford et al., 2011; Delgado et al., 2012). Such an acceleration in sea-level rise falls well within the range of recent predictions for the latter part of the twenty-first century (Pfeffer et al., 2008). However in contrast to the Holocene, impacts of rapid sea-level rise in the coming decades require consideration of substantial and widespread human intervention in coastal systems.

To complement field investigations that have described geomorphological history and sea-level change over the last 13,000 years in the Guadiana Estuary of southwestern Iberia (Boski et. al., 2008, 2002; Delgado et al., 2012), in the present study we take a formalised yet simple and idealized model approach based on the behaviour (i.e., the morphological evolutionary trends) of that system. The specific objectives of this study are: (*i*) to simulate the sedimentary infilling of the Guadiana Estuary palaeovalley due to eustatic sea-level rise during the Holocene, and (*ii*) to evaluate model outputs against previous geomorphological and post-glacial palaeoenvironmental reconstructions based on facies interpretation and ^{14}C dating. The simulations were performed using the Estuarine Sedimentation Model (ESM), which follows

a behaviour-oriented numerical modelling approach (Bruce et al., 2003) that complements process-based modelling (Townend, 2010).

3.2. STUDY AREA

The Guadiana River is 810 km long and traverses extensive rural areas in Spain and Portugal, including the mining areas of the Iberian Pyrite Belt (Delgado et al., 2012). The Guadiana Estuary (Fig. 3.1) is located along the southern border between Spain and Portugal. It is a narrow, deeply incised (ca. 80 m below present MSL), bedrock-controlled estuary experiencing the final stages of sediment infilling, which has led to an incipient coastal progradation (Boski et al., 2008). The estuary, which is ca. 50 km long, has a maximum channel width of 550 m and depths ranging between 5 and 17 m (Wolanski et al., 2006). In 2001, the total dammed area in the watershed increased to 89% with the construction of the Alqueva dam (Gonzalez et al., 2007). Because of the consequent shortage of silt supplied by the river, there has been a rapid decrease in the area of estuarine salt marshes (Sampath et al., 2011). In addition, the construction of jetties at the mouth of the Guadiana River in the 1970s has interrupted the dominant eastward-directed longshore drift. This has resulted in a reduction in the amount of marine sediment supplied to the estuary over the last 35 years. The disruptive effects of the jetties are clearly manifested on the Spanish margin of the estuary, where rapid shoreline retreat at an average rate of 3 m/yr occurred between 1996 and 2005, with a recorded maximum retreat of 4.8 m/yr (Sampath, 2008).

Before the construction of the Alqueva dam, the hydrographic regime of the Guadiana River was characterized by low flows in summer and episodic flooding events in winter. The estuary exhibits a semi-diurnal, meso-tidal regime with a mean range of approximately 2.5 m. The mean neap tidal range is 1.22 m and the mean spring tidal range is 2.82 m (Garel et al., 2009), with a maximum spring tidal range of 3.88 m (Sampath et al., 2011). Tidal wave

propagation in the estuary generates currents with velocities exceeding 0.5 m/s (Morales, 1997). The waves in this coastal region can be classified as medium- to low-energy waves, and in terms of frequency of occurrence, 49% of the waves represent Atlantic swells and 51% local sea waves. The mean annual offshore significant wave height is about 1 m with an average period of 4.7 s (Costa et al., 2001).

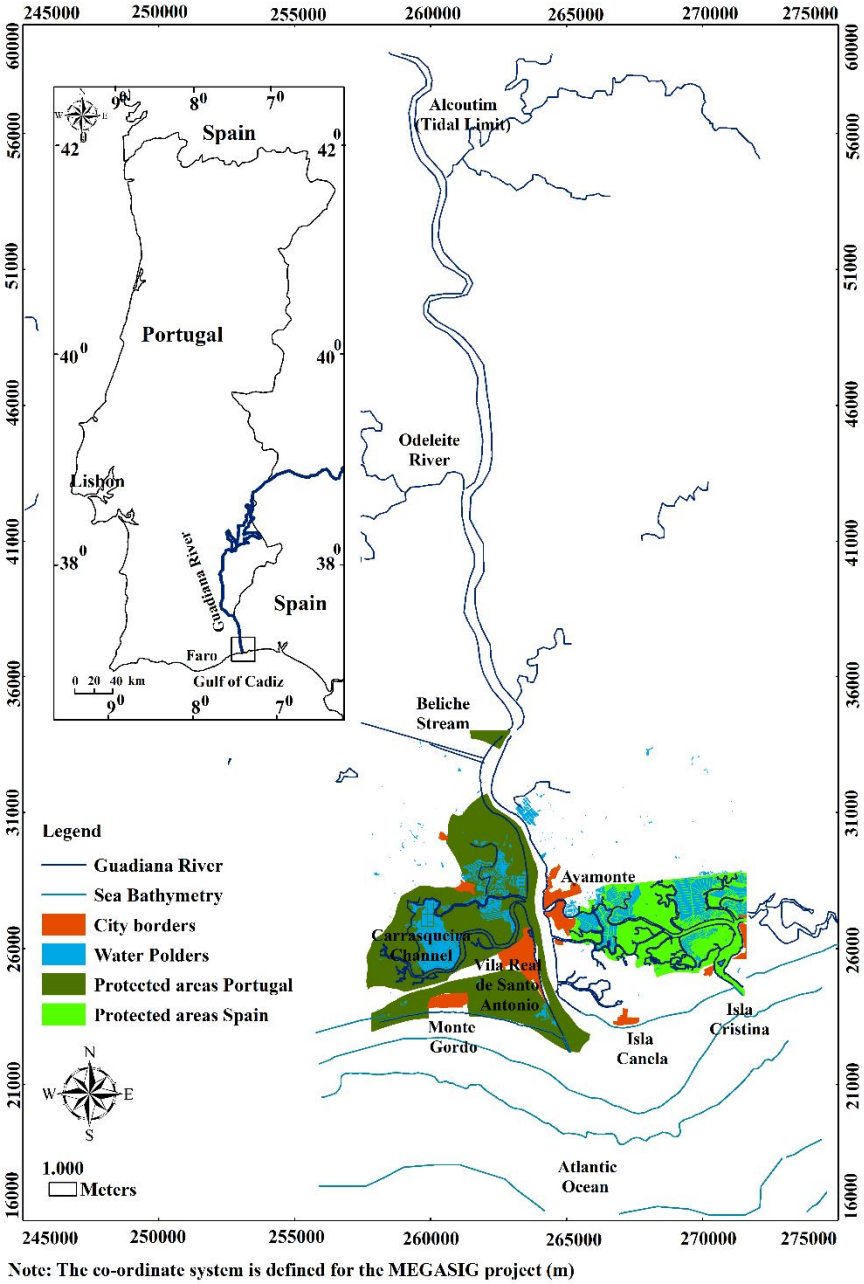

Figure 3.1 Location of the lower Guadiana Estuary.

3.3 METHODOLOGY

3.3.1 ESTUARINE SEDIMENTATION MODEL (ESM)

Hindcasting the morphological evolution of the Guadiana Estuary during the Holocene was performed using ESM. This GIS raster-based model was initially developed by Stolper (1996) and takes into account three factors: (1) changes in the rate of sea-level rise, (2) elevation-dependent accommodation space available for the deposition of sediment, and (3) the inundation-dependent vertical accretion rate of sediment (Bruce et al., 2003). In the context of large-scale coastal behaviour modelling (decades to millennia), estuarine evolution was simulated using the dominant driving factors, which are relative sea-level change, the rate of sediment supply, and tidal inundation. Although wave and river dynamics may influence sediment dynamics in the outer and inner portions of the estuary, respectively, tidal currents play a dominant role in controlling sediment transport in tidal regimes where the tidal range is greater than 2 m (Lanzoni and Seminara, 2002). Tidal inundation is strongly dependent on palaeovalley morphology, which determines the accommodation space for fluvial and marine sediments.

ESM does not explicitly take into account estuarine physical processes, such as tidal hydrodynamics, channel-shoal sediment exchange, and gravitational circulation. This implies that it is not possible to represent dynamic interactions and feedbacks that promote morphological change, because of the limited understanding/record of such processes over a centennial timescale. To partially overcome such limitations, we opted to represent estuarine sediment deposition processes using the net long-term representative sedimentation rates derived from borehole data analysis. In addition, we incorporated semi-empirical formulations given by Prandle (2009) to derive the relationships between the long-term net accretion rate coefficients and water depth below maximum high tide for defined time intervals of several centuries (see section 3.2). The long-term net accretion rate coefficients represent the spatial

and temporal distributions of sediment accretion below the maximum high-tide level of the estuary. With respect to the energy levels of the studied estuary, the lower Guadiana estuary lies within an environment sheltered by the extensive barrier and salt marsh system and mobile sandbank located close to the river mouth, which significantly attenuate ocean waves entering the estuary. Therefore, the sediment grain size across the lower estuary bed is practically uniform, except for some variation in the intertidal zone (Morales et al., 2006). Thus, according to the established relationship between hydraulic energy and corresponding grain size (Hamilton, 1979), the distribution of energy across the lower Guadiana Estuary may be assumed to be relatively uniform. The near-uniform distribution of sediment accretion rates observed in the sedimentary profiles of several boreholes drilled in the Guadiana Estuary (Boski et al., 2008, 2002) further supports this hypothesis.

3.3.2 APPLICATION OF ESM TO THE GUADIANA ESTUARINE SYSTEM

Following similar approaches in a number of previous estuarine aggradation models (e.g., Allen, 1995; Morris et al., 2002; Kirwan and Murray, 2008) applied to estuarine systems composed of intertidal mudflats and salt marshes, the rate of relative elevation change (dZ/dt) at a given point and over a known period of time can be represented in terms of (Eq. 3.1): (1) the rate of sea-level rise (dM_{MSL}/dt), (2) mineral sedimentation rate (dS_{Min}/dt) and organic sedimentation rate (dS_{Org}/dt), (3) erosion due to currents (dE/dt), (4) auto-compaction (dP_{Com}/dt), and (5) deep subsidence (dP_{Sub}/dt):

$$\frac{dZ}{dt} = \frac{dS_{Min}}{dt} + \frac{dS_{Org}}{dt} - \frac{dP_{Com}}{dt} - \frac{dM_{MSL}}{dt} - \frac{dP_{Sub}}{dt} - \frac{dE}{dt} \quad (3.1)$$

In the Guadiana Estuary, deep subsidence has been found to be negligible (Lobo et al., 2003), and because auto-compaction of the accumulated sediments is insignificant as a result of the low organic content (Boski et al., 2008), it was assumed that shallow compaction is

negligible over a centennial timescale. Hence, the determining factors of the model are mineral sedimentation, erosion, and the rate of sea-level rise (Eq. 3.2):

$$\frac{dZ}{dt} = \frac{dS_{Min}}{dt} - \frac{dM_{MSL}}{dt} - \frac{dE}{dt} \quad (3.2)$$

The net annual averaged accretion rate ($\Delta S/\Delta t$) at a given initial depth (h) can be derived by integrating mineral deposition and erosion over each tidal cycle over *M* years with *m* tidal cycles, where ρ_{sed} is the dry density of sediment (Eq. 3.3.). Based on the analysis of annual river discharge from 1947 to 2000, we imposed the estimated six-year (i.e., *M* = 6) cyclic fluctuations of average annual river discharge, namely 380, 300, 25, 75, 150, and 175 m^3/s, to determine the long-term net accretion rates. The calculations were computed for each depth with 0.5-m intervals from low-tide level to the maximum depth. This provides variations in net annual average accretion rates from low tide to the maximum depth.

$$\Delta S/\Delta t|_{\text{at a given location}} = \frac{1}{M \times \rho_{Sed}} \sum_{j=1}^{m} \left\{ \left(\frac{dS_{Min}}{dt} - \frac{dE}{dt} \right) dt \right\} \quad (3.3)$$

Implementation of ESM also requires the long-term net accretion rate coefficients, that is, the long-term net accretion rates relative to the maximum sedimentation rate found within a hypothetical transect from low-tide level to the maximum depth of the estuary (Eq. 3.4):

$$\text{Long-term net accretion rate coefficient} = \frac{\Delta S/\Delta t|_{\text{at a given location}}}{\Delta S/\Delta t|_{Max}} \quad (3.4)$$

If a representative value for the maximum annual sedimentation rate (S^{rep}) for a given period in an estuary can be found, the long-term net accretion rate coefficients enable the spatial distribution of net annual sedimentation rates for the given depth range to be calculated (Eq. 3.5). For simplicity and convenience, we used as S^{rep} the sedimentation rates calculated in radiocarbon-dated time intervals in six boreholes drilled into the Holocene sedimentary column

of the Guadiana estuary. Thus, the net accretion rate at a given depth below the low-tide level can be expressed directly by Eq. 3.5:

$$\frac{\Delta S_{Net}}{\Delta T} = S^{Rep}\left(\frac{\Delta S/\Delta t|_{\text{at a given location}}}{\Delta S/\Delta t|_{Max}}\right) \quad (3.5)$$

As given in Eq. 3.6, the net accretion rates above the low tide were derived by incorporating the tidal inundation frequency (Sampath et al., 2011) and the long-term net accretion rate coefficient at the low-tide level (taken from the Portuguese Hydrographic Chart Datum as 2 m below MSL). Consequently, the curves for the long-term net sediment accretion rate coefficients were computed for the entire depth range (i.e., from high-tide level to the maximum depth at 0.5-m intervals) of the estuary for different periods from 11,500 cal. yr BP. The average granulometric sizes of accumulated sediments were assumed to be indicative of the environmental conditions prevailing over specific periods during the Holocene (see section 3.3.4).

$$\left.\frac{\Delta S_{Net}}{\Delta T}\right|_{\substack{\text{Intertidal}\\ \text{zone}}} = S^{Rep}\left\{\frac{\Delta S/\Delta t|_{@\ z=-2\ m}}{\Delta S/\Delta t|_{Max}}\left[\frac{\text{Tidal Inundation Frequency}|_{@\ z>-2\ m}}{\text{Tidal Inundation Frequency}|_{@\ z=-2\ m}}\right]\right\} \quad (3.6)$$

Finally, the long-term rate of sediment surface elevation change ($\Delta Z/\Delta T$) at a given point of an estuarine system can be expressed in terms of net sedimentation rate ($\Delta S_{Net}/\Delta T$) and sea-level rise rate ($\Delta H/\Delta T$) (Eq. 3.7):

$$\frac{\Delta Z}{\Delta T} = \frac{\Delta S_{Net}}{\Delta T} - \frac{\Delta H}{\Delta T} \quad (3.7)$$

Summarizing the above rationale, our exact input parameters for the ESM model were the long-term net accretion rate coefficients for the depth range, representative sedimentation rates, and cumulative sea-level rise for the total time period of 11,500 years (and using a five-year time step for the modelling).

3.3.3 SEDIMENT DEPOSITION AND EROSION OVER A TIDAL CYCLE

The rate of sediment deposition in sub-tidal channels can be approximated by calculating accretion and erosion rates (Eq. 3.3). As the present study is focused on simulating the long-term morphological evolution of estuaries, the re-suspension of sediment due to turbulence can be neglected and therefore the estuary bed can be considered as fully absorptive (Sanford and Halka, 1993). Consequently, the sediment deposition rate (m/s) can be represented in terms of settling velocity (W_s), sediment concentration near the bed (C_b), and the bulk density of sediment (ρ_{sed}) (Prandle, 2009):

$$\frac{dS}{dt} = \frac{W_s C_b}{\rho_{sed}} \tag{3.8}$$

The settling velocity of fine to medium sand particles ($D_{50} \approx 0.125–0.35$ mm) was estimated in terms of the kinematic viscosity of water, average grain size diameter (D_{50}), and non-dimensional grain diameter (Hallermeier, 1981). The settling velocity of silt to very fine sand fractions ($D_{50} \approx 0.25–0.125$ mm) was derived using the formula of Lane and Prandle (2006) to account for the increase in settling velocity due to the flocculation of particles. Morales (1995) proposed an empirical model for estimating the depth-averaged sediment concentration in the Guadiana estuary in terms of river discharge (m^3/s). The suspended sediment concentration near the bed was related to depth-averaged sediment concentration where sediment deposition occurs via advection and dispersion (Prandle, 2009). The lack of knowledge of river flow rates during the Holocene is also a major constraint. To address this we used the oldest archived data measured in the Guadiana river, available from the Pulo do Lobo gauge station since the 1940s. Although limited in time, this record allows to represent the characteristic torrential river flow regime of the Guadiana river, which we assume to have been similar over the past millennia. Although we used data and relationships that relate to the

recent behaviour of the estuary for hindcasting suspended sediment concentrations in the Guadiana River during the Holocene, these formulae were used because our focus is to conceptualize the problem of the modelling of long-term estuarine morphological evolution. Prandle (2009) showed that time-series of C_b can be related to the depth-averaged sediment concentration in an estuary.

The short-term erosion rate in an estuary can be approximated using the simple formula of Prandle (2004), where γ and f are the sediment erosion coefficient and the bed friction coefficient, respectively:

$$\frac{dE}{dt} = \frac{\gamma f \rho_w (U_t)^2}{\rho_{Sed}} \quad (3.9)$$

The grain density was set to a default value of 2650 kg/m^3, representative of quartz. The expression derived by Jones (1983) was used to estimate the bed friction in terms of bed roughness, which can be related to drag resulting from ripple/dune formations, and the skin friction, which is related to the grain size, D_{50}, of coarse sand for a hydraulically rough flow (Reeve et al., 2004). Values of D_{50} have been given by Morales et al. (2006). As presented by Lane (2004), the main constituents of current speed (U_t) were assumed to be semi-diurnal (M_2) and quarter-diurnal (M_4) tidal currents and residual currents due to river discharge:

$$U_t = U^* \cos(\omega t) - aU^* \cos(2\omega t - \theta) - aU^* \cos\theta \quad (3.10)$$

where $a=\zeta^*/h$ and θ is the phase angle between tidal elevation and tidal current.

Prandle (2009) simplified the equations for motion at any depth by neglecting convective terms and linearising the frictional terms. Thus, the tidal current amplitude U* was presented for synchronous estuarine condition, where the spatial gradient in tidal elevation

amplitude (ζ^*) is zero and k is a unique wave number for the axial propagation of current and surface elevation:

$$U^* = \zeta^* g \frac{k}{(\omega^2+F^2)^{0.5}} \quad (3.11)$$

The linearised dimensionless bed friction coefficient (F) was related to the phase angle (θ) and tidal frequency (ω), and can be estimated using Eq. 3.12, where $\partial h/\partial x$ is the axial bed slope and assumed to be a constant, h is water depth, and g is gravitational acceleration (Prandle 2009).

$$\tan\theta = -\frac{F}{\omega} = \frac{\partial h/\partial x}{0.5hk} \quad (3.12)$$

where

$$k = \frac{\omega}{\sqrt{0.5hg}} \quad (3.13)$$

In the Guadiana Estuary, the tidal wave propagates in synchronic mode up to 50 km from the mouth (Morales 1997). This characteristic may be preserved even during spring tides, as the tidal-range attenuation is less than 20 cm per 10 km along the longitudinal axis of the river (Garel et al., 2009). The use of the above assumption can be justified because we consider only the lower Guadiana estuary (11.6 km). The tidal amplitude (ζ^*) was estimated using the amplitudes (ζ_i), angular frequency (ω_i), and phase (ϕ_i) of the five principal constituents (O1, K1, M2, S2, and M4) given by Pinto (2003) for the Guadiana Estuary.

3.3.4 HINDCASTING OF SEDIMENT INFILLING

There are two distinct linear relationships for radiocarbon ages versus depths of dated materials from six boreholes in the Guadiana estuary. The first comprehends the period from

13000 cal. yr BP to 7500 cal. yr BP and the second the period since 7500 cal. yr BP to present-day (Boski et al., 2002; Boski et al., 2008; Delgado et al., 2012). This suggests that the sediment accretion is almost linear in those two periods, particularly in the sheltered sections of the estuary. To determine the grain size of sediments deposited since 11.500 cal. yr BP, an analysis of sediment characteristics from borehole samples was performed. This allowed to define 12 granulometrically homogenous time intervals with millennial to centennial time scales, each characterized by constant depositional conditions. The sediment erosion coefficient, γ, is a function of sediment diameter (Lane and Prandle, 2006) and is related to the erodibility of sediment. Two different distributions for γ with depth were assumed while maintaining its average value around 0.0001 $m^{-1}s$, as suggested by Prandle (2004). In this way, variability in grain size across the estuary could be indirectly incorporated into the model. For each distribution of γ, we derived 12 long-term net accretion rate coefficient curves (Fig. 3.2) corresponding to time periods during which hydrodynamic and environmental conditions were assumed to be uniform throughout the Holocene period.

Four trials were carried out to find the best function for γ and the corresponding set of long-term net accretion rate coefficient curves. The representative sedimentation rates for the first trial were equal to the rate of sea-level rise derived from the analysis of borehole data (Table 1). However, two boreholes are located in a highly sheltered environment and are not, therefore, representative of the lower estuary as a whole. Consequently, trials two to four were performed using stratigraphic data from the remaining four boreholes to find representative sedimentation rates during the Holocene. Considering specifically the sea-level change since the last glacial maximum (LGM) along the southern Iberia coast, sea-level curves have been presented for coastal areas in the Gulf of Cadiz and in western Portugal (e.g. Dias et al., 2000; Delgado et al., 2012). According to the depth–age diagrams for the Guadiana estuary presented by Boski et al. (2002) and Fletcher et al. (2007), Holocene sedimentation began, respectively,

at depths of 42 m and 38 m below present MSL. Recently, Boski et al. (2008), considering the Guadiana and Gilão-Almargem estuarine systems, placed the beginning of Holocene sedimentation in the southeastern Algarve coast at a depth of 39 m below present MSL. These values are significantly greater than the 30 to 32 m below present MSL extrapolated from the age–depth diagram proposed by Lario et al. (2002) as a synthesis for the Spanish estuaries in the Gulf of Cadiz.

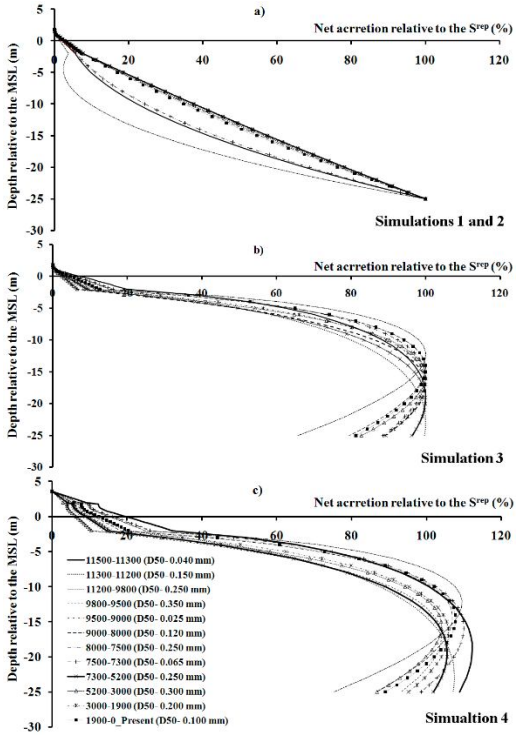

Figure 3.2 Long-term net accretion rate coefficients as a function of depth of the Guadiana Estuary, where (a) and (b) represent two different distributions of sediment erosion coefficients (γ) with depth, and (c) represents the distribution of γ with depth as in the case of (b) but with an additional proportion of net accretion observed at −0.75 m, which results in an equilibrium depth, compared with the observed equilibrium depth, of +2.0 m.

Therefore, considering various estimations of sea level at 11,500 cal. yr BP for the Guadiana estuary, a mean value of 40 m below present MSL was used for simulating the morphological evolution of the Guadiana estuary during the Holocene. In relation to sea-level change since the last glacial maximum (LGM) along the coast of southern Iberia, a sea-level curve has recently been presented for coastal areas in the Gulf of Cadiz and in western Portugal

by Delgado et al. (2012). The average rate of sea-level rise proposed for the period 13,000 to 7000 cal. yr BP was estimated at 7.5 mm/yr and the rate for the period since 7500 cal. yr BP until the present was estimated at 1.3 mm/yr. Such a pattern of sea-level rise is consistent throughout the northern Gulf of Cadiz, as evidenced by Zazo et al. (2008), and even along western Iberia Holocene sea-level rise is characterized by such contrasting linear trends of fast increase before and after 7000 cal. yr BP (Vis et al., 2008). For 11,500 cal. yr BP, the error on the position of sea level is approximately ±5 m. This value was estimated from the results of Delgado et al. (2012). The error contains the uncertainties of ^{14}C dating and the uncertainties of past sea-level determination with respect to MSL.

Table 3.1 Input data used to model Holocene sediment infilling in the Guadiana Estuary.

Simulation	Time (cal yr BP)	Set of net accretion curves (NAR)†	Sediment erosion coefficient (γ)	Sea-level rise rate (mm/yr) #	Sediment deposition rate (S^{Rep}) mm/yr
1	11500–7500 7500–0	1	$\gamma_1 = -2*10^{-7}z^2+9*10^{-6}z-6*10^{-6}$	7.5 1.3	7.5§ 1.3§
2	11500–7500 7500–0	1	$\gamma_1 = -2*10^{-7}z^2+9*10^{-6}z-6*10^{-6}$	7.5 1.3	8.5‡ 1.8‡
3	11500–7500 7500–0	2	$\gamma_2=6*10^{-8}z^2+7.8*10^{-6}z+2.7*10^{-5}$	7.5 1.3	8.5‡ 1.8‡
4	11500–7500 7500–0	3	$\gamma_2=6*10^{-8}z^2+7.8*10^{-6}z+2.7*10^{-5}$	7.5 1.3	8.5‡ 1.8‡

† See Figure 2.

Average value derived from data given by Boski et al. (2002) and Boski et al. (2008).

§ Derived from data given by Boski et al. (2008).

‡ Derived from data given by Boski et al. (2002).

The input and output time-steps were 5 and 10 years, respectively. The simulation of palaeovalley sedimentation from 11,500 cal. yr BP to the present was performed in several blocks with intervals of 100 or 200 years. The final digital elevation model (DEM) of the estuary's bathymetry in each preceding time-step was fed as input into the next step until reaching the present bathymetry. If the simulated elevation values of the DEM corresponding to the present of a particular trial were comparable to the actual elevation values of the present-day topography, then the corresponding series of bathymetries were considered to be the best possible approximation of the morphological evolution of the estuary for the period since 11,500 cal. yr BP. The corresponding γ and the set of long-term net accretion rate coefficient curves were accordingly considered the best functions for the simulations of long-term sediment infilling, providing a basis for decadal forecasting of the morphological evolution of the estuary during the twenty-first century.

3.3.5 DIGITAL TERRAIN MODEL OF THE PRE-INUNDATION GUADIANA PALAEOVALLEY

Exploratory DEMs were created with a suite of the most widely used interpolation methods (Yue et al., 2007; Erdogan, 2009), which are incorporated into the ESRI ArcGIS software used in the present study. Since there is no explicit rule indicating which method is most adequate for a particular surface (Erdogan, 2009), the selection of the interpolation method is more complex, requiring both visual and statistical exploration (Andrews et al., 2002). Methods included TIN (triangulated irregular network with linear interpolation), IDW (inverse distance weighted), Spline and Kriging. ANUDEM, a dedicated interpolation method for creating hydrologically correct DEMs (Hutchinson, 1988, 1989), and implemented in ArcGIS, was also used. As most interpolation methods require input data in the form of individual points, the manually digitized palaeovalley contours were transformed into point

features. Each vertex along the contour lines was converted into a point, retaining the corresponding planimetric coordinates and elevation value.

From simple visual observation, the TIN method was excluded for use due to its unrealistic representation of the terrain surface and overall shape unreliability, confirming the general inability of linear interpolation to produce a smooth and natural terrain surface (DeMers, 2002). The remaining interpolation methods were evaluated using cross-validation on a random sample of 10% of the data points (corresponding to 16,112 points). The differences between the interpolated and observed elevation values at each cross-validation point were analysed using standard descriptive statistics for the assessment of DEM accuracy (Fischer and Tate, 2006). The most common statistical descriptor is the root mean square error (RMSE) (Li, 1988; Fisher and Tate, 2006). Two other descriptors suggested by Li (1988), the mean error (ME) and error standard deviation (S), which are often used for a more complete statistical description of DEM interpolation error (Desmet, 1997; Fisher and Tate, 2006), were also calculated. The two extreme values for the difference between the interpolated and observed elevations (positive maximum and negative maximum) were also calculated, indicating the general location of all the other values (Li, 1988).

The results for the descriptive statistics indicated that no method clearly out-performed the others, although the IDW method presented the best results for the extreme values and ANUDEM the best (lowest) values for RMSE and error standard deviation (S). Nevertheless, the results are very similar for the suite of interpolation methods evaluated, with mean errors in the order of a few centimetres and values of RMSE and error standard deviation between 2 and 2.5 m. Thus, ANUDEM was used as the most reasonable interpolation technique for developing the DEM of the Guadiana estuary palaeovalley of 11,500 cal. yr BP (Fig. 3.3).

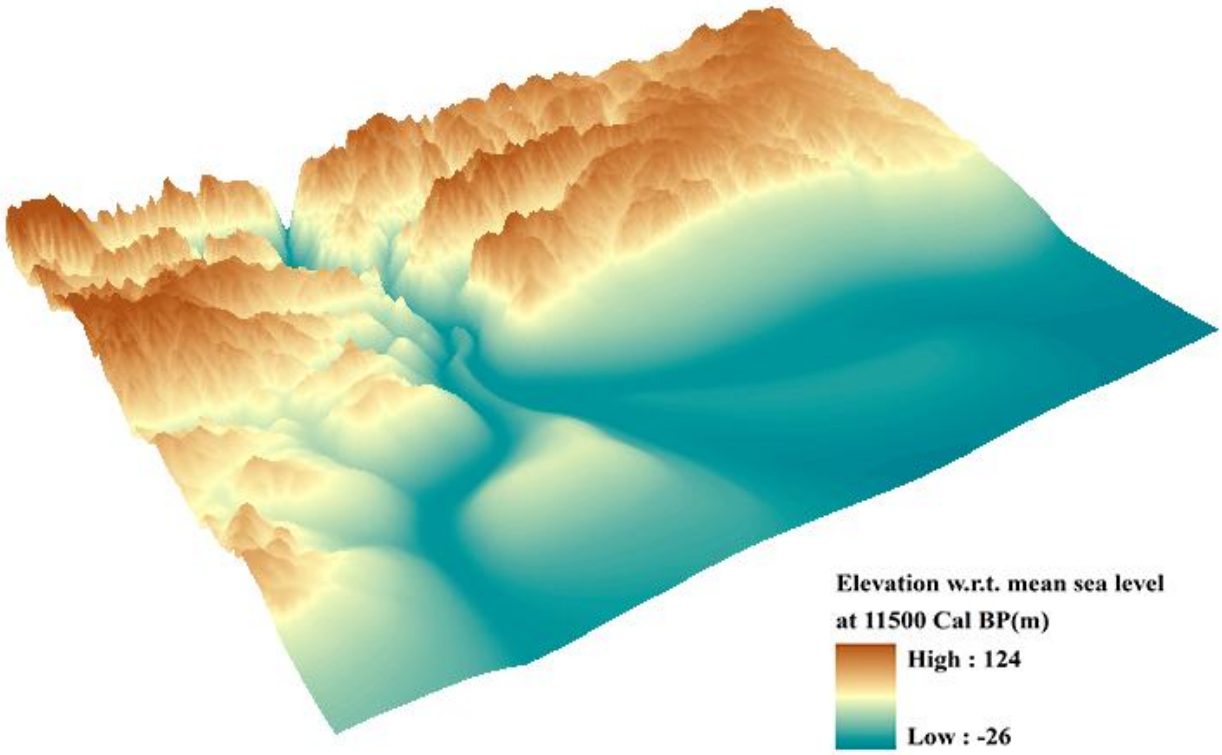

Figure 3.3 Three-dimensional view of the reconstructed palaeovalley of the lower Guadiana Estuary at 11,500 cal. yr BP.

3.4 RESULTS

3.4.1 MORPHOLOGICAL EVOLUTION OF THE ESTUARINE PALAEOVALLEY DURING THE HOLOCENE

The model-generated DEMs of the present topography in the lower Guadiana Estuary corresponding to each of the four simulation trials are shown in Fig. 3.4. The reconstructed palaeovalley DEM at 11,500 cal. yr BP (Fig. 3.4a) and actual present DEM (Fig. 3.4b) were used for assessing the simulated results. The first simulation of present-day topography (Fig. 3.4c) extensively under-predicted the actual topography of the estuary. The only similarity between these two surfaces was in the elevation range from 4 to 5 m.

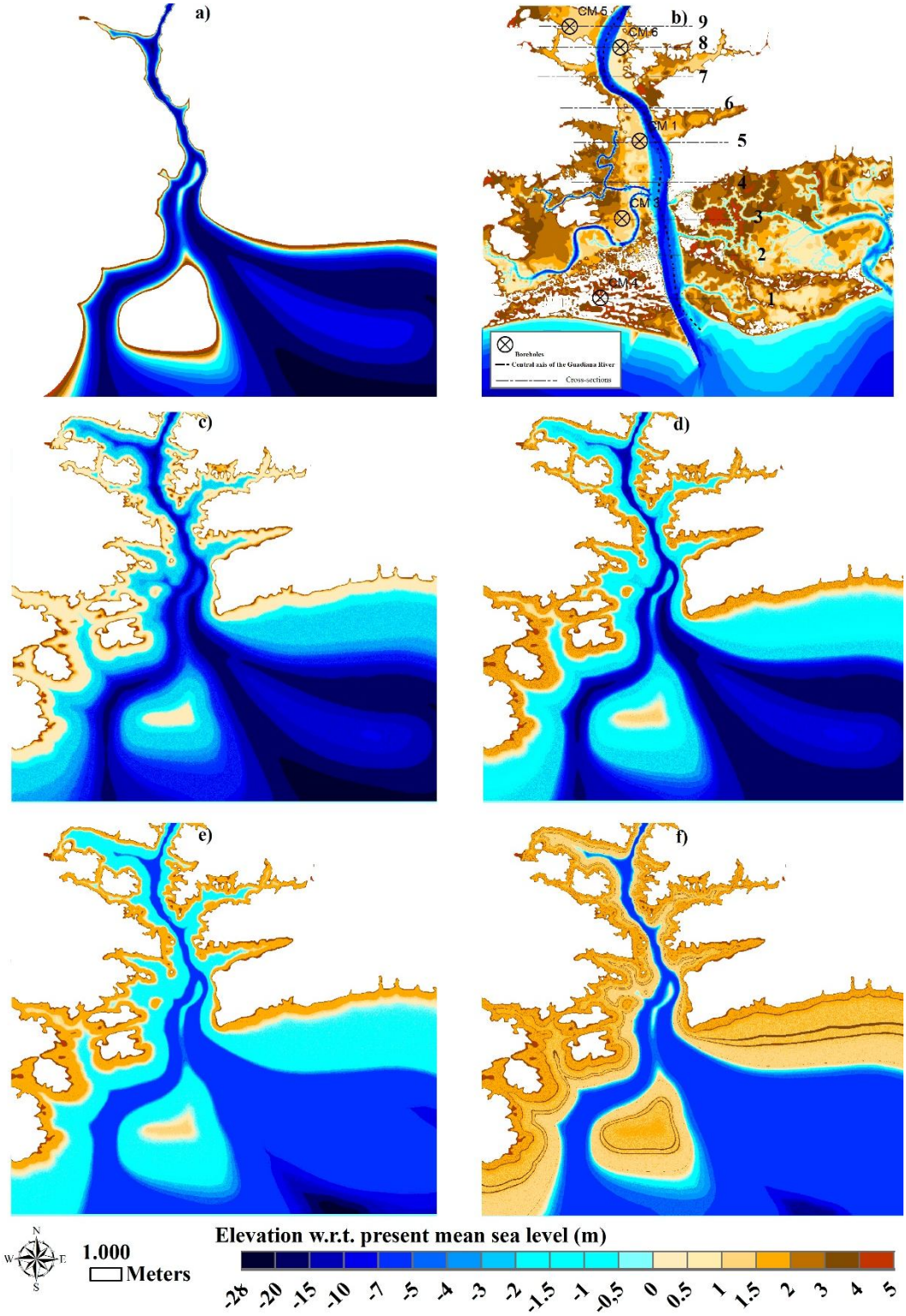

Figure 3.4 Comparison of palaeovalley simulation results corresponding to 0 cal. yr BP with the present-day bathymetry derived from topo-bathymetric surveying in 2000 AD: (a) the palaeovalley of 11,500 cal. yr BP; (b) present-day bathymetry; (c), (d), (e), and (f) simulated present-day bathymetry under simulation runs 1, 2, 3, and 4, respectively.

Various important features of the Guadiana estuarine system, including the morphological evolution of the intertidal zone area, the closure of the second mouth of the Guadiana river due to sand infilling, the morphological evolution of the Vila Real St Antonio delta, and the sand-spit developments of Isla Canela and Isla Cristina resulting in the progradation of the Spanish coastline, were not predicted satisfactorily in the first simulation. Even though high sedimentation rates (see Table 3.1) were used in the second simulation, the simulated topography (Fig. 3.4d) was still under-predicted and very similar to the results of the first simulation. However, there were some improvements in the upper limits of the intertidal zone compared to the actual elevations, despite a continuing submergence of a large part of the delta located near present-day Vila Real city. The complete closure of the second mouth of the Guadiana River, located near present-day Monte Gordo city, was also not satisfactorily simulated.

The simulated present topography of the estuary obtained in the third simulation (Fig. 4e) shows increased sediment infilling in both the intertidal zone area and the ebb delta close to present-day Vila Real de Santo Antonio city (VRSA). However, this simulation still did not satisfactorily predict the actual morphology of the Guadiana Estuary. This third stimulation presented an equilibrium between the reconstructed Holocene sediment surface topography and simulated topography at a depth of approximately −0.75 m (i.e., the estuary bed at around −0.75 m kept pace with sea-level rise). Spatial analysis shows an equilibrium between actual topography and the Holocene topography in the high-tide region (around +1.6 to + 2 m MSL).

As explained in section 3.3.4, the results of the fourth simulation correspond to corrected (i.e., forcing equilibrium near the high-tide region) sedimentation rate coefficients compared with the third simulation. This enabled a realistic sediment infilling in both the intertidal zone and part of the main estuarine channel to be achieved (Fig. 4f), and reflected the new relationship between the long-term net accretion rate coefficients and the depth below

maximum high tide, leading to a realistic improvement in the simulated shoreface. However, the closure of the second mouth of the Guadiana River and the development of the Isla Canela and Isla Cristina sand-spits were again not adequately predicted. Despite an improvement in the area of the VRSA delta, the evolution of the interface between the estuary and shoreface could not be simulated simply by using this idealized aggradation model. It appears that this highly dynamic boundary follows a complex interplay between tidally driven estuarine vertical aggradation and shoreface processes controlled by both along- and cross-shore sediment drift, resulting in the development and migration of sand spits and subsequent aeolian dune formations.

3.4.2 DETAILED ANALYSIS OF SEDIMENT INFILLING IN THE 4TH SIMULATION

The fourth simulation was particularly successful in predicting the present-day elevation/morphology of the sheltered environments of the Guadiana estuary. Fig. 3.5 shows a chronological sequence of sediment infilling along a selected line connecting five boreholes (marked as CM-4, CM-3, CM-1, CM-6 and CM-5 according to their spatial location upstream the estuary mouth) drilled in the Portuguese margin of the estuary. Locations of five boreholes are also shown in Fig. 3.4b. The validity of this modelling approach was further tested using nine cross-sections along the main channel, located at distances of 650 m (CM-4), 2100 m, 3300 m (CM-3), 4500 m, 5800 m (CM-1), 7000 m, 8500 m, 9600 m (CM-6), and 10,400 m (CM-5) m from the mouth of the estuary (Fig. 3.6). Ages obtained from radiocarbon (^{14}C) analysis corresponding to the five boreholes (Boski et al. 2008, 2002; Delgado et al., 2012), are also plotted on Fig. 3.6. Each cross-section consists of 14 profiles, corresponding to profiles at 11,500, 11,000, 10,000, 9000, 8000, 7000, 6000, 5000, 4000, 3000, 2000, and 1000 cal. yr BP, and to the simulated and actual profiles for the present-day.

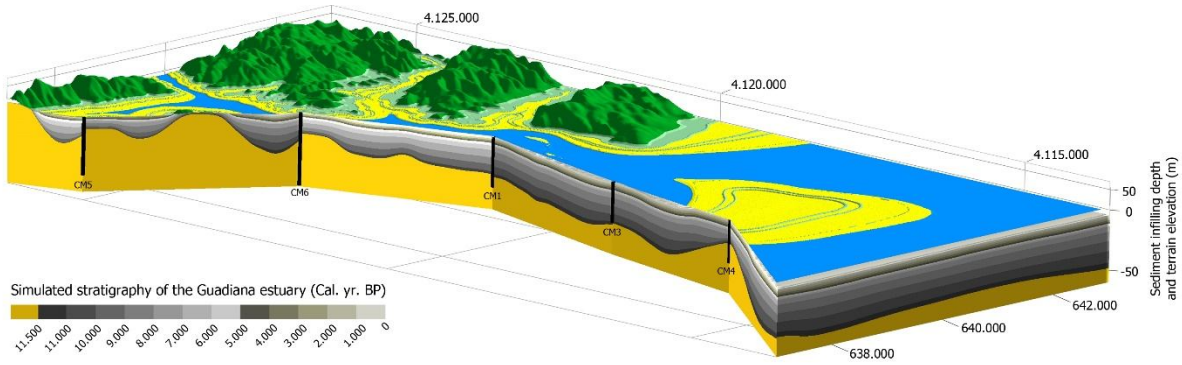

Figure 3.5 Three-dimensional sketch of sediment infilling over the Guadiana estuary palaeovalley from 11,500 cal. yr BP to the present (fourth simulation).

Detailed analysis of sedimentological, mineralogical, paleontological and geochemical data were used to interpret the various sub-environments in the sedimentary columns of the five boreholes, for which details are provided in Boski et al. (2002; 2008) and Delgado et al. (2012). In cross-section 1, borehole CM4 is located approximately 2500 m from the central axis of the estuary channel and on the Monte Gordo dune field (Figs. 3.1 and 3.6i). Seven sedimentological units can be distinguished in the sedimentary column overlying the Palaeozoic substratum (Boski et al., 2002): (1) fluvial from 31 to 27 m below MSL, (2) salt marsh from 27 to 23 m below MSL, (3) swamp/fluvial wetland from 23 to 20 m below MSL, (4) delta fan from 20 to 14 m below MSL, (5) fluvial river channel from 14 to 11 m below MSL, (6) barrier complex from 11 m below MSL to 3 m above MSL, and (7) dune field from 3 to 5 m above MSL (Fig. 3.7a). The depths corresponding to ages obtained from borehole CM-4 are discordant with the simulated depths. As this borehole is close to the shoreline, along-shore and cross-shore sediment transportation would be the dominant processes that determined the formation of the barrier complex at least until c. 6437 cal. yr BP. Ages obtained from radiocarbon analysis corresponding to the five boreholes (Boski et al. 2008, 2002; Delgado et al., 2012), are also on Fig. 3.6, 3.7, 3.8 and 3.9 and fully presented in Table 3.2.

Table 3.2: Summary information for ^{14}C age determinations showing conventional age, δ13C‰, 2 σ range and indicative ages used in the text and Fig. 3.6, 3.7, 3.8 and 3.9.

Borehole/ Sample	Depth MSL (m)	Material	Method	^{14}C Age (yr BP)	δ13C‰ (PDB)	Cal. yr BP 2σ		Indicative Age cal. yr BP
CM1.1	7.87	*C. glaucum*	AMS	3360 ± 31	0.64	3128	3332	3210
CM1.2	8.24	*C. glaucum*	β radiometric	5020 ± 310	1.1	4523	6028	5837
CM1.3	17.12	Peat	β radiometric	6210 ± 220	-25.9	6567	7560	7155
CM1.4	18.60	*C. edule*	AMS	6210 ± 40	2.08	6539	6765	7175
CM1.5	21.27	*C. angulata*	β radiometric	7590 ± 100	20	7855	8282	8848
CM1.6	28.50	*C. glaucum*	β radiometric	8430 ± 380	n/a	8153	10001	9420
CM1.7	36.06	*C. glaucum*	AMS	9500 ± 70	n/a	10209	10510	10765
CM3.1	4.59	*C. angulata*	β radiometric	3300 ± 160	n/a	2749	3496	3598
CM3.2	9.60	*C. angulata*	β radiometric	6710 ± 120	1.6	6951	7454	7594
CM3.3	14.52	*C. angulata*	β radiometric	7080 ± 200	0.7	7201	7951	7936
CM3.4	26.90	Wood	β radiometric	9470 ± 250	-22.9	9968	11601	10738
CM4.1	3.00	*V. nux*	β radiometric	6200 ± 340	1.6	5927	7377	7159
CM4.2	5.75	*S. plana*	β radiometric	5640 ± 90	-0.31	5866	6257	6437
CM4.3	11.75	*C. gibba*	β radiometric	6250 ± 250	1.4	6183	7265	7208
CM5.1	3.33	*S. plana*	AMS	3375 ± 39	-2.9 ± 0.2	3131	3354	3220
CM5.2	5.79	*Venerupis*	AMS	4295 ± 35	n/a	4295	4519	4408
CM5.3	8.90	*C. glaucum*	AMS	6764 ± 45	0.2 ± 0.2	7196	7401	7600
CM5.4	13.45	*Venerupis*	AMS	7585 ± 35	n/a	7958	8143	8017
CM5.5	17.75	*Cardium*	AMS	7725 ± 45	n/a	8063	8313	8169
CM5.6	20.95	Wood	AMS	8256 ± 55	-25.3 ± 0.2	9033	9423	9310
CM5.7	42.70	Wood	AMS	10273 ± 66	-25.5 ± 0.2	11768	12372	11448
CM5.8	47.67	Wood	AMS	10990 ± 40	-25.7	12857	13030	12991
CM6.1	2.00	Organic matter	AMS	830 ± 30	-28.1	686	789	742§
CM6.2	3.10	Organic matter	AMS	1000 ± 45	-31	792	981	897§
CM6.3	4.50	Organic matter	AMS	1215 ± 35	30.6	1059	1189	1155§
CM6.4	14.03	Peat	AMS	6060 ± 50	-25.96	6752	7155	6917§
CM6.5	21.2	*Venerupis*	AMS	7150 ± 50	-8.36	7518	7725	7612§
CM6.6	52.45	Wood	AMS	11110 ± 40	-28.9	12792	13131	13018§
CM6.7	55.00	Organic matter	AMS	11370± 50	-46.01	13125	13357	13265§

Note: § indicates the mean value (Delgado et al., 2012) while other indicative ages are median values (Boski et al., 2002; 2008)

Throughout the text cal. yr BP refer to the median or mid-point date for the two sigma range determined from calibration analysis. For full description of the uncertainty in the radiocarbon ages the reader is referred to Table 2. However, being close to the shoreline, the location of the borehole would have been subjected to episodic extreme events such as storm surges. In such situations, soil layers may not necessarily be in proper chronological sequence in borehole CM-4, and this may explain why the radiocarbon date of c. 7159 cal. yr BP is found above the radiocarbon date of c. 6437 cal. yr BP. Finally, aeolian processes would be the dominant controlling factors of sediment infilling. The discrepancy in the chronology between the measured and modelled infilling is because the above-mentioned processes were not included in the ESM model.

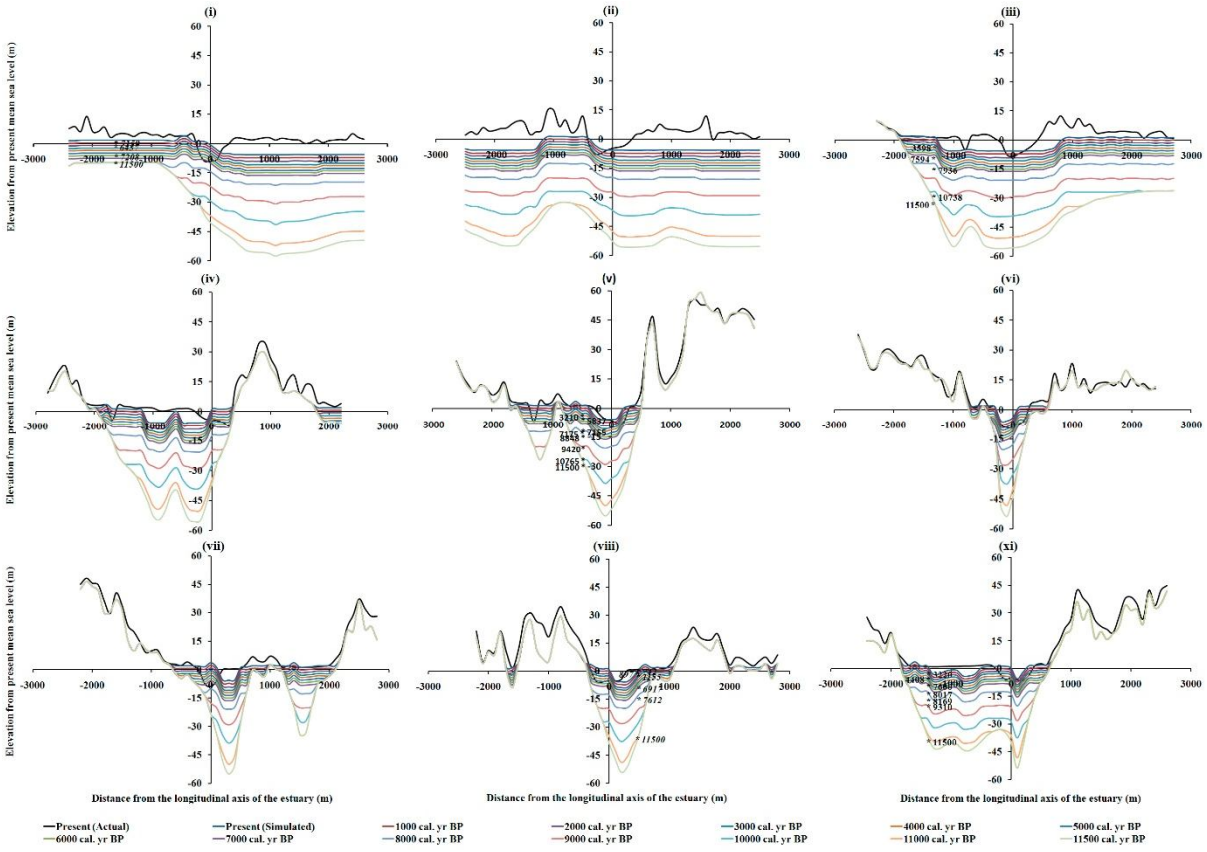

Figure 3.6 Simulated curves of sediment infilling in the Guadiana estuary from 11,500 cal. yr BP to the present and comparison with actual present-day cross-sections.

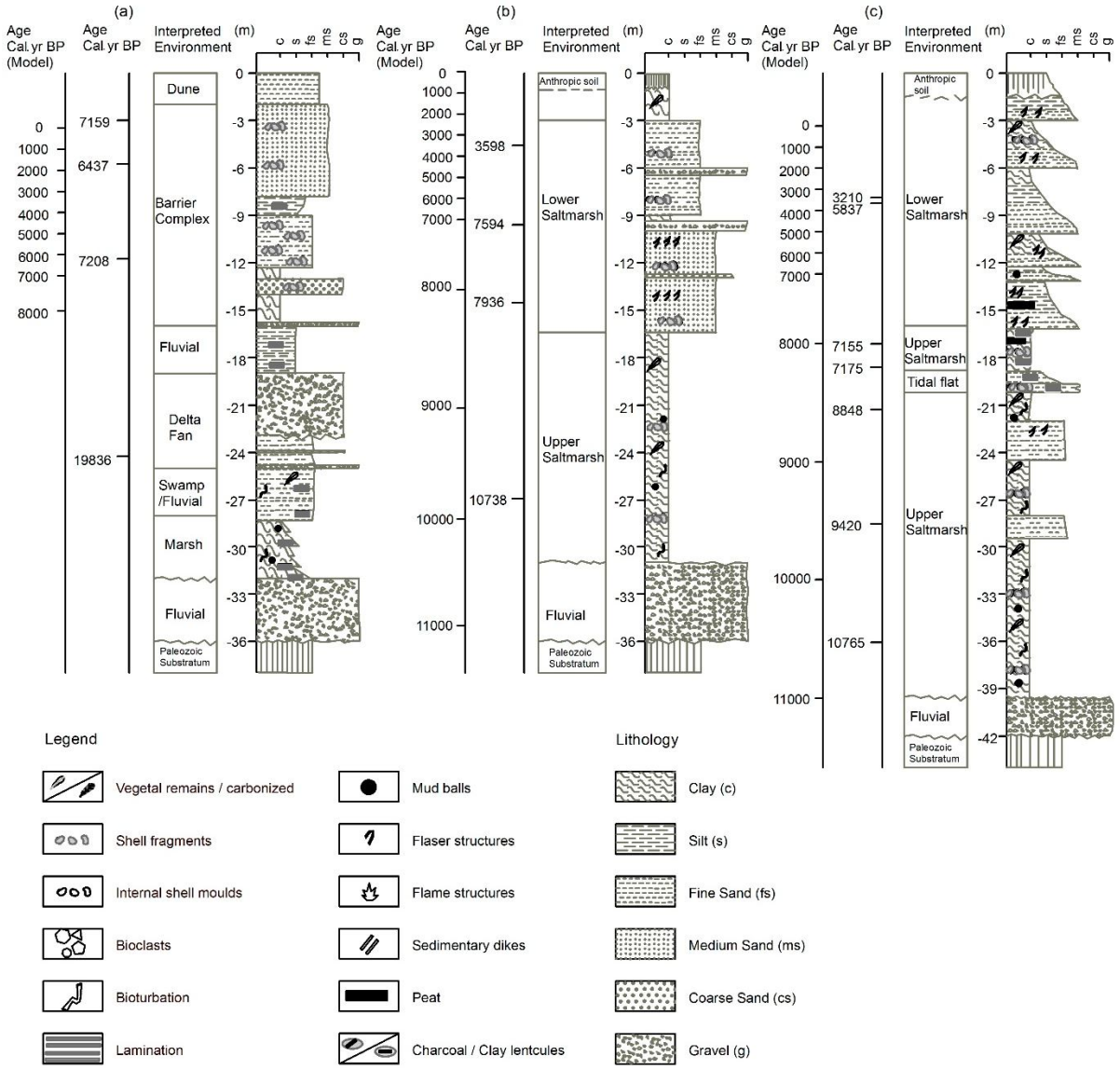

Figure 3.7 Lithostratigraphic sequences of boreholes a) CM-4 (Section 1); b) CM-3 (Section 3); and c) CM-1 (Section 5), showing sedimentary units and comparison of depths for ages obtained from radiocarbon (^{14}C) analysis and model simulations (Adapted from Boski et al., 2002).

In cross-section 3, borehole CM-3 was located close to the river mouth at 11,500 cal. yr BP in the Portuguese margin and approximately 1300 m from the central axis along the estuary channel. The borehole is within the salt marsh affected sporadically by spring tides, and four units of sedimentological facies lying over the Palaeozoic substratum reached at a

depth of 35 m can be identified (Boski et al., 2002): (1) fluvial river channel from 35 to 29.8 m below MSL, (2) upper salt marsh from 29.8 to 15.5 m below MSL, (3) lower salt marsh from 15.5 to 1.8 m below MSL, and (4) present anthropic soil from 1.8 m below MSL to 1.0 m above MSL (Fig. 3.7b). The simulated and actual present topographies are compatible with each other in the location of borehole CM-3 in cross-section 3. Infilling depths for radiocarbon ages of c. 3598, 7594, and 7936 cal. yr BP are comparable with corresponding simulated depths whereas the depth value for c. 10738 cal. yr BP shows a shift to a depth corresponding to that for c. 9815 cal. yr BP (Fig. 3.6iii).

Borehole CM-1 is located in cross-section 5 and is situated in the tidally active salt marsh near Castro Marim. According to Boski et al. (2002), five lithological units can be distinguished above the bedrock at a depth of 41 m below MSL, namely: (1) fluvial river channel from 41 to38 m below MSL, (2) upper salt marsh from 38 to 19 m below MSL, (3) tidal flats from 19 to 18 m below MSL, (4) upper salt marsh from 18 to 15 m below MSL, and (5) lower salt marsh from 15 to 1 m below MSL. In addition, there is a 1-m-deep anthropic soil layer up to the surface (Fig. 3.7c). The simulated and observed present topographies are compatible with each other in the location of borehole CM-1 (Fig. 3.6vi). The depth values for c. 10,765, 9420, 8848, and 3210 cal. yr BP are comparable with those of the simulated depths, whereas the depth values at c. 7175, 7155, and 5837 cal. yr BP cannot be matched to corresponding simulated depth values. The continuity of the upper salt marshes has been disturbed by the deposition of a ~1-m-thick layer of medium sand, forming a tidal flat for a short period.

In cross-section 8 (Fig. 3.6viii), borehole CM-6 is located on mudflats in the Spanish margin and is 500 m from the central axis (near the Beliche bend of the Guadiana River). Sedimentary sequences of borehole CM-6 have accreted on top of a coarse to very coarse basal gravel layer (Fig. 3.8a) that was deposited by the Guadiana River during a past marine lowstand

(Delgado et al., 2012). Although the simulated and actual present topographies are compatible with each other, only two depth values (at c. 897 and 1155 cal. yr BP) approximate the corresponding simulated values, whereas depth values at c. 742, 6917, and 7612 cal. yr BP are not comparable to their respective simulated depths.

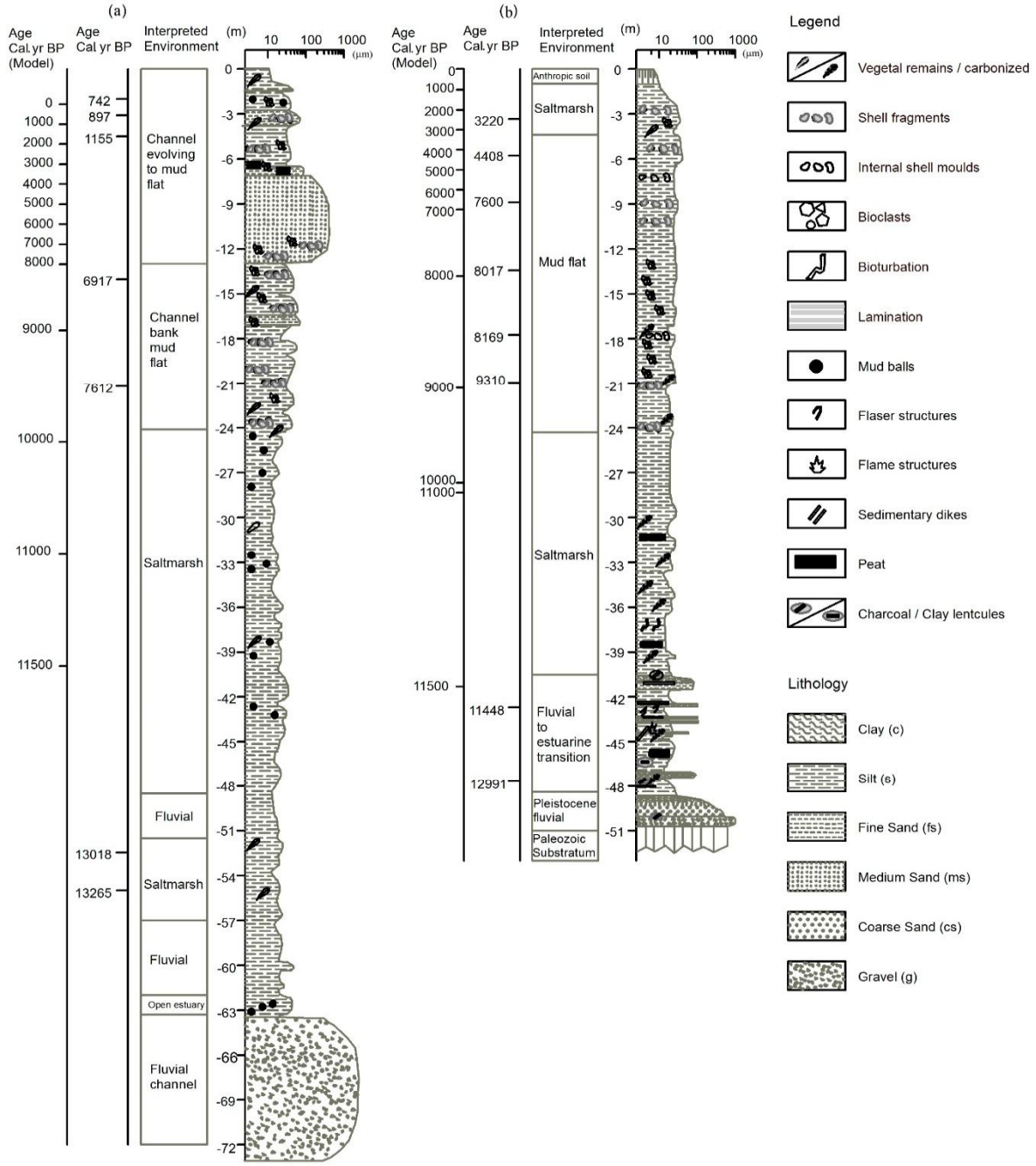

Figure 3.8 Lithostratigraphic sequences of boreholes (a) CM-6 (Section 8); and (b) CM-5 (Section 9), showing sedimentary units and comparison of depths for ages obtained from radiocarbon (^{14}C) analysis and model simulations (Adapted from Delgado et al., 2012).

The sedimentary facies in borehole CM-6 from 11,500 cal. yr BP to the present represent a transition from fluvial river channel to salt marsh and then to a mudflat (Delgado et al., 2012). According to the observed sediment granulometry from c. 6917 cal. yr BP to the present, at least three episodic extreme events may have occurred during this period, and may explain the discordance of the depths at c. 7612 and 6917 cal. yr BP with the corresponding simulated values. However, there is an additional process around bends in rivers and channels that should be considered. Cross-currents in channels produce higher elevations near the outside curve of the channel and low flow near the inside curve of the channel. In such a situation, eddy currents would occur, resulting in a loss of energy. As a result, there would be an increase in sediment deposition near the inside curve of the channel. However, increase of inundation hydroperiod due to elevated water depths near the outside curve of the channel results in increasing current velocity and erosion. This process may explain why the path of the Guadiana estuary profile migrated towards the Portuguese margin while enhancing fluvial sediment deposition in the inner region. Because such processes were not included in the ESM, we may not be able to expect complete agreement between the simulated and observed depositional facies.

In section 9, the most landward borehole, CM-5, is located near the Beliche Rivulet in the Portuguese margin. As in borehole CM-6, sedimentary sequences have accumulated on top of a coarse to very coarse basal gravel layer, which was deposited by the Guadiana River during a past marine lowstand (Delgado et al., 2012). According to Boski et al. (2008), depositional facies can be identified, related to (1) a transition from fluvial river channel to estuarine channel from 47.1 to 39.3 m below MSL, (2) salt marsh from 39.3 to 23 m below MSL, (3) mudflat from 23 to 2.7 m below MSL, (4) salt marsh from 2.7 m below MSL to 0.5 above MSL, and (5) a 1-m-thick layer of anthropic soil from 0.5 m above MSL to the present surface (Fig. 3.8b).

Depth values for the ^{14}C ages can be compared to the corresponding simulated depths. The successful comparability in the present case may be attributed to the sheltered nature of the location of borehole CM-5. In summary, infilling depths related to 16 age determinations are approximately compatible with the corresponding depths simulated using the ESM model, whereas 10 are not. A comparison between the depths and radiocarbon ages of 26 samples and the modelled depths for the same temporal waypoints (Fig. 3.9) demonstrates a very good agreement, with statistical significant correlation at the 0.01 confidence level and a R^2 value of 0.722. This indicates a high accuracy, particularly considering the uncertainties in modelling sedimentation on millennial time scales.

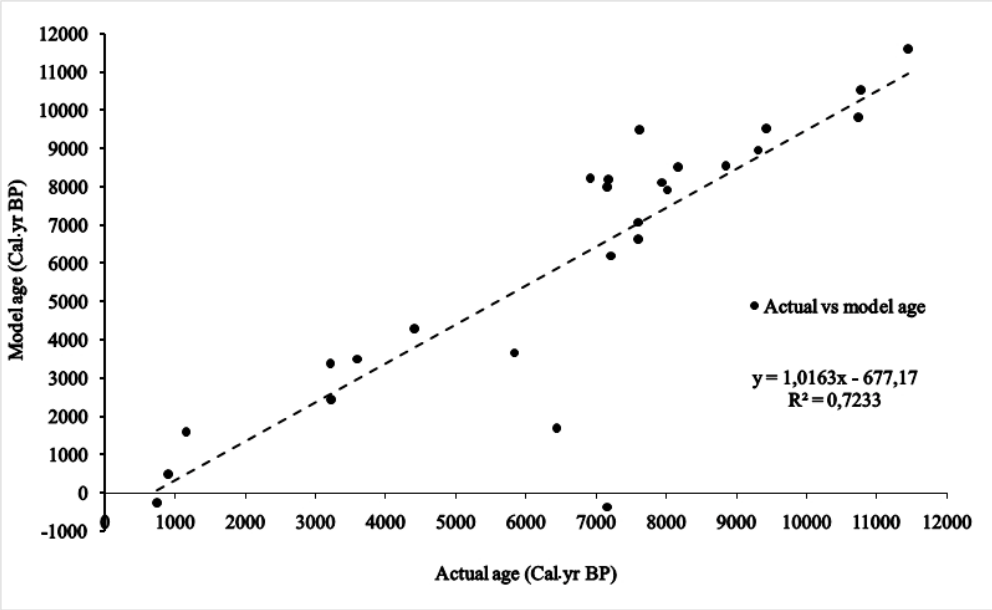

Figure 3.9 Radiocarbon ages of sampled material from the five boreholes in the Guadiana estuary and the equivalent modelled age for the same depths obtained from the simulation of the sediment infilling of the Guadiana estuary.

On the whole, the Portuguese and Spanish margins in cross-section 1 of the simulated profile have to be infilled with sediment by approximately 2.4 and 7 m, respectively, to be compatible with the actual present profile. However, the simulated sub-tidal region of the

estuary was overfilled by about 3.7 m of sediment. There are similar inaccuracies in cross-sections 2, 3 and 4. The errors may have occurred as a result of the formation of sand dunes near to the coastline. However, the average errors in cross-sections 5, 6 and 7 are less than 1 m. Furthermore, the meandering of the main channel of the estuary may have contributed to inaccuracies in the sub-tidal regions of cross-sections 4 to 7. On average, the modelled present-day profiles of cross-sections 8 and 9 have to be infilled with approximately 2.5 m of sediment to make them compatible with the corresponding actual present-day profiles. However, the incompatibilities are seen mainly for the higher elevations, where there is no influence of tides or waves. Therefore, it would appear that the errors are associated mainly with the initial inaccuracies involved in reconstructing the palaeovalley of 11,500 cal. yr BP. The other possible source of error in the sub-tidal region of the estuary is channel dredging for navigation purposes or channel scour/avulsion processes that cannot be captured in the modelling.

3.5 DISCUSSION

3.5.1 ACCURACY OF THE MODEL RESULTS

Stratigraphic sequences provide empirical records of global environmental conditions and changes (Burke et al., 1990). Studies of the magnitude and frequency of past global changes can be used to understand historical trends and to predict near-future conditions (Blum and Törnqvist, 2000). In this context, an understanding of past and present trends in sea-level rise is particularly important for simulating the morphological evolution of coastal areas using a behaviour-oriented modelling approach. For the present study, the definition of the mean sea-level for the start of the Holocene, considering that this occurred at 11,500 cal. yr BP (Bjorck et al., 1998), was based on published regional relative sea-level curves along with published information on discrete relative sea levels and sediment accumulation rates along the Cadiz Gulf during the Late Pleistocene to Holocene transition.

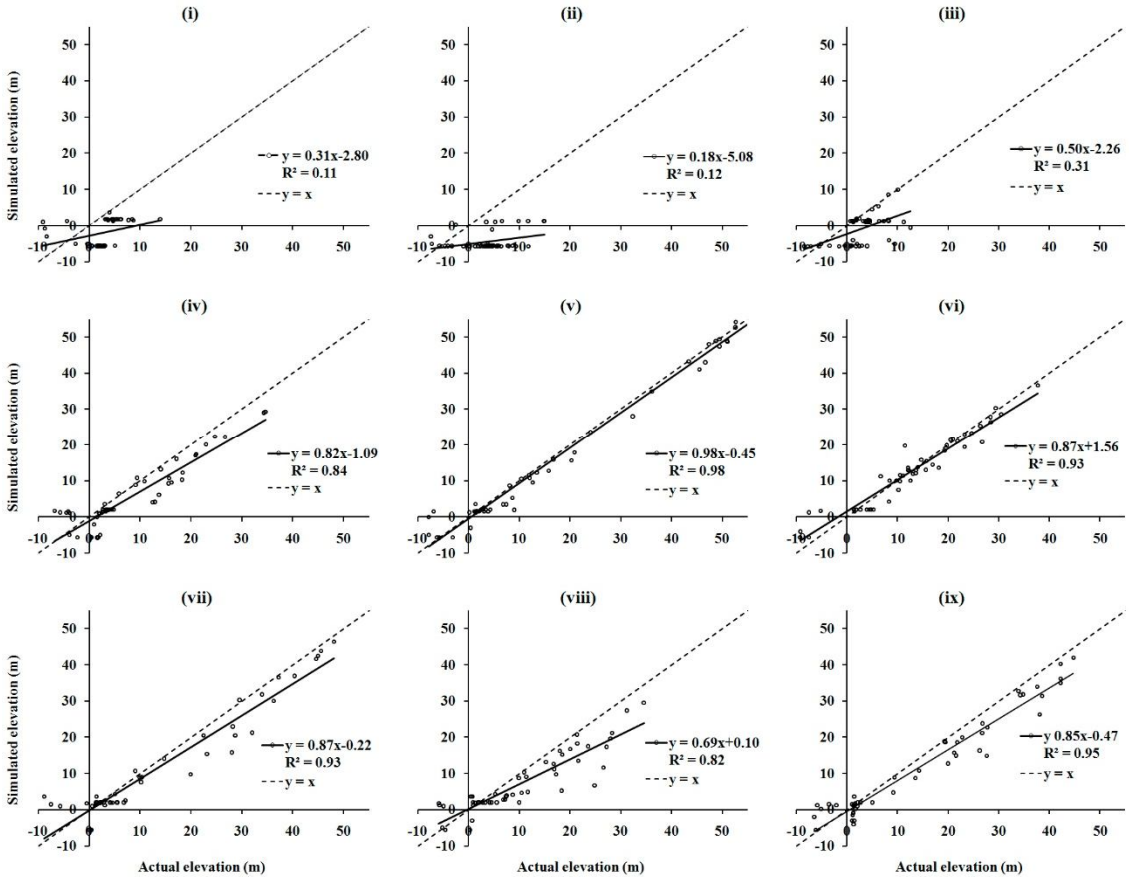

Figure 3.10 Comparison of simulated and actual (observed) elevations for nine cross-sections along the Guadiana estuary for the present-day. The line y = x represents the ideal line for 100% accuracy between simulated and observed elevations.

The simplest assessment of the model results presented here may be achieved by comparing the simulated and actual present-day topographies of the Guadiana Estuary (Fig. 3.10). If the actual and simulated elevations are the same, then the gradient of the corresponding linear regression plots is equal to 1 and the simulation is 100% accurate. However, the direct comparison of two DEMs is compromised by human activities of the past centuries, which has significantly altered local physiography. Since bathymetric data do not cover a period of more than a century, and given that such data may contain signatures of past human activity, we may not be able to achieve perfect validation of the model results. In coastal settings, determining the chronology with good temporal resolution for palaeoenvironmental changes is highly

dependent on availability of organic material for ^{14}C dating (Kortekaas, 2007). In the present study, the determination of ages at different depths of the estuarine system was based on several samples suitable for radio carbon dating measurements. However, the poor temporal resolution of ^{14}C dated sediment samples constrains the validation of the morphological evolution model.

Still, according to the best-fit solution obtained from the four iterations, the linear regression gradients of actual elevation versus simulated elevation along the cross-sections in sheltered environments of the estuary (cross-sections 4 to 9) are greater than 0.67, whereas the gradients of the cross-sections located near the shoreface (cross-sections 1 to 3) are less than 0.50. In addition, the R^2 values for plots corresponding to cross-sections 4 to 9 are greater than 0.82. That is, the model results corresponding to sheltered environments of the estuary are very much within the acceptable limits of accuracy given that the simulations are based on a millennial time scale.

The simplicity of the regression-based assessment means that it does not provide a complete picture of the accuracy of the adopted modelling technique. The RMSE of simulated water depths (Table 3) was therefore used as a more robust estimator of accuracy. For that purpose, we converted the final raster DEMs of the four simulations into point data sets (bathymetry), using ArcGIS tools. Each data set was divided into four topographic sections (Fig. 3.11) and compared with observed present-day (year 2000) morphology. On the whole, there was a significant reduction in the RMSE for all four topographic sections through the successive simulations numbered 1 to 4, except in topographic section 4 of the fourth simulation. For simulations 3 and 4, there was a slight increase in the RMSE in topographic section 4 compared to that in topographic section 3. Nevertheless, it is fair to conclude that the RMSE generally decreases with distance from the mouth of the estuary.

Although the total RMSE of ±4.8 m in the fourth simulation seems high, it is important to consider that the possible errors in determining the MSL at 11,500 cal. yr BP were in the

order of ±5 m (Delgado et al., 2012). The effect on the accuracy of the DEM of the input palaeovalley at 11,500 cal. yr BP caused by interpolation errors can also contribute to the overall accuracy of the model. As proposed by Fisher and Tate (2006) and Li (1988), both the RMSE and error standard deviation were used for determining the accuracy of the DEM of the 11,500 cal. yr BP palaeovalley. Values of both these descriptors lay in the range of 2–2.5 m. The total RMSE in the simulated elevations is, therefore, within this initial error margin.

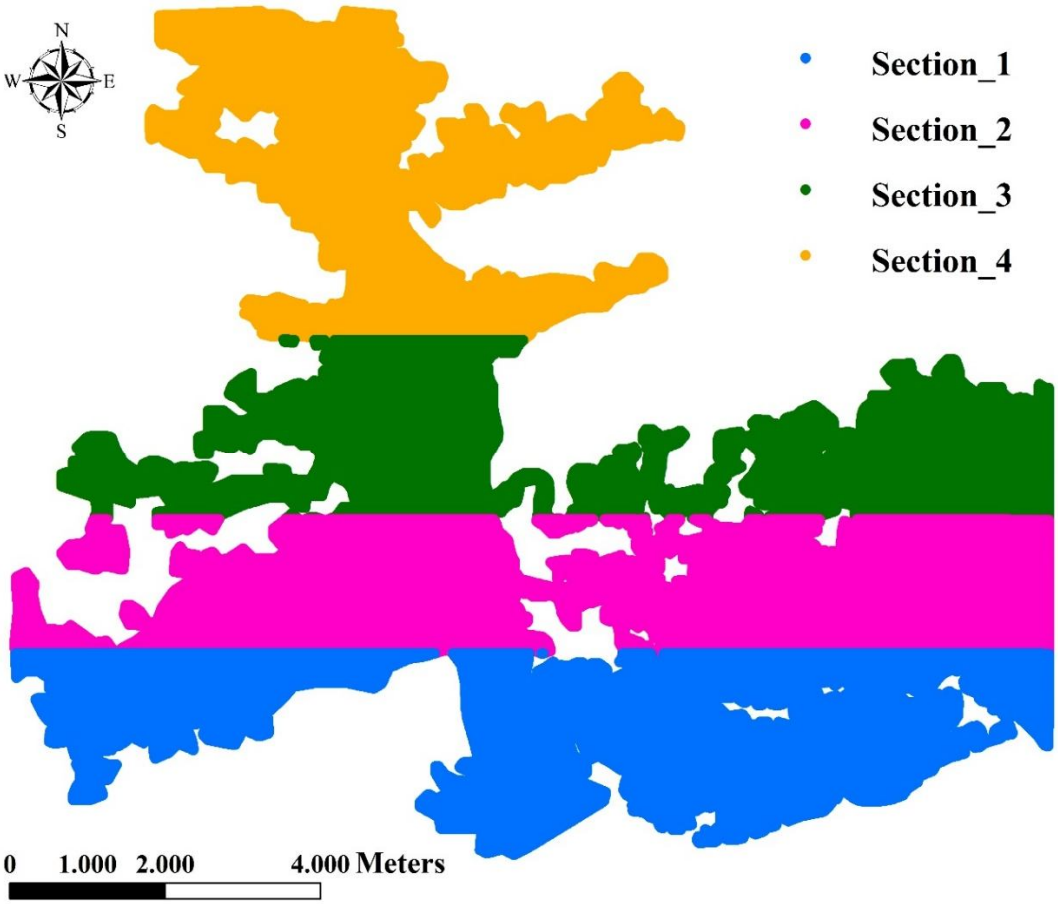

Figure 3.11 Sections of the Guadiana estuarine system used for analysing errors on simulated bathymetries.

Further improvement in the assessment of the quality of modelled palaeotopography was achieved by computing the average error in accretion height (AEAH) of each simulated DEM relative to the average actual accretion height for the whole estuarine system (Table 3.3):

$$AEAH = \frac{\frac{1}{n}\sum_{i}^{n} Error\ in\ simulated\ accretion\ height}{\frac{1}{n}\sum_{i}^{n} Actual\ accretion\ height} \quad (14)$$

where *i* is the particular cell identification and *n* is the number cells in each DEM.

The AEAH of the fourth simulated DEM relative to the actual values was 27.5%, an acceptable figure considering the millennial timescale of simulations. Consequently, we can conclude that the behaviour-oriented approach presented here is satisfactory for simulating the morphological evolution of estuarine systems over centennial to millennial timescales.

Table 3.3 Comparison of root mean square errors on simulated water depths and corresponding actual depths and average errors on simulated accretion heights relative to those of actual accretion heights of the Guadiana estuarine system from 11,500 cal yr BP to the present.

Section	Number of bathymetric points	Root mean square error on simulated water depths (m)				Average error on simulated accretion relative to actual accretion (%)			
		Simulation				Simulation			
		1	2	3	4	1	2	3	4
1	175098	13.8	13.6	7.9	7.0	29.5	29.6	20.7	18.9
2	175113	9.7	9.2	5.6	4.9	35.8	35.4	30.2	28.5
3	147610	5.1	4.7	3.4	3.1	31.3	27.7	26.2	24.0
4	130000	4.5	4.2	3.5	3.7	47.5	42.9	42.3	41.9
Total	627821	8.7	8.3	5.3	4.8	35.6	33.5	29.1	27.5

3.5.2 LIMITATIONS OF THE MODELLING APPROACH

The uncertainties in hindcasting the morphological evolution of the Guadiana Estuary arise from the following causes: (1) a high degree of generalization/simplification of the infilling processes; (2) a lack of comprehensive data to characterise the physical environment of the estuary over the considered period, such as tidal pattern or river discharge (the deduced probable cyclic fluctuations of the average annual river were considered); (3) the bias caused by the antecedent topography. Analysis of global long-term tide gauge datasets obtained under the present rise sea-level conditions (Woodworth, 2010) suggests that there may be feedback effects on regional tidal dynamics (Ward et al., 2012; Pelling et al., 2013). These are likely to modify tidal regimes and tidal ranges along most coastal environments. Absence of reliable data to estimate tidal range variability in the Guadiana estuary during the Holocene transgression, along with the impossibility to explicitly model hydrodynamics and sediment transport in a behaviour-oriented modelling approach, implies that modelling was performed considering always conditions equal to the contemporary tidal regime. Furthermore, the evolution of bathymetry in an estuary is sensitive to bed friction (f) and to sediment erosion coefficient (γ) (Lane, 2004; Lane and Prandle 2006). The approach that we used to develop relationships between non-dimensional net accretion and depth in the sub-tidal channel are dependent on f and γ, whose values along the Holocene are also unknown. To a certain extent, the trial and error approach followed in the four simulations allowed the uncertainties in these parameters to be overcome.

The presented model-based reconstruction relied on the assumption of continuous sedimentation, that is, without periods of non-deposition or erosion that would otherwise reduce the time and space preserved in a sediment column (Sommerfield, 2006). In shallow-marine settings such as estuarine systems, accumulation rates correlate inversely with the time span over which they are averaged, that is, averaging over longer periods typically results in

lower accumulation rates (Sadler, 1999, 1981). Sediment accretion rate depends on the inundation hydroperiod (Cahoon and Reed, 1995). When sediment accretes with time, the inundation hydroperiod decreases, so that less sediment deposits leading to a reduction of accretion rate (Fagherazzi, et al., 2007). This suggests that there is a complex non-linear feedback between sediment infilling and inundation hydroperiod in estuarine systems. In addition, the intense physical and biological reworking of the topmost sediment layer in shallow-estuarine settings filters out low-magnitude events and further increases the incompleteness of the sedimentary record (Crowley, 1984). Therefore, the stratigraphic record should be seen as only a partial record of depositional events (Sommerfield, 2006), and the present model will depend ultimately on the accuracy of long-term representative sedimentation rates derived from borehole data.

The under-prediction of the morphological evolution of the shoreface, in particular the progradation of the coastline of the eastern margin of the estuary, is a salient feature of all four simulations. The shoreface is a highly dynamic zone where waves, currents, tides, cross-shore and longshore sediment transport, local topography and composition of the seabed are interdependent and occur through complex feedback loops (Dronkers, 2005). Likewise, tidal inlets and their associated features, as ebb and flood deltas, add further layers of complexity for modelling entire coastal systems. They act as sources of sediment supply to the coast but with a significant temporal variability, dictated by river discharge (Garel et al., 2014). A complex nearshore sand rotation mechanism proposed by Garel et al. (2014) for the Guadiana estuary, involving feedbacks between sand banks and river flow, which were profoundly altered during cyclic flash-flood events, resulting in migration of sand banks to the eastern margin and subsequent welding to the coastline. This process, conceptualized by Garel et al. (2014) and based on the ebb-tidal delta breaching model by FitzGerald et al. (2000), may have taken place over several millennia on the lower Guadiana estuary, resulting in the progradation

of the eastern margin. Such a combination of wave, tide and fluvial dynamics promotes highly nonlinear processes that, given the lack of knowledge of small-scale residual effects on defining the long-term behaviour, significantly hinders their inclusion in millennia scale predictions (Stive et al., 1995). Therefore, given the averaged nature of behaviour-oriented modelling, similar rates of sedimentation (S^{rep}) were considered for the inner estuary and the eastern margin, recognizing that this is a clear limitation of this approach.

In comparison to the projections of coastal evolution in the lower estuary presented by Morales (1997), the under-prediction of simulations seems to embrace the period from 3000 years BP to the present. Even though the projections of Morales (1997) were based on very limited archaeological data from Ojeda (1988), it seems that the transverse growth of the Monte Gordo beach spit took place on the Portuguese margin synchronously with progradation of the Spanish margin due to new barrier islands forming from active sand bars. As sea-level stabilized during the mid-Holocene, sand bodies located west of the present Monte Gordo beach would have migrated eastwards, causing the closure of the secondary river mouth. There are also evidences for a rapid hillslope erosion in particular from 3000 to 300 yrs BP, that are considered to relate to pre-Roman, Roman, Moorish and early Portuguese phases of settlement and clearance for agriculture and forestry resulting valley floor deposition and estuary siltation (Plater and Kirby 2006). Therefore, the abundance of sediment in the late Holocene would have enhanced progradation of both western and eastern margins of the Guadiana estuary. Subsequent aeolian sand deposition would have enhanced the morphological evolution of the coastline. As the ESM model cannot simulate these dynamic and stochastic processes on the shoreface, increased sediment infilling and subsequent closure of the second mouth of the Guadiana River (near present-day Monte Gordo), along with progradation of the eastern margin, could not be simulated satisfactorily using the present approach. Therefore, it appears that the ESM is more suited for simulating vertical aggradation processes in sheltered

environments of an estuarine system rather than for simulating the lateral movements of sand bodies. A better understanding of the changes in sea-level rise and sediment supply throughout the Holocene is a pre-requisite for long-term modelling of sediment infilling in estuarine systems.

3.5.3 SUGGESTIONS TO IMPROVE THE MODEL APPROACH

There is still room for further improvement of the approach presented. For instance, if a behaviour modelling approach used for simulating the evolution of the shoreface (e.g. Storms et al. 2002) could be incorporated with the present approach of simulating the sheltered environments of an estuary, we would be possible to develop a more generalized application. Incorporating non-linear sediment accumulation rates at least in the shoreface environment would also enhance the accuracy of the simulations. Furthermore, the temporal resolution limitation of dating samples based in ^{14}C could be overcome by optically stimulated luminescence (OSL) as a mean of determining burial ages for sediments (Jacobs 2010). Considering that suitable material such as sand or silt-sized grains of quartz and feldspar is usually available throughout the site, OSL dating technique could be used to improve the chronological sequence of the sedimentary infilling of the Guadiana estuary with higher temporal resolution since 11500 cal. yr BP.

Particle size data can be used to overcome the lack of comprehensive information to characterise the physical environment of the estuary over the study period. For instance, particle size data can be used as a proxy to represent the changing hydrodynamics, different modes of sediment transport and deposition of backbarrier systems including tidal marshes, and open estuaries (Clarke et al., 2014). According to these authors, such data may be used to explain mesoscale system behaviour at subannual resolution over multiple years, and then subannual and multiannual fluctuations in these environmental settings may be superimposed

on a longer-term quasi-stable regimes. A better understanding of the long-term estuarine evolution can thus be achieved and incompleteness of stratigraphic data due to partial recording of depositional events as described by Sommerfield, (2006) can be avoided to a certain extent.

The formation of sand bars, the closure of inlets or a river mouth due to excess sand infilling, and the formation of aeolian dunes by wind are examples of complex behaviours of estuarine systems. However, further studies may include and help to understand the long-term behaviour of such coastal features and processes in numerical models envisaged in the present study.

3.6 CONCLUSIONS

To improve the current understanding of the response of estuarine systems to natural forcing, we simulated the morphological evolution of the Guadiana Estuary due to eustatic sea-level rise during the Holocene. The long-term modelling of the morphological evolution in the estuary complemented previous reconstructions, based on interpretations of the experimental data. Simulations were performed using a behaviour-oriented modelling approach for a time frame established based on 26 radiocarbon age determinations. Six out of nine obtained topographic surface profiles closely matched the actual topographic profiles. The simulations proved to be realistic when applied to the sheltered environments of the estuary, for which the vertical aggradation of sediment is the dominant component of the infilling process.

The best model-based reconstruction of present-day morphology obtained in four different simulations had a total root mean square error of ±4.8 m. This error is comparable with that associated with the estimated mean sea level at 11,500 cal. yr BP and with uncertainties in recreating the palaeovalley surface at 11,500 cal. yr BP. The average error in simulating the elevation of the accreted sediment surface relative to the actual average accretion height was

27.5%, and is considered as acceptable for the millennial timescale adopted. The behaviour-oriented approach that was followed in this study appears to be a useful tool for simulating the morphological evolution of an estuarine system during the period of postglacial sea-level rise. It seems particularly suited to the more sheltered environments of an estuarine system where vertical aggradation dominates the sedimentary infilling of the palaeovalley.

ACKNOWLEDGMENTS: The first author acknowledges FCT for granting a scholarship (SFRH/BD/70747/2010) to carry out this work as part of his PhD research. Carlos Loureiro participation is supported by FCT (grant SFRH/BPD/85335/2012). The authors acknowledge David Stolper, Vivira Cadungog, Peter Cowell and Eleanor Bruce, School of Geosciences, University of Sydney, and the Sydney Olympic Park Authority, for the development of and access to the ESM. The comments of two anonymous reviewers and the Editor, Andrew Plater, have helped to significantly improve an earlier version of the manuscript.

3.7 REFERENCES

Allen, J.R.L., 1995. Salt marsh growth and Flandrian sea level: implication of a simulation model for Flandrian coastal stratigraphy and peat-based sea-level curves. Sedimentary Geology. 100, 21–45.

Andrews, B.D., Gares, P.A., Colby, J.D., 2002. Techniques for GIS modeling of coastal dunes. Geomorphology. 48, 289–308.

Anthony, E.J., Oye´de´, L.M., Lang, J.G., 2002. Sedimentation in a fluvially infilling, barrierbound estuary on a wave-dominated, microtidal coast: the Oue´me´ river estuary, Benin, West Africa. Sedimentology. 49, 1095–1112.

Bjorck, S., Walker, M.J.C., Cwynar, L.C., Johnsen, S., Knudsen, K., Lowe, J.J., Wohlfarth, B., Intimate Members, 1998. The Holocene transgression into the estuarine central basin of the Odiel River mouth (Cadiz gulf, SW, Spain): lithology and faunal assemblages. Journal of Quaternary Science. 13 (4), 283–292.

Blum, M.D., Törnqvist, T.E., 2000. Fluvial responses to climate and sea-level change: a review and look forward. Sedimentology. 47 (Supplement 1), 2–48.

Boski, T., Moura, D., Veiga-Pires, C., Camacho, S., Duarte, D., Scott, D.B., Fernandes S.G., 2002. Postglacial sea-level rise and sedimentary response in the Guadiana Estuary, Portugal/Spain border. Sedimentary Geology. 150, 103–122.

Boski, T., Camacho, S., Moura, D., Fletcher, W., Wilamowski, A., Veiga-Pires, C., Correia, V., Loureiro, C., Santana, P., 2008. Chronology of post-glacial sea-level rise in two estuaries of the Algarve coast, S. Portugal. Estuarine, Coastal and Shelf Science. 77, 230–244.

Bruce, E., Cowell, P., Stolper, D., 2003. Development of a GIS-based estuarine sedimentation model. In: Woodruffe, C.D., Furness, F.A. (Eds.), Coastal GIS 2003 – Wollongong University, Australia, papers on Maritime Policy 14. pp. 271–285.

Burke, K., Francis, P., Wells, G., 1990. Importance of the geological record in understanding global change. Palaeogeography, Palaeoclimatology, Palaeoecology. Global and Planetary Change. 89, 193–204.

Cahoon, D.R, Reed, D.J., 1995. Relationships among marsh surface topography, hydroperiod, and soil accretion in a deteriorating Louisiana marsh. Journal of Coastal Research. 11(2), 357–369.

Clarke, D.W., Boyle, J.F., Chiverrell, R.C., Lario, J., Plater, A.J., 2014. Sediment record of barrier estuary behaviour at the mesoscale: Interpreting high-resolution particle size analysis. Geomorphology. 221, 51– 68.

Cooper, J.A.G., Green A.N., Wright, C.I., 2012. Evolution of an incised valley coastal plain estuary under low sediment supply: a 'give-up' estuary. Sedimentology. 59, 899–916. doi: 10.1111/j.1365-3091.2011.01284.x

Costa, M., Silva, R., Vitorino, J., 2001. Contribuição para o estudo do clima de agitação maritime na costa portuguesa. 2as Jornadas de Engenharia Costeira e Portuária. Aveiro, Portugal. AIPCN, 20 p. (in CD-ROM).

Crowley, K.D., 1984. Filtering of depositional events and the completeness of sedimentary sequences. Journal of Sedimentary Petrology. 54, 127–136.

Delgado, J., Boski, T., Nieto, J.M., Pereira, L., Moura, D., Gomes, A., Sousa, C., García-Tenorio, R., 2012. Sea-level rise and anthropogenic activities recorded in the late Pleistocene/Holocene sedimentary infill of the Guadiana Estuary (SW Iberia). Quaternary Science Reviews. 33, 121–141. DOI: 10.1016/j.quascirev.2011.12.002.

DeMers, M., 1997. Fundamentals of Geographic Systems. Wiley, New York, pp. 486.

Desmet, P.J.J., 1997. Effects of interpolation errors on the analysis of DEM's. Earth Surface Processes and Landforms. 22, 563– 580.

Dias, J. M. A., Boski, T., Rodrigues, A., Magalhães, F., 2000. Coastline evolution in Portugal since the Last Glacial Maximum until present – a synthesis. Marine Geolog. 170, 177–186.

Dronkers, J., 2005. Dynamics of coastal systems. Advanced Series on Ocean Engineering, 25. World Scientific Publishing, Singapore. p 519.

Erdogan, S., 2009. A comparison of interpolation methods for producing digital elevation models at the field scale. Earth Surface Processes Landforms. 34, 366–376. DOI: 10.1002/esp.1731

Fagherazzi, S., Palermo, C., Rulli, M.C., Carniello, L., Defina A., 2007. Wind waves in shallow microtidal basins and the dynamic equilibrium of tidal flats, J. Geophys. Res., 112, F02024, doi:10.1029/2006JF000572.

Fisher, P.F., Tate, N.J., 2006. Causes and consequences of error in digital elevation models. Progress in Physical Geography. 30(4), 467–489.

FitzGerald, D.M., Kraus, N.C., Hands, E.B., 2000. Natural mechanisms of sediment bypassing at tidal inlets. US Army Corps of Engineers. P 11.

Fletcher, W.J., Boski, T., Moura, D., 2007. Palynological evidence for environmental and climatic changes in the lower Guadiana valley (Portugal) during the last 13,000 years. The Holocene. 17, 479–492.

Friedrichs, C.T., Aubrey, D.G. and Speer, P.K., 1990. Impacts of relative sea-level rise on evolution of shallow estuaries. In: Cheng, R.T. (Ed), Residual Currents and Long-term Transport. Coastal and Estuarine Studies, Springer, New York, pp. 106–122.

Ganju, N.K., Schoellhamer, D.H., 2010. Decadal-timescale estuarine geomorphic change under future scenarios of climate and sediment supply. Estuaries and Coasts 33. 15–29.

Garel, E., Sousa, C., Ferreira, Ó. Morales, J.A., 2014. Decadal morphological response of an ebb-tidal delta and down-drift beach to artificial breaching and inlet stabilisation. Geomorphology. 216, 13–25.

Garel, E., Pinto, L., Santos, A., Ferreira, ó., 2009. Tidal and river discharge forcing upon water and sediment circulation at a rock-bound estuary (Guadiana Estuary, Portugal). Estuarine, Coastal and Shelf Science. 84, 269–281. DOI 10.1016/j.ecss.2009.07.002.

Gonzalez, R., Araújo, M.F., Burdloff, D., Cacha˜o, M., Cascalho, J., Corredeira, C., 2007. Sediment and pollutant transport in the Northern Gulf of Cadiz: a multi-proxy approach. Journal of Marine Systems. 68, 1–23.

Hallermeier, R.J., 1981. Terminal velocity of commonly occurring sand grains. Sedimentology. 28, 859–865.

Hamilton, D., 1979. The high energy, sand and mud regime of the Severn Estuary, south-west Britain. In: Severn R.T, Dineley, D., Hawker L.E. (Eds.), Tidal Power and Estuary Management. Colston Papers No. 30, Scientechnica, Bristol, pp. 162–172.

Hibma, A., Stive, M.J.F., Wang, Z.B., 2004. Estuarine morphodynamics. Coastal Engineering. 51, 765–778.

Hutchinson, M.F., 1988. Calculation of hydrologically sound digital elevation models. Proceedings of the Third International Symposium on Spatial Data Handling, August 17–19, Sydney. International Geographical Union, Columbus, Ohio, pp. 117–133.

Hutchinson, M.F. 1989. A new method for gridding elevation and streamline data with automatic removal of pits. Journal of Hydrology. 106, 211–232.

IPCC 2007. Climate Change 2007: The Physical Science Basis. Contribution of Working Group I to the Fourth Assessment Report of the Intergovernmental Panel on Climate Change, In: Solomon, S., Qin, D., Manning, M., Chen, Z., Marquis, M., Averyt, K.B.,

Tignor, M., Miller, H.L. (Eds.), Cambridge University Press, Cambridge, United Kingdom and New York, NY, USA.

Jacobs, Z., 2010. An OSL chronology for the sedimentary deposits from Pinnacle Point Cave 13Bda punctuated presence. J. Hum. Evol. 59 (3-4), 289 – 305.

Johns, B., 1983: Turbulence modelling beneath waves over beaches. In: Johns, B. (Ed.), Physical Oceanography of Coastal and Shelf Seas. Elsevier Oceanography Series. 35, 111–133.

Kirwan, M.L., Murray, A.B., 2008. Ecological and morphological response of brackish tidal marshland to the next century of sea level rise, Westham Island, British Columbia. Global and Planetary Change. 60, 471–486.

Kortekaas, M., Murray, A.S., Bjo¨rck, S., Sandgren, P., 2007. OSL chronology for a sediment core from the southern Baltic Sea: a complete sedimentation record since deglaciation. *Quat. Geochronology. 2*, 95–101.

Lane, A., Prandle, D., 2006. Random-walk particle modelling for estimating bathymetric evolution of an estuary. Estuarine, Coastal and Shelf Science, 68, 1–2. 175–187, doi:10.1016/j.ecss.2006.01.016.

Lane, A., 2004. Bathymetric evolution of the Mersey Estuary, UK, 1906–1997: causes and effects. Estuarine, Coastal and Shelf Science. 59 (2), 249–263. doi:10.1016/j.ecss.2003.09.003.

Lanzoni S., Seminara G., 2002. Long term evolution and morphodynamic equilibrium of tidal channels. Journal of Geophysical Research. 107 (C1), 1–13. DOI:10.1029/2000JC000468.

Lario, J., Zazo, C., Goy, J.L., Dabrio, C.J., Borja, F., Silva, P.G., Sierro, F., Gonz!alez, A., Soler, V., Yll, E., 2002. Changes in sedimentation trends in SW Iberia Holocene estuaries (Spain). Quaternary International. 93–94. 171–176.

Li, Z., 1988. On the measure of digital terrain model accuracy. Photogrammetric Record. 12 (72), 873–877.

Lobo, F.J., Dias, J.M.A., González, R., Hernández-Molina, F.J., Morales, J.A., Díaz del Río, V., 2003. High-resolution seismic stratigraphy of a narrow, bedrock-controlled estuary: the Guadiana estuarine system, SW Iberia. Journal of Sedimentary Research. 73, 973–86.

McGranahan, G., Balk, D., Anderson, B., 2007. The rising tide: assessing the risks of climate change and human settlements in low elevation coastal zones. Environment and Urbanisation.19 (1), 17–37.

Morales, J.A., 1995. Sedimentologia del estuario del Rio Guadiana (S.W. Espanã–Portugal), Servicio de Publicaciones, Huelva University; 1–322.

Morales, J.A., 1997. Evolution and facies architecture of the mesotidal Guadiana River delta (S.W. Spain–Portugal). Marine Geology. 138, 127–148.

Morales, J.A., Delgado, I., Gutierrez-Mas, J.M., 2006. Sedimentary characterization of bed types along the Guadiana Estuary (SW Europe) before the construction of the Alqueva dam. Estuarine, Coastal and Shelf Science. 70, 117–131.

Morris, J.T., Sundareshwar, P.V., Nietch, C.T., 2002. Responses of coastal wetlands to rising sea level. Ecology. 83, 2869–2877.

Nerem, R. S., Chambers, D., Choe, C., Mitchum., G. T., 2010. Estimating Mean Sea Level Change from the TOPEX and Jason Altimeter Missions Marine, Geodesy. 33(S1), 435–446. DOI: 10.1080/01490419.2010.491031

Nichols, M. N., 1989. Sediment accumulation rates and relative sea-level rise in lagoons, Marine Geology. 88, 201– 219.

Nicholls, R.J., Klein, R.J.T., Tol, R.S.J., 2007. Managing coastal vulnerability and climate change: a national to global perspective. In: McFadden, L., Nicholls, R.J., Penning-Rowsell, E. (Eds.), Managing Coastal Vulnerability. Elsevier, Oxford, UK, pp. 223–241.

Ojeda, J., 1988. Aplicaciones de la teledeteccion espacial a la din&mica litoral (Huelva), Geomorfologia y Ordenacion de1 Territorio. Ph.D. Thesis, University of Sevilla, Sevilla, pp. 411 (unpublished).

PALSEA (PALeo SEA level working group), 2010. The sea-level conundrum: case studies from palaeo-archives. Journal of Quaternary Science. 25**,** 19–25.

Pelling, H.E., Uehara, K., Green, J.A.M., 2013. The impact of rapid coastline changes and sea level rise on the tides in the Bohai Sea, China. J. Geophys. Res. Oceans, 118, 3462–3472. doi:10.1002/jgrc.20258.

Perillo, G.M.E., 1995. Definitions and geomorphological classifications of estuaries. In: Perillo, G.M.E. (Ed.), Geomorphology and Sedimentology of Estuaries. Developments in Sedimentology 53, Elsevier, Amsterdam, pp. 17 – 47

Pethick, J.S., 1994. Estuaries and wetlands: function and form. In: Falconer, R.A., Goodwin, P., (Eds) Wetland Management. Thompson Telford, London, 75–87.

Pfeffer, W.T., Harper, J. T., O'Neel, S. 2008. Kinematic constraints on glacier contributions to 21st-century sea-level rise. Science. 321, 1340–1343.

Pinto, L., 2003. Estrataficação salina no Estuário do Guadiana. Master thesis, Faculdade de Ciências da Universidade de Lisboa, Lisboa, pp. 179.

Plater, A., Kirby, J., 2006. The potential for perimarine wetlands as an ecohydrological and phytotechnological management tool in the Guadiana estuary, Portugal. Estuarine, Coastal and Shelf Science. 70, 98–108.

Prandle, D., 2004. How tides and river flows determine estuarine bathymetries. Progress in Oceanography. 61, 1–26. doi:10.1016/j.pocean.2004.03.001.

Prandle, D., 2009. Estuaries: Dynamics, Mixing, Sedimentation and Morphology. Cambridge University Press, New York, pp. 236.

Reeve, D., Chadwick, A., Fleming, C., 2004. Coastal Engineering processes, theory and design practice, Spon press, Oxon, United Kingdom, 461.

Sadler, P.M., 1981. Sediment accumulation rates and the completeness of stratigraphic sections. Journal of Geology. 89, 569–584.

Sadler, P.M., 1999. The influence of hiatuses on sediment accumulation rates. Geo Research Forum 5, 15–40.

Sampath, D.M.R., 2008. Impact of Shoreline Retreat and Inundation due to Sea-level rise along the Coastline adjacent to the Guadiana Estuary, Portugal/Spain Border, MSc. thesis, University of Alagarve, Portugal, pp. 93.

Sampath, D.M.R., Boski, T., Silva, P.L., Martins, F.A., 2011. Morphological evolution of the Guadiana Estuary and intertidal zone in response to projected sea-level rise and sediment supply scenarios. Journal of Quaternary Science. 26(2), 156–170. DOI: 10.1002/jqs.1434.

Sanford, L.P., Halka, J.P., 1993. Assessing the paradigm of mutually exclusive erosion and deposition of mud, with examples from upper Chesapeake Bay. Marine Geology. 114, 37–57.

Schubel J.R. 1971. Classification of estuaries. In: Schubel J.R. (ed.), Estuarine environment: estuaries and estuarine sedimentation Washington D.C., American Geological Institute. Cap. II, pp. 2–8.

Smith, S.V., 2005. Length of the Global Coastal Zone. In: Crossland, C.J., Kremer, H.H., Lindeboom, H.J., Marshall Crossland, J.I., Le Tissier, M.D.A. (Eds.), Coastal Fluxes in

the Anthropocene. The Land–Ocean Interactions in the Coastal Zone Project of the International Geosphere–Biosphere Programme. Springer, New York, pp. 95–143.

Sommerfield, C.K., 2006. On sediment accumulation rates and stratigraphic completeness: lessons from Holocene ocean margins. Continental Shelf Research. 26, 2225–2240.

Stanford, J.D., Hemingway, R., Rohling, E.J., Challenor , P.G., Medina-Elizalde , M., Lester A.J., 2011. Sea-level probability for the last deglaciation: A statistical analysis of far-field records. Global Planet. Change**.** 79, 193–203.

Stevenson, J.C., Ward, L.G., Kearney, M.S., 1986. Vertical accretion in marshes with varying rates of sea level rise. In: Wolfe, D.A. (ed.), Estuarine Variability, Academic Press, San Diego, Calif , pp. 241– 259.

Stive, M. J. F., H. J. De Vriend, P. J. Cowell, and A. W. Niedoroda. 1995. Behavior-oriented models of shoreface evolution. Proceedings of Coastal Dynamics' 95, ASCE. 998–1005.

Stolper, D., 1996. The Impact of sea-level rise on estuarine mangroves: Development and Application of a Simulation Model. Honours Thesis, University of Sydney, Sydney, pp. 90.

Storms, J.E.A., Weltje, G.J., van Dijke, J.J., Geel C.R., Kroonenberg, S.B., 2002. Process-Response Modeling of Wave-Dominated Coastal Systems: Simulating Evolution and Stratigraphy on Geological Timescales. Journal of Sedimentary Research. 72, 226-239.

Syvitski, J.P.M., Harvey, N., Wolanski, E., Burnett, W.C., Perillo, M.E., Gornitz, V., 2005. Dynamics of the Coastal Zone. In: Crossland, C.J., Kremer, H.H., Lindeboom, H.J., Marshall Crossland, J.I., Le Tissier, M.D.A. (Eds.), Coastal Fluxes in the Anthropocene. The Land–Ocean Interactions in the Coastal Zone Project of the International Geosphere–Biosphere Programme. Springer, New York, pp. 39–94.

Townend, I., Pethick, J., 2002. Estuarine flooding and managed retreat Philosophical Transactions Royal. Society, London, 360, 1477–1495.

Townend, I., 2010. An exploration of equilibrium in Venice Lagoon using an idealised form model. Continental Shelf Research. 30 (8), 984–999 doi:10.1016/j.csr.2009.10.012

Valiela, I., 2006. Global Coastal Change. Water Framework Directive, 2000 (2000/60/EC)). Blackwell Publishing, Oxford pp. 368.

Vis, G., Kasse, C., Vandenbergue, J., 2008. Late Pleistocene and Holocene palaeogeography of the Lower Tagus Valley (Portugal): effects of relative sea level, valley morphology and sediment supply. Quaternary Science Reviews, 27, 1682-1709. DOI: 10.1016/j.quascirev.2008.07.003.

Ward, S.L., Green, J.A.M., Pelling, H.E., 2012. Tides, sea-level rise and tidal power extraction on the European Shelf. Ocean Dyn. 62, 1153–1167. doi:10.1007/s10236-012-0552-6.

Wolanski, E., Boorman, L.A., Chı´charo, L., Langlois-Saliou, E., Lara, R., Plater, A.J., Uncles, R.J., Zalewski, M., 2004. Ecohydrology as a new tool for sustainable management of estuaries and coastal waters. Wetlands Ecology and Management. 12, 235–276.

Wolanski, E., Chicharo, L., Chicharo, M.A., Morais, P., 2006. An ecohydrology model of the Guadiana Estuary (South Portugal) Estuarine. Coastal and Shelf Science. 70, 132–143.

Woodworth, P. L., 2010. A survey of recent changes in the main components of the ocean tide. Cont. Shelf Res. 30, 1680–1691. doi:10.1016/j.csr.2010.07.002.

Yue, T., Du, Z., Song, D., Gong Y., 2007. A new method of surface modelling and its application to DEM construction. Geomorphology. 91, 161–172.

Zazo, C., Dabrio, C.J., Goy, J.L., Lario, J., Cabero, A., Silva, P.G., Bardají, T., Roquero, E., 2008. The coastal archives of the last 15 ka in the Atlantic-Mediterranean Spanish linkage area: sea level and climate changes. Quaternary International, 181, 72–87. DOI: 10.1016/j.quaint.2007.05.021

Chapter 4

Assessment of Impacts on Intertidal zone Habitats of the Guadiana Estuary due to Sea-level Rise during the 21st century

This chapter is partly based on the following three conference papers and a planned peer reviewed journal paper on decadal morphological evolution in the Guadiana estuary in response to sea-level rise and sediment supply reduction during the 21st century.

Sampath, D.M.R. Boski, T., 2013. Assessment of Impacts on Intertidal zone Habitats of the Guadiana Estuary due to Sea-level Rise during the 21st century. Geo-Temas, 14, 199-202.

Sampath, D.M.R., Boski, T., 2013. An assessment of significance of the uncertainty in sea-level rise on habitat translation in the Guadiana estuarine system in the 21st century, 2ª Conferência sobre morfodinâmica estuarina e costeira, Uni. Aveiro, 9-10 Maio 2013, Portugal.

Dissanayake, Sampath, Boski, Tomasz., Flavio Martins, Carlos Sousa, Francisco Pinheiro Lima Filho, Francisco H. Bezerra, 2011. Forecasting and hindcasting long-term morphological evolution of the estuaries and lagoons in response to the sea-level rise, Journal of Coastal Research, SI 64, 691-695.

ABSTRACT

In order to achieve sustainable management of estuaries it is fundamental to have a better understanding of the behaviour of estuarine systems to both natural and anthropogenic forcing. This paper focuses on the impacts on intertidal zone habitats of the Guadiana estuary due to sea-level rise during the 21st century. Assessment of impacts was carried out by simulating the morphological evolution due to sea-level rise during this century using a behaviour-oriented modelling approach. The model was approximately validated by analysing the comparability of the present-day bathymetry with that of simulated bathymetries that are reconstructed based on the palaeovalley of 11500 Cal. BP years. Decadal-timescale forecasting of morphological evolution was based on an improved IPCC's projections for sea-level rise and local sedimentation scenarios for the 21st century in the Guadiana estuary

The forecasting results of the model indicated that, if the biogeochemical properties of the Guadiana estuarine system are ideally suitable for landward migration and adaptation of salt marshes with rising sea levels; the only risk would be the reduction of high marsh habitats in the Portuguese margin by 0. 05 and 0.6 km^2 in response to lower and upper limit scenarios of sea-level rise and sedimentation, respectively. If the adaptation capacity for salt marsh vegetation in the newly migrated zones is very poor, the low- and mid-marsh communities will be threatened with extinction both in the Portuguese and Spanish margin under the upper limit scenarios. Under the worst environmental and sea-level rise conditions, the land available for high marshes from the estuarine system will be about 1.4 km^2 by the end of the 21st century. The total newly inundated area due to tides and the projected increase of sea-level will be 3.2 and 11.8 km^2 for lower and upper limit scenarios, respectively.

Keywords: coastal zone management, estuaries, intertidal habitats, sea-level rise

4.1 INTRODUCTION

From an ecological point of view, estuaries are complex systems composed of tidal channels, sand flats, mudflats and salt marshes, whose functioning is physically controlled mainly by river, tidal and wave dynamics. Estuarine wetlands are among the most productive ecosystems and, therefore, provide a wide range of ecological services. However, they are fragile and highly sensitive to human interferences and natural changes, which affect tidal inundation and sediment supply. An increase in sea-level in an estuarine system initially results in channel deepening and expansion of accommodation space, thereby enhancing ebb and wave asymmetry. Subsequently, more sediment enters into the estuary resulting in an increase of sediment deposition rates and decrease of depth (Pethick, 1994). If there is a decrease in sediment supply and/or increase in sea-level above the self-adjusting capacity of the system, the feedback mechanisms may not be sufficient to maintain stable water depths in an estuary. Dams and coastal defences generally reduce the sediment supply to estuaries, resulting in a reduction of vertical accretion and a decrease in their capacity to keep pace with changing sea-levels. Such constraints on the adaptive capacity of estuaries to sea-level rise will likely drive a decrease in wetland areas and drowning of estuarine habitats in the future (Townend and Pethick, 2002).

The Guadiana estuary, located along the southern border between Spain and Portugal is a good example of an estuarine system with a long history of impacts caused by human

activities (Fig. 4.1). Recently, the estuary has been subjected to decreasing river flow and drastically reduced sediment supply due to the emplacement of approximately 100 dams along the drainage basin (Dias et al., 2004). The recent geological history of the Guadiana estuary is well described in terms of sea-level change over the last 13000 years. But in order to be useful for planning and holistic management, it is important to understand and estimate potential impacts due to projected sea-level rise and sediment supply scenarios for at least next 100 years. Therefore, the main objectives of this study are twofold: 1) to simulate the morphological evolution of the Guadiana Estuary and its intertidal zone under the worst case sea-level rise and sedimentation scenarios (lower and upper limit) for the 21st century; and 2) to assess potential morphological impacts and risk of the habitat shift, which will assist in the formulation of long-term management policies for the entire estuarine system.

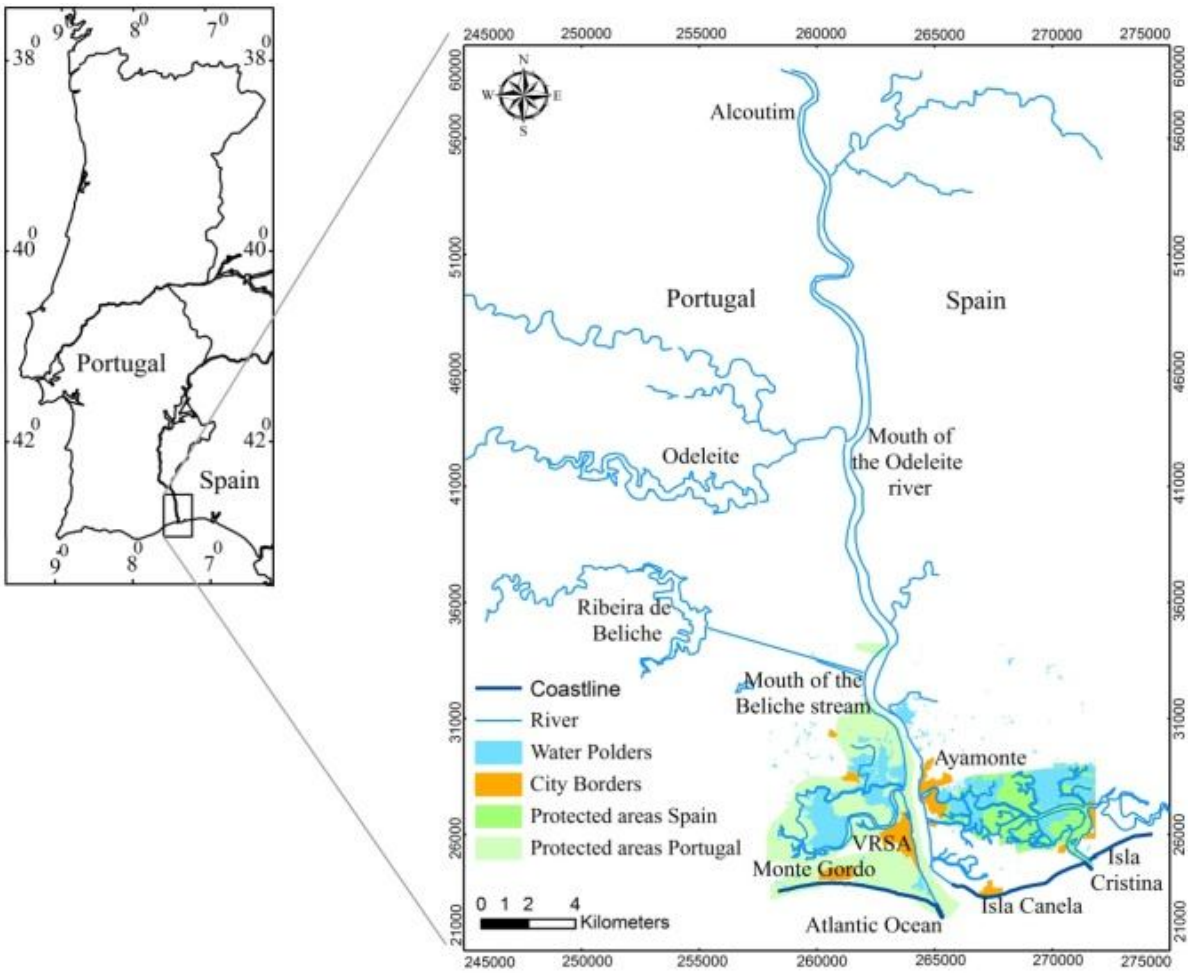

Figure 4.1. Location of the lower Guadiana estuary

4.2 METHODOLOGY

In the context of large-scale coastal behaviour modelling (decades to millennia), estuarine evolution was simulated using the dominant driving factors, which are relative sea-level changes, rate of sediment supply and tidal inundation. The latter is, however, strongly dependent on the initial morphology, which determines the accommodation space for fluvial and marine sediments. The millennial/centennial timescale simulation, which was described in the chapter 3 also enables the establishment of a suitable base for long-term forecasting of morphological evolution in the estuary for the scenarios projected for the 21st century. Good comparison of the model results with the chronostratigraphy of the Guadiana estuary's post-glacial sedimentary infilling detailed by Boski et al. (2002, 2008) serves to validate the numerical modelling approach in this chapter. Thus, the forecasting the morphological evolution of the Guadiana estuary was approached using the GIS raster based *Estuarine Sedimentation Model*, originally developed by Stolper (1996). The net accretion coefficients that were used for simulating the Holocene sediment infilling from the 1900 Cal. yr BP to present day (simulation 4) were used for forecasting the morphological evolution in the Guadiana estuary during the 21st century. The same erodibility function ($\gamma_2=6*10^{-8}z^2+7.8*10^{-6}z+2.7*10^{-5}$) that is used in the fourth simulation of the palaeovalley sediment infilling were used for forecasting as well.

4.2.1 SEA-LEVEL RISE SCENARIOS

Predicting the long-term behaviour of estuarine systems in response to sea level change and other forcings (e.g. a drastic reduction in sediment supply due to damming) is important for coastal zone management. Taken conservatively, due to uncertainties in determining the magnitude of sea-level rise and the sediment supply into the Guadiana estuary during the 21st century, we proposed a conceptual scenario-based approach to model the morphological

evolution of the estuary in response to the above pressures. Decadal-timescale forecasting of morphological evolution was based on the upper and lower limit of A1FI sea-level rise projections (IPCC, 2007) that are updated by Hunter (2010). As the recent sea level change trend, at the Portuguese continental margin, was attributed to the global causes (Dias and Taborda, 1992), we used the upper limit (95%) of mean sea-level rise projections under the globalized economy and intensive use of fossil fuel (A1FI) scenario (Fig. 4.2a and 4.2b) given by Hunter (2010). The lower limit (5%) of the A1FI scenario serves to estimate the uncertainty of the projections for the 21st century.

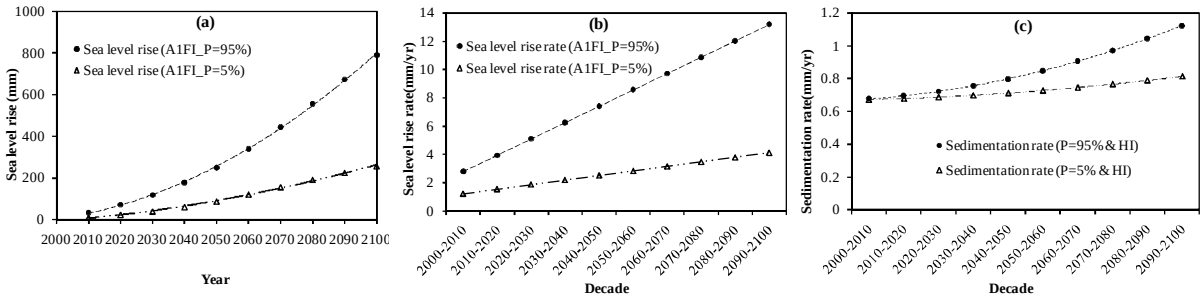

Figure 4.2 Time series used for forecasting morphological evolution in the Guadiana estuary during the 21st century: (a) sea level rise envelop of updated A1FI scenario; (b) corresponding decadal average sea level rise rate; and (c) the envelop of sedimentation scenario corresponding to A1FI sea level rise scenario and sediment supply reduction from fluvial sources.

4.2.2 SEDIMENTATION SCENARIOS

Sedimentation scenarios for the 21st century were derived using available data for the Guadiana Estuary. The estimated present maximum sediment deposition rate value approximately would be 0.65 mm/yr (Sampath et al., 2011). Decadal variability of the sedimentation rate in the estuarine system will be dependent mainly on the temporal variability of the marine sediment supply during the 21st century:

$$S_t^{Rep} = \alpha S_0^F + \beta S_0^M \quad (4.1)$$

where α and β will represent the temporal variability of fluvial and marine sediment supply, respectively; and S^F_0 and S^M_0 are the contributions to representative sediment rate from fluvial and marine sediment supply, respectively at present (t_0=0).

Cluster Analysis of resemblance of the grannulometric distribution of marine sediment and fluvial sediment shows the Euclidian distance dissimilarity is about 60% (Fig. 4.3). Therefore, we assume it is an indicator of the ratio of marine sediment to fluvial sediment supply. However, for conservative estimation we assume the ratio to be 1:1. As the present representative sedimentation rate was estimated to be 0.65 mm/yr, we can estimate the individual contributions from fluvial and marine sources (i.e. $S_0^M = S_0^F = 0.325$ mm/yr).

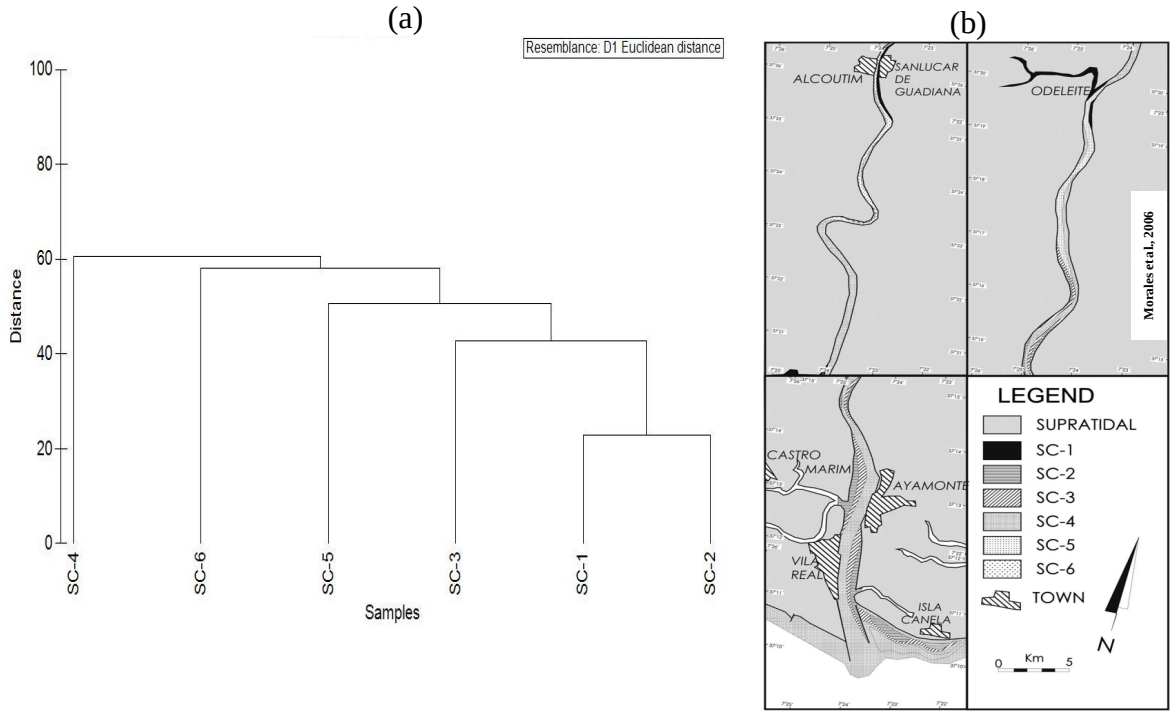

Figure 4.3 Comparison of sediment types in the Guadiana estuary (a) Cluster Analysis of resemblance of the grannulometric distribution of marine sediment and fluvial sediment (b) the sediment types based on granulometric analysis of Morales et al., 2006.

For simplicity, the temporal variability of the suspended sediment supply from fluvial sources is assumed to be negligible, because of the low temporal variability of the river's discharge after the construction of the Alqueva dam (i.e. α=1). This assumption is applicable as long as there will be no drastic change in tapping of river water in the Guadiana basin by means of new dam constructions or due to natural phenomenon. We assume that the factor of increase of the marine sediment supply into the estuary will be equal to the ratio of cross-shore sediment transportation increase due to projected sea-level rise (Fig 4.2c). In the context of conceptual approach, we defined β at a given time t_t based on the concepts of cross-shore transportation theorem developed by Kiribel and Dean, 1985; 1991).

$$\beta = \left\{ \frac{\frac{\tan\delta}{2}\left[h_{avg} + \frac{dM_{MSL}}{dt}(t_t - t_0)\right]^{0.5} - \frac{1}{3}A^{3/2}}{\frac{\tan\delta}{2}(h_{avg})^{0.5} - \frac{1}{3}A^{3/2}} \right\} \quad (4.2)$$

Shoreface slope δ is assumed to be constant over a 100 year period. h_{avg} is the average depth in the shoreface. The constant A is related to the sediment diameter (Dean, 1991) and it can be found in the Coastal Engineering Manual, 2008. The above data and the net accretion rate coefficients from 1900 Cal. yr BP to present day were used to forecast the morphological evolution of the Guadiana estuary during the 21st century using the ESM.

4.3 RESULTS

4.3.1 WATER DEPTH CHANGES DUE TO LOWER LIMIT (P=5%) SCENARIOS.

Under the projected sediment supply reduction and increased sea level (257 mm) as given by the lower limit case of the A1FI scenario, the morphological evolution will result in a slight increase of water depths throughout the estuary (Fig. 4.4). The estimated minimum increase of effective water depth of the main sub-tidal channel is about 110 mm and the maximum increase is about 200 mm. The order of magnitude of decadal water depth increase

will be of the order of a few centimetres. In the intertidal zone, the minimum increase of water depth relative to the maximum high tide limits is about 210 mm and the maximum is 250 mm. The landward limits of the intertidal zone would not significantly translate further inland. There can be landward migration of intertidal zone limits associated with Beliche stream. There will also not be a comparable decadal translation of depth classes in the intertidal zone of the Portuguese (western) margin. There is a little lateral translation of the intertidal zone limits and mean sea level contours of the main channel near to VRSA city limits and below. The main reason is the rubble mound jetty with steep artificial slopes. On the whole, we will not expect significant transgression of mean sea level contours in the Portuguese margin.

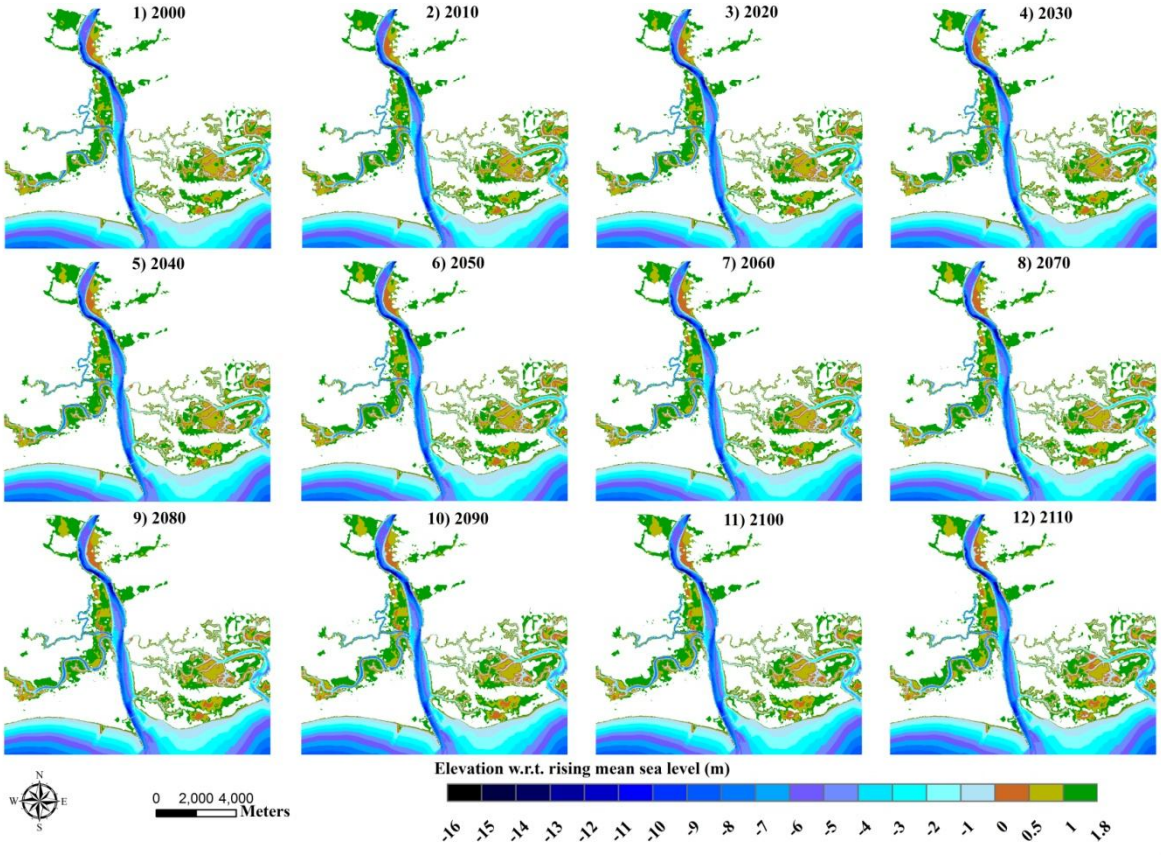

Figure 4.4 Comparison of spatial changes in the depth of the estuary below the maximum high tide level at present (2000) and at the end of each decade during the 21st century in response to the lower limit of A1FI sea level rise projections updated by Hunter (2010).

In the Spanish (eastern) margin, the decadal expansion of the intertidal zone area in response to A1FI sea level rise scenario (P=5%) will be mainly associated with the secondary channel located near the river mouth and the tidal channels of the Isla Cristina inlet. During this century, there will be a little expansion of the landward tidal limits in the secondary channels that are the boundary of the present built-up area of Ayamonte city. That is further restricted by some agricultural area in the same area. In fact, a little intertidal zone area exists at present due to the human activities. However, there would be a comparable transgression of the mean sea level contour in the upper reach of the lower Guadiana estuary. The rate of transgression of the mean sea level will increase after 2060. But there is no significant lateral translation of the landward limits of the intertidal zone.

4.3.2 WATER DEPTH CHANGES DUE TO UPPER LIMIT (P=95%) SCENARIOS

Under the worst case of the projected sediment supply reduction and sea level rise (791 mm) as given by the upper limit (P=95%) of the A1FI scenario, the morphological evolution in the Guadiana estuary and its intertidal zone will result in a significant increase of water depths throughout the estuary (Fig. 4.5). The minimum increase of effective water depth of the main sub-tidal channel is 645 mm and the maximum would be 715 mm. In the intertidal zone, the minimum increase of water depth is about 710 mm and the maximum increase is about 730 mm. Thus, the order magnitude of water depth increase in the estuarine system is four fold compared to the lower limit scenario. We may experience translation of the estuary channel towards the Spanish margin at the end of this century in the lower reach of the study area while there is a deepening of the sub-tidal channel above the north limits of VRSA city. There would be overall channel deepening in the sub-tidal area where Beliche stream meets the main channel. On the whole, the rapid landward translation of upper limits of the intertidal can be expected under the worst case scenario where the projected sea level rise is exponential. Lateral

expansions of intertidal zone limits in the Portuguese margin are mainly associated with: 1) the first secondary channel from the river mouth; 2) the associated region of the main channel above the Vila Real do Santo Antonio (VRSA) built-up area; and 3) intertidal zone limits of Beliche stream. As in the lower case scenario, a little lateral translation can be expected of the intertidal zone limits and mean sea level contours of the main channel near to VRSA city limits and below due to their artificial slopes, during this century. Due to the same reason we will not expect significant transgression of mean sea level contours in the Portuguese margin as a whole.

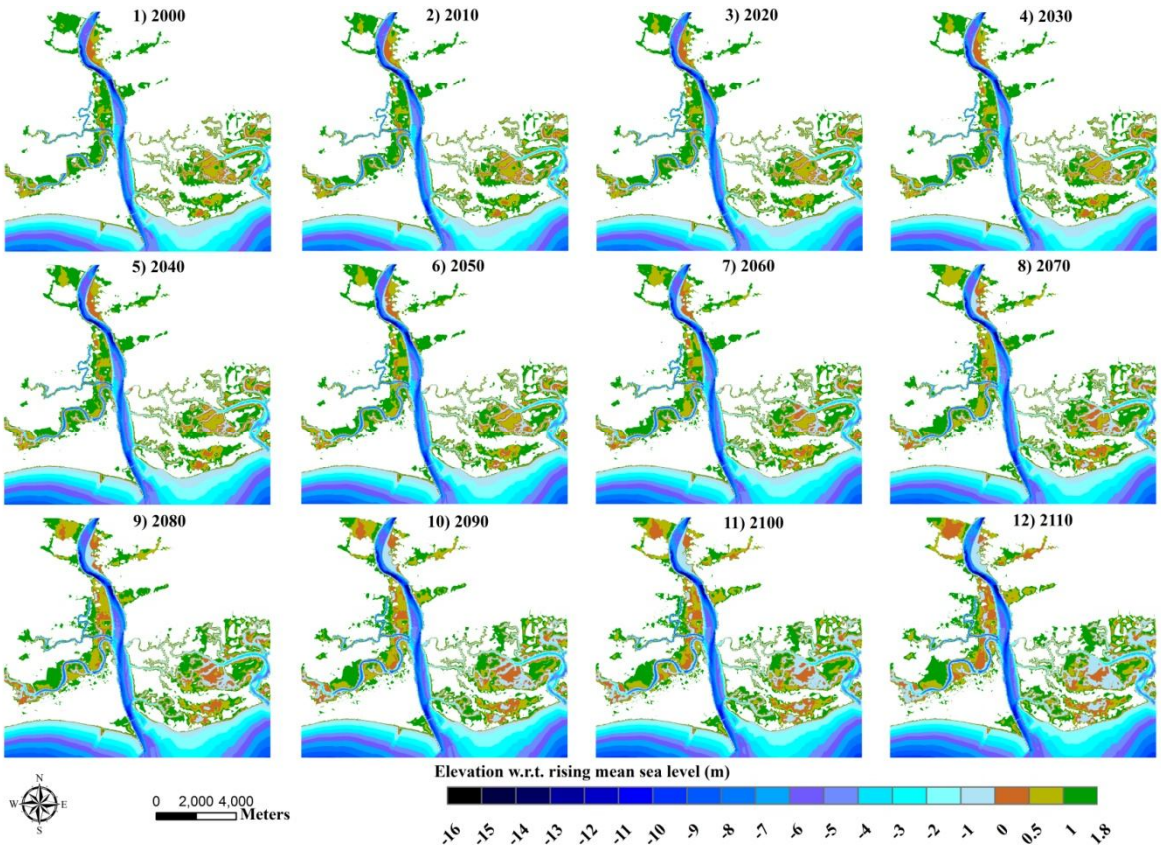

Figure 4.5 Comparison of spatial changes in the depth of the estuary below the maximum high tide level at present (2000) and at the end of each decade during the 21st century in response to the upper limit of A1FI sea level rise projections updated by Hunter (2010).

Similar to the lower case scenario, in the Spanish margin, the decadal expansion of the intertidal zone area in response to the upper limits of A1FI sea level rise scenario (P=95%) will be mainly associated with the secondary channel located near the river mouth and the tidal channels of the Isla Cristina inlet. Very little expansion of the landward tidal limits in the secondary channels that limits the built-up area of Ayamonte city can be expected during the 21st century. However, there would be a significant transgression of the mean sea level contour in the upper reach of the lower Guadiana estuary and tidal channel network associated with the Isla Cristina inlet. The rate of transgression of the mean sea level will be seen approximately after 2030. Loss of land due to the transgression of mean sea level may be able to compensate slightly. However, exiting land will be converted to entirely different depth class.

4.3.3 DECADAL NET ACCRETION DUE TO LOWER LIMIT (P=5%) SCENARIOS

According to the results, morphological response to the lower limit of projected sea level rise and sediment supply constraints can be understood and visualized by analysing the decadal behaviour of the net sediment accretion throughout the estuary (Fig. 4.6). In response to the lower limit of sea level rise and corresponding sediment supply scenario, there is no significant spatial variability in sediment deposition throughout the estuarine system until 2040. After that, there will be two distinct behaviours of sediment deposition over the estuarine system: 1) along the sub-tidal channel bed; and 2) on the intertidal zone bed. Until 2040, the maximum net sediment accretion depth is approximately 3 cm, and then it starts exhibiting increased sedimentation in the sub-tidal channel. By 2070, the net accretion depth of the sub-tidal channel is about 8 cm while that is about 4-5 cm in the intertidal zone. At the end of the 21st century, maximum depth of net accretion in the sub-tidal channel would be about 12 cm and that is in the intertidal zone is about 7 cm. Thus we can see a mild exponential behaviour of the net accretion depth in the sub-tidal channels.

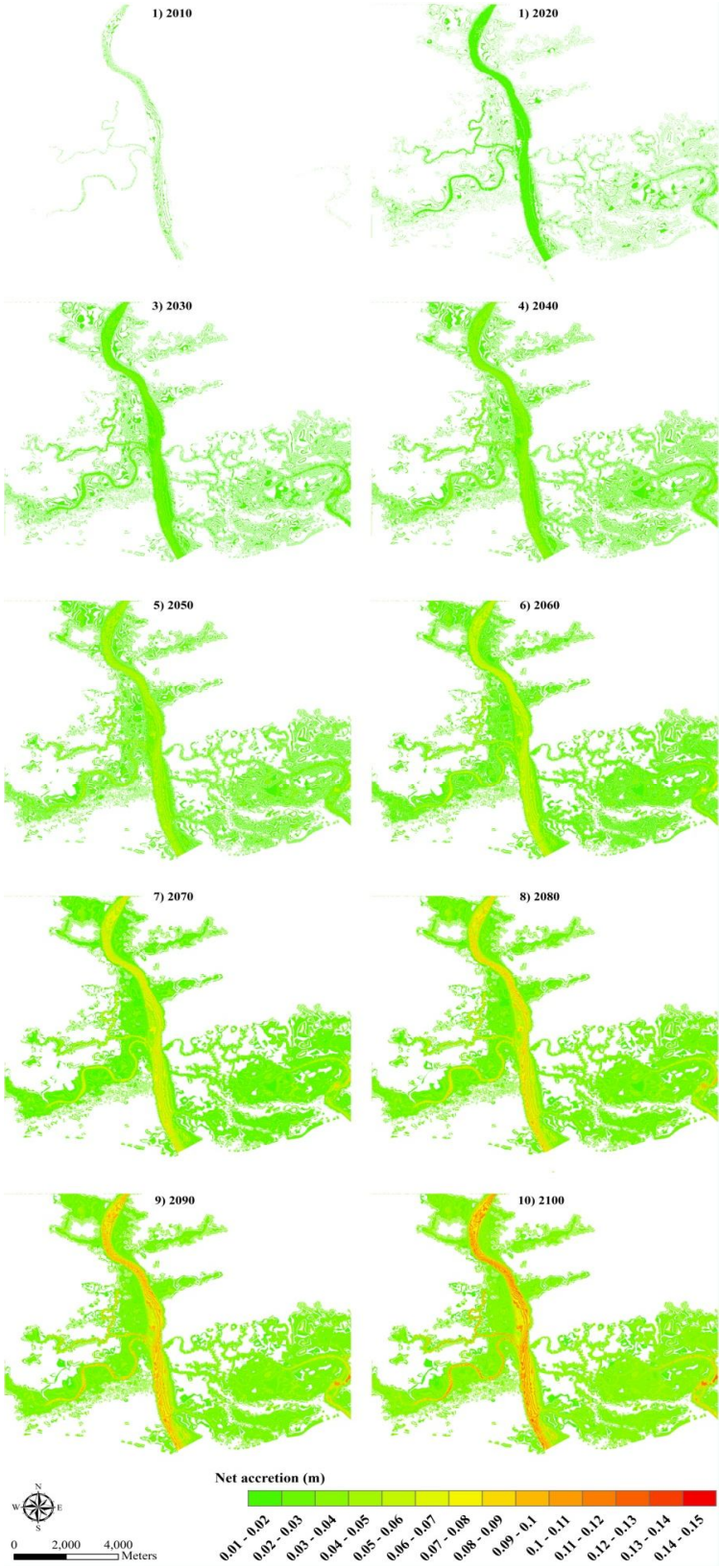

Figure 4.6 Comparison of spatial changes in net accretion of the estuary below the maximum high tide level at the end of each decade during the 21st century in response to the lower limit of A1FI sea level rise projections updated by Hunter (2010).

In the intertidal zone, the first time derivative of net accretion depth is positive (i.e. an increase of accretion depth with time) while the second time derivative of the net sediment accretion would be negative (i.e. decrease in the accretion rate with time). This behaviour implies that there would be a maximum limit for depth of sediment deposition under the imposed conditions of sea level rise and reduction of sediment supply. Even though, there is an increase of accommodation space due to sea level rise, the intertidal zone area may not be resilient enough to maintain the depth under high tide situation and with time there would be an exponential deepening of depths below high tide in the intertidal zone. This observation may be applicable to the sub-tidal region, but the rate at which channels deepen would be less than that of in the intertidal zone.

For instance, the water depth increase would be 13 cm for a rise of sea level of approximately 26 cm under the lower limit scenarios. The corresponding depth increase in the intertidal zone will be about 20 cm. Furthermore, we can see the development of ripple-like landforms from 2050. At the end of the 21st century, these landforms are fully developed and the average height of these ripples will be about 4 cm. From VRSA to the mouth of the river, these forms are longitudinal while further upstream these forms are oblique to the flow direction. In the upper reach of the study area, such directional patterns cannot be seen even if net accretion depths are comparable to that in the lower reach.

4.3.4 DECADAL NET ACCRETION DUE TO UPPER LIMIT (P=95%) SCENARIOS

The behaviour of decadal morphological evolution is very much comparable with the behaviour expected under the lower case scenario (Fig. 4.7). Until 2030, depths of net accretion (2 cm) are approximately identical in response to both lower and upper limit scenarios. After that there is slightly enhanced sedimentation in the sub-tidal channel where the maximum net accretion depth will be approximately 15 cm at the end of the 21st century.

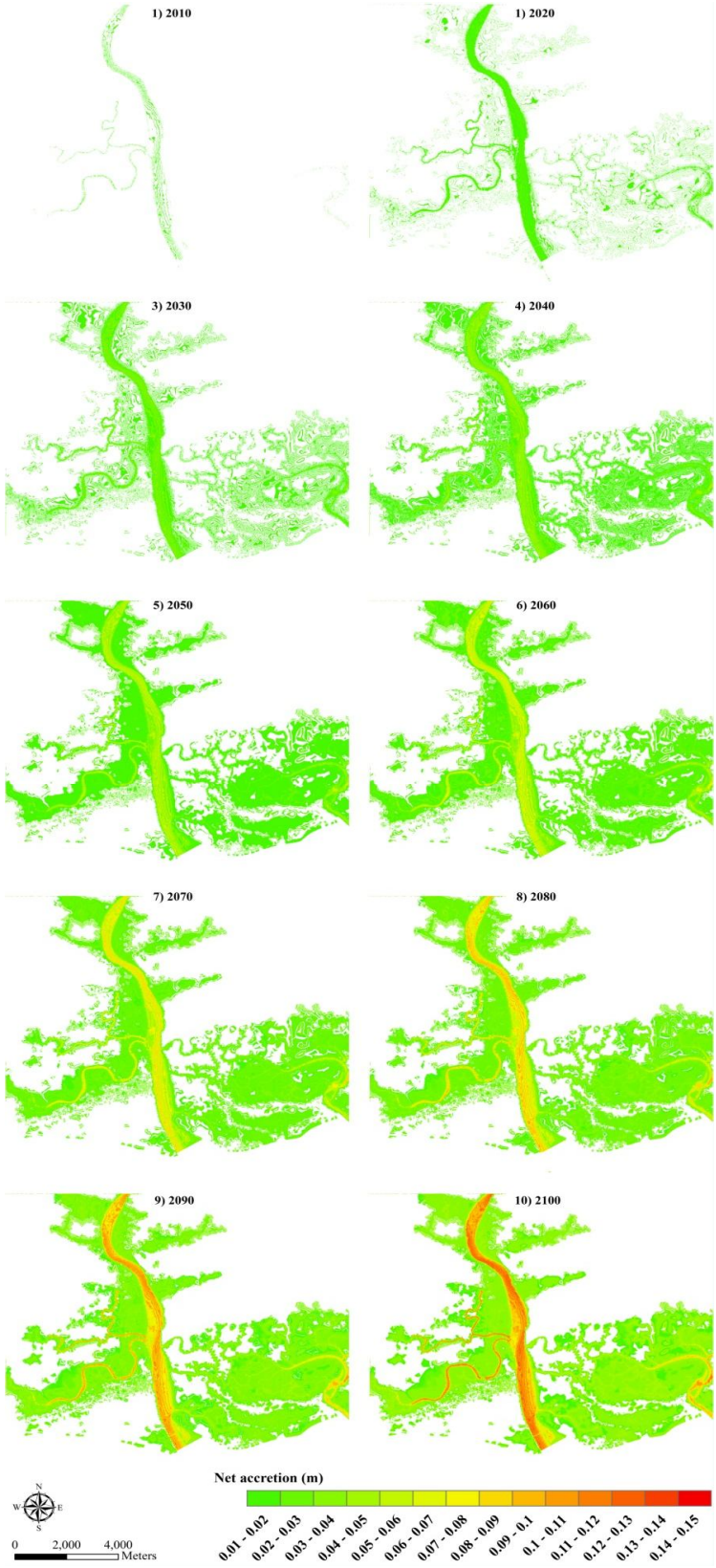

Figure 4.7 Comparison of spatial changes in net accretion of the estuary below the maximum high tide level at the end of each decade during the 21st century in response to upper limit of A1FI sea level rise projections updated by Hunter (2010).

But the corresponding maximum net sediment deposition in the intertidal zone area is comparable with the lower limit scenario (i.e. 7 cm). This morphological response is due to 79 cm rise of sea level by the end of the 21st century. Thus, under the sediment starvation conditions, sub-tidal channel would deepen at least by 65 cm and that is in the intertidal zone is 72 cm. Therefore, existing habitats would experience extremely deleterious impact. If the biogeochemical characteristics of the estuarine system would be suitable for fauna and flora to adapt to the new environmental conditions with landward lateral translation of habitats with sea level rise, the impact may be reduced. If not, the salt marsh habitats may disappear from the estuarine system during this century.

As in the lower limit scenario, similar development of landforms along the sub-tidal channel can be seen under the worst case scenario and they reach their fully developed state by 2080. The relative heights of ripples range from 6 to 8 cm. The spatial distribution of the net accretion depths in the sub-tidal channel in response to the upper limit scenarios by 2090 will be approximately comparable with the accretion depths in response to the lower limit scenarios by 2100. Thus we may suggest 10 to 20 year phase shift in morphological response between the upper limit and lower limit scenarios. Even though we imposed constraints to fluvial sediment supply during the 21st century, enhancement of net accretion may be mainly attributed to the increased marine sediment supply and increased accommodation space.

4.3.5 SEDIMENT VOLUME DEPOSITED IN THE ESTUARINE SYSTEM

The decadal sediment volume deposited in the estuary during the 21st century shows different behaviour based on the percentile limit of the A1FI sea level rise scenario (Fig. 4.8a). The projected decadal sediment volume deposition corresponding to the lower limit of the A1FI sea level rise scenario is almost constant while there will be an exponential increase of expected sediment volume deposited on the estuary corresponding to the upper limit of sea level rise scenario. However, until 2050, the decadal volume of sediment deposition is almost similar in

response to both lower limit and the upper limit of sea level rise projections. This is because sea level may not rise above the modified linear banks of the estuary during this period. When sea level rises further, even flat terrains submerges where there will be a rapid increase of the area under water resulting in increased sedimentation.

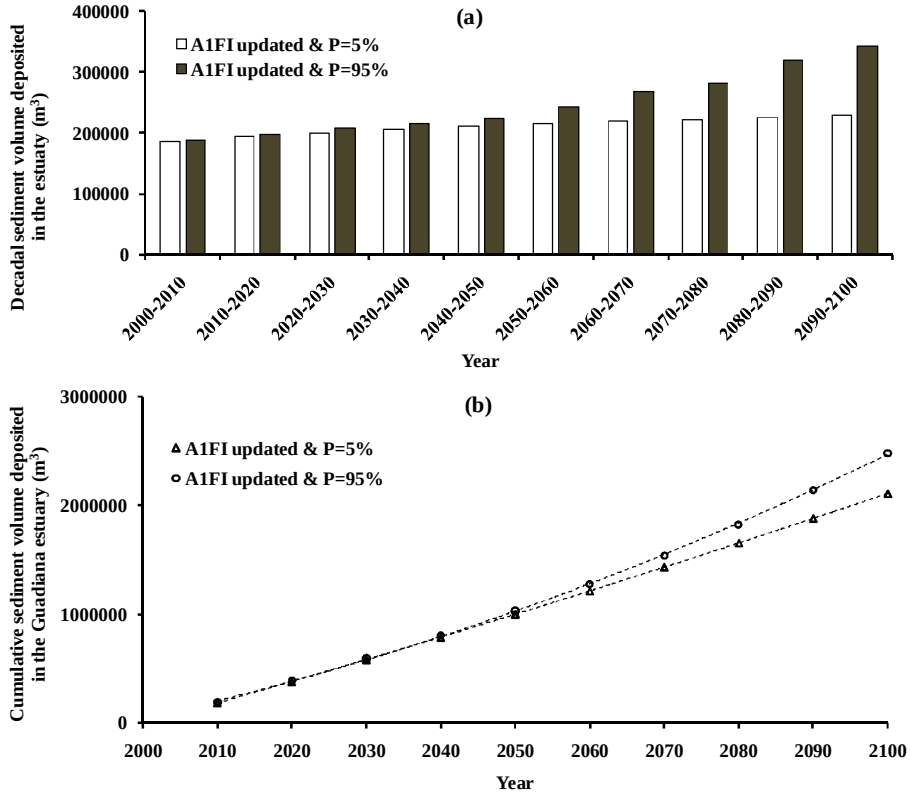

Figure 4.8 Projected (a) decadal and (b) cumulative volume of sediment deposited on the estuary and its intertidal zone in response to the lower and upper limits of updated A1FI sea-level rise scenario during the 21st century.

The deposited volume is almost constant when P= 5%, as sea level rise would not rise above the linear modified slopes of the estuary. Thus the cumulative sediment volume trapped within the estuary would be linearly increase for the lower limit of sea level rise projections during the 21st century. In case of respective upper limit of sea level projections, there would be an exponential increase of cumulative sediment volume deposited in the estuary during this century (Fig. 4.8b).

4.4 DISCUSSION

4.4.1 IMPACTS OF SEA LEVEL RISE ON THE INTERTIDAL ZONE

Impacts of the sea-level rise on the estuarine system were assessed quantitatively in terms of changing the land area within a defined set of depth classes. The intertidal zone of the estuary (-2.0-+1.8 m MSL) was classified into two major classes: 1) the area below the mean sea level (likely to include mud/sand flats; 0 - -2.0 m); and 2) the area above the mean sea level (potential area for salt marsh growth; 0 - +1.8 m MSL). The latter class was classified into three sub-classes, approximately representing land area likely to be available for sub-habitats for: 1) low marsh communities (0- 0.5 m); 2) mid marsh communities (0.5-1.0 m); and 3) high marsh communities (1.0-1.8 m). Shifting and adaptation of a type of marsh communities under changing sea level depends on the characteristics of plants soil types and influence of the tide. But the above classification was loosely defined based only on the tidal influence on evolving estuarine bathymetry due to sea level rise and sedimentation because the adopted estuarine sedimentation model is not integrated with a biogeochemical model.

4.4.2 DECADAL IMPACTS OF SEA LEVEL RISE ON THE MAIN DEPTH CLASSES

The intertidal zone area will increase both in the Portuguese margin (Fig. 4.9a-i and 4.9a-ii) and in the Spanish margin (Fig. 4.9b-i and 4.9b-ii) in response to both lower (P=5%) and upper (P=95%) limits of A1FI sea-level rise scenario and corresponding sedimentation scenarios resulting from the reduced fluvial sediment supply during the 21st century. In the Portuguese margin, the gradient is almost constant of three curves shown in the 4.9a-i (lower limit scenario), indicating a gradual increase of the area with the rise of sea-level. However, there are two gradients in curves of 4.9a-ii (upper limit scenario), indicating increase of the rate of expansion of the area influenced due to both sea-level rise and high tide. As the curve of 0 - -2 m is almost linear in 4.9a-ii, the total effect will be due to the expansion of the area within

the depth class of 0 - +1.8 m. That indicates rapid submergence of ground above the mean sea-level due to its flatness compared to relatively steep slope below the mean sea-level.

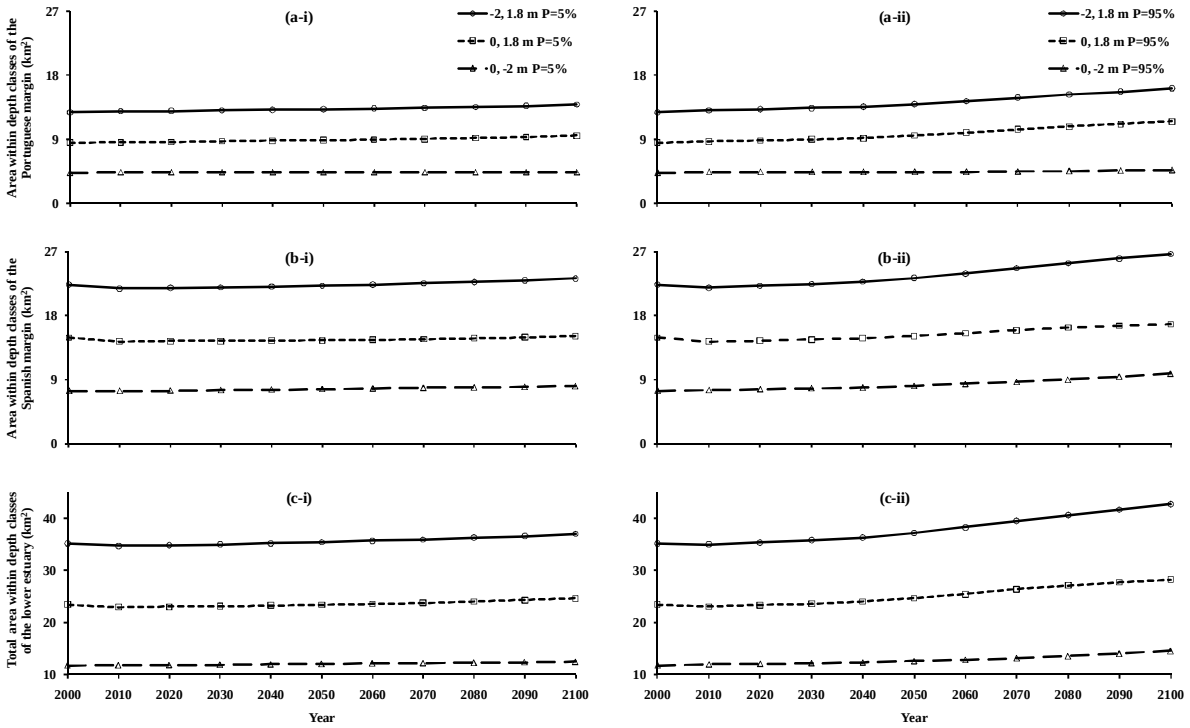

Figure 4.9 Decadal changes of area within depth classes (habitats) in the intertidal zone of the Guadiana estuary as a whole, above the mean sea level and below mean sea level during the 21st century in response to: (i) lower limit and (ii) upper limit of A1FI sea level rise projections updated by Hunter (2010): (a) Changes in the Portuguese margin; (b) changes in the Spanish margin; and (c) Total changes

In the Spanish margin, there is an insignificant expansion of the area within habitat classes in response to the lower limit scenario, but for upper limit projections, there is a slightly exponential expansion of area over each decade. This shows the influence of sea-level rise will be experienced differently by the people in two sides of the river. However, under the projected lower limits of sea-level rise, the expansion of the total intertidal zone area (within the contours of -2 and +1.8 m) due to lateral translation of high tide limits over the 21st century would be

insignificant (Fig. 4.9c-i). Whereas a mild exponential expansion of the total intertidal zone area is likely under the upper limit scenarios of sea level rise and sedimentation (Fig. 4.9c-ii). The exponential nature of the overall expansion of the intertidal zone area is mainly due to the expansion that occurs above the mean sea level (0 – +1.8 m) in the Spanish margin.

4.4.3 DECADAL IMPACTS OF SEA LEVEL RISE ON SUB-HABITAT CLASSES

The decadal variability of subtidal habitat classes both in the Portuguese margin (Fig. 4.10a-i and 4.10a-ii) and in the Spanish margin (Fig. 4.10b-i and 4.10b-ii) behave differently in response to both lower (P=5%) and upper (P=95%) limits of A1FI sea-level rise scenario and corresponding sedimentation scenarios.

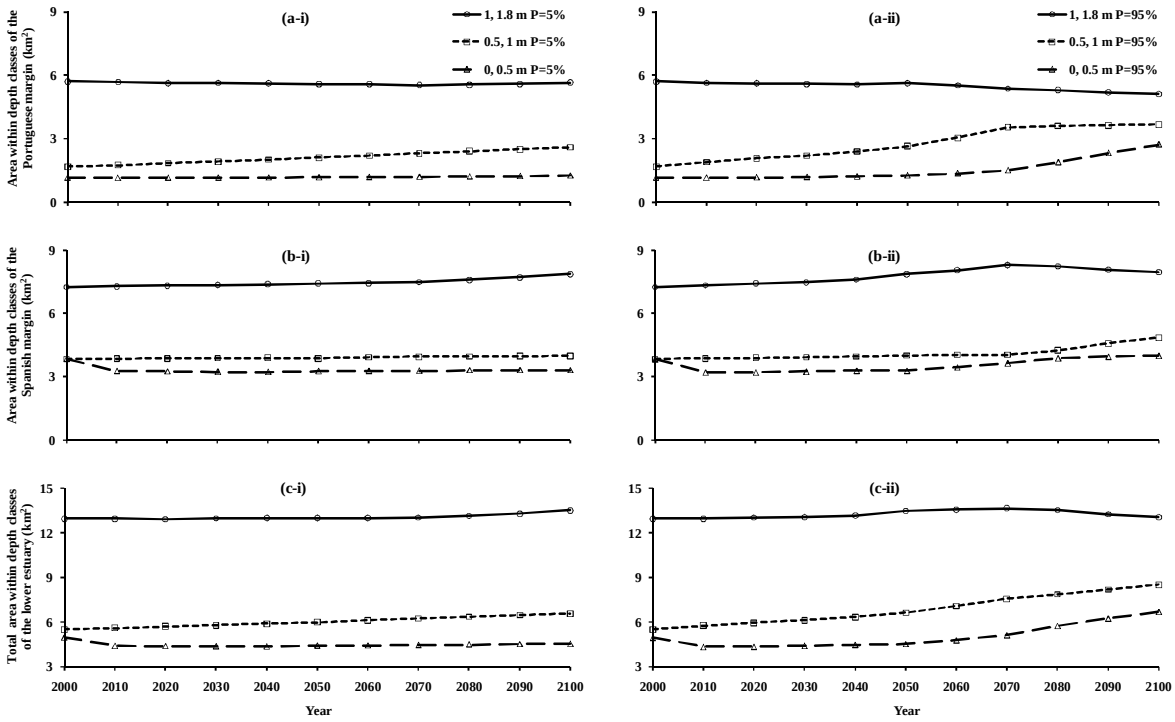

Figure 4.10 Decadal changes of the area within three depth classes (habitats) above the mean sea level of the Guadiana estuary during the 21st century in response to: (i) lower limit and (ii) upper limit of A1FI sea level rise projections updated by Hunter (2010): (a) Changes in the Portuguese margin; (b) changes in the Spanish margin; and (c) Total changes.

In the Portuguese margin, area of the depth classes of 0 – 0.5 m and 0.5 – 1.0 m increase gradually while the area of the depth class of 1 – 1.8 m remains almost constant over this century in response to lower limit projections of forcings. In response to the upper limits of forcings, depth classes show two gradients. The area within the depth classes of 0 – 0.5 m increases slowly until 2070 and then show rapid increase. Area of the depth classes of 0.5 – 1 m increases until 2070 and then remains almost constant while the area of the depth class of 1 – 1.8 m remains almost constant until 2050 and then decreases. In the Spanish margin, under the lower limit scenario, the area within 0 – 0.5 m decrease at the beginning and then remains almost constant while the area within 0.5 – 1 m and 1 – 1.8 m remains almost constant. Under the upper limit projections, the area within 0 – 0.5 m decrease at the beginning but increase slowly, whereas the area within 0.5 – 1 m remains almost constant until 2070 and then increases. However, the area within 1 – 1.8 m increases until 2070 and then starts to decrease. The cumulative effect will be controlled by the behaviour of the Spanish margin in response to the considered forcing acts (Fig. 4.10 c-i and 4.10c-ii).

4.4.4 OVERALL IMPACTS OF SEA LEVEL RISE ON HABITAT CLASSES.

In the Portuguese margin, - 2m contour or the Portuguese Hydrographic Datum, will transgress inland by 0.486 and 1.55 km2 in response to lower limit and upper limit scenarios, respectively. That is 0.832 and 2.586 km2 in the Spanish margin. The area within the depth class of -2 – 0 m will expand slightly due to lower limit scenarios. But the expansion of area at the end of 2100, due to upper limit projections will result in translation of mud flats partly into the present depth class of 0.5 – 1 m, in which likely habitat class is the mid-marsh (Table 4.1). Thus, the present low-marsh system will be completely occupied by mud flats, resulting poor biodiversity. Similarly, under these worst conditions, the depth class 0 – 0.5 m will completely transgress into mid marsh and partially into high marsh habitats. Only 0.194 km2 will remain

from the present high marsh depth class at the end of this century. There will be 4.926 km2 of new land that comes under the influence of tides by 2100.

Table 4.1 Predicted translation of area of the likely habitat types in the intertidal zone of the Portuguese margin in response to lower and upper limit scenarios of sea level rise and sedimentation by the year 2100, compared to their existing area by 2000.

Habitat types (likely)	**Area – km^2 (2000)**	**Occupied from the original habitat types of**	**Area of likely habitats in the Portuguese margin (km^2) by 2100**	
			A1FI (P = 5%)	**A1FI (P = 95%)**
Mud flats (-2 – 0 m)	4.268	Mud flat	3.782	2.718
		Low marsh	0.59	1.144
		Mid marsh	0	0.779
		Total	**4.372**	**4.641**
		Expansion (%)	**(2)**	**(9)**
Low-marsh (0 – 0.5 m)	1.144	Low marsh	0.554	0
		Mid marsh	0.692	0.900
		High marsh	0	1.817
		Total	**1.246**	**2.717**
		Expansion (%)	**(9)**	**(137)**
Mid-marsh (0.5 – 1 m)	1.679	Mid marsh	0.987	0
		High marsh	1.604	3.699
		Total	**2.591**	**3.699**
		Expansion (%)	**(54)**	**(120)**
High-marsh (1 – 1.8 m)	5.710	High marsh	4.106	0.194
		Newly inundated land	1.556	4.926
		Total	**5.662**	**5.120**
		Expansion (%)	**(-1)**	**(-11)**
Intertidal zone (Total) (-2 – 1.8 m)	12.801	Existing intertidal zone	12.315	11.251
		Newly inundated land	1.556	4.926
		Total	**13.871**	**16.177**
		Expansion (%)	**(8)**	**(26)**

If the biogeochemical properties are not suitable for healthy growth of salt marsh vegetation, there will be almost complete extinction of those much sensitive systems. Even if those properties are suitable, there would be a 11% reduction of high marsh habitats from the

Portuguese margin due to upper limit scenarios of sea-level rise and sediment supply changes over this century. The situation is even vulnerable under lower limit scenarios as there would be a 1% reduction. Thus, the high marsh systems are highly vulnerable habitats for these forcings in the Portuguese margin.

Table 4.2 Predicted translation of area of the likely habitat types in the intertidal zone of the Spanish margin in response to lower and upper limit scenarios of sea level rise and sedimentation by the year 2100, compared to their existing area by 2000.

Habitat types (likely)	**Area – km^2 (2000)**	**Occupied from the original habitat types of**	**Area of likely habitats in the Spanish margin (km^2) by 2100**	
			A1FI (P = 5%)	**A1FI (P = 95%)**
Mud flats (-2 – 0 m)	7.454	Mud flat	6.622	4.868
		Low marsh	1.449	3.828
		Mid marsh	0	1.180
		Total	**8.071**	**9.876**
		Expansion (%)	**(8)**	**(32)**
Low-marsh (0 – 0.5 m)	3.828	Low marsh	2.379	0
		Mid marsh	0.917	2.669
		High marsh	0	1.324
		Total	**3.296**	**3.993**
		Expansion (%)	**(-14)**	**(4)**
Mid-marsh (0.5 – 1 m)	3.849	Mid marsh	2.932	0
		High marsh	1.059	4.849
		Total	**3.991**	**4.8**
		Expansion (%)	**(4)**	**(24)**
High-marsh (1 – 1.8 m)	7.251	High marsh	6.192	1.078
		Newly inundated land	1.674	6.880
		Total	**7.866**	**7.958**
		Expansion (%)	**(8)**	**(10)**
Intertidal zone (Total) (-2 – 1.8 m)	22.382	Existing intertidal zone	21.550	19.796
		Newly inundated land	1.674	6.880
		Total	**23.224**	**26.7**
		Expansion (%)	**(4)**	**(19)**

This situation is applicable for the Spanish margin as well. There will be near extinction of marsh habitats if the biogeochemical properties are not suitable for healthy translation in response to worst case upper limit scenarios (Table 4.2). However, if those environmental conditions are suitable there will not be habitat squeezing as in the case of Portuguese margin. Interestingly, under the lower limit scenario, there would be a 14% reduction of area of depth class 0 – 0.5 m by the year 2100. This is because area reduction due transgression of the 0 m contour may not be compensated by the increase of the area by the transgression of the 0.5 m contour. The newly inundating area due to high tides would be 6.88 km^2.

On the whole, under the lower limit scenarios and very limited capacity for marsh communities to adapt in their newly migrated areas, there would remain 2.9, 3.9 and 10.3 km^2 of original low-, mid- and high-marsh habitats, respectively by the year 2100 (Fig. 4.11). Interestingly, under ideal biogeochemical conditions for marshes to adapt to new environments, and under the upper-limit sea-level rise (79 cm) and sedimentation scenarios, there will be no overall reduction of any habitat areas at the end of the 21st century. But we may find that low-marshes will migrate into an area where there were mid- and high-marshes originally. Mid-marshes will completely translate into original high-marsh habitats. From 13.1 km^2 of new high-marsh habitats, only 1.3 km^2 will remain in their original lands during next 100 years. Thus, if the adaptation capacity of existing habitats is very less for their lateral translation with the sea-level rise, the land available for low and mid marsh habitats will be at high risk of disappearing from the whole estuarine system in response to the worst-case sea-level rise and sedimentation scenarios. There would be geographical limitations for high-marsh habitats translation towards land with the sea-level rise in the Portuguese margin. The newly inundated land area is about 3.2 and 11.8 km^2 for the lower and the upper limit scenarios, respectively.

In conclusion, Considering the ecological importance of enhancing adaptation of salt-marshes and that these lands are prone to tidal inundation during the next 100 years, it would

be beneficial to implement a planned retreat program. Such a retreat will reduce artificial constraints for marsh communities to adapt under challenging new environmental conditions. In conclusion, uncertainty in sea-level rise projection is one of the important aspects to be considered in making policy decisions for managing resources in this estuarine system.

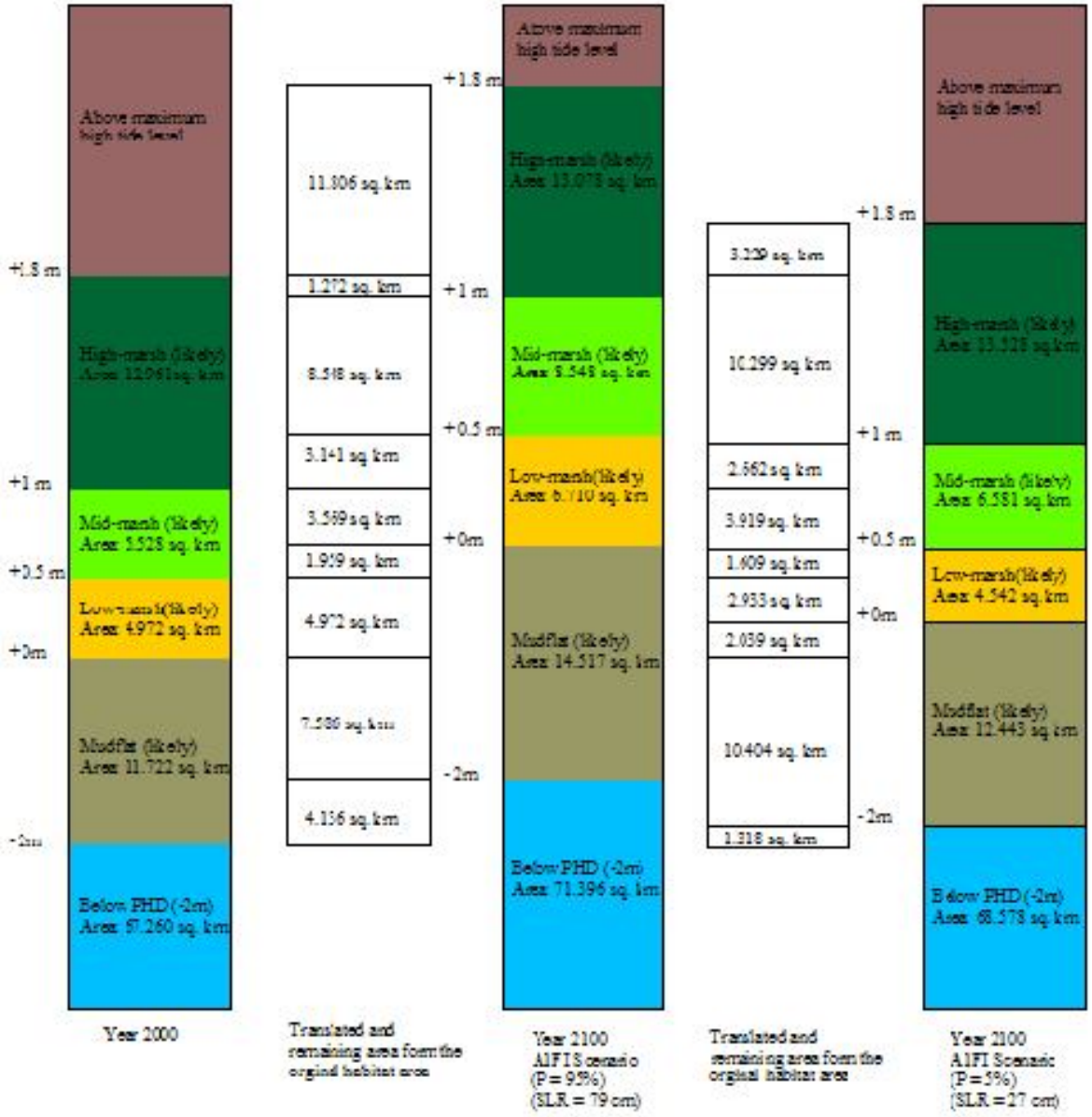

Figure 4.11 Areas available at present for different habitat types likely to be in the estuarine system and their landward translation in the lower Guadiana Estuary in response to the lower and upper limits of A1FI Sea-level rise and sedimentation scenarios for the 21st century, if soil conditions are perfectly suitable for adaptation.

4.4.5 COMPARISON OF BEHAVIOUR-ORIENTED ESTUARINE SEDIMENTATION MODEL AND HYBRID MODEL

Since the assumptions and approaches are different, the comparison of simulations using Estuarine Sedimentation Model and its intermediate Hybrid approach may not be directly feasible. Sea-level rise and sedimentation scenarios that were used in both cases are different. However, in the approach of direct application of ESM, the sea-level rise rate projections under the human-intervention (HI) case was the upper limit of A1FI scenario (59 cm) as given in the IPCC, 2007. In the hybrid approach, the updated A1FI scenario (Hunter, 2010) was used for the simulations, in which sea-level rise projection for the end of the 21st century was 79 cm relative to the year 2000. This increase is due to accounting of land-ice processes, resulting increased ice sheet melting (Hunter, 2010; Meehl et al. 2007). However, increase of ice sheet melting has been estimated on the basis of the projected global average temperature (Hunter 2010), but Rahmstorf 2007 emphasises that the sea-level rise depends, largely, on the integral of past global-average temperature.

The sedimentation scenarios were dependent on the sea-level rise rate. But the comparison is mainly to focus on the morphological features for two approximately close sea-level rise scenarios. The difference between two sea-level rise scenarios by the end of 2100 is 20 cm. In the case of direct application of ESM model, the maximum accretion height is 12.6 cm and that is estimated to be 14.3 cm using the hybrid approach (Fig. 4.12). According to simulated morphology using the hybrid approach, there is formation of bars along the main channel (Fig. 4.12a). At present there are more than 570 bars or dunes, of which the height is more than 25 cm and there are many smaller dunes (Lobo et al., 2004). The orientation of the simulated bars below the section of Belichi stream can be comparable with the observations of Lobo et al., (2004).

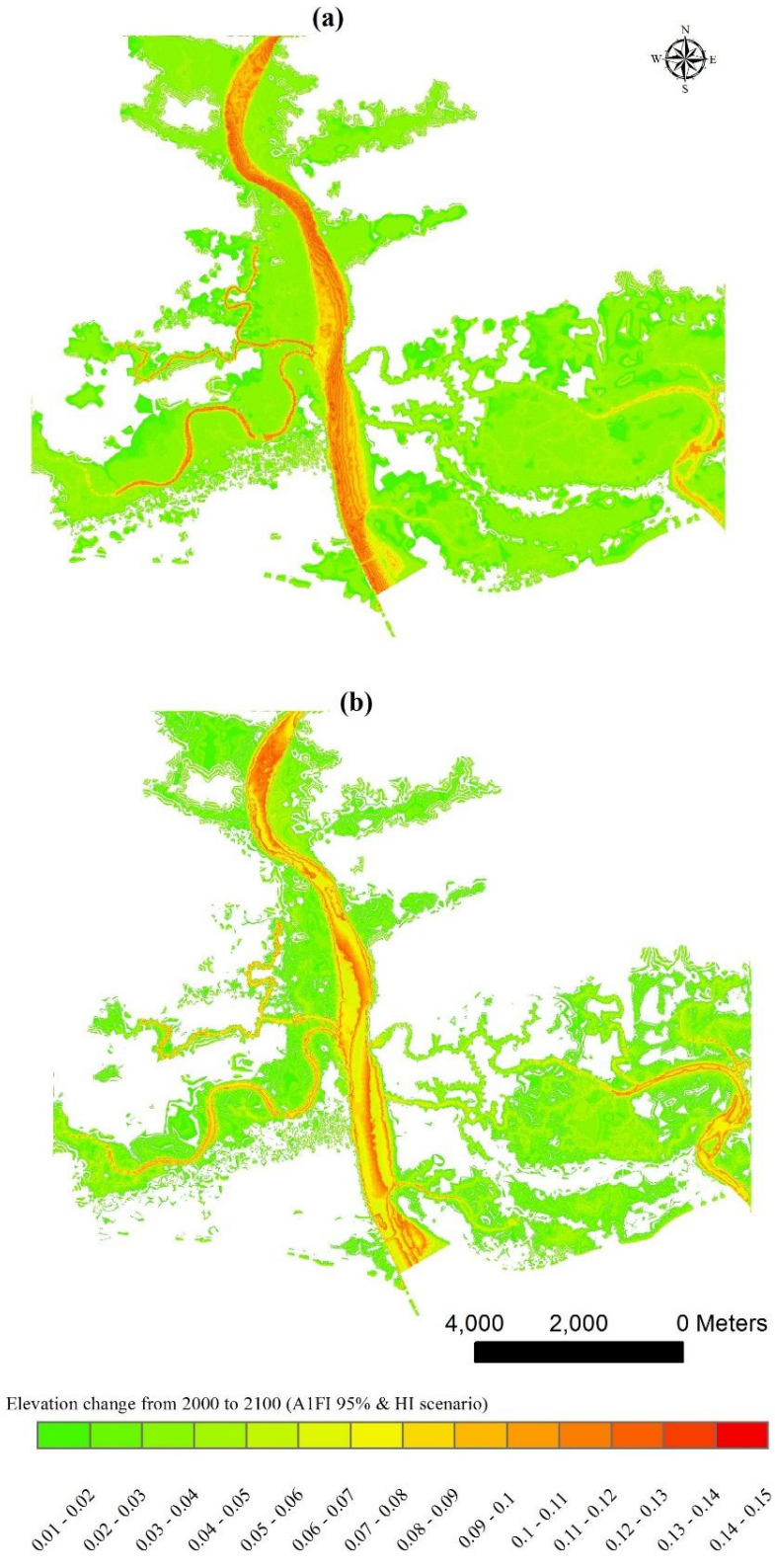

Figure 4.12 Comparison of morphological evolution using the direct application of behaviour-oriented Estuarine Sedimentation Model and modified ESM model based on hybrid rule-based theoretical framework of Prandle, (2006) and (2009).

But the orientation of simulated dunes above the Belichi steam is almost in the opposite direction compared to the observations. That does not mean the simulations may be wrong, because those orientations are for the end of the 21st century. In case of the direct application of the ESM model, results show formation of sand bars (Fig. 12b), which are likely to differentiate the ebb and flood channels as observed by Van Veen (1950) and Ahnert (1960). However, as the heights of these bars are less than 12 cm, there will not be shoal formation (Hibma, et al 2004). The sedimentation in the intertidal zone is very much similar in both applications. In the case of hybrid approach, the extent height of sedimentation in the intertidal zone is high relative to the direct application.

4.5 CONCLUSIONS

In order to improve the current understanding of the response of estuarine systems to both natural and anthropogenic forcing, we simulated the morphological evolution of the Guadiana estuary due to sea-level rise during the 21st century. Simulations were performed using a behaviour-oriented modelling approach, which was previously validated based on the chronostratigraphic ^{14}C data. As explained in the chapter 3, the ability of the model to reconstruct palaeovalley sedimentary infilling was used as an indirect validation of the approach. The simulations proved to be realistic when applied to the sheltered environments of the estuary, where a vertical aggradation of sediment may be assumed as the dominant component of the infilling process. The results of the optimized run were used for decadal-scale forecasting of morphological evolution. The forecasting results of the model indicated that, if the biogeochemical properties of the Guadiana estuarine system are ideally suitable for landward migration and adaptation of salt marshes with rising sea levels; the only risk would be the reduction of high marsh habitats in the Portuguese margin by 0. 05 and 0.6 km^2 in response to lower and upper limit scenarios of sea-level rise and sedimentation, respectively.

If the adaptation capacity for salt marsh vegetation in newly migrated zones is very poor, the low- and mid-marsh communities will be threatened with extinction both in the Portuguese and Spanish margin under the upper limit scenarios. They will be replaced by mud or sand flats or new low marsh with low species richness. Under the worst environmental and sea-level rise conditions, the land available for high marshes from the estuarine system will be about 1.4 km^2 by the end of the 21st century. The total newly inundated area due to tides and the increased sea-level will be 3.2 and 11.8 km^2 for lower and upper limit scenarios, respectively. Although we recognize that there is room for further improvement of this hybrid modelling approach, the present forecasting results can produce a broad view of the impacts related to sea-level rise for holistic management purposes.

ACKNOWLEDGMENTS

The first author acknowledges FCT for granting a scholarship (SFRH/BD/70747/2010) to carry out this work as part of his PhD research. The authors acknowledge Dr. David Stolper, Vivira Cadungog, Dr. Peter Cowell and Dr. Eleanor Bruce, School of Geosciences, University of Sydney, and the Sydney Olympic Park Authority for access to the ESM.

4.6 REFERENCES

Ahnert, F., 1960. Estuarine meanders in the Chesapeake Bay area. Geographical Review 50, 390–401.

Boski, T., Moura, D., Veiga-Pires, C., Camacho, S., Duarte, D., Scott, D.B., Fernandes S.G., 2002. Postglacial sea-level rise and sedimentary response in the Guadiana Estuary, Portugal/Spain border. *Sedimentary Geology*, 150: 103–122.

Boski, T., Camacho, S., Moura, D., Fletcher, W., Wilamowski, A., Veiga-Pires, C., Correia, V., Loureiro, C., Santana, P., 2008. Chronology of post-glacial sea-level rise in two estuaries of the Algarve coast, S. Portugal. *Estuarine, Coastal and Shelf Science*, 77: 230-244.

Coastal Engineering Manual, 2008. Coastal Engineering Manual - Part V, EM 1110-2-1100, US Army Corps Engineers Washington, USA, 1-667.

Dean, R.G., 1991. Equlibrium beach profiles: Characteristics and applications. *Journal of Coastal Research*, 7(1), 53-84.

Dias J, Taborda R. 1992. Tidal gauge data in deducing secular trends of relative sea-level and crustal movements in Portugal. *Journal of Coastal Research* 8 (3): 655- 659.

Dias, J.M.A., Gonzalez, R., Ferreira, Ó., 2004. Natural versus anthropic causes in variations of sand export from river basins: an example from the Guadiana river mouth (Southwestern Iberia). *Polish Geological Institute Special Papers*, 11: 95-102.

Hibma, A., Stive, M.J.F., Wang, Z.B., 2004. Estuarine morphodynamics. Coastal Engineering 51, 765– 778

Hunter, J.R., 2010. Estimating sea-level extreams under conditions of uncertain sea-level rise. *Climate Change*, 99: 331-350.

IPCC 2007. *Climate Change 2007: The Physical Science Basis. Contribution of Working Group I to the Fourth Assessment Report of the Intergovernmental Panel on Climate Change*, In Solomon S, Qin D, Manning M, Chen Z, Marquis M, Averyt KB, Tignor M, Miller HL. (eds.). Cambridge University Press, Cambridge, United Kingdom and New York, NY, USA.

Kriebel, D.L. and Dean, R.G., 1985. Numerical simulation of time-dependent beach and dune erosion. Coastal Eng., 9: 221-245.

Kriebel, D.L., Kraus N.C. and Larson M., 1991. Engineering methods for predicting beach profile response. In: ASCE, Coastal Sediments '91, Seattle, WA, Vol. 1, pp. 557-571.

Lobo, J., Plaza, F., Gonza´ les, R., Dias, J., Kapsimalis, V., Mendes, I., Rio, V.D., 2004. Estimations of bedload sediment transport in the Guadiana estuary (SW Iberian Peninsula) during low river discharge periods. Journal of Coastal Research SI 41 12-26.

Meehl G, Stocker T, Collins W, Friedlingstein P, Gaye A, Gregory J, Kitoh A, Knutti R, Murphy J, Noda A, Raper S, Watterson I, Weaver A, Zhao Z-C., 2007. Climate change 2007: the physical science basis. In: Contribution of working group I to the fourth assessment report of the intergovernmental panel on climate change, chapter 10. Cambridge University Press, Cambridge, pp 747–845.

Morales, J.A., Delgado, I., Gutierrez-Mas, J.M., 2006. Sedimentary characterization of bed types along the Guadiana Estuary (SW Europe) before the construction of the Alqueva dam. Estuarine, Coastal and Shelf Science. 70, 117–131.

Pethick, J.S., 1994. Estuaries and wetlands: function and form. In: *Wetland Management*. Thompson Telford, London, 75-87.

Prandle, D., 2006. Dynamical controls on estuarine bathymetry: Assessment against UK database. Estuarine, Coastal and Shelf Science 68, 282-288.

Prandle, D., 2009. Estuaries: Dynamics, Mixing, Sedimentation and Morphology. Cambridge University Press, Cambridge, UK, ISBN 978 05 2129 781 3, p. 235.

Rahmstorf, S., 2007. A semi-empirical approach to projecting future sea-level rise. Science 315(5810):368–370.

Sampath, D.M.R., Boski , T., Silva P.L. and Martins F.A. 2011. Morphological evolution of the Guadiana estuary and intertidal zone in response to projected sea-level rise and sediment supply scenarios, *Journal of Quaternary Science* 26(2): 156–170. DOI: 10.1002/jqs.1434.

Stolper, D., 1996. *The Impact of sea-level rise on estuarine mangroves: Development and Application of a Simulation Model*. Honours Thesis, University of Sydney, Sydney, 90p.

Townend, I., Pethick, J., 2002. Estuarine flooding and managed retreat. *Philosophical Transactions Royal. Society, London*, 360: 1477-1495.

van Veen, J., 1950. Ebb and flood-channel systems in the Netherlands tidal waters (in Dutch, English summary). KNAG, 2e Series, Part 67. Republished, translated and annotated by Delft University of Technology, 2001. ISBN 9040723389

Chapter 5

Sensitivity of controlling parameters of a decadal scale morphological evolution model: Application to the Guadiana Estuary - SW Iberia

Sampath, D.M.R., Boski, T., 2015. Sensitivity of controlling parameters of a decadal scale morphological evolution model: Application to the Guadiana Estuary - SW Iberia. Expected to submit to Geomorphology**.**

ABSTRACT

Focussing on predicting large-scale morphological evolution of an estuarine system, in response to environmental and anthropogenic forcings, a hybrid model was developed and applied to the Guadiana estuary – SW Iberia. The model first simulates the decadal-scale evolution of the system using a rule-based approach to find the spatial variability of annual average net sediment accretion, to simulate the centennial scale morphology by using a behaviour-oriented approach. This paper presents an assessment of the accuracy of the decadal scale module and its sensitivity to bed friction (f), the power of the current velocity of the erosion rate function (n), sea-level rise rate and time span of morphological evolution.

The normal probability distribution of the modelled sediment surface elevation change from 2000 to 2014 approaches that of the observed distribution for n = 1.8, 2, 2.5 and 3 while the friction was 0.8f, f, 1.5f, and 2.07f, respectively. Both average elevation change and standard deviation exhibit logarithmic relationships with n when it was increased from 1.5 to 3. If n was further increased both average elevation change and standard deviation tend to be constants. The difference between the average elevation change with and without sea-level rise relative to the increasing rate of the accommodation space converges to zero with the increase of sea-level rise rate above the present global mean sea-level rise rate. Thus, sea-level rise by 5 mm/yr would cause significant destruction to the sensitive ecosystem of the Guadiana estuary. The simulations produced spatial variability of eroding and accretion, comparable with observed changes. Estuarine mudflats were most affected by erosion. Under reduced fluvial sediment supply salt-marshes will experience a similar increase of water depth threatening the stability of the intertidal ecosystem.

Key words: Morphological evolution, estuary, sea-level rise, human intervention, sensitivity analysis of behaviour-oriented models

5.1 INTRODUCTION

The Intergovernmental Panel on Climate Change in its latest report (IPCC, 2014) emphasizes the importance and urgency of finding adaptation and mitigating solutions for the global threats due to climate change and an accelerating pace of the mean sea level (MSL) rise. Thus, there is increasing interest in synthesizing available data and modelling bathymetric evolution of estuaries, specifically to determine historical changes, and predicting future trends over periods of ≈100 years (Lane, 2004). Many researchers have approached this problem by developing different models with different complexities for accurately predicting morphological evolution in estuarine systems in response to projected scenarios of sea-level rise and acute human interventions in the catchment.

Geomorphological evolution or behaviour-oriented models (top-down) and process-based models (bottom-up) are generally used to predict the morphological behaviour of estuaries (Karunarathna et al., 2008). These two approaches may be considered as complementary with respect to time scales embraced by simulations. The first approach (Dennis et al., 2000; Bruce et al., 2003; Karunarathna and Reeve, 2008; Sampath et al., 2011) is based on empirical rules or expert analysis of long-term morphology data, thus, these types

of models are more appropriate for predicting large scale and long-term physical responses of an estuary to natural changes in forcing (e.g. sea level rise) and human interference (Karunarathna et al., 2008). These types of models does not explicitly take into account the estuarine physical processes like tidal hydrodynamics, channel-shoal sediment exchange, and gravitational circulation and do not allow to represent dynamic interactions and feedbacks intervening in morphological changes (Sampath et al., 2011). Process-based models (Dronkers, 1998; Fortunato and Oliveira, 2003; Dastgheib, et al., 2008; Van der Wegen and Roelvink, 2008; Dissanayake et al., 2009; Lesser, 2009) use the knowledge of physical principles underlying hydrodynamic and sediment transport and are suitable to describe the short-term morphodynamics, using two- or three-dimensional hydrodynamic models combined with sediment transport and morphodynamic modules (Karunarathna et al., 2008; Dissanayake et al., 2011). These models are more appropriate to simulate coastal evolutions up to decadal time scales (Dissanayake et al., 2011).

Because estuaries are ephemeral features in the geological time-scale, the usefulness of morphological models will depend on their ability to simulate the long-term estuarine morphological changes during the postglacial eustatic sea-level rise of the last 15,000 years which drowned fluvial valleys (Schubel, 1971; Perillo, 1995) worldwide.. However, a better understanding of the sensitivity of the estuarine system to long-term forcings like sea level rise and human interference is required if the sustainable management of the estuary is to be achieved. In this regard, it is desirable to accommodate theoretical solutions of physical processes in behaviour oriented models and that way improve their trustworthiness.

Sampath et al., 2015 presented a semi-behaviour-oriented approach to simulate the morphological evolution of the Guadiana estuary during sedimentary infilling that accompanied Holocene sea-level rise. The centennial to millennial scale extrapolations were conducted using the Estuarine Sedimentation Model, which uses a behaviour-oriented

approach, supported by the chronostratigraphy of the estuary's sedimentary sequence. Implementation of ESM also requires the long-term net accretion rate coefficients of each cell of the topo-bathymetry, that is, the long-term net accretion rates at a given location relative to the maximum sedimentation rate found within a hypothetical transect from maximum high-tide level to the maximum depth of the paleovalley of the estuary. The long-term net accretion rate coefficients of the sub-tidal region of the paleovalley of the estuary were estimated using a decadal scale model based on the theoretical framework developed by Prandle (2009). Then the long-term net accretion rate coefficients in the intertidal region of the estuary were derived by rescaling the sedimentation rates derived in terms of the inundation frequency from the low tide to the maximum high tide level relative to the coefficient at the low tide level or the Portuguese Hydrographic Datum at 2m below the mean sea-level (Sampath et al., 2011).

The theoretical framework of the Prandle (2009) is based on the analytical solutions to the one-dimensional and cross sectionally averaged shallow-water wave equations. The equations were simplified for the first-order tidal simulations by neglecting the convective terms and by linearizing the quadratic friction term of the shallow-water wave equation. This approach is valid only for the synchronous estuaries, as the surface gradients associated with axial amplitude variations in ς^* is assumed to be significantly less than those associated with corresponding phase variations. These assumptions are shown to be valid except in the shallowest conditions at the tidal limit (Prandle, 2003). The complexity of estuaries and in particular the stochastic nature of the intervening processes (De Vriend, 2001) requires several assumptions in order to be able to provide analytical solutions for a diverse range of dynamic interactions and mixing processes (Prandle and Lane, 2015).

The long-term net accretion rates the sub-tidal region of the estuary were linked to variables like bed friction, current velocity, sediment erodibility coefficient, settling velocity and suspended sediment concentration. The bed roughness of an estuary has been identified as

a highly sensitive parameter for sediment transport model applications (van Rijn 2007). The presence of medium to large scale bedforms can modify the flow pattern, through the generation of vortices enhancing the spatially-averaged bed shear stress (Villaret et al., 2011). Furthermore, sediment transport predictions are generally highly sensitive to the local skin friction, which represents the part of friction acting locally on individual grains (Villaret et al., 2010). Current velocity can determine sediment transport through the estuary channels and thereby it is determining factor its morphology (Liu and Aubrey, 1993). On the other hand, how the tidally dominated estuaries respond to rises in mean sea-level and changes in river flows and sediment supply associated with human activities in the catchments are important aspects for long-term planning of the local ecosystems (Lane and Prndle, 2007).

Consequently, the first objective of this paper is twofold: (1) to assess the sensitivity of bed friction coefficient, the power of the current velocity, and sea-level rise rate in determining the decadal scale morphological evolution in the Guadiana estuary and (2) to understand the effect of dam construction along the Guadiana river on the estuarine morphology. These parameters can be considered as main sources of uncertainty in the present approach to the long-term morphological evolution in the system. The model simulations, scripted with MATLAB, were carried out in the Guadiana estuarine system because this area is affected with fluvial sediment starvation due to construction of large number of dams over the past 50 years (Sampath et al., 2015) to which adds the observed presently sea-level rise.

5.2 STUDY AREA.

5.2.1 GEOGRAPHICAL AND GEOLOGICAL SETTING

The Guadiana River drainage basin is the fourth largest on the Iberian Peninsula, with an area of 66 960 km^2 (Garel et al., 2009). It is 810 km long and traverses extensive rural areas in Spain and Portugal, including the mining areas of the Iberian Pyrite Belt (Delgado et al., 2012). The

Guadiana Estuary (Fig. 5.1) is located along the southern border between Spain and Portugal and extends for about 80 km, from its mouth to the weir of Moinho dos Canais where the tidal wave is virtually dampened (Silva et al., 2000; Garel et al 2009). The estuary, which, in physical terms is ca. 50 km long, has a maximum channel width of 550 m and depths ranging between 5 and 17 m (Wolanski et al., 2006). The depth of the channel is generally less than 10 m (referred to the average water level), with a mean depth about 5 m from the mouth to 50 km that slowly decreases upstream (Garel et al., 2009). The local depth variations reaches up to 18 m generally in front of the creeks (Lobo et al., 2004).

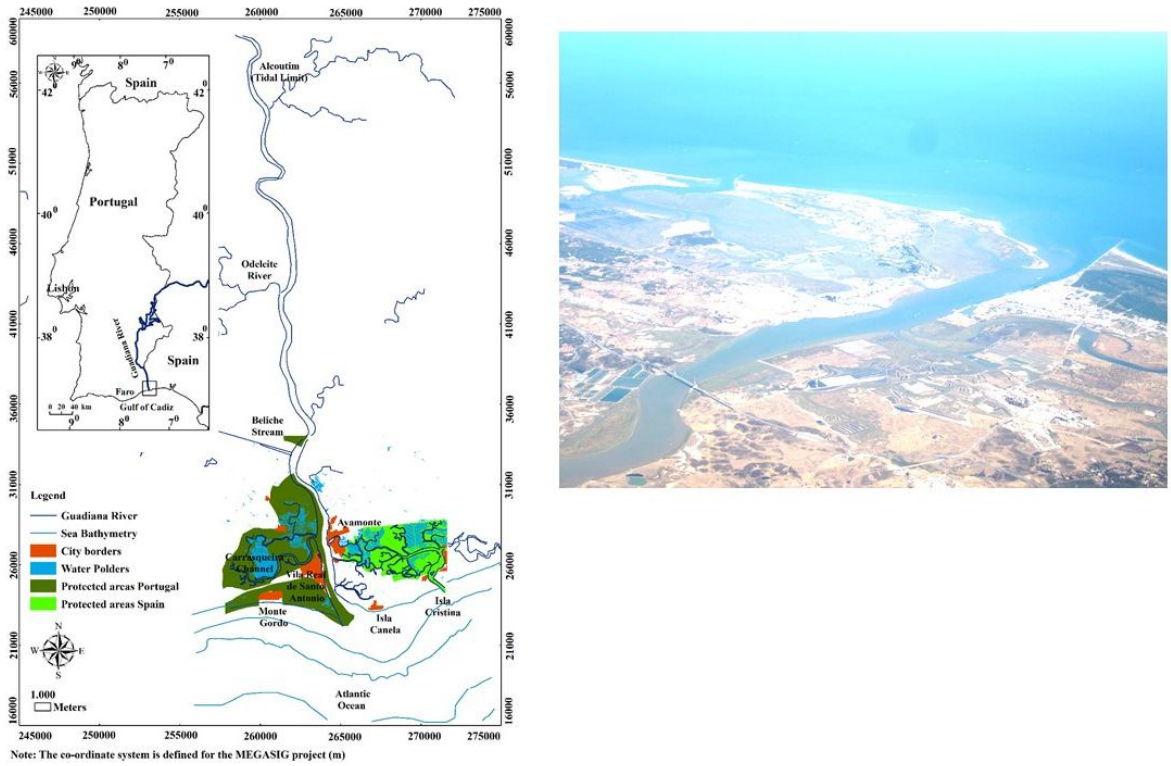

Figure 5.1 The Guadiana estuary and an aerial photograph of the lower estuary.

It is a narrow, deeply incised (down to ca. 80 m below present MSL), bedrock-controlled estuary experiencing the final stages of sediment infilling, experiencing an incipient coastal progradation (Boski et al., 2008). The prograding system near to the river mouth is constituted by successive sandy barriers separated by salt marshes that configure a wave-

dominated delta (Morales, 1997). Within the estuary, the channel reaches the maximum depth at the Portuguese margin close to the mouth of the river. It migrates towards the Spanish margin further upstream from the mouth and reaches more than 6 meters depth under the Extreme Equinox Low Water. A near horizontal lateral tidal bar is developed between 2 and 4 meters depth and separated from the intertidal areas by a high slope step of 2 meters (Morales et al., 2014). Water circulation within the estuary is almost exclusively confined within this narrow so-called bypassing channel which connects directly the river to the open littoral zone (Garel et al., 2009). The marine sector of the estuarine channel consists of successive meanders imposed by the hard geology of the substrate (Lobo *et al.*, 2004; Morales *et al.*, 2006; Morales et al., 2014). Curved sectors of the channel present a section characterized by a pool in the concave margin and a lateral tidal bar in the convex one and inflection points between successive curved tracks, presents a symmetric bed profile with an intermediate depth and without pools and bars (Morales, 1997; Morales et al., 2014).

5.2.2 BED SEDIMENT TYPES

Only about 7 km of the channel from the mouth is embedded in soft sediment (Garel et al., 2009). Bottom sediments are predominantly sands, with mean diameters of about 600 μm, except near the margins where significant amounts of mud are present (Fortunato and Oliveira 2003). Morales et al., 2014 have distinguished four types of beds in the lower estuary. They are : (1) about 3 km from the mouth, the sediment is characterized by a mean grain size of coarse sand, but with an important population of medium sand, a moderate sorting, a mesokurtic shape and a lightly positive skewness (with tail towards the fine); (2) about 3.5 km from the mouth, the sediment is characterized by a mean grain size of medium sand, but with abundant populations of coarse and fine sands, present also a moderate sorting and a positively skewed distribution (with tail towards the fine), but with a leptokurtic shape; (3) after another 0.5 km upstream of

the previous area, the abundance of fine sediment increases; and (4) further upstream sediment types presents a very high dispersion, an extremely poor sorting, a negative skewness (tail towards the coarse) and a platykurtic (plane) shape.

5.2.3 HYDROLOGIC AND HYDRODYNAMIC SETTING

The river inputs to the Guadiana estuary are highly variable, at a seasonal and inter-annual scale producing severe droughts and episodic floods in the river basin (Garel et al, 2009). The maximum historical peak discharges are estimated around 11000 m^3/sec in winter 1876 (Rocha and Correia, 1994; Ortega and Garzo´ n, 2009). The monthly river discharge ranged from <10 m^3/sec to 4660 m^3/sec for the period 1947–2001 (Garel et al., 2009). The flow is forced mostly by tides and river flow (Fortunato and Oliveira 2003) and the system is strongly flood-dominant because it has few tidal flats (Fortunato *et al.*, 2002). The estuary exhibits a semi-diurnal, meso-tidal regime with a mean range of approximately 2.5 m. The mean neap tidal range is 1.22 m and the mean spring tidal range is 2.82 m (Garel et al., 2009) with a maximum spring tidal range of 3.5 m (Fortunato and Oliveira 2003). Tidal wave propagation in the estuary generates currents with velocities exceeding 0.5 m/s (Morales, 1997). The waves in this coastal region can be classified as medium- to low-energy waves, and in terms of frequency of occurrence, 49% of the waves represents Atlantic swells and 51% local sea waves. The mean annual offshore significant wave height is about 1 m with an average period of 4.7 s (Costa et al., 2001).

5.2.4 HUMAN PRESSURES IN THE AREA

The estuarine system consists of extensive salt marsh areas on both sides of the inlet (Boski et al., 2002), whose extension of the salt marshes is much reduced compared to the period with unhindered sedimentation during the Holocene (Boski et al., 2008). This intense

transformation of the system is due to strong anthropogenic pressure, including dams, coastal defenses (Sampath et al., 2015), urbanization, farming and aquaculture (Me´nanteau et al., 2005). In 2002, the total dammed area in the watershed increased to 89% with the construction of the Alqueva dam (Gonzalez et al., 2007). Before the construction of the Alqueva dam, the hydrographic regime of the Guadiana River was characterized by low flows in summer and episodic flooding events in winter (Fig. 5.2). Since then, the total fluvial discharge has varied between 7 and 57m^3/s on average years, and reach 280m^3/s on wet years (Fortunato and Oliveira 2003). As a result, the shortage of silt supplied by the river, there has been a rapid decrease in the area of estuarine salt marshes (Sampath et al., 2011).

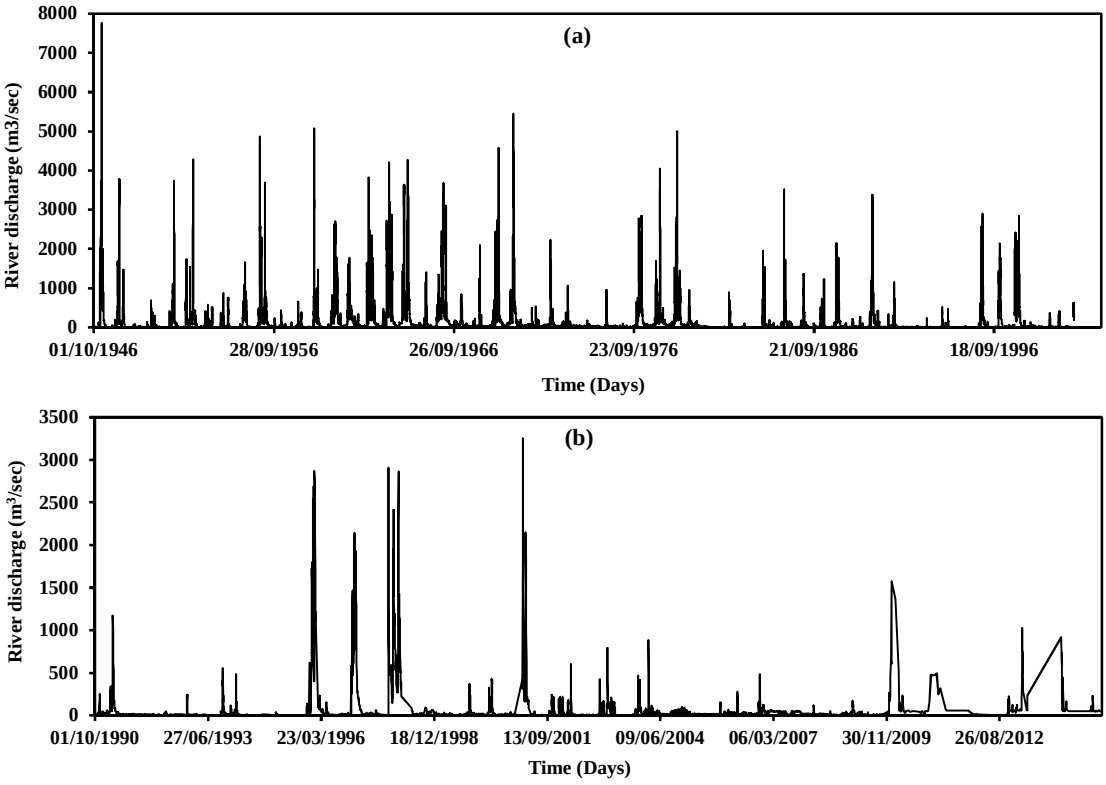

Figure 5.2 River discharge of the Guadiana estuary as measured at the gauge station of Pulo do Lobo: (a) from 1946 to 2000 and (b) from 1990 to 2014 May.

In addition, the construction of jetties at the mouth of the Guadiana River in the 1970s has interrupted the dominant eastward-directed longshore drift. This has resulted in a reduction

in the amount of marine sediment supplied to the estuary over the last 35 years. The disruptive effects of the jetties are clearly manifested on the Spanish margin of the estuary, where rapid shoreline retreat at an average rate of 3 m/yr occurred between 1996 and 2005, with a recorded maximum retreat of 4.8 m/yr (Sampath, 2015).

5.2.5 NATURAL PRESSURES

Global vulnerability analyses by Nicholls et al. (2007) and IPCC (2013) have predicted a climatically driven increase in vulnerability of the coastal zones due to sea-level rise, increased storminess, and climate change. Indeed, the assembled records of altimetric data from the TOPEX/Poseidon, Jason-1, and Jason-2 satellite missions indicate that the average rate of sea-level rise during the period 1993–2009 was 3.2 ± 0.4 mm/yr (Nerem et al., 2010),. Linear regression analysis of tide gauge datasets from Cascais and Lagos estimates that sea-level rise along the Portuguese coastline will be 14–57 cm above the contemporary level by the end of the 21st century (Dias and Taborda, 1992). This value is comparable with the upper limit projection (59 cm) of sea-level rise under the A1FI sea-level rise scenario of the IPCC (2007). Dias and Taborda (1992) conclude that most of the signals indicating sea-level rise at these stations are of global origin, which emphasizes the validity of global projections for the study area. In addition, the (annual and wintertime) Guadiana River discharge shows an inverse correlation with the North Atlantic Oscillation (NAO), which is the dominant mode of the winter climate variability in the north Atlantic region (Dias et al., 2004; Trigo et al., 2004).

5.3. METHODOLOGY

Assessment of the sensitivity of bed friction coefficients, the power of the current velocity in the erosion rate function, and sea-level rise rate in determining the decadal scale morphological evolution in the Guadiana estuary were mainly based on the theoretical

framework of the Prandle (2009) to represent the estuarine dynamics. The framework is based on the analytical solutions to the one-dimensional and cross sectionally averaged shallow-water wave equations. The equations were simplified for the first-order tidal simulations by neglecting the convective terms and by linearizing the quadratic friction term of the shallow-water wave equation. This approach is further simplified for a triangular shaped synchronous estuaries, as the surface gradients associated with axial amplitude variations in ς^* is assumed to be significantly less than those associated with corresponding phase variations. These assumptions are shown to be valid except in the shallowest conditions at the tidal limit (Prandle, 2003).

According to Sampath et al. (2015), in the Guadiana estuarine systems composed of intertidal mudflats and salt marshes, the rate of relative elevation change (dZ/dt) at a given point and over a known period of time can be represented in terms of sedimentation rate, erosion rate and sea-level rise rate (Eq. 5.1). In this estuary, deep subsidence has been found to be negligible (Lobo et al., 2003). Shallow compaction is negligible as a result of the low organic content (Boski et al., 2008).

$$\frac{dZ}{dt} = \frac{dS_{Min}}{dt} - \frac{dE}{dt} - \frac{dM_{MSL}}{dt} \quad (5.1)$$

The elevation change (ΔZ) at a given initial depth (h) over Δt time step can be derived by integrating mineral deposition and erosion over each tidal cycle over *M* years with *m* tidal cycles, where ρ_{sed} is the dry density of sediment (Eq. 5.2).

$$\Delta Z_{\text{ at a given location}} = \sum_{j=1}^{m} \left\{ \left(\alpha \frac{dS_{Min}}{dt} - (1-\alpha) \frac{dE}{dt} \right) \Delta t \right\} \quad (5.2)$$

where α= 0 or 1 if there is accretion or erosion respectively, over the time period considered.

We assumed that the deposition and erosion processes do not occur simultaneously. It was shown by Partheniades, (2009), erosion and deposition of cohesive sediments do not take place simultaneously. Thus, it is assumed that the sedimentation occurs over a certain period from the start of slack periods of low and high tides (Brown 2013). The slack periods start ca 1 and 2 h after the high and low tides of the Guadiana estuary, respectively (Garel et al. 2009). The instant of accretion (Eq. 5.3) or erosion (Eq. 5.4) will be given by decimal values 2t/T where t is instantaneous time of the tidal cycle and T is the Tidal period.

$$\alpha = 0 \quad if\ 0.25 < \left\{\left(\frac{2t}{T}\right) - \left(Int.\ \frac{2t}{T}\right)\right\} < 0.75 \tag{5.3}$$

$$\alpha = 1 \quad if\ \left\{\left(\frac{2t}{T}\right) - \left(Int.\ \frac{2t}{T}\right)\right\} < 0.25\ and\ \left\{\left(\frac{2t}{T}\right) - \left(Int.\ \frac{2t}{T}\right)\right\} > 0.75 \tag{5.4}$$

In process-based approaches the instant of erosion or accretion is determined by the critical bed shear stress because the bottom stress is a first-order term in the momentum equation that describes the coastal circulation and sediment transport (Ganju and Sherwood, 2010). In reality, there would period where there is no erosion or accretion. However, in the context of behaviour-oriented model, such simplifications would be justified.

5.3.1 SEDIMENT DEPOSITION OVER A TIDAL CYCLE

The sediment deposition rate in sub-tidal channels can be approximately estimated by calculating accretion and erosion separately. Steady advective settlement and intermittent contacts of sediments with the bed via vertical turbulent excursions are the dominant processes that govern the sediment deposition rate in an estuary (Prandle, 2009). We assume the deposition occurs only in the slack period. The slack period of the Guadiana estuary is approximately 1 h after high tide (Garel et al., 2009). As the present study is focused on

simulating the long-term morphological evolution of estuaries, we can conveniently assume that the resuspension of the sediment due to turbulence is not important as all dispersive collisions settles during this time frame. That is the estuary bed is fully absorptive (Sanford and Halka (1993). Hence, sediment deposition rate (mm/sec) can be represented in terms of settling velocity (W_s) sediment concentration near the bed (C_b) and bulk density of sediment (Prandle, 2009):

$$\frac{dS}{dt} = \frac{W_s C_b}{\rho_{sed}} \tag{5.5}$$

The settling velocity of fine to medium sand particles ($D_{50} \approx 0.125 – 0.35$ mm) was estimated in terms of the kinematic viscosity of water (ν), average grain size diameter (D_{50}) and non-dimensional grain diameter D_* (Hallermeier, 1981 and van Rijn 1984):

$$W_s = \frac{\upsilon}{D_{50}}\left[(10.36^2 + 1.049D_*^{0.3})^{0.5} - 10.36\right] \tag{5.6}$$

$$D_* = \left[\frac{g(s-1)}{\nu}\right]^{1/3} \tag{5.7}$$

where g being the gravitational acceleration, and s the ratio of the grain density to the water density. The grain density is set to a default value of 2650 kg m^3, representative of quartz sediments.

Settling velocity of silt to very fine sands ($D_{50} \approx 0.25 – 0.125$ mm) was derived using the formula of Lane and Prandle (2006) to account for the increase of settling velocity due to flocculation of particles (Eq. 5.8). Prandle (2009) shows time series of C_b can be related to depth-averaged concentration (Eq. 5.9).

$$W_S = D_{50}^2 \tag{5.8}$$

$$C_b \approx \frac{h}{\sqrt{\pi E t}} \bar{C} \tag{5.9}$$

Morales (1995) proposed an empirical model for estimating the depth-averaged sediment concentration in the Guadiana estuary in terms of river discharge Q_R (m^3/sec). There is a fundamental issue of using this relationship for hindcasting suspended sediment concentrations in the Guadiana river during the Holocene. But we used this formula because the present approach mainly focus on conceptualizing the problem of long-term modelling of morphological evolution in estuaries.

$$\bar{C} = \left(\frac{Q_R}{0.03}\right)^{0.5} \tag{5.10}$$

As explained in the section 5.2.4, the discharge of the Guadiana River was drastically reduced after 2002 with the closure of the Alqueva dam for impounding the reservoir. Though it is possible to model the time series of River Discharge using Fourier analysis, a simple approximation of the available archived data from Pulo do Lobo gauge station of the Guadiana River was used in the model (Fig. 5.3). Large discharges with high fluctuations over a considerable period were averaged for simplicity and reduce the MATLAB scripts in the program. Suspended sediment concentration at peak discharge occasions were obtained by scaling the value estimated using Eq. 5.10 to comparable with concentrations observed during similar situations by Marchado et al. (2007) and Garel et al. (2009).

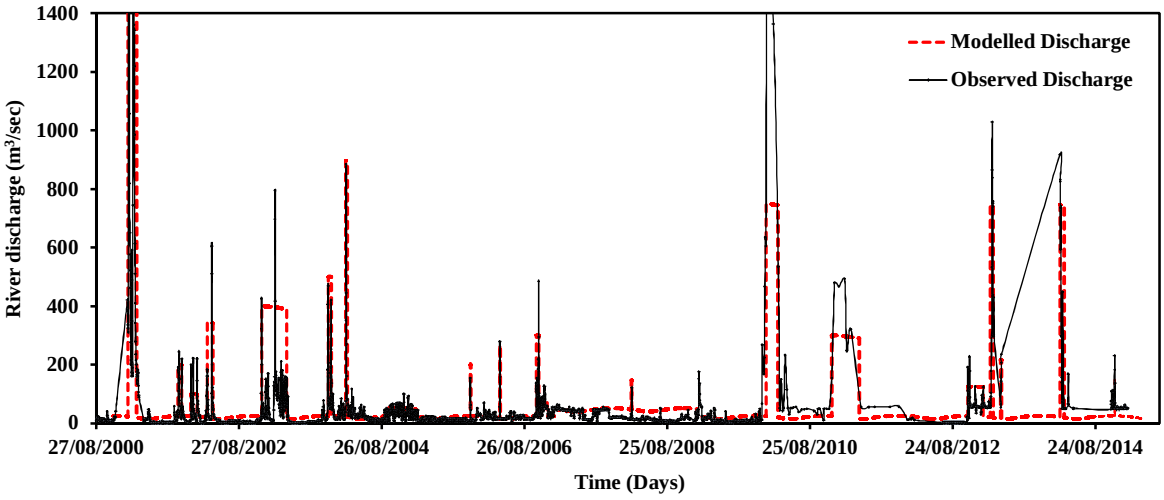

Figure 5.3 Observed and approximated river discharge of the Guadiana estuary from 2000 to 2014 May and pulse like large discharges with high fluctuations over a considerable period were averaged for simplicity in the Matlab script.

The dispersion coefficient E, can be approximated by (Prandle, 1982):

$$E = fU^{*}h \tag{5.11}$$

where *f*, is the bed friction coefficient, h is the water depth and U* is the tidal current amplitude.

We used the expression derived by Jones (1983) to estimate the bed friction in terms of bed roughness, Z_0 (Eq. 5.12).

$$f = 0.74Z_0^{0.71} \tag{5.12}$$

We assume bed roughness consists of the form drag resulting from ripple/dune formation with wave length of λ_r (=1000D_{50}) and the skin friction related to the coarse sand with grain size D_{50} for hydraulically rough flow (Reeve et al., 2004).

$$Z_0 = \frac{\lambda_r}{49} + \frac{2.5D_{50}}{30} \tag{5.13}$$

Prandle (2009) presents a solution for the tidal current amplitude, U* for synchronous estuary condition where the spatial gradient in tidal elevation amplitude (ζ*) is zero (Eq. 5.14). That is the unique wave number (k) for axial propagation of current (U) and surface elevation (ζ). In the Guadiana estuary the tidal wave propagates in synchronic mode up to 50 km from the mouth (Morales 1993). This characteristic may be preserved even during the spring tides as the tidal range attenuation is less than 20 cm per 10 km along the longitudinal axis of the river (Garel et al., 2009).

$$U^* = \zeta^* g \frac{k}{(\omega^2 + F^2)^{0.5}} \quad (5.14)$$

The linearized dimensionless bed friction coefficient (F) was related to the phase angle (θ) and tidal frequency (ω) and it can be estimated using the Eq. 5.15 where and ∂h/∂h is the axial bed slope (Prandle 2009).

$$\tan\theta = -\frac{F}{\omega} = \frac{\partial h/\partial x}{0.5hk} \quad (5.15)$$

$$k = \frac{\omega}{\sqrt{0.5hg}} \quad (5.16)$$

5.3.2 SEDIMENT EROSION OVER A TIDAL CYCLE

The short-term erosion rate in an estuary can be approximated using the simple formula of Prandle (2004) where γ is the sediment erosion coefficient (Eq. 27). For tidally dominated estuarine regimes, erosion rate is relatively insensitive to the power N (= 2-5) and U_c (Prandle, 2004). On the other hand, Lane and Prandle (2006) suggested that the precise calibration of

hydrodynamics and sediment modules are likely to be unsuitable for long-term applications. Thus we assume U_c=0 and N=2 (Eq. 5.18).

$$\frac{dE}{dt} = \frac{\gamma' \rho_w (U_t - U_c)^N}{\rho_{Sed}} \quad (5.17)$$

$$\frac{dE}{dt} = \frac{\gamma' \rho_w (U_t)^2}{\rho_{Sed}} \quad (5.18)$$

As given by Lane (2004), the main constituents of current velocity speed (Ut) were assumed to be current velocitys (U_0) due to river discharge and semi-diurnal (M_2) and quarter diurnal (M_4) currents.

$$U_t = U^* \cos(\omega t) - aU^* \cos(2\omega t - \theta) - aU^* \cos\theta \quad (5.19)$$

Where a=ζ*/h.

5.3.3 TIDAL HEIGHTS AND WATER DEPTHS OF THE ESTUARY.

Tidal heights, ζ^* for the model were estimated using the Eq. 5.20, based on the tidal parameters of constituents given by Pinto (2003).

$$\zeta^* = z + \sum_{i=1}^{N} \zeta_i \cos\left(\frac{2\pi t}{T_i} - \frac{\pi \phi_i}{180}\right) \quad (5.20)$$

where, ζ_i, ϕ_i, T_i were tidal amplitude, phase lag and period of the i^{th} tidal constituent and N is the number of tidal constituents considered for calculating the water level.

Compared to the observed archived data for the Guadiana estuary by the Instituto Hidrografico, (1990), the maximum and minimum tidal levels and the maximum tidal range were able to predict with good accuracy (Fig. 5.4). Then the estuary water depth at a given cell,

h(t) will be determined by the elevation z relative to the mean sea level and the sea-level rise. Though the analytical solutions were derived by Prandle (2009) for tidal propagation of estuaries were based on dominant tidal constituents, the water depths in the estuary have to be estimated with good accuracy because the net accretion rates were related to the water depths in the model. Therefore, the tidal heights were estimated using 10 tidal constituents.

Table 5.1 Tidal constituents used for determining the tidal heights in the model (Pinto, 2003).

Tidal constituent (i)	**Amplitude (ς_i) (m)**	**Period (T_i) (Seconds)**	**Phase (ϕ_i) (Degree)**
M2	1.03	44712	198.7
M4	0.021	22356	39.4
S2	0.34	43200	91.8
O1	0.0503	92969	66.5
K1	0.062	86170	64.7
MSf	0.02	1275721	313.5
N2	0.21	45570	357.8
K2	0.07	43082	117.1
MS4	0.004	21972	229.8
M6	0.01	14904	250.0

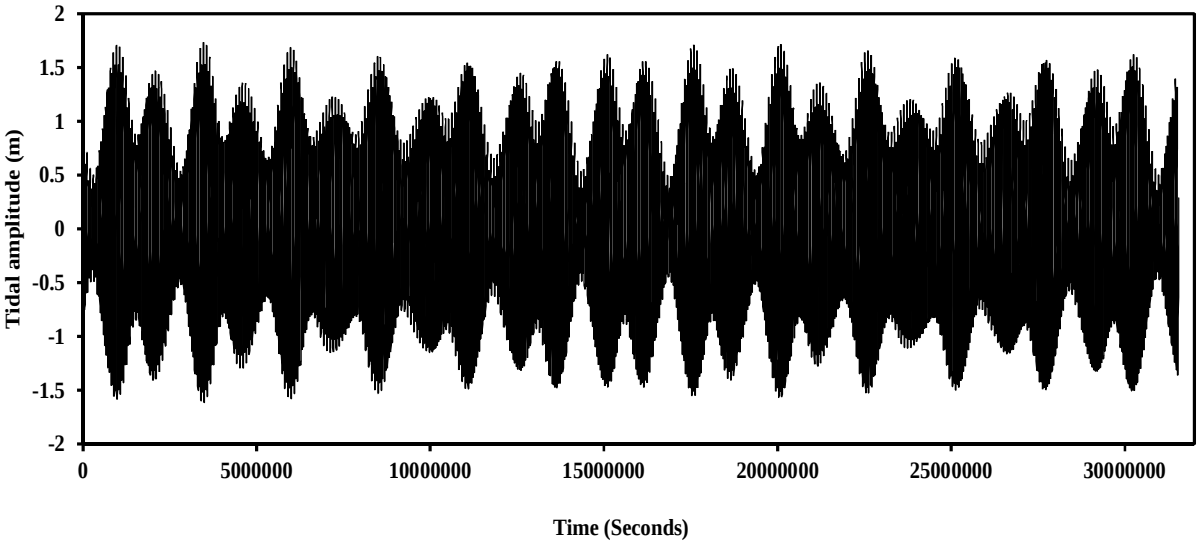

Figure 5.4 Modelled tidal heights of the Guadiana estuary for a year in terms of 10 tidal constituents.

5.3.4 SENSITIVITY OF POWER OF CURRENT VELOCITY, FRICTION AND SEA-LEVEL RISE ON ESTUARINE MORPHOLOGICAL EVOLUTION.

As different values were proposed for the index n, the power of the current velocity of the erosion rate function by various authors. Therefore, we simulated the morphological evolution of the Guadiana estuary for n values of 1.8, 2, 2.5, 3, 4, 5, 6, 7, and 8. The sea-level rise rate was assumed as 3.2 mm/yr for these simulations. Bed friction of the each cell was derived by the expression of Jones (1983). The input elevation data set was derived from the observed bathymetric map of the Guadiana estuary for the year 2000 and the simulation carried out until 2014 May with 1200 second time step.

The bed friction f appears in both the sediment deposition rate and erosion rate functions. Thus, the effect of the bed friction will be non-linear on the elevation change in estuaries. Simulations were carried out by increasing or decreasing the values of the empirically estimated bed friction of each cell by ±50, ±30, -20%, ±10%, +80%, 90%, 100% and +107% for n =1. 8, 2, 2.5 and 3. The sea-level rise rate was assumed as 3.2 mm/yr for these simulations. The resulting modelled morphology for 2014 May was compared with the corresponding observed elevation data set to derive the elevation change and the average net accretion rate for the above conditions.

The study of the sensitivity of bed friction on morphological evolution revealed that there is an interrelation between the bed friction and the power n. There were four optimum modelled solutions for the observed elevation change over 14 years. We used those four solutions to access the sensitivity of sea-level rise rates on estuarine morphological changes in decadal time scale. Simulations were carried out by changing the sea-level rise rates to 1, 2, 3.2, 4 and 5 mm/yr. The observed rate of global mean sea-level (GMSL) rise is +3.2 ± 0.4 mm yr^{-1} since 1993 (Church, et al 2013; Masters et al., 2012).

For the above four combinations of the friction factor and n value, we studied the effect of dam construction (in particular the Alqueva dam) along the Guadiana river on the estuarine morphology. The temporal variability of the average elevation change over the lower estuary were assessed from 2000 to 2014 May. The model was scripted with MATLAB, an advanced scientific computational language and spatial analysis were carried out using Geo-processing and 3D Analysis tool of ESRI ArcGIS software.

5.4 RESULTS

5.4.1 OBSERVED AND SIMULATED DISTRIBUTIONS OF ELEVATION CHANGE

According to the results, the observed elevation change from 2000 to 2014 shows and normal distribution (Fig. 5.5a and 5.5b). The observed average elevation change ($\overline{\Delta Z_{obs}}$) of the normal distribution is 0.369 m and the standard deviation (σ_{obs}) is 0.766 m. The maximum accretion and erosion in the 10 km stretch of the channel from the mouth is 4.5 and 3.2 m, respectively. Simulated elevation changes over the same period for different powers (n) of the current velocity of the erosion rate function (Prandle, 2009) do not show much difference in the case of standard normal distribution curves.

However, compared to the standard normal distribution, there are clear variations of the distribution patterns of elevation change for different n values. Simulated average elevation change ($\overline{\Delta Z_{Sim}}$) increase from negative to positive value when the value n increases from 1.5 to 3 and then it is almost constant in between n=3 and 8. Standard deviations of simulated distributions of elevation change also show a similar behaviour.

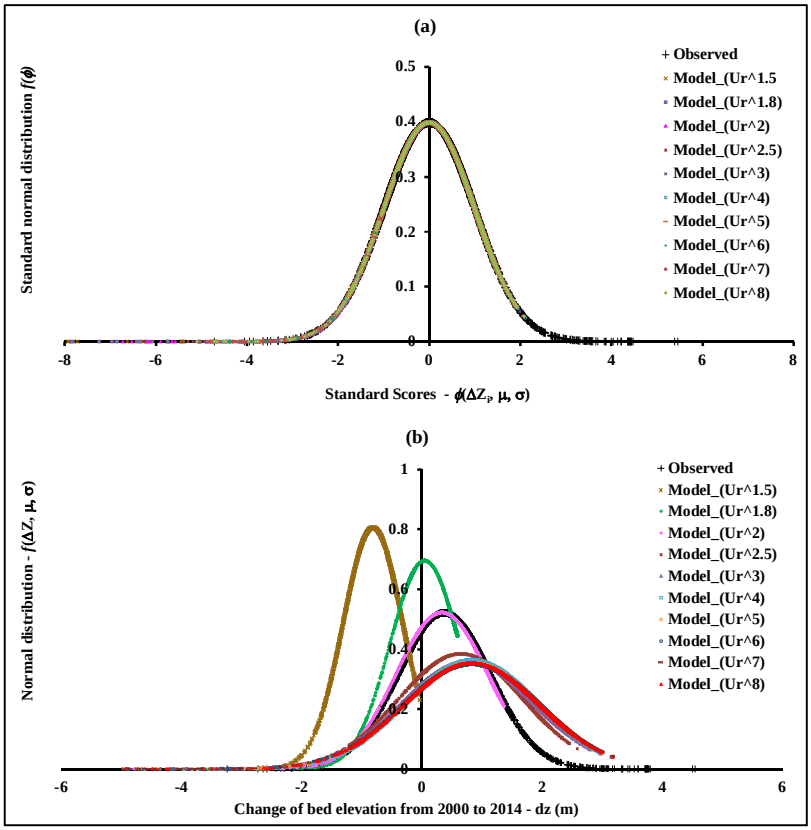

Figure 5.5 Observed and simulated distributions of elevation change of the Guadiana estuary from 2000 to 2014. (a) Standard normal distribution and (b) normal distribution.

$$f(\Delta Z_i, \overline{\Delta Z}, \sigma) = \frac{1}{\sigma\sqrt{2\pi}} e^{-(\Delta Z_i - \overline{\Delta Z})^2/2\sigma^2} \quad (5.\ 21)$$

$$\overline{\Delta Z} = \frac{1}{N}\sum_{i=0}^{N} \Delta Z_i \quad (5.22)$$

$$\sigma = \sqrt{\frac{\sum_{i=0}^{N} \Delta Z_i{}^2 - \frac{1}{N}\left(\sum_{i=0}^{N} \Delta Z_i\right)^2}{N-1}} \quad (5.23)$$

$$f(\Phi, \mu = 0, \sigma = 1) = \frac{1}{\sqrt{2\pi}} e^{-(\Phi)^2/2} \quad (5.24)$$

$$\Phi = \frac{\Delta Z_i - \overline{\Delta Z}}{\sigma} \quad (5.25)$$

where ΔZ_i is the elevation change from 2000 to 2014 of the the i^{th} cell and N is the number of cell in the domain considered in the simulation.

The observed normal distribution elevation change and the simulated distribution corresponding to n=2 shows a good agreement with each other despite the extreme accretions were not able to be simulated properly. For n=2, the model was able to produce maximum erosion about 5m and maximum accretion 1.7 m. All the simulated curves show this deficiency, but when the n value is increased, it is possible to simulate high accretion cells, though the distribution curves deviate from the observed pattern significantly. These extreme accretion cells may be due to transportation of sand bars and sand waves as the rivers are highly dynamic. Prandle, 2009 suggest that n is typically in the range of 2-5 and Lane and Prandle (2006) found that n=2 can be used to reproduce the sediment concentration in the Mersey Estuary. Lavelle et al (1984) inferred a value of n=8 for fine sediments. Van Rijn (1993) found transport rates of fine sands proportional to powers of current between 2.5 and 4 depending on wave conditions.

As explained under the methodology, the friction factors for all the simulations were estimated based on empirical equation of Jones (1983) where bed roughness can be related to drag resulting from ripple/dune formations, and the skin friction, which is related to the grain size, D_{50}, of coarse sand for a hydraulically rough flow (Reeve et al., 2004). The sea-level rise rate is 3.2 mm/yr which was the global mean sea-level rise rate estimated from satellite altimetry data (Watson et al., 2015).

5.4.2 SENSITIVITY OF FRICTION COEFFICIENT ON MORPHOLOGICAL EVOLUTION.

As the empirically estimated bed friction of each cell has increased from 0.5*f to 2.07*f (changed by ±50, ±30, -20%, ±10%, +80%, 90%, 100% and +107%), mean value of the distribution curve of the elevation change shift towards negative showing increased erosion (Fig. 4). When the power (n) of the current velocity increased from 1.8 to 3, the mean value

shift towards positive showing increased accretion. This behaviour is only valid for a case of Ur < 1 m/sec (Fig. 5.6). Interestingly, it is possible to find normal distribution patterns approximately similar to the observed distribution of the elevation change in the Guadiana estuary bed from 2000 to 2014. They are: (1) for n = 1.8, and when the friction factor is reduced by 20% (0.8*f); (2) for n = 2 and no change in friction factor; (3) for n = 2.5, and when the friction factor is increased by 50% (1.5*f); (4) for n =3, and when the friction factor is increased by 107% (2.07*f). However, these similar situations may not imply that the estuary bed experience the same dominant process under those four situations. This aspect will be discussed in the section 5.4.4. The extreme accretions were able to simulate for reduced values of the friction coefficients but there would be a clear shift in the average elevation change and the standard deviation of the data sets.

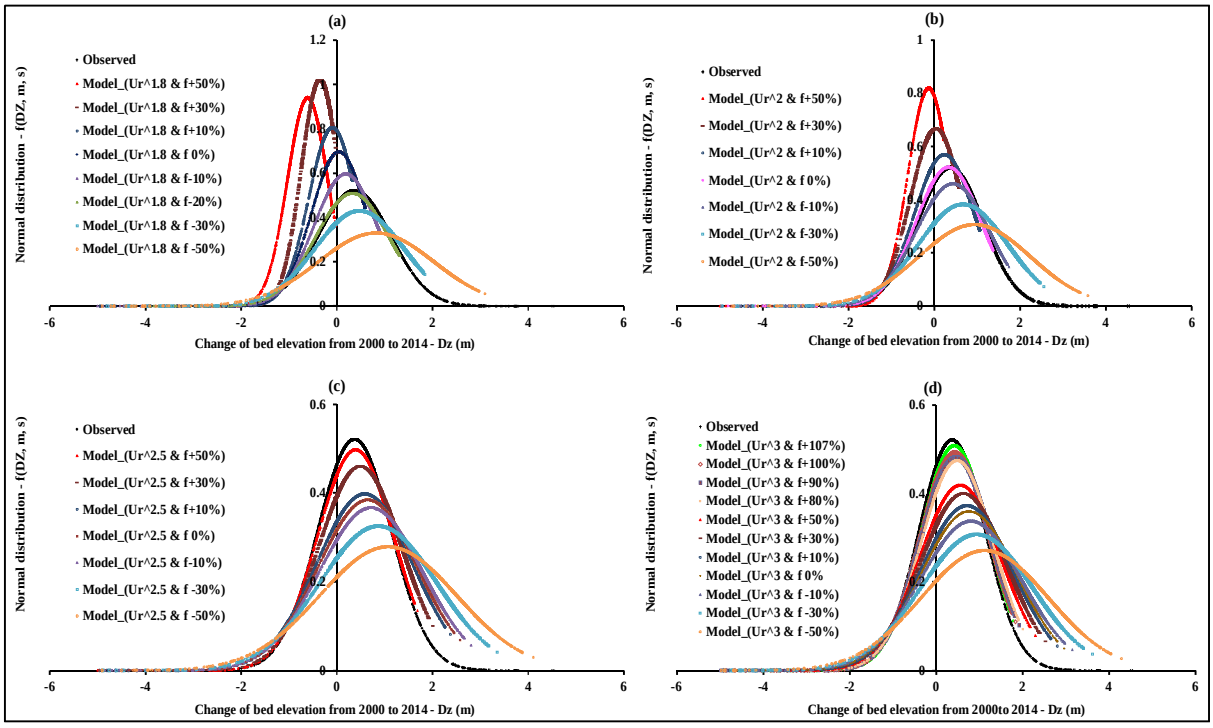

Figure 5.6 Sensitivity of bed friction coefficient (f) and power (n) of current velocity in the erosion rate function on determining the probability distribution of the elevation change of the Guadiana estuary from 2000 to 2014.

For the changes in friction coefficient and the power n, the variation of the average accretion and standard deviation are shown in Figure 5.7a and 5.7b, respectively. Variation of average elevation change and standard deviation over this period for the case n = 8 were also shown in respective figures. This simulation was carried out to find the extreme limit of n. The trend in the average elevation change is almost linear when the n values are 1.8 and 2. For the cases of n= 2.5 and above, the average elevation change exhibits a non-linear behaviour and may be approximated with polynomial function.

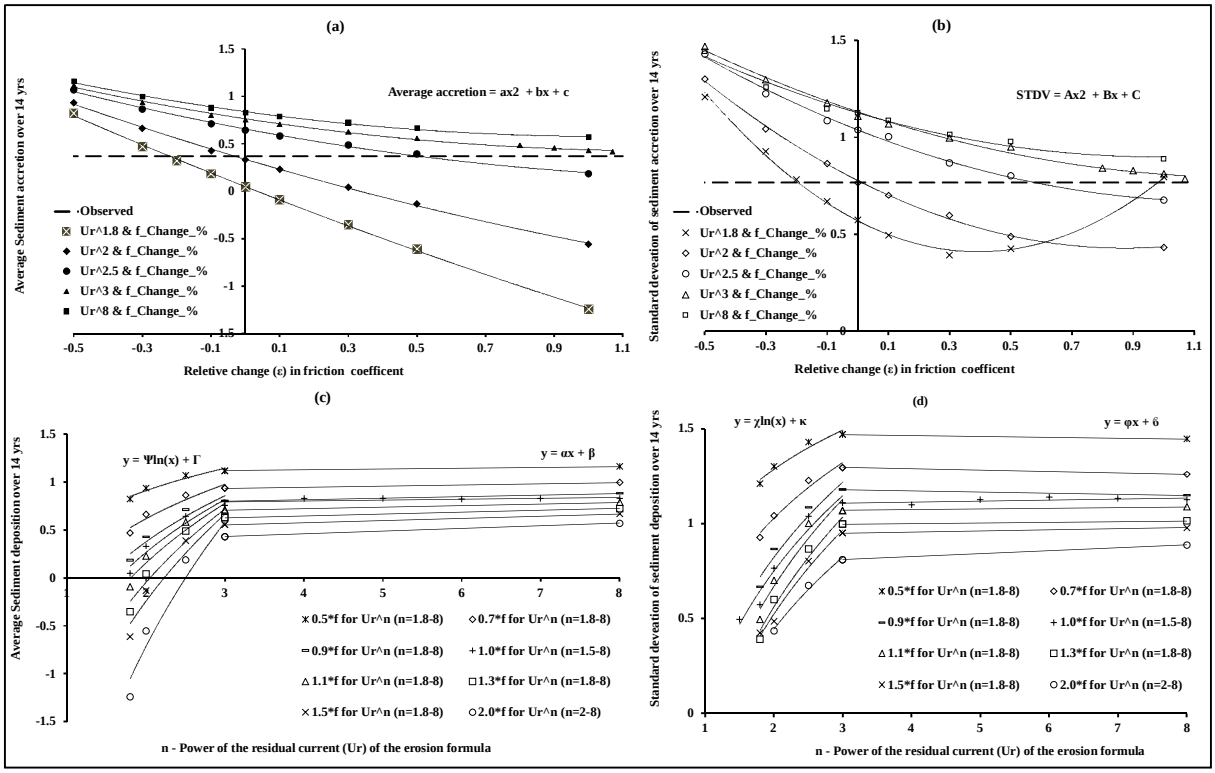

Figure 5.7 Sensitivity of estimated bed friction coefficient and power (n) of the current velocity of the erosion function on the average elevation change and corresponding standard deviation based on the simulated bathymetries of the Guadiana estuary for 2014.

The standard deviation and change in friction coefficient for above cases are non-linear relationship for all n values. The horizontal dashed lines in both figures represent the observed

average value of the elevation change and corresponding standard deviation during this period. Thus, the n =3 would be the limiting case where we can obtain an approximate normal distribution that is similar to the observed data set. For n =8, the polynomial curves will not intersect the horizontal line. This will suggests that the most suitable values for power n of the current velocity in the erosion function would be between 1.8 and 3.

Average elevation change and standard deviation show a logarithmic relationship with the power (n) of the current velocity for n =1. 8 to 3 and for n > 3, both parameters do not depend on the value of the n (Fig. 5.7c and 5.7d). If the friction factor decreased and limits to zero, we can expect that the average elevation and standard deviation does not correlate with the value n and there would be constant average elevation for any n values. That would be an ideal case of smooth channel.

5.4.3 MORPHOLOGICAL EVOLUTION IN THE GUADIANA ESTUARY BED.

Simulated bathymetries of the Guadiana estuary that corresponding to the four cases explained previous section, show good agreement with the observed bathymetry obtained using the single beam echo-sounding technique (Fig. 5.8). There are extensive shallow regions in the main channel that are less than 4 m in depth. However, a mildly meandering deep channel with an average depth of 8 m is a characteristic of the both maps of 2000 and 2014 of the Guadiana estuary. On the other hand it is recognized that the vessels which navigate through this channel generate locally significant turbulence and waves and therefore, sediment deposition and/or erosion will not be solely/directly governed by the tidal currents in the estuary.

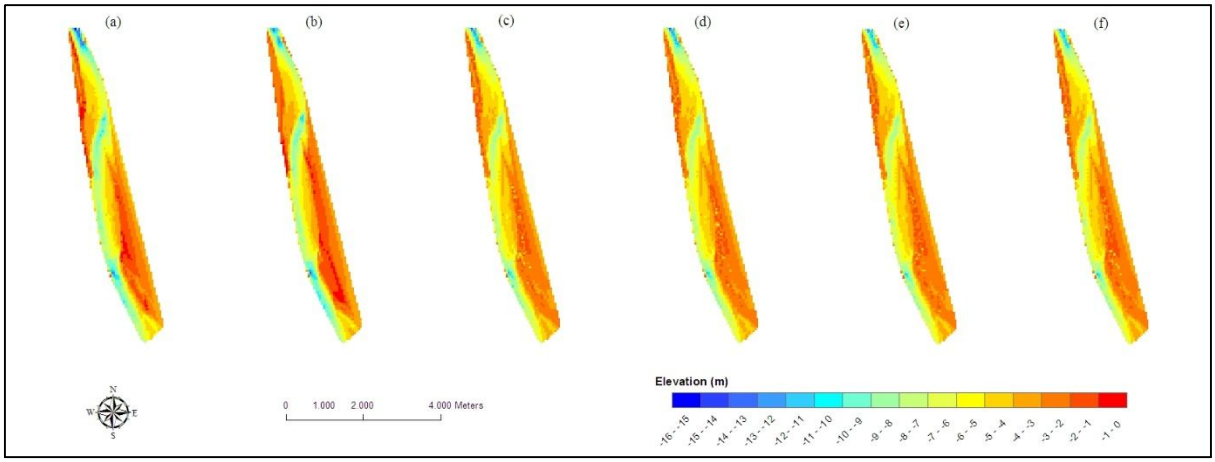

Figure 5.8 Observed bathymetries (z) and simulated bathymetries of year 2014 of the Guadiana estuary with respect to mean sea-level of the year 2000. (a) Observed z of the 2000; (b) observed z of the 2014; (c) simulated z (n = 1.8 and empirically estimated friction coefficients were reduced by 20%; (d) simulated z (n = 2 and empirically estimated friction coefficients were not changed; (e) simulated z (n = 2.5 and empirically estimated friction coefficients were increased by 50%; (f) simulated z (n = 3 and empirically estimated friction coefficients were increased by 107%.

The morphological evolution in the Guadiana estuary can be understood from the elevation change of the bed over this period. The observed map shows erosion mainly in the Portuguese margin of the channel and shallow regions close to the mouth of the river (Fig. 5.9). Accretion has taken place in other areas where average value would be about 20 cm over this period. However, there is a significant increase in the accretion depth (about 4 m) near to the Spanish margin and 6 Km from the mouth. Adjacent to this highly localized accretion region, there is a channel with increased erosion about 2 m. That is nearly perpendicular to the river flow. The highly localized erosion and adjacent accretion area would be trough and crest regions of sand waves moving towards the ocean. Sometimes this special feature may be due to frequent maneuvering of vessels along this path to a loading and unloading location situated in the Spanish margin.

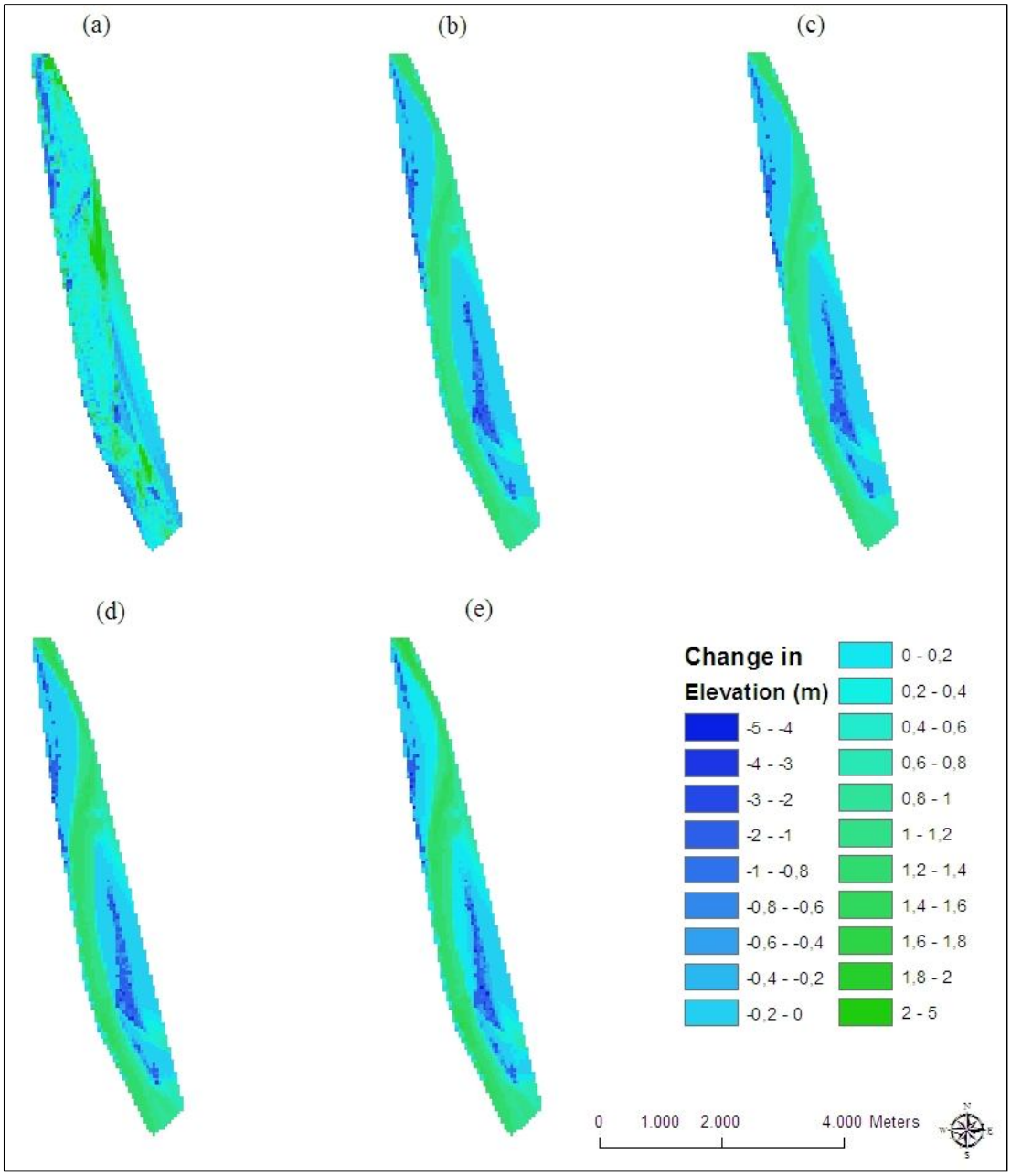

Figure 5.9 Observed and simulated elevation change of the Guadiana estuary from 2000 to 2014. (a) Observed ΔZ; (b) simulated ΔZ (n = 1.8 and empirically estimated friction coefficients were reduced by 20%; (c) simulated ΔZ (n = 2 and empirically estimated friction coefficients were not changed; (d) simulated ΔZ (n = 2.5 and empirically estimated friction coefficients were increased by 50%; (e) simulated ΔZ (n = 3 and empirically estimated friction coefficients were increased by 107%.

On the whole, the observed and simulated elevation change patterns corresponding to the four cases discussed here can be very much comparable. Simulated maps also show high erosion in the Portuguese margin and shallow regions near to the mouth. However, simulated erosion near to the mouth is approximately four-fold higher than that in the observed map. In case of n = 1.8 and 2 and corresponding friction coefficients, erosion of this shallow region extends up to the Spanish bank and the average erosion height was 0.5 m. In the other two cases, the erosion height is about 0.2 m. The increase of accretion near to the downstream of the bridge (farthest limit from the river mouth considered in the analysis can be highly comparable between both observed and simulated ΔZ maps. The simulated elevation changes show an increased accretion of 1m height in the deep section of the channel of the Guadiana estuary. That is not clearly visible in the observed map. However, there is an increase, but scattered accretion along this sub-channel in the simulated maps. This may be resuspension and transportation of the sediment away from this channel due to the disturbances for flows and currents with frequent navigation of large vessels. Possible impacts due to navigation on the hydrodynamic characteristics that govern the flow patterns near the bed of the deep channel and thereby the sedimentation were not considered in the model development. Therefore, we may not be able to expect accurate sedimentation patterns in that region.

5.4.4 ANNUL VARIABILITY OF THE ELEVATION CHANGE IN THE ESTUARY.

Simulation results for the four cases considered in this study were used to understand the annual variability of the elevation change relative to the year 2000 (Fig. 5.10). At present, the river water discharge is regulated by more than 100 dams (Wolanski et al. 2006). The Alquea dam that forms the largest reservoir in Europe (Dias et al., 2004) was closed in February 2002 (Garel 2009). The simulated models corresponding to the four cases show almost same rate in the average elevation change until 2002. During 2002 and 2003, the simulated average

elevation changes increase, but with slower rate compared to the rate before 2002. This implies that the lower estuary has experienced immediate response of the closure of the dam. Then, the average elevation change corresponding to n = 1.8 and 2 decreases until 2005. Those two cases show a near equilibrium situation in the estuary bed from 2005 to 2010 as the average elevation change was approximately constant. As the downstream experiences low flow conditions further, the simulated average elevation change corresponding to n = 1.8 and 2 started to decrease showing identical rates for both cases. This would coincide with the year at which the reservoir reached its full capacity with the 250 km^2 surface area.

When n = 2.5, the simulated average elevation change slowly increases from 2002 to 2010 and then it showed a near equilibrium until now. The simulated average elevation change corresponding to n = 3 also showed a comparatively high rate of increase until 2010 but slow down afterwards. Thus, the effect of reduction of river discharge and thereby fluvial sediment supply to the estuarine system can be visible in all four cases. However, they do not undergo identical processes. At present, cases corresponding to n = 1.8 and 2 represent dominant erosion process while the case n = 2.5 represents a near equilibrium situation in the bed. The case represents an accretion phase. However, according to our understanding of the estuary, the case of n = 1.8 and 2 would be more applicable to the Guadiana estuary.

According to the simulation results corresponding to four cases, the standard deviations of elevation change in the lower estuarine bed were approximately identical (Fig. 5.10b). That was changed after 2002 reflecting the disturbance to the fluvial sediment supply of the system after closure of the Alqueva dam. However, at present the standard deviations of elevation change in the whole lower estuary are approaching to an approximately identical value and tend to be a constant implying less time dependency except in the case of n = 1.8.

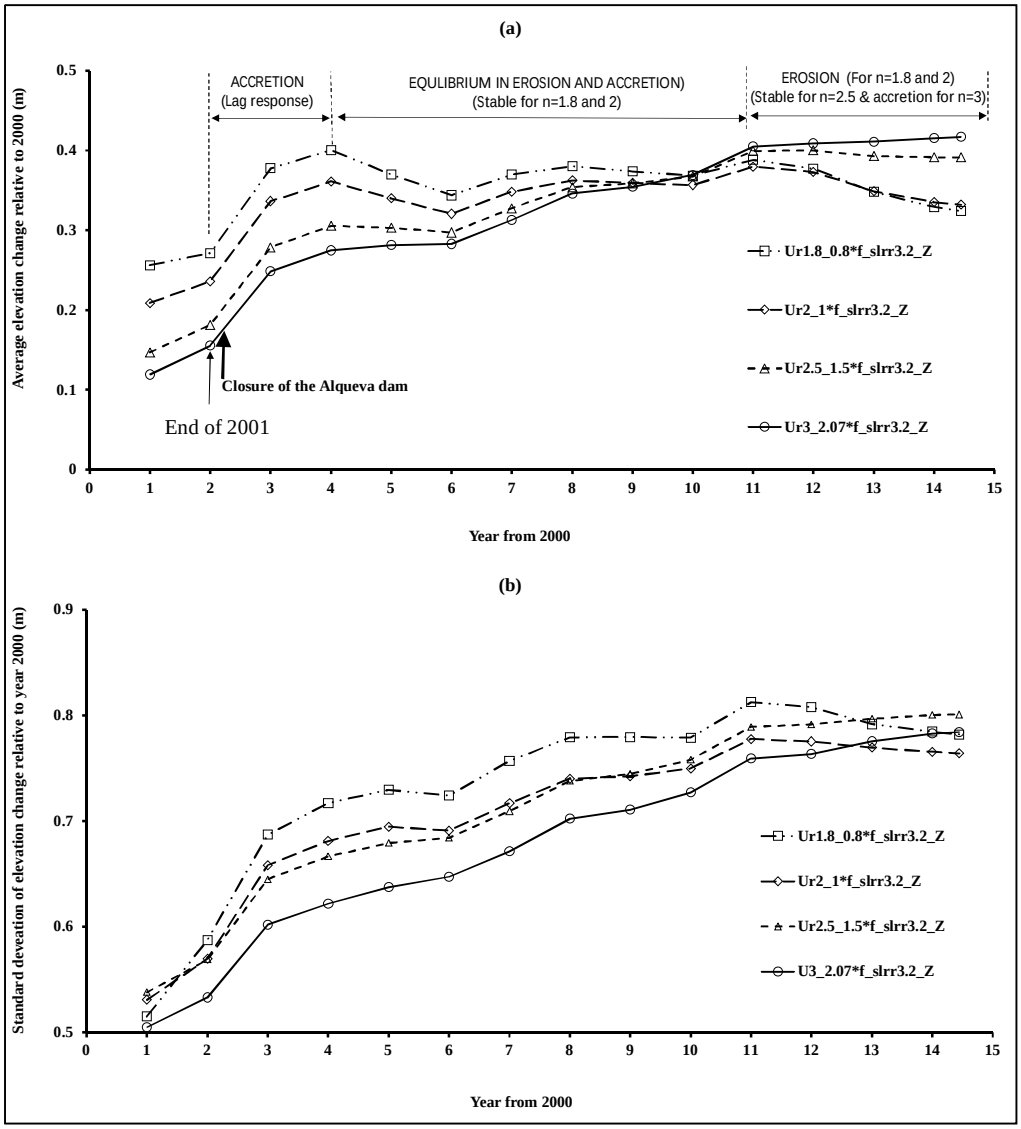

Figure 5.10 (a) Annual average elevation change (simulated) relative to the year 2000 and (b) corresponding changes in the standard deviation for four cases of (1) n = 1.8 and friction coefficients were reduced by 20%; (2) n = 2 and no change in friction coefficients; (3) n = 2.5 and friction coefficients were increased by 50%; (4) n = 3 and friction coefficients were increased by 107%.

5.4.5 Sensitivity of sea-level rise rate on the decadal scale morphological evolution

Sensitivity of the sea-level rise rate on the elevation change in the estuary over a 14 year period was estimated using the average elevation change and standard deviation (Fig. 5.11a and 5.11b). Average elevation change from 2000 to 2014 increases linearly, but mildly with the

increase of sea-level rise rate from 1 to 5 mm/yr. However, the standard deviation of the elevation change in the whole system shows a weak decreasing linear relationship with the increase of sea-level rise rate. All four cases corresponding to n = 1.8, 2, 2.5 and 3 shows this identical behaviour.

Furthermore, whether the increase of the accommodation space would be infilled to maintain the stable water depths by keeping pace with the sea-level rise was assessed in terms of the relationship between additional relative net accretion rate (Eq. 26) and sea-level rise rate (Fig. 5.11c). The additional net accretion rate is the difference between the rate of elevation change with and without sea-level rise. The main assumption is that the dominant process that determine the long-term morphological evolution of an estuary is sea-level rise. The Increasing rate of the accommodation space can be assumed as same as the sea-level rise rate.

$$Additional\ relative\ net\ accretion\ rate = \frac{(\overline{\Delta Z_{With\ SLR}} - \overline{\Delta Z_{No\ SLR}})\ /\Delta T}{Increasing\ Rate\ of\ accomodation\ space} \quad (26)$$

The Variation of additional relative net accretion rate with sea-level rise rate shows different behaviour according to the value of n and the corresponding friction coefficients of the optimum solutions that corresponding to the observed behaviour of the system. For n = 1.8 and 2, additional relative net accretion rate increases logarithmically with the increase of sea-level rise rate. For n = 2.5 and 3, additional relative net accretion rate decreases logarithmically with the increase of sea-level rise. This is mainly due to the dominant processes that govern the estuary are different, as explained in the section 5.4. However, all the curves converge to a near zero value when the sea-level rise rate is 5 mm/yr. This implies that there is no additional relative net accretion in the system. Thus the sedimentation process in the system will be governed by the tidal dynamics under the rapid sea-level rise and significant reduction in sediment supply due to human interventions. Therefore, the Guadiana estuary may behave as a give-up estuary in the future as described by Cooper et al. (2012).

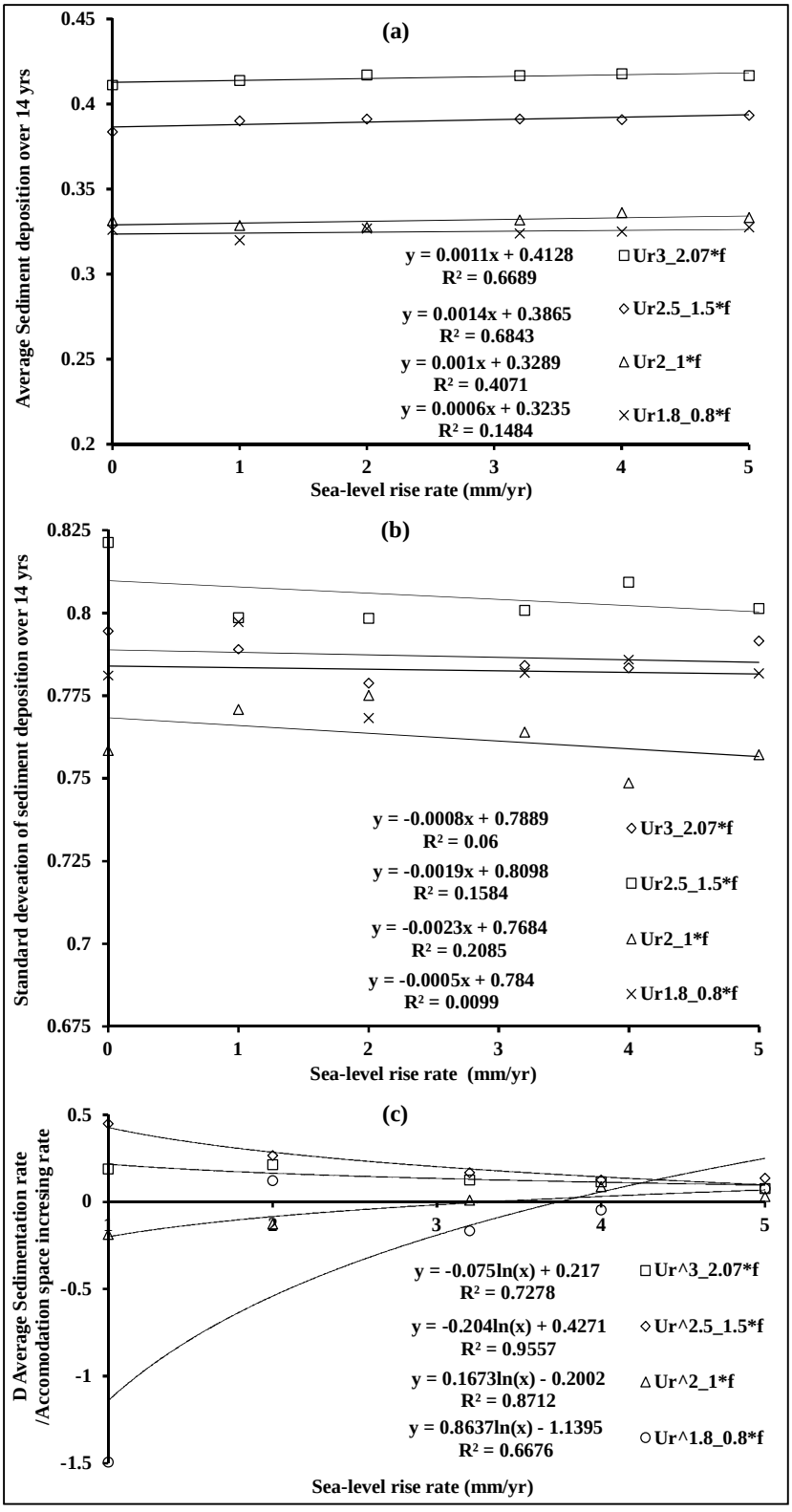

Figure 5.11 Sensitivity of sea-level rise rate on the elevation change of the estuary bed. (a) Average elevation change with sea-level rise rate, (b) standard deviation with sea-level rise rate and (c) additional relative net accretion rate with sea-level rise rate.

Such situation would result in an increase of water depth and submergence of salt-marshes and increase of mud-flat areas. Therefore, rapid sea-level rise would lead to deleterious consequence to the entire ecosystem due to the reduction in the biodiversity of the estuarine habitats. Therefore, it is advisable to maintain a minimum fluvial discharge by regulating the reservoir capacity of the Alqueva dam.

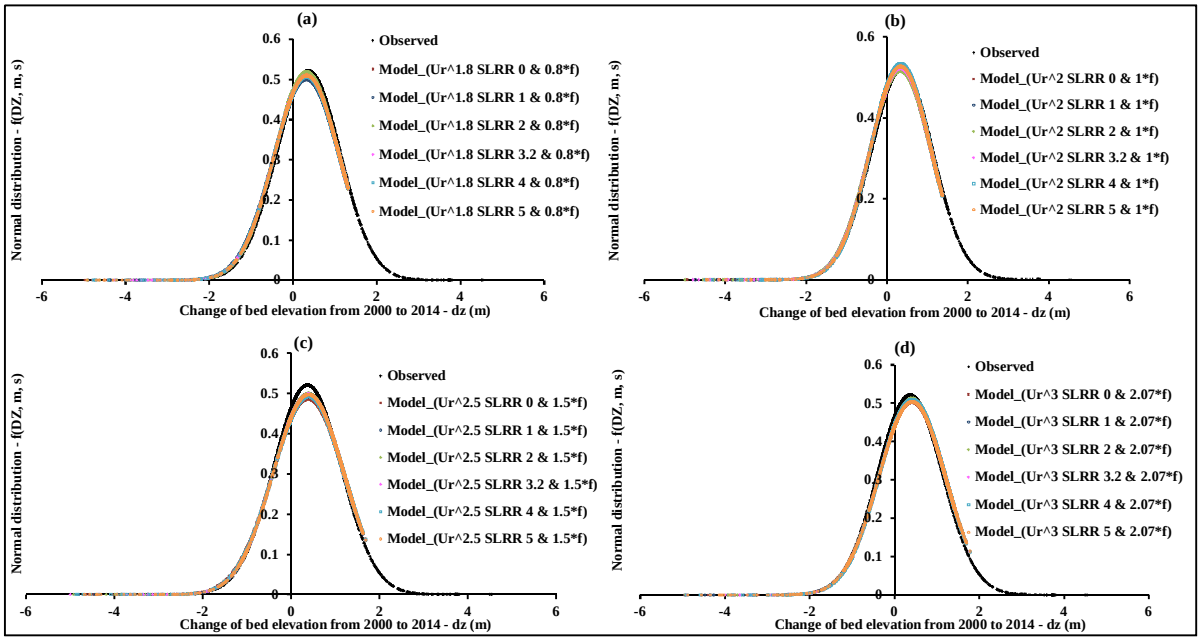

Figure 5.12 observed and simulated normal distribution of the elevation change in the Guadiana estuary from 2000 to 2014 for four cases of (1) n = 1.8 and friction coefficients were reduced by 20%; (2) n = 2 and no change in friction coefficients; (3) n = 2.5 and friction coefficients were increased by 50%; (4) n = 3 and friction coefficients were increased by 107%.

The simulated normal distributions of the elevation change in the Guadiana estuary from 2000 to 2014 (for four cases of (a) n = 1.8 and friction coefficients were reduced by 20%; (b) n = 2 and no change in friction coefficients; (c) n = 2.5 and friction coefficients were increased by 50%; (d) n = 3 and friction coefficients were increased by 107%) show no significant difference for increasing sea-level rise rate (Fig. 10). However, the mean values of

normal curves shift positive side while there is no clear relationship between the probability density with the sea-level rise rate. For instance, the maximum probability density at the mean value does not depend on the sea-level rise rate.

5.5 DISCUSSION

5.5.1 ASPECTS OF LONG-TERM PREDICTIONS OF MORPHOLOGICAL EVOLUTION OF ESTUARINE SYSTEMS.

Predictability of long-term morphological changes in estuaries is limited because of the non-linear and stochastic in nature of the external forcings, sensitivity analysis of idealized models can be considered as a method of investigation of the behaviour of these systems (De Vriend, 2001). In this context, the accuracy and the sensitivity of the simulated morphological evolution of the Guadiana estuary from 2000 to 2014 May have to be assessed in terms of dominant controlling parameters of the model. Long-term simulations of the morphological evolution of estuarine systems in response to global and local forcings are complicated due to the incompatibility between scales of short-term hydrodynamic processes and long-term morphological processes. Long-term and large-scale predictions will be related to the time scale of predominant processes like waves, tides, and settling and advection of suspended sediment; or the time scale of external forcing like sea-level rise or inherent time scale of predominant morphological changes like life time of a sand wave or bed forms (De Vriend, 2001). Though the simplification of estuarine processes is unavoidable in model studies, it should be cautioned the reliability of the results. It is possible to understand the solutions from idealized model simulations are one possible scenario of stochastic behaviour of the system. For instance, when sediment diposits with time, the inundation hydroperiod decreases, so that less sediment deposits leading to a reduction of accretion rate (Fagherazzi, et al., 2007). In

estuarine systems, sediment movement initially leads to morphological changes at the special and temporal scales of the water and sediment motion resulting in changes in the flow and sediment transportation processes (De Vriend, 2001). This suggests that there is a complex non-linear feedback between sediment infilling and inundation hydroperiod in estuarine systems (Sampath et al., 2015).

5.5.2 SENSITIVITY OF f ON MORPHOLOGICAL EVOLUTION OF ESTUARIES.

Bed shear stress is a critical parameter in determining the coastal circulation and sediment transport (Ganju and Sherwood, 2010). The total bed shear stress can be related to three contributors, namely: (1) the skin friction or gain-related friction; (2) the form drag resulting from ripple/dune formation; and (3) sheet flow conditions arises due to turbulent momentum exchange between the particles (Reeve et al., 2004). However, the present model does not use bed shear stress but the bed friction will be calculated to estimate the axial current velocity to determine the erosion rate using the formulation presented by Prandle (2009). In the model, the bed friction coefficients (f) of each cell with its own unique grain size were estimated using the expression derived by Jones (1983), which related to the bed roughness, Z_0. However, for simplicity, we assumed bed roughness consists of only the first two components given by Reeve et al., (2004). The form drag also will be only due to ripple formation with wave length of λ_r (=$1000D_{50}$) (Reeve et al., 2004) and the skin friction related to the coarse sand with grain size D_{50} for hydraulically rough flow where the Nikuradse roughness length ks was $30Z_0$ (Nikuradse, 1933). However, according to the study of Lobo et al., 2002, more than 570 medium and large dunes of H > 0.25 m were identified and there are many other small dunes and in the marine estuary Seaward-directed dunes were higher (average value of 0.6 m) than symmetric dunes (average value of 0.4 m). Therefore, the estimated bed friction will be under-predicted.

Despite this weakness, understanding the sensitivity of the bed friction is important because, according to the tidal theory, tides and river discharge interact through quadratic bed friction, which diminishes and distorts the tidal wave as fluvial discharge increases (Moftakhari et al., 2013). The present study shows the decrease in friction factor resulted in decrease of sediment erosion as it can be inferred from the formulation of Prandle (2009). The friction coefficient play role in the sedimentation rate function as it determines the increase of the suspended sediment concentration due to resuspension. Thus, non-linearity of the bed friction on the average elevation change over decadal scale can be expected as the coefficient is increased beyond the estimated values using the expression of Jones (1983). In reality, if the bed friction is decreased, there would feedback effect to increase the water depths because according to Lane (2004), if the bed friction is reduced, the amplitudes of tidal constituents tend to increase and decrease in phase lead while the increasing of the friction results in the opposite effect. Furthermore, the role of bed friction on the morphological evolution does not depend only on the f, but the model includes the linearized bed friction (F) for determining the current velocity. This coefficient in the model will indicate whether the tidal dynamics are frictionally dominated if the tidal amplitudes are greater than h/10 or otherwise (Prandle, 2004).

5.5.3 SENSITIVITY OF THE POWER OF CURRENT VELOCITY.

According to Prandle, 2004, erosion rate is relatively insensitive to either the power n for a tidally dominated regime and the n is encountered in the range 2–5. The present model simulations suggest that average elevation change would be almost constant for $n > 3$. This observation will be held for any friction values that we used in the simulations. If the n is reduced the erosion will be increased significantly. The model would be unstable and inaccurate if the $n < 1.5$. However, Prandle, (2004) suggests that the currents are insensitive to the bed friction (f) if the tidal amplitudes are greater than h/10.

5.5.4 THE IMPACT OF SEA-LEVEL RISE ON THE GUADIANA ESTUARY FROM 2000 TO 2014.

Use of different sea-level rise rates as input parameters in the model simulations helped to understand the sensitivity of sea-level rise rate on morphological evolution. It seems if the sea-level rise rate increased beyond the present global mean-sea-level projection of +3.2 ± 0.4 mm/yr (Church, et al., 2013; Masters et al., 2012), the estuary may not be able to keep pace with increasing accommodation space. Thus channel deepening and translation of salt-marshes into mud flats where the biodiversity is very poor can be expected in the future. As understood in terms of annual variability of the average elevation change from 2000 to 2014, the estuary behaves differently though the model can simulate the bathymetry for the year 2014 with good accuracy comparable to the observed for four optimum combinations of the friction factor and power of the current velocity. If these simulations were further extended for different scenarios of river discharges, we may be able to find the minimum rate of water discharge from the Alquava dam to sustain the marsh systems in the future.

5.5.5 STRENGTHS AND LIMITATION AND POSSIBLE IMPROVEMENTS OF THE MODEL

The ability to accurately predict the large-scale spatial and temporal evolution of an estuarine system in response to natural forcing or human interferences is increasingly important as the system may be under pressure beyond its carrying capacity (De Vriend, 2001). Thus, such models serve the need for sustainable management of these tidal systems to understand whether they will keep up with forcing like sea-level rise and due to the shortages of fluvial sediment supply due to reduction in river discharge. Most of the deterministic models ignores the stochastic nature of the forcings affecting natural systems like estuaries, and they are often dependent on representative conditions like dominant river discharge (Jansen, 1979; Sampath

et al., 2015), sediment grain size (Sampath et al., 2015) and a few tidal constituents (Latteux, 1995) or representative waves (De Vriend, et al., 1993) .

In the present behaviour-oriented model application, we try to represent the temporal variation of water level due to tides using 10 tidal constituents. The stochastic nature of the river discharge was absorbed into the model by including an approximated time series instead of the measured data. Therefore, the future predictions may reflect the probabilistic nature of the input data to certain extend. That is because the measured time series will not reflect the total stochastic nature of centennial time scale (De Vriend,, 2001). Instead of using one representative mean grain size for the cell, accuracy of the settling of suspended sediment within the estuary can be improved, if the sediment composition can be represented. The spatial variability of sediment size within the estuary will have signatures of morphodynamic behaviour of the systems in the past. That will help to predict the morphological evolution in decadal time scale. However, the inability of the model to update the special variability of sediment distribution in the estuary with the advection of new sediment into the system, is a weakness in the model. The tidal constituents also will vary with the increase of sea-level, but the model does not take such variations into consideration.

Furthermore, the long-term model of simulating the morphological evolution over centennial to millennial time scale was validated with stratigraphic data of radiocarbon ages of six borehole in the Guadiana estuary (Sampath et al., 2015). This paper presents the results of sensitivity analysis of the decadal simulations of the scale sub-model of the above long term model. The decadal scale simulations of the Guadiana estuary were validated using the data of the bathymetric surveying carried out using single beam echo sounder and real time kinematic method to correct the variation in tides over surveying period. The river discharges were based on the observed time series and tidal heights were derived using tidal constituents. Suspended sediment concentration projections related to the river discharge (Morales 1995) and scaled to

with the data of Machado et al., (2007) and Garel et al., (2009) obtain peak SSC during the flash discharges during this period. However, still there would be inaccuracies of these field measurements it would be noteworthy to mention that if the models are over calibrated and parametrized its essential dynamics using the data from the past, a model may lose its predictive capacity in general De Vriend, 2001).

5.6 CONCLUSIONS

A conceptual model was developed to simulate long-term morphological evolution of the Guadiana Estuary in response to dominant forcings such as sea-level rise and sediment supply changes. The model first simulates the decadal-scale evolution of the estuarine system to find the spatial variability of the annual average of the net sediment accretion in the estuary. The results are applicable to simulate the centennial scale morphodynamics by means of behaviour-oriented approach. The decadal-scale hydrodynamics and morphological evolution were simulated by using the generalized analytical solutions within a theoretical framework, in which the tidal propagation in the estuary was represented by the one-dimensional and cross-sectionally averaged shallow-water wave equations while frictional terms were linearized in a triangular-shaped and synchronous estuarine channel.

1. The decadal-scale model produced elevation change distribution from 2000 to 2014 in the Guadiana estuary, approximately similar to the observed normal probability distribution for the same period.
2. The variation of average elevation change ($\overline{\Delta Z}$) and standard deviation (σ) exhibit a logarithmic relationship for the powers of current velocity of the erosion rate function (n) from 1.5 to 3 and then there is no significant change in $\overline{\Delta Z}$ and σ for further increase of n.
3. A combined effect on $\overline{\Delta Z}$ and σ is identified between the n and friction factor for the modelled current velocity less than 1 m/sec.

4. The optimum modelled distribution of elevation change similar to the observed can be obtained for n = 1.8, 2, 2.5 and 3 while the friction is changed -20 %, (0.8f), 0 %, (f), +50 %, (1.5f), and 107 % (2.07f) respectively relative to its estimated value by using empirical expression derived by Jones (1983).
5. The difference between $\overline{\Delta Z}$ with and without sea-level rise relative to the increasing rate of the accommodation space converges to zero with the increase of sea-level rise rate above the present global mean sea-level rise rate, thus sea-level rise rate with 5 mm/yr would cause significant destruction to the sensitive ecosystem of the Guadiana estuary.
6. After 2010, there is increasing erosion for n = 1.8 and 0.8f and n = 2 and f and equilibrium condition can be expected for n = 2.5 and 1.5f as there is approximately zero net accretion over this period but a logarithmic increase of net accretion for n=3 and 2.07f case. This suggests, though the simulations show elevation change distributions comparable to the observed elevation change for four combinations of friction and the power of the current velocity, the estuarine system is under different state according to the dominant processes. The field observations suggest that increased erosion and transport of sediment into the ocean, the most applicable combination would be given by n = 1.8 and 0.8f or n = 2 and f.
7. The model was able to produce spatial variability of eroding and accreting regions, though there may be a discrepancy in magnitude. The erosion has taken place mainly in shallow mudflats. That will imply that that the mud plat will deepen with sea-level rise.
8. Finally, even though the complete model is formulated to simulate long-term morphological evolution in estuarine systems, the decadal scale module of the model would be useful to simulate short-term bathymetries of estuarine channels and to estimate the volume of the channel dredging for navigation. However, it is important to establish the normal distribution of ΔZ in estuaries by carrying out several bathymetric surveying at least annually.

ACKNOWLEDGMENTS: The first author acknowledges FCT (SFRH/BD/70747/2010) and the **CIMA - Centro de Investigação Marinha e Ambiental**, Universidade do Algarve (**UID / MAR / 00350/2013)** for granting a scholarship to carry out this work as part of his PhD research. The comments of two anonymous reviewers and the Editor, have helped to significantly improve an earlier version of the manuscript.

5.7 REFERENCE

Boski, T., Moura, D., Veiga-Pires, C., Camacho, S., Duarte, D., Scott, D.B., Fernandes S.G., 2002. Postglacial sea-level rise and sedimentary response in the Guadiana Estuary, Portugal/Spain border. Sedimentary Geology. 150, 103–122.

Boski, T., Camacho, S., Moura, D., Fletcher, W., Wilamowski, A., Veiga-Pires, C., Correia, V., Loureiro, C., Santana, P., 2008. Chronology of post-glacial sea-level rise in two estuaries of the Algarve coast, S. Portugal. Estuarine, Coastal and Shelf Science. 77, 230–244.

Brown J., 2013. Waves, Tides and Shallow-Water Processes: Prepared by an Open University Course Team Elsevier, Science, p187.

Bruce, E., Cowell, P., Stolper, D., 2003. Development of a GIS-based estuarine sedimentation model. In: Woodruffe, C.D., Furness, F.A. (Eds.), Coastal GIS 2003 – Wollongong University, Australia, papers on Maritime Policy 14. pp. 271–285.

Church, J. A. *et al.* in *Climate Change 2013: The Physical Science Basis* (eds Stocker, T. F. *et al.*) Ch. 13. IPCC, Cambridge Univ. Press, 2013.

Cooper, J.A.G., Green A.N., Wright, C.I., 2012. Evolution of an incised valley coastal plain estuary under low sediment supply: a ‘give-up’ estuary. Sedimentology. 59, 899–916. doi: 10.1111/j.1365-3091.2011.01284.x

Costa, M., Silva, R., Vitorino, J., 2001. Contribuição para o estudo do clima de agitação maritime na costa portuguesa. 2as Jornadas de Engenharia Costeira e Portuária. Aveiro, Portugal. AIPCN, 20 p. (in CD-ROM).

Dastgheib, A., Roelvink, J.A., Wang, Z.B., 2008. Long-term process-based morphological modelling of the Marsdiep Tidal Basin. Marine Geology 256, 90–100.

Delgado, J., Boski, T., Nieto, J.M., Pereira, L., Moura, D., Gomes, A., Sousa, C., García-Tenorio, R., 2012. Sea-level rise and anthropogenic activities recorded in the late Pleistocene/Holocene sedimentary infill of the Guadiana Estuary (SW Iberia). Quaternary Science Reviews. 33, 121–141. DOI: 10.1016/j.quascirev.2011.12.002.

Dennis, J.M., Spearman, J.R., Dearnaley, M.P., 2000. The development of Regime models for prediction of the long term effects of civil engineering activities of estuaries. Physics and Chemistry of the Earth, Part B: Hydrology, Oceans and Atmosphere 25, 45-50.

De Vriend, H.J., Capobianco, M., Chesher, T., De Swart, H.E., Latteux, B., Stive, M.J.F., 1993. Approaches to long-term modelling of coastal morphology: a review. Coastal Eng., 21 (1–3), 225–269.

De Vriend, 2001. Long-term morphological Prediction. In: River, Coastal and Estuarine Morphodynamics, Eds. Seminara, G., and Blondeaux, P. Springer Science & Business Media. (163-190), P211.

Dias J, Taborda R. 1992. Tidal gauge data in deducing secular trends of relative sea-level and crustal movements in Portugal. *Journal of Coastal Research* 8 (3): 655- 659

Dias, J.M.A., Gonzalez, R., Ferreira, O., 2004. Natural versus anthropic causes in variations of sand export from river basins: an example from the Guadiana river mouth (Southwestern Iberia). Polish Geological Institute Special Papers 11, 95-102.

Dissanayake, D.M.P.K.; Van der Wegen, M. and Roelvink, J. A, 2009. Modelled channel pattern in schematized tidal inlet. *Coastal Engineering*, 56, 1069 – 1083.

Dissanayake, D.M.P.K., Ranasinghe, R., Roelvink, J.A., Wang, Z.B., 2011. Process-based and semi-empirical modelling approaches on tidal inlet Evolution. Journal of Coastal Research SI 64 1013 - 1017 ICS2011 (Proceedings) Poland ISSN 0749-0208.

Dronkers, J., 1998. Morphodynamics of the Dutch Delta. In: Dronkers, J., Scheffer, M. (Eds.), Physics of Estuaries and Coastal Seas. Balkema, Rotterdam, pp. 297e304.

Fagherazzi, S., Palermo, C., Rulli, M.C., Carniello, L., Defina A., 2007. Wind waves in shallow microtidal basins and the dynamic equilibrium of tidal flats, J. Geophys. Res., 112, F02024, doi:10.1029/2006JF000572.

Fortunato, A.B., Pinto, L., Oliveira, A., Ferreira, J.S., 2002. Tidally generated shelf waves off the western Iberian coast. Continental Shelf Research 22, 1935–1950.

Fortunato, A B ., Oliveira, A., 2003. A modeling system for tidally driven long-term morphodynamics. *Journal of Hydraulic Research* Vol. 00, No. 0 (2003), pp. 1–9.

Ganju, NK., Sherwood, CR. 2010. Effect of roughness formulation on the performance of a coupled wave, hydrodynamic, and sediment transport model Ocean Modelling 33, 299–313

Garel, E., Pinto, L., Santos, A., Ferreira, ó., 2009. Tidal and river discharge forcing upon water and sediment circulation at a rock-bound estuary (Guadiana Estuary, Portugal). Estuarine, Coastal and Shelf Science. 84, 269–281. DOI 10.1016/j.ecss.2009.07.002.

Gonzalez, R., Araújo, M.F., Burdloff, D., Cacha˜o, M., Cascalho, J., Corredeira, C., 2007. Sediment and pollutant transport in the Northern Gulf of Cadiz: a multi-proxy approach. Journal of Marine Systems. 68, 1–23.

Hallermeier, R.J., 1981. Terminal velocity of commonly occurring sand grains. Sedimentology 28, 859-865.

IPCC 2007. Climate Change 2007: The Physical Science Basis. Contribution of Working Group I to the Fourth Assessment Report of the Intergovernmental Panel on Climate Change, In: Solomon, S., Qin, D., Manning, M., Chen, Z., Marquis, M., Averyt, K.B., Tignor, M., Miller, H.L. (Eds.), Cambridge University Press, Cambridge, United Kingdom and New York, NY, USA.

IPCC, 2013. Climate Change 2013: The Physical Science Basis. Contribution of Working Group I to the Fifth Assessment Report of the Intergovernmental Panel on Climate Change [Stocker, T.F., D. Qin, G.-K. Plattner, M. Tignor, S.K. Allen, J. Boschung, A. Nauels, Y. Xia, V. Bex and P.M. Midgley (eds.)]. Cambridge University Press, Cambridge, United Kingdom and New York, NY, USA, 1535 pp.

IPCC, 2014. In: Core Writing Team, Pachauri, R.K., Meyer, L.A. (Eds.), Climate Change 2014: Synthesis Report. A Contribution of Working Groups I, II, and III to the Fifth Assessment Report of the Intergovernmental Panel on Climate Change. IPCC, Geneva, Switzerland, ISBN 978 92 9169 143 2, p. 151.

Jansen, P.Ph. (Ed.) 1979. Principles of River Engineering. Pitman Publ. Ltd., London, 509 pp.

Johns, B., 1983: Turbulence modelling beneath waves over beaches. In: Johns, B. (Ed.), Physical Oceanography of Coastal and Shelf Seas. Elsevier Oceanography Series. 35, 111–133.

Karunarathna, H. and Reeve, D.E., 2008. A Boolean Approach to Prediction of Long-term Evolution of Estuary Morphology, Journal of Coastal Research, Vol. 24(2B), pp. 51-61. DOI: 10.2112/05-0542.1

Karunarathna, H.; Reeve, D., and Spivack, M., 2008. Long-term morphodynamic evolution of estuaries: an inverse problem. *Estuarine Coastal Shelf Science*, 77, 385–395.

Latteux, B. (1995) Techniques for long-term morphological simulation under tidal current action. Marine Geology, 126, 129–141.

Lane A, Prandle D., 2007. Changing flood risks in estuaries due to global climate change: forecasts from observations, theory and models. Int J Appl Math Eng Sci 1(11):69–88.

Lane, A., Prandle, D., 2006. Random-walk particle modelling for estimating bathymetric evolution of an estuary. *Estuarine, Coastal and Shelf Science,* 68(1-2): 175-187, doi:10.1016/j.ecss.2006.01.016.

Lane, A., 2004. Bathymetric evolution of the Mersey Estuary, UK, 1906-1997: causes and effects. *Estuarine, Coastal and Shelf Science* 59 (2), 249-263. doi:10.1016/j.ecss.2003.09.003.

Lavelle, JW., Mojfeld, HO., Baker, ET., 1984. An in-situ erosion rate for a fine grained marine sediment. Journal of Geophysical Research, 89 (4), 6543-6552.

Liu, JT. and Aubrey, DG., 1993. Tidal residual currents and sediment transport through multiple tidal inlets. American Geophysical Union, 44, 113-157

Lesser, G.R., 2009. *An approach to medium-term coastal morphological modelling*, PhD dissertation, UNESCO-IHE Institute for Water Education, Delft, the Netherlands.

Lobo, F.J., Dias, J.M.A., González, R., Hernández-Molina, F.J., Morales, J.A., Díaz del Río, V., 2003. High-resolution seismic stratigraphy of a narrow, bedrock-controlled estuary: the Guadiana estuarine system, SW Iberia. Journal of Sedimentary Research. 73, 973–86.

Lobo, J., Plaza, F., Gonza´ les, R., Dias, J., Kapsimalis, V., Mendes, I., Rio, V.D., 2004. Estimations of bedload sediment transport in the Guadiana estuary (SW Iberian Peninsula) during low river discharge periods. Journal of Coastal Research 41 (Special Issue): 12–26.

Machado, A., Rocha, F., Gomes, C., Dias, J., 2007. Distribution and composition of suspended particulate matter in Guadiana estuary (southwestern Iberian Peninsula). Journal of Coastal Research 50, 1040–1045. Proc. International Coastal Symposium, Special Issue.

Masters, D. *et al*. Comparison of global mean sea level time series from TOPEX/Poseidon, Jason-1, and Jason-2. *Mar. Geod.* **35**, 20–41 (2012).

Menanteau, L., Chadenas, C., Choblet, C., 2005. Les marais du Bas-Guadiana (Algarve, Andalousie): emprise, de´ prise et reprise humaines. 1er colloque internations du Groupe d´ Histoire des Zones Humides, Le Blanc.

Moftakhari, H. R., D. A. Jay, S. A. Talke, T. Kukulka, and P. D. Bromirski (2013), A novel approach to flow estimation in tidal rivers, Water Resour. Res., 49, 4817–4832, doi:10.1002/wrcr.20363.

Morales, J.A., 1993. Sedimentologı´a del Estuario del Guadiana (S.W. Espan˜a– Portugal). Ph.D. thesis, University of Sevilla, Sevilla, Spain, p. 274.

Morales, J.A., 1995. Sedimentologia del estuario del Rio Guadiana (S.W. Espanã–Portugal), Servicio de Publicaciones, Huelva University; 1–322.

Morales, J.A., 1997. Evolution and facies architecture of the mesotidal Guadiana River delta (S.W. Spain–Portugal). Marine Geology. 138, 127–148.

Morales, J.A., Delgado, I., Gutierrez-Mas, J.M., 2006. Sedimentary characterization of bed types along the Guadiana Estuary (SW Europe) before the construction of the Alqueva dam. Estuarine, Coastal and Shelf Science. 70, 117–131.

Morales, JA., Sedrati, M., Cantano, M. Ramírez, AR., Delgado, I., Lozano, C., Flor-Blanco, G., 2014. From the continent to the coast: the bedload transport across the lower sector of the Guadiana River Mouth (Spain-Portugal). Géomorphologie : relief, processus, environnement, 2014, n° 3, 55-64.

Nerem, R. S., Chambers, D., Choe, C., Mitchum., G. T., 2010. Estimating Mean Sea Level Change from the TOPEX and Jason Altimeter Missions Marine, Geodesy. 33(S1), 435–446. DOI: 10.1080/01490419.2010.491031

Nicholls, R.J., Klein, R.J.T., Tol, R.S.J., 2007. Managing coastal vulnerability and climate change: a national to global perspective. In: McFadden, L., Nicholls, R.J., Penning-Rowsell, E. (Eds.), Managing Coastal Vulnerability. Elsevier, Oxford, UK, pp. 223–241.

Nikuradse, J., 1933. Laws of flow in rough pipes. VDI Forschungsheft, p. 361.

Ortega, J.A., Garzo´ n, G., 2009. A contribution to improved flood magnitude estimation in base of palaeoflood record and climatic implications – Guadiana River (Iberian Peninsula). Natural Hazards and Earth System Sciences 9, 229–239.

Perillo, G.M.E., 1995. Definitions and geomorphological classifications of estuaries. In: Perillo, G.M.E. (Ed.), Geomorphology and Sedimentology of Estuaries. Developments in Sedimentology 53, Elsevier, Amsterdam, pp. 17 – 47.

Partheniades E., 2009. Cohesive Sediments in Open Channels: Erosion, Transport and Deposition**.** Butterworth-Heinemann, - Technology & Engineering - 384 p.

Pinto, L., 2003. Estrataficação salina no Estuário do Guadiana. Master thesis, Faculdade de Ciências da Universidade de Lisboa, Lisboa, p. 179.

Prandle, D., 1982. The vertical structure of tidal currents and other oscillatory flows. Continental Shelf Research 1, 191-207. doi:10.1016/0278-4343(82)90004-8.

Prandle, D., 2003. Relationships between tidal dynamics and bathymetry in strongly convergent estuaries. J. Phys. Oceanogr. 33 (12), 2738e2750. http://dx.doi.org/ 10.1175/1520-0485(2003)033<2738:RBTDAB>2.0.CO;2.

Prandle, D., 2004. How tides and river flows determine estuarine bathymetries. Progress in Oceanography 61, 1-26. doi:10.1016/j.pocean.2004.03.001.

Prandle, D., 2006. Dynamical controls on estuarine bathymetry: assessment against UK database. Estuar. Coast. Shelf Sci. 68 (1e2), 282e288. http://dx.doi.org/ 10.1016/j.ecss.2006.02.009.

Prandle, D., 2009 Estuaries: Dynamics, Mixing, Sedimentation and Morphology. Published by Cambridge University Press. New York, 236p.

Prandle, D., Lane, A., 2015. Sensitivity of estuaries to sea level rise: Vulnerability indices, Estuarine, Coastal and Shelf Science 160, 60-68

Reeve, D., Chadwick, A., Fleming, C., 2004. Coastal Engineering processes, theory and design practice, Spon press, Oxon, UK; 1- 461.

Rocha, J.S., Correia, F.N., 1994. Defence from floods and floodplain management in middle size catchments. In: Gardiner, J., Starosolszky, O., Yevjevich, V. (Eds.), Defence from Floods and Floodplain Management. NATO ASI Series, Series E, Applied Sciences, vol. 299. Kluwer Academic Publishers, Dordrecht, The Netherlands, pp. 395–417.

Sampath, D.M.R., Boski, T., Silva, P.L., Martins, F.A., 2011. Morphological evolution of the Guadiana Estuary and intertidal zone in response to projected sea-level rise and sediment supply scenarios. Journal of Quaternary Science. 26(2), 156–170. DOI: 10.1002/jqs.1434.

Sampath, D.M.R., Boski, T., Loureiro, C., Sousa, C., 2015. Modelling of estuarine response to sea-level rise during the Holocene: application to the Guadiana Estuary-SW Iberia. Geomorphology 232, 47–64. http://dx.doi.org/10.1016/j.geomorph.2014.12.037

Schubel J.R. 1971. Classification of estuaries. In: Schubel J.R. (ed.), Estuarine environment: estuaries and estuarine sedimentation Washington D.C., American Geological Institute. Cap. II, pp. 2–8.

Silva, M.C., Fortunato, A.B., Oliveira, A., Rocha, J.S., 2000. Condiço˜es ambientais no estua´ rio do Guadiana: o conhecimento actual. In: 5_ Congresso da A´ gua. Associaça˜o Portuguesa de Recursos Hı´dricos, APRH, Lisbon, Portugal CD-ROM.

Sanford, L.P., Halka, J.P., 1993. Assessing the paradigm of mutually exclusive erosion and deposition of mud, with examples from upper Chesapeake Bay. Marine Geology. 114, 37–57.

Trigo, R.M., Pozo-Va´squez, D., Osborn, T.J., Castro-Dı´ez, Y., Ga´ miz-Fortis, S., Esteban-Parra, M.J., 2004. North Atlantic oscillation influence on precipitation, river flow and water resources in the Iberian Peninsula. International Journal of Climatology 24, 925–944.

Van der Wegen, M., Roelvink, J.A., 2008. Long-term morphodynamic evolution of a tidal embayment using a two-dimensional, process-based model. Journal of Geophysical Research 113, C03016. doi:10.1029/2006JC003983.

van Rijn, L.C., 1984. Sediment transport: part II: suspended load transport. Journal of the Hydraulic Division, ASCE 110 (HY11), 1613-1641

Van Rijn, LC., 1993. Principals of sediment transportation in rivers, estuaries, and coastal seas. Aqua publications, Amesterdam.

Van Rijn, L.C., 2007. Unified view of sediment transport by currents and waves, I: Initiation of motion, bed roughness and bed-load transport. Journal of Hydraulic Engineering, ASCE 133 (6), 649–667.

Villaret C., Hervouet J.M., Huybrechts N., Van L.A., Davies A.G., 2010. Effect of bed friction on morphodynamic modelling: Application to the central part of the Gironde estuary In: *River, Coastal and Estuarine Morphodynamics: RCEM 2009 – Vionnet et al. (eds), Taylor & Francis Group, London, ISBN 978-0-415-55426-8.*

Villaret, C., Huybrechts, N., Davies, A.G., Way O., 2011. Effect of bed roughness prediction on morphodynamic modelling: Application to the Dee estuary (UK) and to the Gironde estuary (France). 34th IAHR World Congress - Balance and Uncertainty, 33rd Hydrology & Water Resources Symposium 10th Hydraulics Conference 26 June - 1 July 2011, Brisbane, Australia

Watson, CS., White, NJ., Church, JA. King, MA., .Burgette, RJ.& Legresy, B., 2015. Unabated global mean sea-level rise over the satellite altimeter era. *Nature Climate Change* **5**, 565–568 ***NATURE CLIMATE CHANGE* | LETTER** doi:10.1038/nclimate2635

Wolanski, E., Chicharo, L., Chicharo, M.A., Morais, P., 2006. An ecohydrology model of the Guadiana Estuary (South Portugal) Estuarine. Coastal and Shelf Science. 70, 132–143.

Chapter 6

Estimation of denudation rate of the Guadiana basin using the sediment budget approach.

This chapter is mainly based on the following abstract and foreseen for publication with the co-authors in a peer reviewed journal after including the results of the denudation rate estimation by ^{10}Be isotope method.

Sampath, D.M.R., Padilla, S., Delgado, J., López-Gutiérrez¨ J. M., Nieto, J.M., Boski, T., 2013. Estimation of denudation rates of the drainage basin of the Guadiana river using ^{10}Be isotope method and sediment budget method. V Regional Committee on Neogene Atlantic Stratigraphy **RCANS 2013** 24-26 September 2013, Huelva

ABSTRACT

The denudation rate within the Guadiana basin is estimated for the purpose of assessment of landscape evolution in millennial time scale. The study was carried out using the estimated data of suspended and bed load transport to the ocean from the Guadiana river and an estimation of the sediment volume deposited in the process of sediment infilling of Guadiana palaeovalley in response to eustatic sea-level rise between 11500 Cal. yr BP and pre anthropogenic period. The latter estimation was carried out by simulating the sediment infilling using a hybrid estuarine sedimentation model. The study will serve to understand the controls and efficiencies of relevant geomorphic processes, and to establish the relationship between climate change and landscape response. The estimations can be used to achieve the objectives of soil/sediment management of the whole basin, in particular for the Transboundary Rivers.

According to the sediment budget approach, the average denudation rate of the Guadiana river basin in the considered period is $1.58*10^{-3}$ cm/yr**.** That is one order of magnitude less than the result obtained using the ^{10}Be isotope method. However, if we apply retention factor for the value estimated using the sediment budget approach, to account for the sediment load trapped behind the dam, the results would be comparable. On the other hand, the estimation of denudation rate using the sediment budget method and the ^{10}Be isotope method can be used as a novel approach for estimating sediment retention by dams. This study proves the validity of the approach and the applicability of the model. Further studies are necessary to improve the estimations.

Keywords: Denudation rate, Sediment budget, Guadiana drainage basin, ^{10}Be isotope, Long-term hindcasting models

6.1 INTRODUCTION

Denudation is the overall degradation and levelling of continental land masses (Ahnert, 1996, Smithson et al. 2008) due to exogenic processes, including weathering, mass wasting and erosion by wind, running water, waves and glaciers (Olvmo, 2010). Erosion can result either from mechanical or biological mobilization, transport and carrying away of rock and soil material, by external agents, surface or subsurface (Slaymaker, 2003). These materials ultimately are transported into continental basins and oceans by surface runoff, river flow, ground water seepage, ice and wind while discontinuous transfer will take place into sedimentary basins from storage of fine material in valleys, on flood plains, lakes or man-made reservoirs (Einsele, 2013).

Denudation rate usually represents the spatially averaged rate of erosion for the entire basin with particular physiographic settings with similar geologic, climatic, and land use conditions (Ahnert, 1970; Einsele, 2013). Therefore, it is required to measure erosion and weathering rates, in different geomorphic settings and across various temporal and spatial scales, to quantify the rates of landscape evolution, to understand the controls and efficiencies of relevant geomorphic processes, and to establish the relationship between climate change and landscape response (Small, et al., 1997). The estimations serve the objectives of sediment

management of the whole basin, in particular for the transboundary rivers (Naden et al., 2004). Erosion can result in very deleterious impacts on the landscape and the ecosystems (Dymond et al., 2010), while that can be hazardous when the mass movement of the earth is involved (Hovius et al., 1997). Thus, the main objective of this chapter is to estimate and compare the denudation rate of the Guadiana river catchment using the ^{10}Be isotope method and the sediment budget method. This will serve as a validation of the strength and skills of the model.

6.2 CHARACTERISTIC OF THE GUADIANA BASIN

The transboundary Guadiana River is 810 km long, and its basin area is about 66'960 km^2 (Garel et al., 2009), of which 55260 km^2 (83%) are Spanish, and 11'700 km^2 (17%) Portuguese (Gonzalez, et al 2001). Oliveira et al. (1992) and Linan et al. (1994) as adapted by Gonzalez, et al. (2007) provide a classification of geology in the basin, accordingly, the basin consists of (1) Shists and greywackes of the Ossa-Morena zone (Proterozoic and Paleozoic); (2) Meso-Cenozoic sediment cover; (3) flysch deposits and Iberian Pyrite belt (Devonian-Carboniferous); (4) Magmatic-hercinian Intrusive rocks (Gabbros of the Beja massif); (5) Magmatic-hercinian Intrusive rocks (acid to basic rocks); and (6) metagabbros, sheeted dike complex, and metabasalts (Paleozoic) in Beja Acebuches ophiolitic complex. The monotonous sequence of schists and dark grey greywackes exhibit brown colour when deeply weathered (Machado et al., 2007). Eroded sediments from these sources will be eventually transported into the river and some part of it will deposited in the estuary while the rest is carried up to the continental shelf. According to Morales (1993), gravel and sand from the drainage basin are deposited in the upper estuary, while in the middle estuary, poorly sorted sediment with grain size ranging from gravels to clay and silt dominate. Well sorted medium sand including quartz, feldspar and bioclasts are typical in the lower estuary (Lobo et al., 2004; Geral et al., 2009). As

the grain size of the subtidal channel near to the mouth of the estuary and open coast is approximately same (Morales et al., 2006), sediment will be mainly from the sea.

The hinterland of the Guadiana River Basin is extremely dry, in particularly during the summer (Gonzalez, et al 2001) and as consequence water consumption for irrigation amounts to 95% of total water consumption in the basin as a whole (Aldaya and Llamas, 2008). The course of the river is mainly through rural areas and the mining area of the South Iberian Pyritic Belt (Machado et al., 2007) creating high potential for the anthropogenic soil erosion. At present, the river water discharge is regulated by more than 100 dams, including the Alqueva dam that forms the largest reservoir in Europe after its completion in 2002 and (Dias et al., 2004). The Guadiana River Basin and its adjacent coastline of the southwestern Iberia were subject to high seasonal variability in its flow regime prior to the closure of Alqueva dam and low flow after its completion (Gonzalez, et al 2001).

6.3 METHODOLOGY

The sediment budget concept was introduced with a landmark study of inventorying sources, sinks and movements of sediment by Jackli, (1957). Swanson et al. (1982) presented the first detailed explanation of the sediment budgeting methodology. Sediment budget method of estimating the denudation rate is essentially a mass balance based approach, which accounts the sources, sinks and redistribution pathways of sediments in a unit region over unit time (Slaymaker, 2003). Sediment budget can be defined as a quantitative statement of the rates of sediment production, transport, and discharge of detritus which account for the sources and deposition of sediments as it travels from its point of origin to its eventual exit from the drainage basin (Reid and Dune, 1996). According to Gregory and Goudie, (2011), the simple form of the sediment mass balance relates the sediment inputs *(I)* from upstream, tributaries,

and slopes to outputs *(O)* and a change in sediment storage *(DS)* due to deposition and erosion of the valley, floodplain and lacustrine sediment stores:

$$I = O \pm \Delta S \quad (6.1)$$

According to Swanson et al. (1982), the three components of sediment budget have to be established: (1) recognition and quantification of transport processes, (2) recognition and quantification of storage processes, and (3) identification of linkages amongst transport processes. As the estimation of direct denudation measurements on slopes can lead to pitfalls, the denudation rate is usually derived from the determination of the sediment transport of streams or rivers (Ahnert, 1970). Accordingly, sediment load estimations or measurements give a value for the total weight of rock or soil removed from the drainage basin per unit time. If the average density of material is known, this weight can be converted in volume per unit time (usually year; kilo year; mega year). If the basin area is known, then the thickness of removed material or the average denudation rate can be derived for the whole basin. Sediment budget method of estimating the denudation rate is a powerful tool, generally used at the scale of sedimentary basins (Guerit et al., 2015). Despite its inadequate justification, the main assumption in this approach is that the rate of rock waste production, and rate of transport of that material, within the drainage basin is during the short period of measurement in equilibrium with the rate at which the rock material is removed from the basin (Ahnert, 1970).

Though there are no measured values for the suspended load and bedload sediment transport in the Guadiana estuary, estimation of the same parameters by Morales, (1993), and Portela, (2006) was used for this preliminary estimation of the denudation rate using the sediment budget method. The estimation of the annual rate of deposition of the sediment in the estuarine system, including the intertidal area was carried out by using the modified estuarine

sedimentation model. Its methodology was described in the chapter 3 under the simulation of sediment infilling during the Holocene in response to eustatic sea-level rise.

6.4 ESTIMATION OF DENUDATION RATE FOR THE GUADIANA ESTUARY

There are no published data on the sediment discharge from the Guadiana river (Morales, 1997), but according to Portela (2006), the order of magnitude of both suspended load and bedload sediment discharge from 1980-2000 (before the Alqueva dam) were 10^5 m^3/yr. According to Morales 1993, the suspended sediment load is approximately 579000 m^3/yr and the bed load is 439600 m^3/yr. Thus, the total sediment load from the Guadiana basin to the ocean is approximately $1.02*10^6$ m^3/yr. The accumulation of the sediments within the area of the present estuarine system started very early, ca 13,000 Cal. yr BP (Boski et al., 2008). The sea-level rise rate from 11500 Cal. yr BP to 7500 Cal yr BP was 7.5 mm/yr and then up to the present pre-anthropogenic period, it was about 1.3 mm/yr and it has kept pace with sea-level rise during the Holocene as there were no significant human activities in the catchment area that obstructed the natural sediment supply into the coastal system (Boski et al., 2002; 2008 and Delgado et al., 2012). Based on morphological simulations using the Estuarine Sedimentation Model, the total volume deposited from 11500 to 7500 Cal yr BP was about $3.05x10^9$ m^3 while the infilling volume of sediment since then was about $1.63x10^9$ m^3 to compensate for increase of accommodation space due to sea-level rise during the Holocene period. Thus, the fluvial sedimentation rate from 11500 Cal yr BP to present was about $0.08x10^6$ m^3/yr. Therefore, the Total fluvial sediment load from the river basin would be $1.1*10^6$ m^3/yr. As the basin area of the Guadiana river is 66960000000 m^2, the average denudation rate would be $1.58*10^{-3}$ cm/yr.

6.5 DISCUSSION

The average denudation rate of the Guadiana estuary derived from the annual average flux of ^{10}Be isotope was $1.3 \pm 0.2x10^{-2}$ cm/yr while the same derived using the directly estimated monthly averages was $0.79 \pm 0.62 \ x10^{-2}$ cm/yr (Sampath, et al., 2013). That is one order of magnitude higher than the same derived using the sediment budget method. However the denudation rate of the Guadiana river derived from the sediment budget method is comparable with that of the Miñor river in the northern Spain. As the Guadiana river flow is highly regulated during the last 50 years, the recent estimations of fluvial sediment discharges (Morales, 1993, Portela, 2006) may not be representative of the pre-anthropogenic periods. In 1990, about 70% of the Guadiana drainage basin was regulated (Morales, 1995) and resulted in drastic reduction of sediment supply to estuary and ocean basin. Therefore, denudation rates of the Guadiana river basin derived using the sediment budget method would be an under-estimation.

Table 6.1 Corrected average denudation rate of the Guadiana river basin by applying assumed sediment retention factor due to dams.

Total sediment load into the ocean [1] (m^3/yr)	**1020000**	**1020000**	**1020000**
Sediment retention by dams (%)	80	85	90
Corrected total sediment load into the ocean (m^3/yr)	5100000	6800000	10200000
Sedimentation rate in the estuary[2] (m^3/yr)	80000	80000	80000
Corrected total sediment load from the basin (m^3/yr)	5180000	6880000	10280000
Corrected denudation rate (cm/yr)	$7.74*10^{-3}$	$1.03*10^{-2}$	$1.54*10^{-2}$

Note
[1]as estimated by Morales, 1993
2 as estimated using the simulations of ESM model

It is widely accepted that the sediment volume retained by dams would be reach up to 90%. Table 6.1 gives corrected denudation rates for assuming sediment retention factors, which has to be established scientifically by further research. At present, the river water discharge has reduced by 90 % compared to its unregulated river flow discharge (Wolanski et al., 2006). If we assume that the sediment supply into the ocean and the estuary is also reduced by the same percentage we may apply correction for sediment accumulation behind dams along the Guadiana river. Accordingly, if we apply 90% retention factor for the value estimated using the sediment budget approach, the results would be comparable with the upper limit of denudation rate estimated using the ^{10}Be isotope method. The correction factor of 85% would agree with the lower limit of the denudation rate measured using the isotope method while 80% would approximately represent the value estimated using monthly averages of ^{10}Be isotope concentrations. Therefore, denudation rates of the Guadiana river basin derived from the ^{10}Be isotope method may be directly comparable with those obtained from the sediment budget method only after correcting for attenuation of solid discharge caused by dams. On the other hand, the estimation of denudation rate using the sediment budget method and the ^{10}Be isotope method can be used as a novel approach for estimating sediment retention factor (SRF_{Dam}) by dams (Eq. 6.2).

$$SRF_{Dam} = 100 - \left(\frac{A \times DR_{10Be} - LSDR_{Estuary}}{100}\right) \times (q_{Sus} + q_{Bed}) \qquad (6.2)$$

where DR_{10Be} is the denudation rate using the ^{10}Be isotope method; A is the basin area; q_{Sus} and q_{Bed} is the recent estimation of suspended and bed load into the ocean and SRF_{Dam} is a percentage.

The main assumption is that the long-term (millennial scale) sediment deposition rate ($LSDR_{Estuary}$) would not be affected significantly due to the changes of sediment supply in an

estuarine system during recent anthropogenic period of the catchment. The present estimation of bed load and suspended load into the ocean will be mainly affected due to damming. The denudation rate is characteristic of the whole drainage basin, and not the river. The river flow is obstructed by dams resulting retention of sediments. If there are no dams or regulations of river discharge, thereby sediment supply, the denudation rate estimated using the sediment budget should be a higher value reflecting the increase of sediment erosion in the catchment due to human activities including irrigation and agriculture. There are also evidences for a rapid hillslope erosion in particular from 3000 to 300 yrs BP, that are considered to relate to pre-Roman, Roman, Moorish and early Portuguese phases of settlement and clearance for agriculture and forestry resulting valley floor deposition and estuary siltation (Plater and Kirby 2006). Therefore the above correction factor has to be refined further in the future studies.

6.6 CONCLUSIONS

The denudation rate of the Guadiana basin represents a generalized process of landscape evolution in millennial time scale. It has a paramount importance to understand the controls and efficiencies of individual geomorphic processes, and to establish the relationship between climate change and landscape response. Such estimations can support the sediment management in the whole basin, what is particularly relevant for the Transboundary Rivers. In order to check the trustworthiness of the denudation rate figures the results obtained by ^{10}Be isotope method and the sediment budget method were confronted.

According to the sediment budget approach, the average denudation rate of the Guadiana river basin is $1.58*10^{-3}$ cm/yr**.** The average denudation rate of the Guadiana estuary derived from the annual average flux of ^{10}Be isotope was $1.3 \pm 0.2x10^{-2}$ cm/yr while the same derived using the monthly averages was $0.79 \pm 0.62\ x10^{-2}$ cm/yr. ie. One order of magnitude higher than the first method. The inclusion of the correction for sediment retention by dams

into the sediment budget approach, in the widely accepted range of 90 – 80% makes the results obtained by two methods fully comparable. Conversely, the estimation of denudation rate by the sediment budget method and the ^{10}Be isotope method can be used as a novel approach for estimating sediment retention by dams. Further studies to improve the estimations are needed.

ACKNOWLEDGMENTS

The first author acknowledges FCT for granting a scholarship (SFRH/BD/70747/2010) to carry out this work as part of his PhD research. The authors acknowledge Dr. David Stolper, Vivira Cadungog, Dr. Peter Cowell and Dr. Eleanor Bruce, School of Geosciences, University of Sydney, and the Sydney Olympic Park Authority for access to the ESM.

6.7 REFERENCE

Ahnert, F., 1970. Functional relationships between denudation, relief and uplift in large mid-latitude drainage basins. American Journal of Science, 268, pp 243–263.

Ahnert F, 1996. Introduction to geomorphology. London: Arnold. 352p.

Aldaya MM., Llamas, MR., 2008. WATER FOOTPRINT ANALYSIS FOR THE GUADIANA RIVER BASIN. Complutense University of Madrid, PAPELES DE AGUA VIRTUAL NO: 3. 114p.

Boski, T., Moura, D., Veiga-Pires, C., Camacho, S., Duarte, D., Scott, D.B., Fernandes S.G., 2002. Postglacial sea-level rise and sedimentary response in the Guadiana Estuary, Portugal/Spain border. *Sedimentary Geology*, 150: 103–122.

Boski, T., Camacho, S., Moura, D., Fletcher, W., Wilamowski, A., Veiga-Pires, C., Correia, V., Loureiro, C., Santana, P., 2008. Chronology of post-glacial sea-level rise in two estuaries of the Algarve coast, S. Portugal. *Estuarine, Coastal and Shelf Science,* 77: 230-244.

Delgado, J., Boski, T., Nieto, J.M., Pereira, L., Moura, D., Gomes, A., Sousa, C., García-Tenorio, R., 2012. Sea-level rise and anthropogenic activities recorded in the late Pleistocene/Holocene sedimentary infill of the Guadiana Estuary (SW Iberia). Quaternary Science Reviews. 33, 121–141. DOI: 10.1016/j.quascirev.2011.12.002

Dias, J.M.A., Gonzalez, R., Ferreira, Ó., 2004. Natural versus anthropic causes in variations of sand export from river basins: an example from the Guadiana river mouth (Southwestern Iberia). *Polish Geological Institute Special Papers*, 11: 95-102.

Dymond, J., Betts, H., & Schierlitz, C. (2010a). An erosion model for evaluating regional landuse scenarios. Environmental Modelling and Software, Vol. 25 , 289-298.

Einsele, G., 2013. Sedimentary Basins: Evolution, Facies, and Sediment Budget. Springer Science & Business Media.792p.

Garel E, Pinto L, Santos A, Ferreira ó. 2009. Tidal and river discharge forcing upon water and sediment circulation at a rock-bound estuary (Guadiana estuary, Portugal). *Estuarine, Coastal and Shelf Science* 84: 269-281. DOI 10.1016/j.ecss.2009.07.002.

Gonzalez R, Dias JMA, Ferreira O. 2001. Recent Rapid Evolution of the Guadiana Estuary Mouth (Southwestern Iberian Peninsula). *In*: Healy TR. (ed.), *ICS 2000 (Proceedings), Journal of Coastal Research* Special Issue, 34: 516-527.

Gonzalez, R., Araújo, M.F., Burdloff, D., Cacha˜o, M., Cascalho, J., Corredeira, C., 2007. Sediment and pollutant transport in the Northern Gulf of Cadiz: a multi-proxy approach. Journal of Marine Systems. 68, 1–23.

Gregory, KJ., Goudie, AS., 2011 The SAGE Handbook of Geomorphology, SAGE. 648P.

Guerit, L., Barrier, L., Métivier, F., Jolivet, M., Fu, B., 2015. Denudation rates from mass balance on alluvial fans in the Chinese Tian Shan. Geophysical Research Abstracts. Vol. 17, EGU2015-1323,

Hovius, N., Stark, C., & Allen, P. (1997). Sediment flux from a mountain belt derived by landslide mapping. Geology, 25(3), 231-234.

Jackli, H., 1957. Gegenwartsgeologische bundnerischen Rheingebietes: ein beitrag zur exogenen dynamik alpiner gebirgslandschaften. Swiss Geotech. Commission. Geotech. Series 36. Kummerley and Frei, Bern.

Liñán, C.C., de Alvaro, M., Apalategui, O., Baena, J., Balcells, R., Barnolas, A., Barrera, J.L., Bellido, F., Cueto, L.A., Diáz de Neira, A., Elízaga, E., Fernández-Gianotti, J.R., Ferreiro, E., Gabaldón, V., García-Sansegundo, J., Gómez, J.A., Heredia, N., Hernández.Urroz, J., Hernández-Samaniego, A., Lendínez, A., Leyva, F., Lopez-Olmedo, F.L., Lourenzo, S., Martín, L., Martín, D., Martín-Serrano, A., Matas, J., Monteserín, V., Nozal, F., Olive, A., Ortega, E., Piles, E., Ramírez, J.I., Robador, A., Roldán, F., Rodríguez, L.R., Ruiz, P., Ruiz, M.T., Sánchez- Carretero, R., Teixell, A., 1994.Mapa Geológico de la Península Ibérica, Baleares y Canarias (1:1 000 000). Instituto Tecnológico Geominero de España.

Lobo, J., Plaza, F., Gonza´ les, R., Dias, J., Kapsimalis, V., Mendes, I., Rio, V.D., 2004. Estimations of bedload sediment transport in the Guadiana estuary (SW Iberian Peninsula) during low river discharge periods. Journal of Coastal Research 41, 12–26. Special Issue.

Machado A, Rocha F, Gomes C, Dias J. 2007. Distribution and Composition of Suspended Particulate Matter in Guadiana Estuary (Southwestern Iberian Peninsula), Journal *of Coastal Research***,** Special Issue 50: 1040-1045.

Morales, J.A., 1993. Sedimentología del Estuario del Guadiana (S.W. Espa~na- Portugal) (PhD thesis). University of Sevilla, Sevilla, Spain, p. 274

Morales, J.A., 1995. Sedimentologia del estuario del Rio Guadiana (S.W. Espanã–Portugal), Servicio de Publicaciones, Huelva University; 1–322.

Morales, J.A., 1997. Evolution and facies architecture of the mesotidal Guadiana River delta (S.W. Spain–Portugal). Marine Geology. 138, 127–148.

Morales, J.A., Delgado, I., Gutierrez-Mas, J.M., 2006. Sedimentary characterization of bed types along the Guadiana Estuary (SW Europe) before the construction of the Alqueva dam. Estuarine, Coastal and Shelf Science. 70, 117–131.

Naden P, Smith B, Bowes M, Bass J. 2004. Fine sediment in the aquatic environment: issues for successful management. BHS Occasional Paper no. 14; 13–19.

Oliveira, J.T., Pereira, E., Ramalho, M., Antunes, M.T., Monteiro, J.H., Almeida, J.P., Carvalho, D., Carvalhosa, A., Ferreira, J.N., Gonçalves, F., Oliveira, V., Ribeiro, A., Ribeiro, M.L., Silva, A.F., Noronha, F., Young, T., Barbosa, B., Manupella, G., Pais, J., Reis, R.P., Rocha, R., Soares, A.F., Zbyszewski, G., Gaspar, L., Moreira, A.P., Moitinho da Almeida, F., Dâmaso, B., Dâmaso, L., 1992. Notícia explicativa da carta geológica de Portugal (folha 8; 1:200000). Serviços Geológicos de Portugal.

Olvmo, M., 2010. Review of denudation processes and quantification of weathering and erosion rates at a 0.1 to 1 Ma time scale. Technical Report, TR-09-18, University of Gothenburg. 50p.

Plater, A., Kirby, J., 2006. The potential for perimarine wetlands as an ecohydrological and phytotechnological management tool in the Guadiana estuary, Portugal. Estuarine, Coastal and Shelf Science. 70, 98–108.

Portela L., 2006. Sediment delivery from the Guadiana estuary to the coastal ocean. J Coastal Res SI 39:1819–1823

Reid, L.M. and T. Dunne. 1996. Rapid evaluation of sediment budgets. Catena Verlag GMBH, Reiskirchen, Germany. 164p

Sampath, D.M.R., Padilla, S., Delgado, J., López-Gutiérrez, J. M., Nieto, J.M., Boski, T., 2013. Estimation of denudation rates of the drainage basin of the Guadiana river using ^{10}Be isotope method and sediment budget method. V Regional Committee on Neogene Atlantic Stratigraphy RCANS 2013 24-26 September 2013, Huelva.

Slaymaker O., 2003. The sediment budget as conceptual framework and management tool. Hydrobiologia 494: 71–82.

Small, E.E., Anderson, R.S., Repka, J.L., and Finkel, R., 1997, Erosion rates of alpine bedrock summit surfaces deduced from in situ 10Be and 26Al: Earth and Planetary Science Letters, v. 150, no. 3–4, p. 413–425.

Smithson P, Addison K, Atkinson K, 2008. Fundamentals of the physical environment. 4th ed. London: Routledge. 776p

Swanson, F. J., R. J. Janda, T. Dunne & D. N. Swanston (eds), 1982. Sediment Budgets and Routing in Forested Drainage Basins. U.S.D.A. Forest Service, Portland. General Technical Report PNW-141.

Wolanski, E., Chicharo, L., Chicharo, M.A., Morais, P., 2006. An ecohydrology model of the Guadiana Estuary (South Portugal) Estuarine. Coastal and Shelf Science. 70, 132–143.

Chapter 7

Sensitivity of estuarine morphological response to fluvial discharge of the Guadiana River after the Alqueva dam: Conceptualization of the preliminary estimation of environmental flow to maintain salt-marsh habitats

Sampath, D.M.R., Boski, T., 2015. Modelling of estuarine response to increase of river discharge of the Guadiana river after Alqueva dam: Conceptualization of the preliminary estimation of environmental flow to maintain saltmarsh habitats. In preparation for the submission to Special Issue on Sustainability of Future Coasts and Estuaries in Estuarine, Coastal and Shelf Science.

ABSTRACT

In the context of rapid sea-level rise during the 21st century and beyond, managing estuarine ecosystems systems is a demanding task if there is significant reduction of fluvial sediment supply due to regulation of river discharge for different purposes. Methods applied to estimate environmental flow does not take into consideration the fluvial discharge required for maintaining the saltmarsh habitats and does not consider the impacting process of sea-level rise. The present study aims in filling this gap and assess sensitivity of morphological evolution of the estuary to the river discharge in the worst case sea-level rise and sedimentation scenarios. Assessment were mainly based on the theoretical framework, a set of analytical solutions to simplified equations of wave motion in shallow waters. Simulations were carried out for three cases in terms of the base river flow. The first case represents the observed base flow of the river, approximated in terms of trigonometric functions, of which amplitudes are 35, 25, 10 and 8 m^3/sec. The other two cases were derived by multiplying amplitudes by 1.5 and 2 to increase the annual average base flows by 1.37 and 1.75, respectively. For the two latter conditions the estimated net eroded sediment volume was reduced by 25 and 40% with respect to the estimated net eroded volume for the observed river discharge. Based on linear regression analysis, net erosion may be avoided by increasing the amplitudes of the base flow function by 3.5. But that is not sufficient to avoid submergence of habitat area due to the projected 79 cm rise of sea-level by the year 2100. The results suggest the deficiencies of defining the environmental flow as a percentage of dry season flow. Determination of environmental flow should be based on a full spectrum of natural flows, in terms of temporal and spatial variability. A multi-dimensional approach has to be adopted to mitigate the consequences of sea-level rise and strong flow regulations on the ecosystem of the Guadiana estuary.

Keywords: Long-term morphological evolution, Estuary, saltmarsh, sea-level rise, Environmental flow

7. 1 INTRODUCTION

Estuarine ecosystems, including saltmarshes provide economic, social and environmental benefits, which includes distinctive biodiversity and important ecosystem services, such as coastal defence, supporting fisheries and nutrient cycling (Mossman, et al., 2012). But they are vulnerable to rising sea levels, coastal developments, pollution and disturbance (Boorman, et al., 2002). The negative impacts on entire estuarine systems receive less attention when dams and irrigation farming are proposed upstream or when development and land reclamation sites are demarcated with hard engineering structures for flood protection within the littoral zone (Wolanski et al., 2006). Principal among fragile coastal habitats that are at risk from a variety of anthropogenic and natural forces are saltmarshes (lower, middle and upper marsh) associated with inter-tidal areas made up with fine-grained sediments (Dijkema 1987, Burd 1989). Therefore, Saltmarshes are now less extensive around the coasts of Europe than they were before the anthropogenic period (Dixon *et al.* 1998). The Health of an estuarine ecosystem is determined by natural interaction and feedback physical, biological and environmental processes, thus involve with number of important variables (Balls, 1994). According to Boorman, et al. (2002), a salt marsh develops naturally when an intertidal mud flat accumulates fine sediments to a level at which pioneer salt marsh plant species can colonise, if the suitable

conditions for their germination and establishment exist. For long term survival of and development, sediment from the water, which covers the marsh at high tide has to be trapped by the salt marsh plants and then incorporated into the marsh substrate (Boorman, et al., 2002).

The ecosystem health of an estuarine system can be degraded when the systems are poorly flushed, a characteristic during the low flow conditions either due to droughts or flow regulations by dams (Wolanski et al., 2006). The river discharge of the Guadiana River is regulated by more than 100 dams, including the Alqueva dam, constructed in 2002, forming the largest reservoir in Europe (Dias, et al., 2004). Therefore, the river discharge into the estuary is generally less than 20 m^3/sec (Garel and Ferreira, 2012). This significant reduction of river discharge leading to man-made droughts due to excessive trapping of water behind the Alqueva dam, and pulse-like, unseasonal river flows were the characteristic of the post dam Guadiana river (Wolanski et al., 2006). Area of the salt marsh habitat is reduced compared to the natural fluvial sedimentation prevailed in the system during the Holocene period (Boski et al., 2008). The situation can be further aggravated due to strong anthropogenic pressure, including urbanization, farming and aquaculture (Me´nanteau et al., 2005). Therefore, the ecosystem health of the Guadiana estuary is severely affected at present (Wolanski et al., 2006).

One of the strategy of mitigating negative consequences of river runoff regulations is to define environmental flow to inform on how much water should be released into a river, or the limit of abstraction from it, or the restoration of flows (King et al., 2003). The objective of the environmental flow is to mimic components of the rivers natural flow variability, including the magnitude, frequency, timing, duration, and rate of change and the predictability of flow events (Arthington et al., 2006). Environmental flows may be defined as the minimum water requirement that is left in a river system, or released into it, for the specific purpose of managing the condition of that ecosystem (King et al., 2003). There are about 100 different approaches to determine the environmental flow for the management of water resources (Tharme, 1996;

King *et al.*, 1999). The main types of flow-assessment approaches are: (1) hydrological, (2) hydraulic rating, (3) habitat rating, and (4) holistic (King *et al.*, 1999). The first approach is based solely on hydrological data and use summary statistics of flow, which may or may not be ecologically relevant, to advise on suitable flows, often for fish habitat (King et al., 2003). Due to the lack of sensitivity of the first approach to individual rivers, hydraulic-rating methods were developed which use field measurements to describe channel–discharge Relationships (King et al., 2003). Though providing river-specific data, the second method failed to indicate the significance of changes in the measured physical conditions for the aquatic biota and this led to the development of habitat-rating approaches (Reiser *et al.*, 1989a; 1989b; Stalnaker *et al.*, 1995). Though hydrodynamic habitat models have long been used worldwide to facilitate Environmental Flow Assessments (EFAs) in deriving defensible flow recommendations these models have been primarily focused on fish, neglecting the habitat requirements of other biotic elements of the whole ecosystem (Theodoropoulos, et al., 2015). These methods do not pay attention to the fluvial discharge required for maintaining the saltmarsh habitats and does not consider the threat of sea-level rise. Though the Alqueva water management authorities are intended to maintain environmental flow, which is not compulsory according to existing Portuguese water resources legislation and this is very simply calculated as a value > 2.5 to 5% of the modular water flow to be maintained throughout the year, if conditions permit (Galvão, et al., 2012). The adequacy of this approach has been challenged by several studies (e.g. Alves and Bernardo, 1998; Alves and Gonçalves, 1994; Chicharo et al., 2006; Chicharo et al., 2009; Wolanski et al., 2008).

Though, this study is not aimed to present a method of determining the environmental flow for such scenarios, but try to understand the sensitivity of river discharge on maintaining the depth of intertidal zone where the salt marshes can colonize. Thus, in the context of hybrid approach extending from chapter 5, which is a simple and idealized scripted with MATLAB

using a set of theoretical framework based on rule-based morphological expressions derived by Prandle (2004; 2009), this study is focused to understand the effect of dam construction along the Guadiana river on the estuarine morphology. Therefore, the main objectives of this chapter are twofold: (1) to assess the sensitivity of river discharge under the worst case sea-level rise rate scenario (A1FI – Intensive use of fossil fuel and 95% limit of the envelop) on determining the decadal scale morphological evolution in the Guadiana estuary and (2) to understand the effect of dam construction along the Guadiana river on the estuarine morphology. The model simulations were carried out in the Guadiana estuarine system because this region is affected with increased rate of sea-level and starvation of fluvial sediment due to the construction of a large number of dams over the past 50 years (Sampath et al., 2015). The model was scripted with MATLAB, an advanced scientific computational language.

7.2 STUDY AREA

Extensive details of the geographical and hydrodynamic setting of the Guadiana estuary are given previously. Therefore, the most important and relevant characteristics of the area are explained briefly here. Guadiana River is located in a semi-arid region with a Mediterranean climate (Aldaya and Llamas, 2008). Average annual precipitation is ca. 500 mm, and the hydrographic regime is torrential with concentrated rainy periods and a prolonged dry season, usually from May to September (Galvão et al., 2012). The Mediterranean climate irregularity shows a strong interannual variability, with intense rainy years, alternating with years of extended droughts (Daveau, 1987). Since the managing water requirements for different purposes under such demanding conditions has led to the construction of hundreds of dams, from which almost 90 have a volume capacity over $1hm^3$ (Galvão et al., 2012). These dams will trap sediment increasingly eroded from the catchment but without allowing them to reach the coastal system (Ferreira and Panagopoulos, 2014).

The Guadiana estuary is located along the southwestern boundary of Portugal and Spain. On the Portuguese margin, the salt marshes are sheltered by an ebb-tidal delta and it drains into the estuarine channel while the eastern margin is a mosaic of barrier islands and spits separated by wide salt marsh habitats that drain mainly to the sea through the Carreras tidal inlet (Garel et al., 2009). Under low flow conditions (Q_R < 50 m^3/sec), the Guadiana estuary can be considered as well-mixed in salinity (Fortunato et al., 2002). Under these conditions, seaward vertical velocity regime due to barotropic tide exists at spring tides, while the lower estuary is partially stratified during the neap tide (Garel et al., 2009). The estuary may have trapped approximately 10% of the total fluvial sediment contribution (0.5 to 1.5 x 10^6 t/yr) to the littoral zone from 1980 to 2000 (Portela, 2006). Under the low flow conditions, the suspended sediment concentration (SSC) is 10 mg/L at the mouth and it is about 100 mg/L at the middle estuary, where the turbidity maximum locates (e.g. Wolanski et al., 2006; Machado et al., 2007). However, before the Alqueva dam, the Guadiana River runoff was highly variable, at a seasonal and inter-annual scale resulting severe droughts or episodic floods. Thus, monthly river discharge ranged from <10 to 4660 m^3/sec and 50% of are less than 110 m^3/sec during the period 1947–2001 (Garel et al., 2009). Mean river flow measured at Pulo do Lobo (ca. 85 km upstream from river mouth) during summer reached 20 – 25 m^3/Sec during 1997 – 1998 previous to Alqueva, and decreased below 10 m^3/Sec from 1999 to 2003 during Alqueva construction and filling. Afterwards, summer river flow increased to 10 – 15 m^3/Sec during 2004 – 2005 reaching 20 – 25 m^3/Sec during 2007 – 2008, but decreased back below 10 m^3/Sec during 2008 – 2009 (Galvão, et al., 2012). From 2010 onwards, data is scattered, but in general there is an increase of summer flow except in 2012 (Fig. 7.1). The environmental flow of the Guadiana River is 2 m^3/sec, which is the river run-off during the dry season (Wolanski, et al., 2006).

7.3 METHODOLOGY

The methodology for this chapter extends from the chapter 5. Therefore, the additional information required for the analysis of sensitivity of river discharge on morphological evolution is briefly explained in this chapter. Assessment of the sensitivity of river discharge in the context of rising sea-level on determining the decadal scale morphological evolution in the Guadiana estuary were mainly based on the theoretical framework of Prandle (2009) to represent the estuarine dynamics. The local physical parameters including tidal constituents (Pinto, 2003), sediment size distribution (Morales et al., 2006), and suspended sediment concentration (e.g. Garel et al., 2009; Marchado et al., 2007; Morales, 1995) were obtained from previous studies carried out in the Guadiana estuary. The river discharge data and rating curves to derive the river discharge from 2000 to 2014 May were obtained from the archived data. The theoretical framework is based on the analytical solutions to the one-dimensional and cross sectionally averaged shallow-water wave equations (Prandle, 2009). The equations were simplified for the first-order tidal simulations by neglecting the convective terms and by linearizing the quadratic friction term of the shallow-water wave equation. This approach is further simplified for a triangular shaped synchronous estuaries, as the surface gradients associated with axial amplitude variations in ς^* is assumed to be significantly less than those associated with corresponding phase variations (Prandle, 2003). The assumption of synchronous estuary is shown to be valid for the Guadiana estuary as the study area extends only to 11 km from the mouth of the river (Geral et al., 2009).

The river discharge in the model consists of a base flow and pulses. The base flow represents the usual river discharge throughout the year and pulses represent the instantaneous increase of river discharge due to heavy rain or dam flushing. Sometimes, pulses were averaged over the time, if there were several pulses in a short time span. The base flow of the Guadiana river discharge is approximated as a combination of sinusoidal and cosine functions that define

the base characteristic river discharge after the closure of the Alqueva dam. Coefficients or amplitudes of the trigonometric functions were 35, 25, 10, and 8 m^3/sec (Table 7.1). For the sensitivity analysis, these coefficients of the trigonometric function of base flow were increased by 1.5 and 2. Thus, the modelled annual average base river discharge is equivalent to 1.37 and 1.75 of the observed annual average base river discharge from 2000 to 2014 for the factor 1.5 and 2, respectively. According to the empirical formulation of Morales, 1995, the suspended sediment concentration was increased by 1.225 and 1.41 compared to the SSC corresponding to each coefficient.

Table 7.1 Coefficients that used to change the base flow of the Guadiana river discharge, which is approximated as a combination of sinusoidal and cosine functions.

Coefficients of sinusoidal and cosine functions that define the base river discharge of the Guadiana estuary	**1.5*Q_R**	**2*Q_R**
	Modelled annual average base river discharge =1.37* Observed annual average base river discharge from 2000 to 2014	**Modelled annual average base river discharge =1.75* Observed annual average base river discharge from 2000 to 2014**
Q_R		
m^3/sec	**Factor of increase of SSC w.r.t initial SSC due to Q_R, based on Morales, 1995 empirical formulation**	
35	1.225	1.410
25	1.225	1.410
10	1.225	1.410
8	1.225	1.410

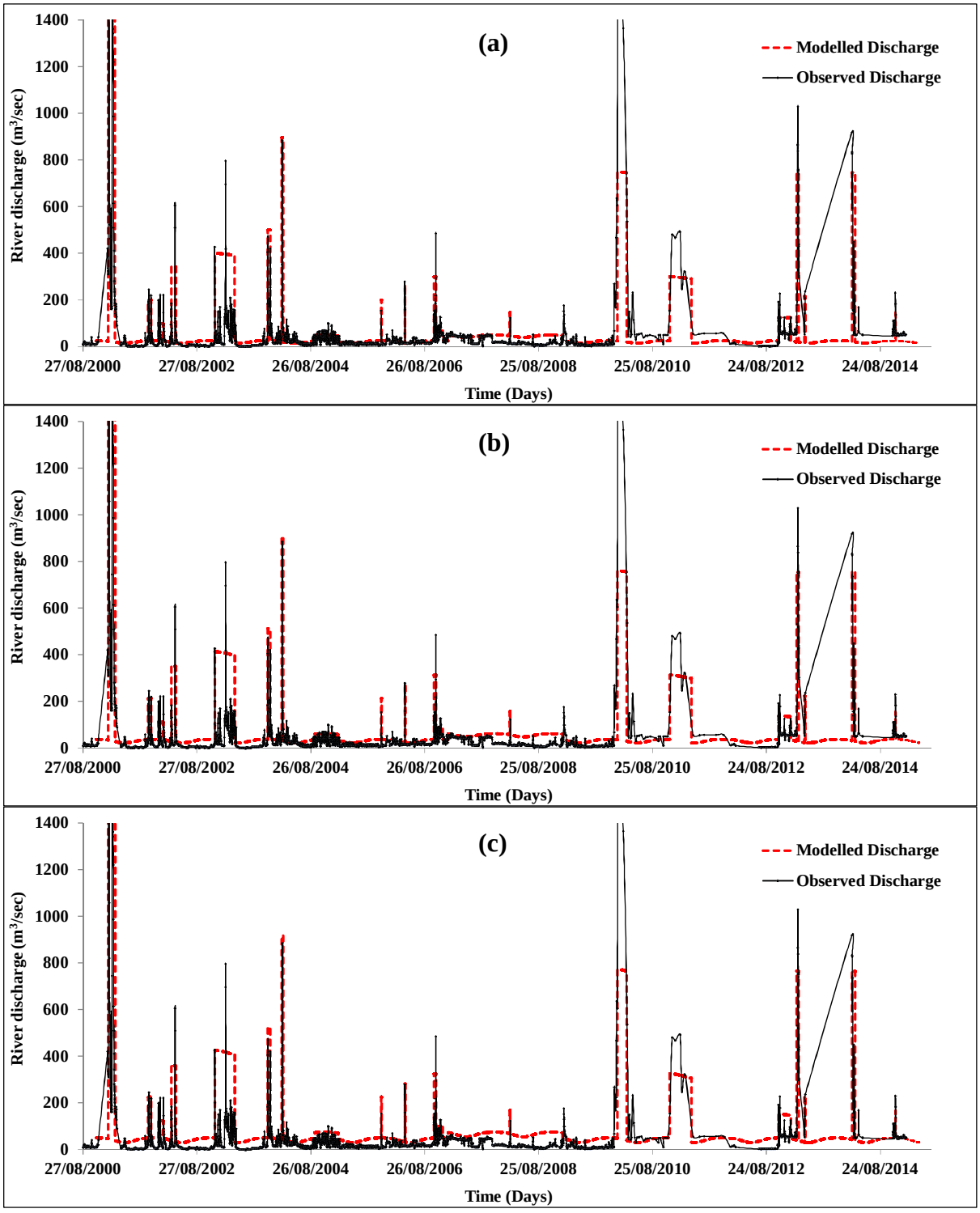

Figure 7.1 The observed and modeled river discharge of the Guadiana River from 2000 to 2014 May. (a) Comparison of the observed river discharge with the modeled river discharge (b) Comparison of the observed river discharge with modeled river discharge, but the coefficients of the trigonometric function (base flow) were increased by 1.5; and (c) the same was increased by 2.

The Observed River discharge at the Pulo do Lobo Guage station represents 91% of the runoff of the Guadiana basin (Geral et al., 2009). However, the data from 2010 are scattered (Fig. 7.1a). Therefore, river discharge during such time periods were assumed to represent only the base flow without peaks. As this is a preliminary study, the sensitivity analysis of the river discharge on the long-term morphological evolution were carried out for two cases, where the base flow coefficients were increased by factor 1.5 and 2 (Fig. 7.2b and 7.2c, respectively).

Fig. 7.2 shows the representative sedimentation rate functions for modelled river discharge, which was approximated to the observed river discharge of the Guadiana River from 2000 to 2014 and modelled river discharge for the same period, but the coefficients of the trigonometric function (base flow) were increased by 1.5 and 2.

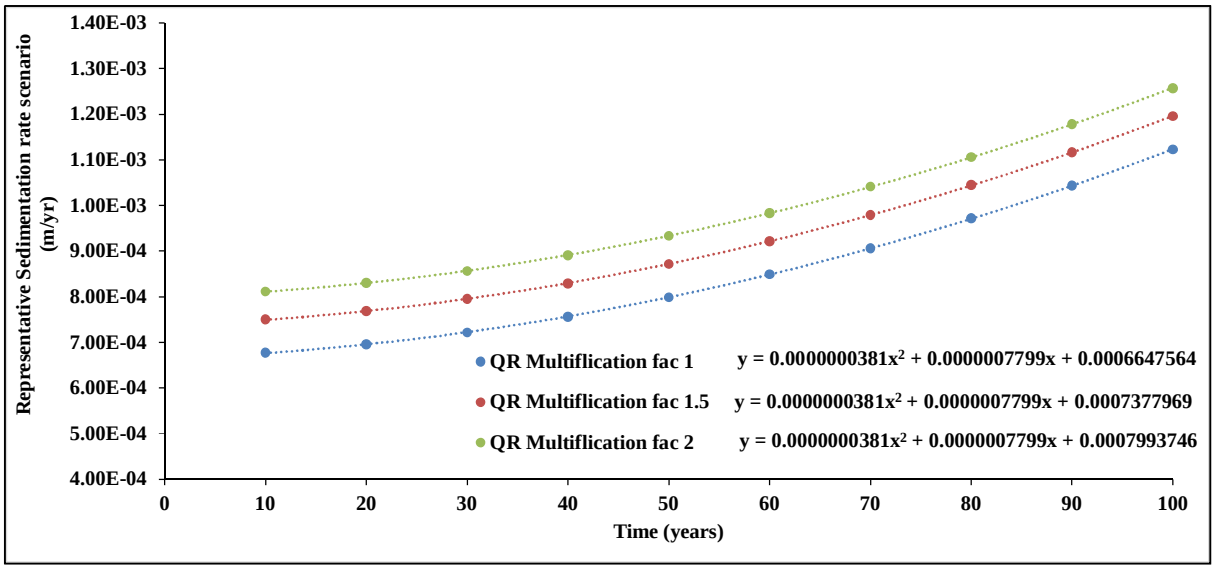

Figure 7.2 Representative sedimentation rate functions for modeled river discharge, which was approximated to the observed river discharge of the Guadiana River from 2000 to 2014 and modeled river discharge for the same period, but the coefficients of the trigonometric function (base flow) were increased by 1.5 and 2.

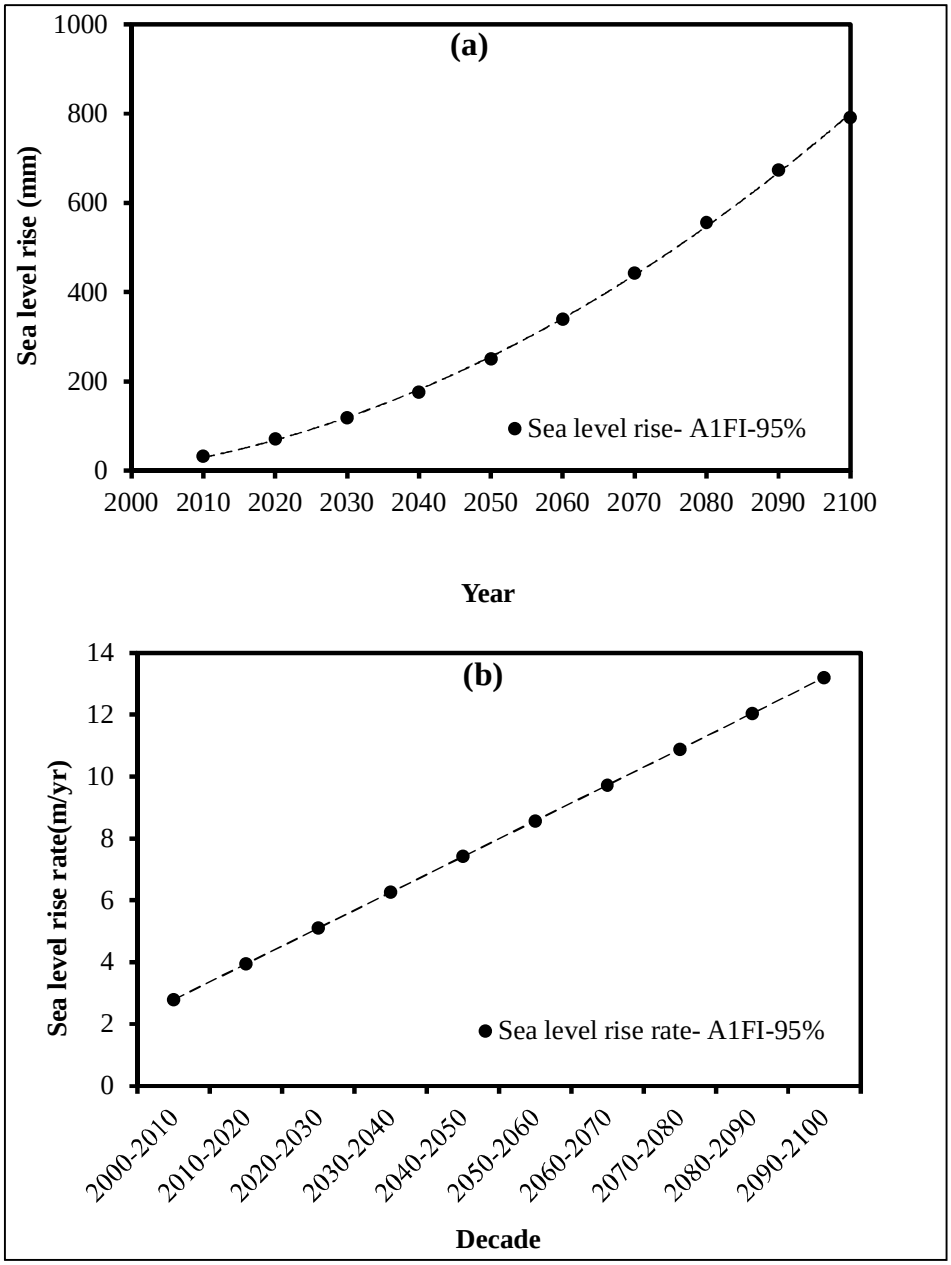

Figure 7.3 Sea-level rise projections: (a) The upper limit projection of A1FI (Intensive use of fossil fuel) sea-level rise scenario based on the IPCC, 2007 report, but updated, including the effect of ice sheet melting (Hunter, 2010); and (b) Corresponding sea-level rise rate variations.

Decadal-timescale forecasting of morphological evolution for different river discharge functions was based on the upper limit of A1FI sea-level rise projections (IPCC, 2007) that are updated by Hunter (2010). As the recent sea level change trend, at the Portuguese continental margin, was attributed to the global causes (Dias and Taborda, 1992), we used the upper limit

(95%) of mean sea-level rise projections under the globalized economy and intensive use of fossil fuel (A1FI) scenario (Fig. 7.3a and 7.3b) given by Hunter (2010). The projection is relative to the year 2000, though the Hunter, (2010) used 1990 as the base year. The sea-level rise scenario was assumed as a second order polynomial function of time and first time derivative of this function was used to derive the sea-level rise rate function for each decade. The assembled records of altimetry data from the TOPEX/Poseidon, Jason-1, and Jason-2 satellite missions indicate that the average rate of sea-level rise during the period 1993–2009 was 3.2 ± 0.4 mm/yr (Nerem et al., 2010).

As explained in chapter 5, the model was scripted with MATLAB, an advanced scientific computational language and spatial analysis were carried out using geo-processing and 3D Analysis tool of ESRI ArcGIS software. Time step for hydrodynamic simulations were 20 minutes and long-term morphodynamic simulation were carried out with 1 year time step. In contrast to methodology in chapter 3 and 4, the hydrodynamic model based on the theoretical framework of Prandle, (2009) calculates the long term accretion coefficients for the both sub-tidal and intertidal regions. In the chapter 3 and 4, the coefficients were calculated in terms of tidal inundation frequency and net accretion coefficient at the Portuguese Hydrographic Datum.

7.4 RESULTS

Though the output time step of the model simulation was 10 years from the year 2000, bathymetries shown in Fig. 7.4 represents the bathymetry of the Guadiana estuary observed in 2000 and the simulated bathymetries for 2020, 2050, 2070 and 2010. In this case, the modelled river discharge is equivalent to the observed river discharge pattern at the Pulo do Lobo Guage station (Fig. 7.1a) Expansion of area prone to tidal inundation with sea-level rise is very prominent near to the secondary channels in the Portuguese margin.

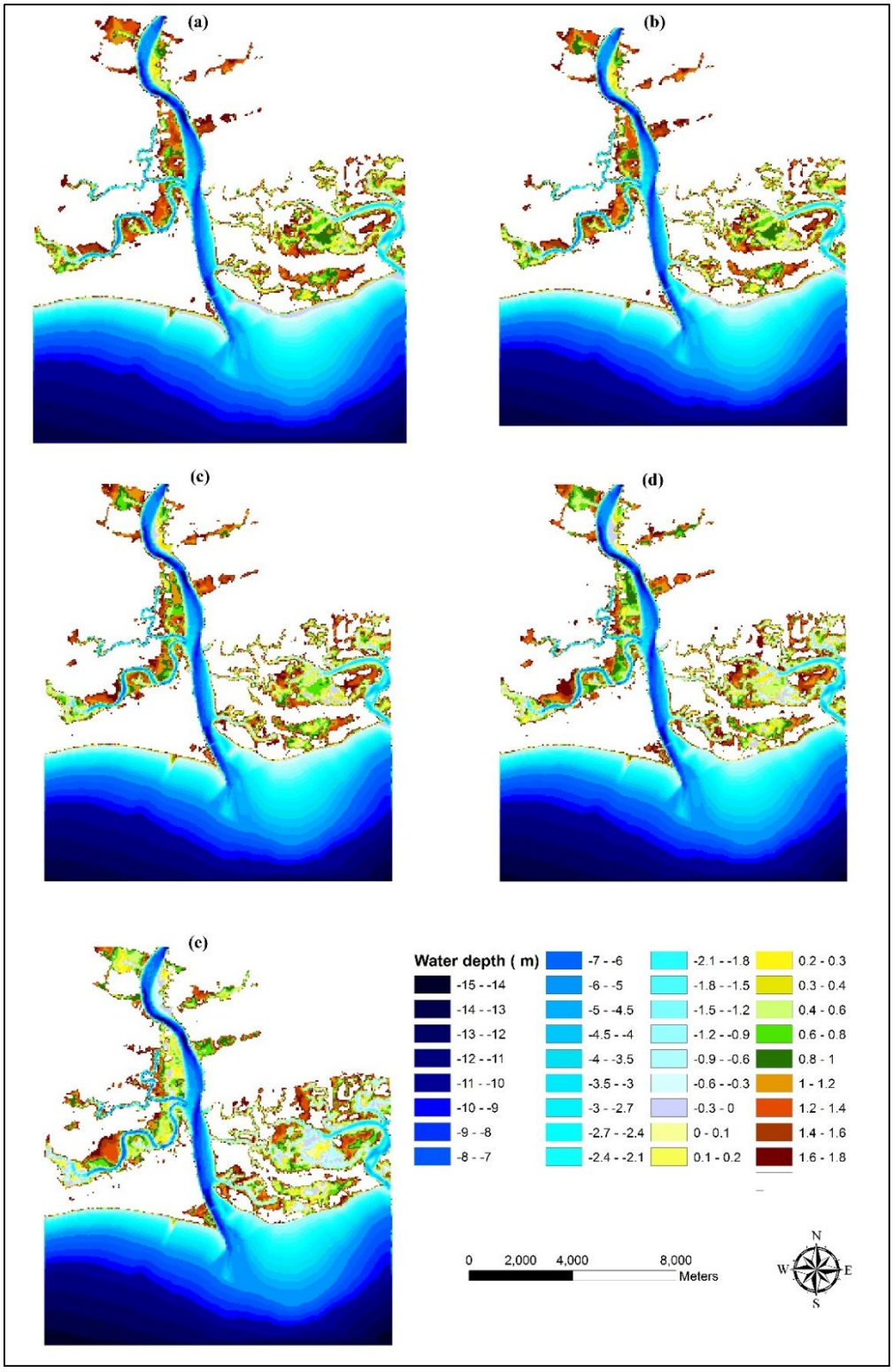

Figure 7.4 Bathymetry of the Guadiana estuary (a) observed in 2000 and the simulated bathymetries for (b) 2020, (c) 2050, (d) 2070 and (e) 2100, in response to the A1FI sea-level rise scenario and the modelled river discharge, which equivalent to the observed river discharge pattern at the Pulo do Lobo Guage station.

Table 7.2 Predicted translation of area of the likely habitat types in the intertidal zone of the Guadiana estuary in response to upper limit scenarios of sea level rise and sedimentation scenarios by the year 2100, compared to their existing area by 2000.

Habitat types (likely)	**Area – km^2 (2000)**	**Occupied from the original habitat types of**	**Area of likely habitats in the Portuguese margin (km^2) by 2100**		
			A1FI (P = 95%) Factor 1	**A1FI (P = 95%) Factor 1.5**	**A1FI (P = 95%) Factor 2**
Mud flats (-2 – 0 m)	11.14	Mud flat	6.67	6.68	6.69
		Low marsh	4.16	4.16	4.16
		Mid marsh	3.52	3.48	3.45
		Total	**14.35**	**14.32**	**14.3**
		Expansion (%)	**(28.9)**	**(28.6)**	**(28.3)**
Low-marsh (0 – 0.5 m)	4.16	Low marsh	0	0	0
		Mid marsh	2.51	2.55	2.58
		High marsh	4.59	4.54	4.50
		Total	**7.10**	**7.09**	**7.08**
		Expansion (%)	**(70.9)**	**(70.5)**	**(70.2)**
Mid-marsh (0.5 – 1 m)	6.03	Mid marsh	0	0	0
		High marsh	8.08	8.11	8.14
		Total	**8.08**	**8.11**	**8.14**
		Expansion (%)	**(34.0)**	**(34.6)**	**(35.1)**
High-marsh (1 – 1.8 m)	13.98	High marsh	1.31	1.33	1.34
		Newly inundated land	11.98	11.98	11.98
		Total	**13.29**	**13.31**	**13.32**
		Expansion (%)	**(-4.9)**	**(-4.7)**	**(-4.7)**
Intertidal zone (Total) (-2 – 1.8 m)	35.31	Existing intertidal zone	29.53	29.52	29.52
		Newly inundated land	11.98	11.98	11.98
		Total	**41.51**	**41.50**	**41.5**
		Expansion (%)	**(17.6)**	**(17.5)**	**(17.5)**

The expansion of intertidal zone limits in the Spanish margin is visible on the banks of secondary tidal channels of the Carreras inlet. Though the base flow component of the total river discharge is increased by factor 1.5 and 2, the expansion of tidal prone areas is very much similar (Table 7.2). The expansion of the mud flat area is prominent under three cases. That is the area between -2 to 0 m, would be 14. 35 km^2. Compared to the approach adopted in the chapter 4, there is additional transgression of the mean sea-level by 1 km^2. The landward

movement of – 2 m contour, increases the area below the Portuguese Hydrographic Datum, approximately by 4.45 km^2.

As in the chapter 4, for simplicity, the area prone to tidal heights up to 0.5, 1 and 1.88 m are assumed to be the likely habitats of the low and mid and high saltmarsh systems. Under the worst case sea level rise scenario, low and mid marsh will completely translate into new regions. Very little amount of area will retain from the high marsh regions compared to existing area at the year 2000. If the biogeochemical properties are not suitable for the successful translation of these habitats under rising sea-level, these habitats may extinct from the ecosystem. Even if the base flow was increased by factors of 1.5 and 2, which resulted in an increase of sedimentation rate by 1.2 and 1.4 times relative to rates predicted for the approximated river discharge given in Fig. 1a, the risk of habitat extinction may not be able to effectively overcome. This would suggest the deficiencies of defining the environmental flow as a percentage of dry season flow.

Compared to the available area, the survival of marsh system is dependent on the water depth. If the saltmarsh habitats are submerged with water level, that will increase the vulnerability of different species of saltmarsh vegetation. Fig. 7.5 shows the change in water depth of the Guadiana estuary and its intertidal zone region due to A1FI sea-level rise scenario and sedimentation scenario based on river discharge (a) approximately equivalent to the observed river discharge pattern from 2000 to 2014 May, measured at the Pulo do Lobo station; (b) the base flow of the modelled river discharge in the case a was increased by factor 1.5; and (c) by a factor 2. The change of water depth ranges from 0.7 to 0.86 m in response to 0.79 m rise of sea-level by the end of the year 2100. In the first case water depth in the intertidal zone can increase by 0.78 to 0.86 m. In the case b and c, water depth change in the intertidal zone will be approximately by 0.78 to 0.84 and 0.78 to 0.82, respectively. This shows reductions of change of water depth by 2 and 4 cm for the case b and c, respectively. However, it is not

possible to predict the effect of such reduction of water depth due to the increase of base flow by 1.5 and 2 on the reduction of the stress on salt marsh vegetation for their survival.

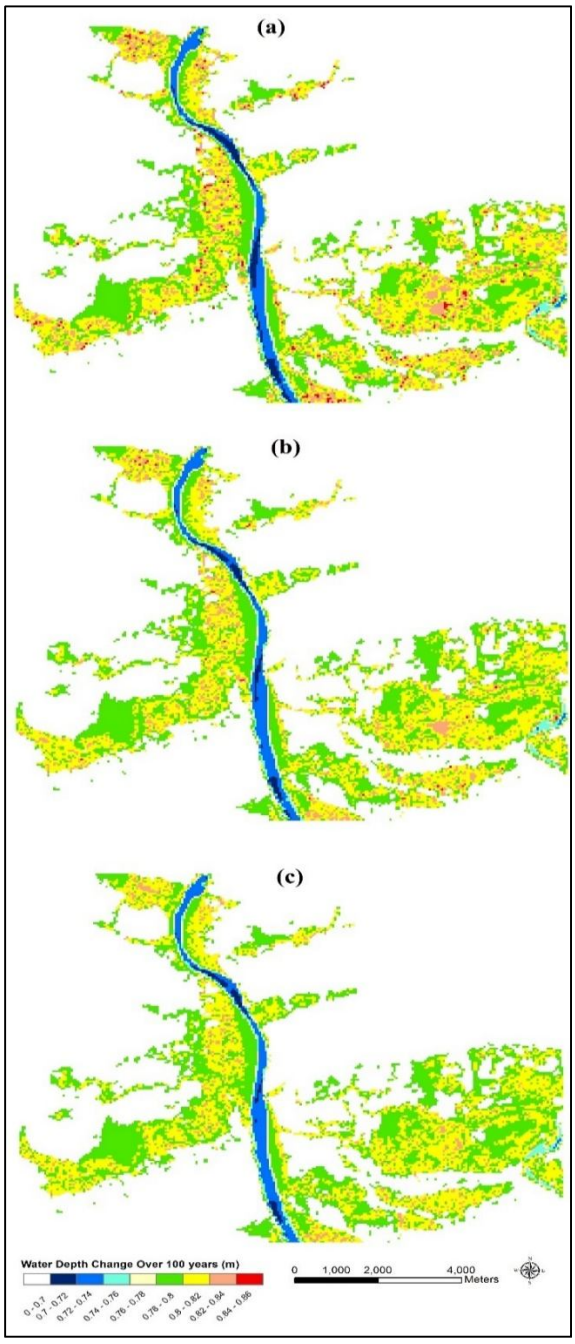

Figure 7.5 Change in water depth of the Guadiana estuary and its intertidal zone region due to A1FI sea-level rise scenario and sedimentation scenario based on river discharge (a) approximately equivalent to the observed river discharge pattern from 2000 to 2014 May; (b) the base flow of the modelled river discharge in the case a was increased by factor 1.5; and (c) by a factor 2.

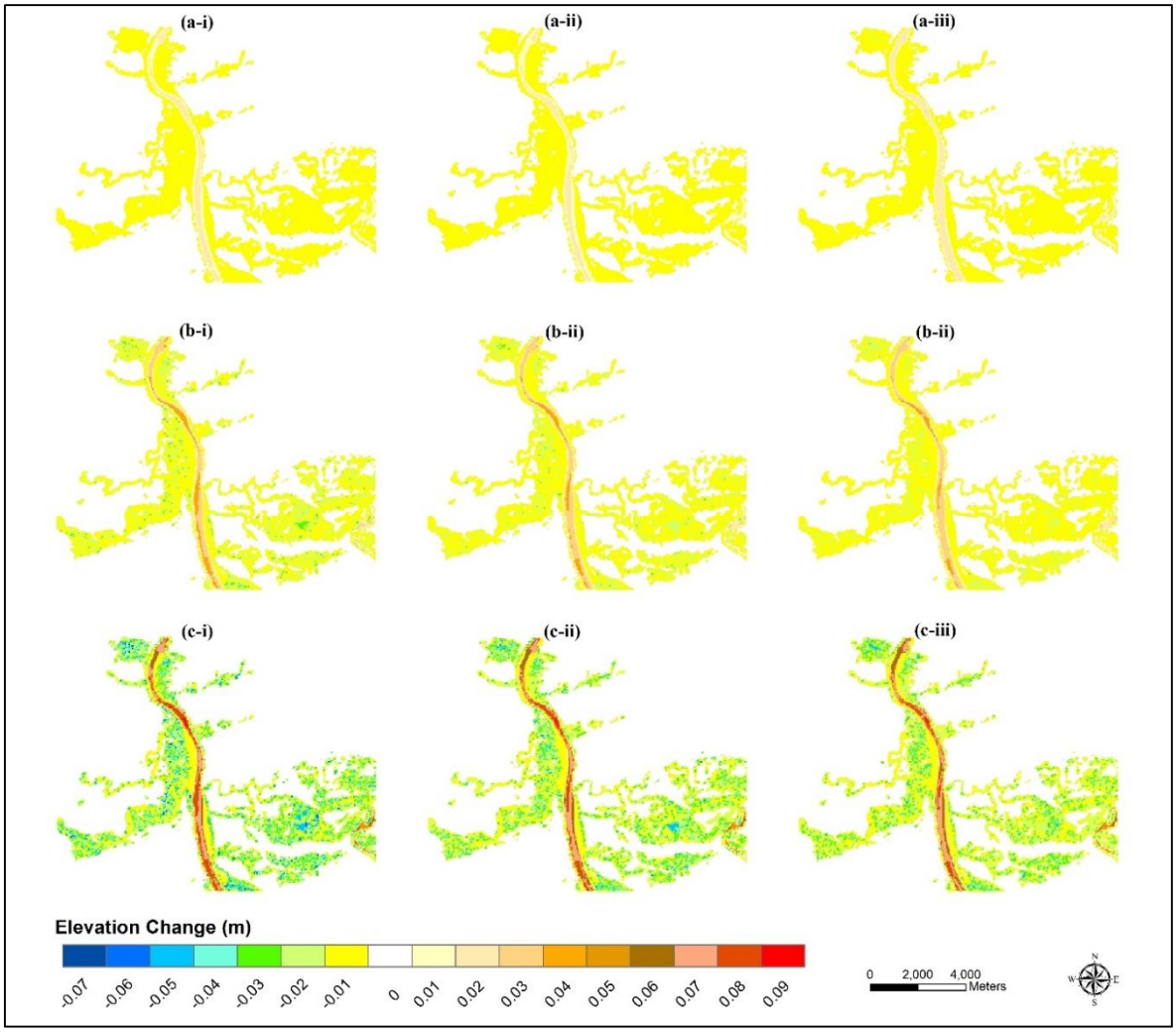

Figure 7.6 Change of elevation of the Guadiana estuary at the end of the year (a) 2020; (b) 2050; and (c) 2100 in response to sea-level rise by 79 cm (The upper limit of the A1FI scenario) and sedimentation scenario based on river discharge (i) approximately equivalent to the observed river discharge pattern from 2000 to 2014 May; (ii) the base flow of the modelled river discharge in the case a was increased by factor 1.5; and (iii) by a factor 2.

According to the bathymetric surveying carried out in 2014 May, there are erosional and accretion areas relative to the observed bathymetry of year 2000. The tidal inundation frequency curves were used in the Estuarine Sedimentation Model explained in chapter 2, 3 and 4. Simulation of erosional areas using this approach was not possible as it uses a generalized sedimentation behaviour for the depth range of the estuary from the maximum high

tide limit. Such approach would be suitable for unhindered sediment supply conditions where there is a net accretion throughout the estuary. However, in the context of drastic reduction of fluvial sediment supply due to a large number of dams along the Guadiana River, it is not possible to expect net accretion throughout the estuary as it was the case in the Holocene period. As in the chapter 5, erosional and accretion areas were able to simulate during the 21st century using the theoretical frame of Prandle, 2009. According to the results, intertidal zone is eroding and there is a low depositional trend in the sub tidal channel for the increase of water level as the sea-level rise from 2000 to 2100 (Fig. 7.6). At the beginning, the erosional and accretion heights are uniform for the three cases. For instance, by 2020, there would be 1 cm of erosion from the intertidal zone and 2 cm of accretion throughout the subtidal channel. However, with the increase of sea level by 2100, there is a significant spatial variability of accretion and erosion. The maximum erosion occurs in the associated intertidal areas of secondary channels, such erosion occurs in the region associated with a complex network of secondary channels of the Carreras inlet. With the increase of base flow by a factor of 1.5 and 2, the erosive strength will reduce by an order of a few centimetres.

The simulation of decadal scale morphological evolution in response to sea-level rise and reduced sedimentation scenarios shows net erosion from the system (Fig. 7.7). In the context, that the Guadiana estuary is at the terminal stage, such result can be expected over this century. Studies by Geral, et al., (2009; 2012), shows the dominance of the ebb tides in the estuary as the residual currents are seaward. By increasing the base flow river discharge by a factor of 1.5 and 2, the net eroded sediment volume can be reduced by 25 and 40% with respect to the net eroded volume given by factor 1 (i.e. modelled river discharge is approximately same as the observed discharge at the Pulo do Lobo station. However, this reduction will not be effective, even under such conditions, there can be an increase of water depth in saltmarsh habitats.

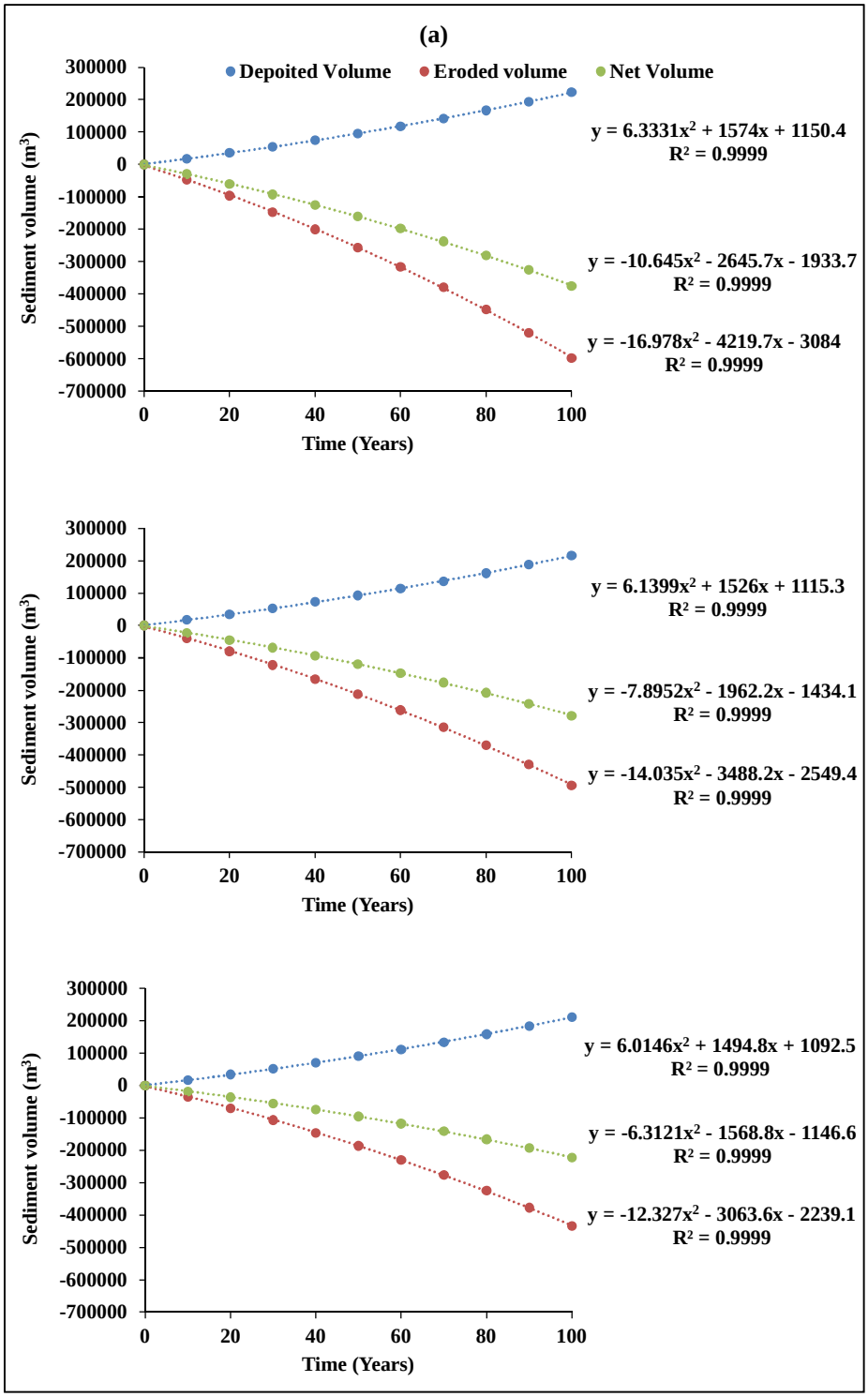

Figure 7.7 Decadal volume of sediment erosion, accreted and net erosion from the lower Guadiana estuary due to A1FI sea-level rise scenario and sedimentation scenario based on river discharge (a) approximately equivalent to the observed river discharge pattern from 2000 to 2014 May; (b) the base flow of the modelled river discharge in the case a was increased by factor 1.5; and (c) by a factor 2.

7.5 DISCUSSION

7.5.1 IMPACTS DUE TO SEA-LEVEL RISE AND RIVER REGULATIONS

As there conclusive evidence of accelerated sea-level rise during this century (IPCC, 2014), coastal managers and scientist are increasingly concerned over the future survival of salt marshes (Kirwan et al., 2010). According to Day et al. (2000), the critical factor in determining the health of a saltmarsh is the availability of fluvial sediment rather than the sea-level rise. According to Mudd, (2011), if there is morphological evolution of marsh platform to an elevation lower than mean high tide, either due to reduced sedimentation or an increased rate of SLR, then these marsh plants will die while the marsh habitats drown. If these two conditions are imposed a stress on saltmarsh growth, such systems are highly vulnerable, which would be the case in the Guadiana estuarine system. The feedback effect of drowning of marsh systems is the increase of erosion as the plants die and thus these habitats can rapidly convert to subtidal flats where the richness of species are minimum (Fagherazzi et al., 2006). However, such feedback effect is not considered in this study. That is because this work is a preliminary conceptualization of determining environmental flow to maintain the saltmarsh ecosystems.

However, it is important to note that, as concluded by Siams, et al., 2001, that the salt marshes of the mesotidal estuaries such as the case of Guadiana are susceptible to sea-level rise only in a worst case scenario. Though, the IPCC, (2007) report does not include the ice sheet melting of the Greenland and the Atlantic, the IPPC (2014) has included the ice sheet melting for their latest projections. In this study, the sea-level rise time series for the worst case scenario is based on the projections by Hunter, (2010), which was scaled the IPCC, 2007 scenarios based on the projections ice sheet melting estimations given in IPCC, 2001. These projections are very much closer to the projections in the latest IPCC report. Though there is great uncertainty is still exist regarding the fate of the ice sheets, losses from both Greenland and Antarctic ice sheets have accelerated, doubling over recent years due to increased melting

(Velicogna 2009). The present study showed that the saltmarshes would not be under stress if there is no man made disturbance like sea walls or concrete coastal defence structures inhibiting the landward migration of saltmarshes with rising sea-level. When determining the two dimensional surface area of different habitats under the considered scenarios, there was a little discrepancy between the measured area in this chapter and the chapter 4. This is because the resolution considered in the chapter is 10 m and in this chapter the resolution is 50 m to reduce the time required for the computing. It takes approximately 8 days to simulate evolution of morphology in response to one case of sea-level and sedimentation scenarios, which is highly demanding. It is recognized that the MATLAB scripts can be rewritten with efficient codes. This chapter is also based on the theoretical framework explained in the chapter 5, constraints discussed under that chapter on the model is valid for this work. The methodology developed in this study can be further improved by integrating the present morphological model with biogeochemical and demographic modelling, remote sensing and geographical information analysis as explained by Siams et al., 2001.

7.5.2 MITIGATING THE SALTMARSH EROSION

The present study shows that the saltmarsh habitats are increasingly at high risk of extinction due to the increase of water depth change. Though the base flow, which is related to the environmental flow, is increased by factors of 1.5 and 2, the erosion cannot be effectively reduced nor will the threat of submergence of habitats be reduced. Therefore, following remedial measures are recommended to minimize the effect of sea-level rise and reduction of fluvial sediment supply to the estuarine system.

Holistic management of water resources in the Guadiana River catchment is still a complex transnational problem though there has been negotiations between Portugal and Spain for several decades (Galvão et al., 2012). In 1998, Portugal and Spain signed, at Albufeira, a

Convention to regulate access to their common rivers. Most of them have their upstream basins in Spain and flow into Portugal (Costa et al., 2008). As an outcome of these bilateral Agreements, both countries agreed to adopt an integrated management of water and territory plan, covering quantitative and qualitative features, stipulating minimum flows (under normal rainfall conditions), and foreseeing the permanent exchange of hydrologic and environmental data and information (Mendes, 2010). However, in the context of strong flow regulations on the Guadiana River in the era of rapid sea-level rise, a multi-dimensional approach has to be adopted to mitigate their negative consequences on estuarine ecosystem including the saltmarsh habitats associated with the Guadiana estuary. As King et al. (2003), explained, the first step should be the determination of environmental flow in the Guadiana River based on the holistic approach. Since all major abiotic and biotic components constitute the ecosystem to be managed, the full spectrum of flows, and their temporal and spatial variability, constitute the flows to be managed. Aquatic scientists and engineers from many disciplines should use methods of her/his choice to develop an understanding of flow–ecosystem relationships, and then works with the other team members, within the overarching process of the holistic approach to integrate data and knowledge (King et al., 2003) so that projected time series of environmental flow can be determined by the additional data including weather forecast for the region.

Then it is recommended to remove all the unnecessary coastal defensive structures to allow the natural process to take place. The second approach of managed realignment will support the natural survival of saltmarsh systems. However, allowing the tidal flow does not automatically lead to the early reestablishment of a creek system (Boorman et al., 2002). Therefore, development of an effective drainage system may be useful for the speedy removal of the surface water as the tide ebbs is important for the dewatering of the soil which aids the establishment of marsh vegetation (French *et al.* 1995; Boorman 1999, Dixon *et al.* 1998).

Acceleration of the rate of sedimentation can be enhanced by the use of various types of structures and the best examples of this approach are the Schleswig-Holstein method (Boorman, et al., 2002). This method was applied in Dutch and German Wadden Sea (Kamps 1962); in England (Toft *et al.* 1995); and in the USA (Turner and Streever 2002). Furthermore, other soft engineering measures to retain and stabilize the sediment are the use of geotextile membranes, wave breakers and vegetation protection (Colenutt, 2001).

The required fine fluvial sediment can be supplied using water wheels with buckets, a centuries old traditional water pumping mechanism. In this regard, several water wheels can be installed along the margin of the river and water is conveyed to marsh systems. In this method water will not be lost as in the case of a diversion structure because water will re-enter the main river while the fine sediment is trapped by the existing vegetation canopy. This approach is simple, less maintenance requirements and no energy required to pump the water as it will work with the energy of the river flow. The enhancement of the natural processes of marsh development will be effective when conditions are favourable for example where marshes are threatened by large scale environmental pressures including rising sea levels (Boorman 1992, Dahl and Johnson 1991).

Some species can colonize in managed realigned sites. However, managed realigned marsh systems may not have the same species richness as in natural systems (Mossman, et al., 2012). If all other methods are not feasible, the transplanting of a species of *Spartina* would be an alternative but the planting may be difficult in a relatively high energy environment and proved ineffective (Colenutt, 2001). Considering the inherent variation in natural saltmarshes and projected environmental change, these additional management interventions of planting of mid- and upper-marsh species, while manipulating the topographic heterogeneity can be applied to achieve at least the minimum levels of ecosystem functioning (Mossman, et al., 2012).

7.6 CONCLUSIONS AND RECOMMENDATIONS

The present study was focused on assessing the sensitivity of river discharge on morphological evolution in the estuary in response to the worst case sea-level rise and sedimentation scenarios. For that purpose simulations were carried out for three cases in terms of the base flow of the river: i) an approximately equivalent to the observed base flow component of the Guadiana River. ii) 1.37 times increase of observed annual average base flow and iii) 1.75 times increase of observed annual average base flow. The corresponding suspended sediment concentrations were increased by 1.225 and 1.41 compared to the SSC of each coefficient. Expansion of area under tidal inundation and rising sea-level is very prominent near to the secondary channels in the Portuguese margin. The expansion of intertidal zone limits in the Spanish margin is visible on the banks of secondary tidal channels of the Carreras inlet. A significant increase of the mud flat area is prominent under three cases. Such increase can result a system with poor species richness. Under the worst sea level rise scenario, low and mid marsh will translate into a new upwards setting, if the biogeochemical conditions are appropriate and there is no man made obstructions. The high salt marsh areas will be drastically reduced when compared to the situation observed in 2000. The modelled base flow increases were not sufficient to overcome the risks of habitat extinction and point to the deficiencies of defining the environmental flow as a percentage of dry season flow. The reduction of sediment erosion by 25 and 40% associated with the modelled conditions will not be effective to protect the marsh because increase of water depth in saltmarsh habitats.

Thus, in the context of strong flow regulations on the Guadiana River in the era of rapid sea-level rise, we propose a 4 step multi-dimensional approach for the conservation of the estuarine system.

1. Determination of environmental flow based on a full spectrum of natural flows, in terms of temporal and spatial variability.

2. Removal all the unnecessary coastal defensive structures to allowing the natural sedimentation process to take place within the system.
3. The fine fluvial sediment needed to sustain the marshes should be supplied by an appropriate bypassing system
4. A possible transplanting of the dominant marsh species can be envisaged as an alternative

ACKNOWLEDGMENTS: The first author acknowledges FCT (SFRH/BD/70747/2010) and the **CIMA - Centro de Investigação Marinha e Ambiental**, Universidade do Algarve (**UID / MAR / 00350/2013)** for granting a scholarship to carry out this work as part of his PhD research. The comments of two anonymous reviewers and the Editor, have helped to significantly improve an earlier version of the manuscript.

7.7 REFERENCES

Aldaya, MM, Llamas, MR, 2008. Water footprint analysis for the Guadiana river basin. Value of Water Research Report Series No. 35, UNESCO–IHE Delft, The Netherlands. 86p.

Alves, M. H. & Bernardo, J. M., 1998. Novas perspectivas para a determination do caudal ecológico em regiões semi-áridas. Proceedings of *Seminário sobre barragens e ambiente*. Comissão nacional Portuguesa da Grandes barragens, ISBN 92-894-5122-X, Porto, Maio de 1998.

Alves, M. H. & Gonçalves, H., 1994. O caudal ecológico como medida de minimização dos impactes nos ecossitemas lóticos. Métodos para a sua determinação e aplicações. Proceedings of: "*Actas do 6ºSILUSB/1ºSILUSBA, Simpósio de Hidráulica e Recursos dos Países de Língua oficial Portuguesa*", (Abril de 1994), Lisboa

Arthington AH, Bunn SE, Poff LN, Naiman RJ. 2006. The challenge of providing environmental flow rules to sustain river ecosystems. Ecological Applications 16: 1311–1318.

Balls, P.W., 1994. Nutrient inputs to estuaries from nine Scottish east coast rivers: influence of estuarine processes on inputs to the North sea. Estuarine, Coastal and Shelf Science 39, 329-352.

Boorman, L.A., 1999. Salt Marshes – present functioning and future change. *Mangroves and Salt Marshes*; 3: 227-241.

Boorman, L. Hazelden, J. Boorman, M., 2002. New Salt Marshes for Old - Salt Marsh Creation and Management. Littoral 2002. The Changing Coast. EUROCOAST / EUCC, Porto – Portugal Ed. EUROCOAST – Portugal. 35-45.

Boski, T., Camacho, S., Moura, D., Fletcher, W., Wilamowski, A., Veiga-Pires, C., Correia, V., Loureiro, C., Santana, P., 2008. Chronology of the sedimentary processes during the postglacial sea level rise in two estuaries of the Algarve coast, Southern Portugal. Estuarine, Coastal and Shelf Science 77, 230–244.

Burd, F., 1989. Saltmarsh survey of Great Britain. An inventory of British Saltmarshes. *Research and Survey in Nature Conservation No. 17*. Nature Conservancy Council, Peterborough.

Chícharo, L., Ben Hamadou, R., Amaral, A., Range, P., Mateus, C., Piló, D., Marques, R., 2009. Application and demonstration of the Ecohydrology approach for the sustainable functioning of the Guadiana estuary (South Portugal). *Ecohydrology and Hidrobiology*, Vol. 9, No.1, pp. 55-71

Chícharo, L., Chícharo, M.A., Ben-Hamadou, R. (2006). Use of a hydrotechnical infrastructure (Alqueva Dam) to regulate planktonic assemblages in the Guadiana estuary: basis for

sustainable water and ecosystem services management. *Estuarine Coastal and Shelf Science*, Vol. 70, No. 1-2, (October 2006), pp. 3-18, ISSN 0272-7714.

Colenutt, A., 2001. SALTMARSH MANAGEMENT TECHNIQUES: A REVIEW. NEW FOREST DISTRICT COUNCIL, COAST PROTECTION GROUP. UK, 29P

Costa, L., Vergés, J.C., Barraqué, B., 2008. Shaping a new Luso Spanish convention, Working Paper no. 08/2008, Universidade Católica Potuguesa, Porto 13P.

Dahl, T.E., Johnson, C.E., 1991. *Status and trends of wetlands in the conterminous United States, mid-1970's to mid-1980's.* US Department of the Interior, Fish and Wildlife Service, Washington, DC.

Daveau, S., 1987. Comentários e actuaçizações. In : *Geografia de Portugal II.* O ritmo climático e a paisagem. Edições São José da Costa, ISBN 972-9230-16-1, Lisboa

Day, J.W., Shaffer, G.P., Britsch, L.D., Reed, D.J., Hawes, S.R., Cahoon, D., 2000, Pattern and process of land loss in the Mississippi Delta: A spatial and temporal analysis of wetland habitat change: Estuaries, v. 23, p. 425– 438, doi:10.2307/1353136.

Dias J, Taborda R. 1992. Tidal gauge data in deducing secular trends of relative sea-level and crustal movements in Portugal. *Journal of Coastal Research* 8 (3): 655- 659.

Dias, J.M.A., Gonzalez, R., Ferreira, O´., 2004. Natural Versus Anthropic Causes in Variations of Sand Export from River Basins: an Example from the Guadiana River Mouth (Southwestern Iberia). Rapid Transgression into Semi-enclosed Basins. Polish Geological Institute Special Papers, Gdansk, pp. 95–102.

Dijkema, K.S., 1987. Geography of the Salt Marshes in Europe. *Zeitschrift für Geomorphologie*; 31: 489-499.

Dixon, A.M. Leggett, D.J., Weight, R.C., 1998. Habitat creation opportunities for landward coastal re-alignment: Essex case studies. *Journal of the Chartered Institute of Water and Environmental Management;* 12: 102-112.

Fagherazzi, S., Carniello, L., D'Alpaos, L., Defina, A., 2006. Critical bifurcation of shallow microtidal landforms in tidal fl ats and salt marshes: Proceedings of the National Academy of Sciences of the United States of America, v. 103, p. 8337–8341, doi:10.1073/pnas .0508379103.

Ferreira, V., Panagopoulos, T., 2014. Seasonality of soil erosion under Mediterranean conditions at the Alqueva Dam Watershed. Environmental Management. 54:67–83

Fortunato, A.B., Pinto, L., Oliveira, A., Ferreira, J.S., 2002. Tidally generated shelf waves off the western Iberian coast. Continental Shelf Research 22, 1935–1950.

French, J.R., Spencer,T. , Murray, A.L., Arnold, N.S. 1995. Geostatistical analysis of sediment deposition in two small tidal wetlands, Norfolk, UK. *Journal of Coastal Research*; 11: 308-321.

Galvão, HM., Reis, MP., Domingues, RB., Caetano, SM., Mesquita, S., Barbosa, AB., Costa, C., Vilchez C., Teixeira, MR., 2012. Ecological Tools for the Management of Cyanobacteria Blooms in the Guadiana River Watershed, Southwest Iberia, In: Kumarasamy M., (Ed.), Studies on Water Management Issues. InTech, 174 p.

Garel E., Ferreira, Ó., 2012. Fortnightly changes in water transport direction across the mouth of a narrow estuary. Estuaries and Coasts. 36 (2), 286–299. DOI 10.1007/s12237-012-9566-z

Garel, E., L. Pinto, A. Santos, and Ó. Ferreira. 2009. Tidal and river discharge forcing upon water and sediment circulation at a rockbound estuary (Guadiana estuary, Portugal). Estuarine, Coastal and Shelf Science 84: 269–281.

Hunter, J.R., 2010. Estimating sea-level extreams under conditions of uncertain sea-level rise. *Climate Change*, 99: 331-350.

IPCC, 2001. *Climate Change 2001: The Scientific Basis. Contribution of Working Group I to the Third Assessment Report of the Intergovernmental Panel on Climate Change (IPCC*

TAR). J. T. Houghton et al. eds (Cambridge University Press, Cambridge, UK and New York, NY, USA).

IPCC, 2007. Climate Change 2007: The Physical Science Basis. Contribution of Working Group I to the Fourth Assessment Report of the Intergovernmental Panel on Climate Change, In: Solomon, S., Qin, D., Manning, M., Chen, Z., Marquis, M., Averyt, K.B., Tignor, M., Miller, H.L. (Eds.), Cambridge University Press, Cambridge, United Kingdom and New York, NY, USA.

IPCC, 2014. In: Core Writing Team, Pachauri, R.K., Meyer, L.A. (Eds.), Climate Change 2014: Synthesis Report. A Contribution of Working Groups I, II, and III to the Fifth Assessment Report of the Intergovernmental Panel on Climate Change. IPCC, Geneva, Switzerland, ISBN 978 92 9169 143 2, p. 151.

Kamps, L.F., 1962. *Mud distribution and land reclamation in the eastern Wadden shallows.* Rijkswaterstaat, The Hague, The Netherlands.

King, JM, Tharme RE, Brown CA., 1999. *World Commission on Dams Thematic Report: definition and implementation of instream flows.* World Commission on Dams: Cape Town.

KING, J., BROWN C. SABET, H., 2003. A SCENARIO-BASED HOLISTIC APPROACH TO ENVIRONMENTAL FLOW ASSESSMENTS FOR RIVERS RIVER RESEARCH AND APPLICATIONS *River Res. Applic.* **19**: 619–639 (2003)

Kirwan, M.L., Guntenspergen, G.R., D'Alpaos, A., Morris, J.T., Mudd, S.M., and Temmerman, S., 2010, Limits on the adaptability of coastal marshes to rising sea level: Geophysical Research Letters, v. 37, p. L23401, doi:10.1029/2010GL045489.

Machado, A., Rocha, F., Gomes, C., Dias, J., 2007. Distribution and composition of suspended particulate matter in Guadiana estuary (southwestern Iberian Peninsula). Journal of

Coastal Research 50, 1040–1045. Proc. International Coastal Symposium, Special Issue.

Mendes, A., 2010. Water Scarcicity and drought management in transboundary river basin: Convenio da Albufeira » In: Procceding from International Conference on Water Scarcity and Drought: Path to Climate Change Adaptation .Madrid 18th-19th February.

Me´nanteau, L., Chadenas, C., Choblet, C., 2005. Les marais du Bas-Guadiana (Algarve, Andalousie): emprise, de´ prise et reprise humaines. 1er colloque internations du Groupe d´ Histoire des Zones Humides, Le Blanc.

Morales, J.A., 1995. Sedimentologia del estuario del Rio Guadiana (S.W. Espanã–Portugal), Servicio de Publicaciones, Huelva University; 1–322.

Morales, J.A., Delgado, I., Gutierrez-Mas, J.M., 2006. Sedimentary characterization of bed types along the Guadiana Estuary (SW Europe) before the construction of the Alqueva dam. Estuarine, Coastal and Shelf Science. 70, 117–131.

Mossman, HL., Davy, AJ., Grant, A., 2012. Does managed coastal realignment create saltmarshes with 'equivalent biological characteristics' to natural reference sites? Journal of Applied Ecology, 1-11. doi: 10.1111/j.1365-2664.2012.02198.x

Mudd, SM., 2011. The life and death of salt marshes in response to anthropogenic disturbance of sediment supply GEOLOGY 39 (5), 511–512; doi: 10.1130/focus052011.1.

Nerem, R. S., Chambers, D., Choe, C., Mitchum., G. T., 2010. Estimating Mean Sea Level Change from the TOPEX and Jason Altimeter Missions Marine, Geodesy. 33(S1), 435–446. DOI: 10.1080/01490419.2010.491031

Portela, L., 2006. Sediment delivery from the Guadiana estuary to the coastal ocean. Journal of. Coast. Res. 1819-1823.

Pinto, L., 2003. Estrataficação salina no Estuário do Guadiana. Master thesis, Faculdade de Ciências da Universidade de Lisboa, Lisboa, p. 179.

Prandle, D., 2003. Relationships between tidal dynamics and bathymetry in strongly convergent estuaries. J. Phys. Oceanogr. 33 (12), 2738e2750. http://dx.doi.org/ 10.1175/1520-0485(2003)033<2738:RBTDAB>2.0.CO;2.

Prandle, D., 2004. How tides and river flow determine estuarine bathymetry. Prog. Oceanogr. 61, 1e26. http://dx.doi.org/10.1016/j.pocean.2004.03.001.

Prandle, D., 2009. Estuaries: Dynamics, Mixing, Sedimentation and Morphology. Cambridge University Press, Cambridge, UK, ISBN 978 05 2129 781 3, p. 235.

Reiser DW, Ramey MP, Wesche TA., 1989a. Flushing flows. In *Alternatives in Regulated River Management*, Gore JA, Petts GE (eds). CRC Press: Florida.

Reiser DW, Wesche TA, Estes C., 1989b. Status of instream flow legislation and practice in North America. *Fisheries* 14(2):22–29.

Sampath, D.M.R., Boski, T., Loureiro, C., Sousa, C., 2015. Modelling of estuarine response to sea-level rise during the Holocene: application to the Guadiana Estuary-SW Iberia. Geomorphology 232, 47–64. http://dx.doi.org/10.1016/j.geomorph.2014.12.037

Simas, T., Nunes, J.P., Ferreira J.G., 2001. Effects of global climate change on coastal salt marshes *Ecological Modelling* 139, 1–15

Stalnaker C, Lamb BL, Henriksen J, Bovee K, Bartholow J. 1995. *The Instream Flow Incremental Methodology: A primer for IFIM*. Biological Report 29. US Department of the Interior, National Biological Service: Washington, DC.

Tharme RE. 1996. *Review of international methodologies for the quantification of the instream flow requirements of rivers*. Water Law Review: final report for policy development, for the South African Department of Water Affairs and Forestry: Pretoria. Freshwater Research Unit: University of Cape Town.

THEODOROPOULOS C., PAPADONIKOLAKI G., STAMOU A., BUI M., RUTSCHMANN P., SKOULIKIDIS N., 2015. A METHODOLOGY FOR THE

DETERMINATION OF ENVIRONMENTAL FLOW RELEASES FROM DAMS BASED ON HYDRODYNAMIC HABITAT MODELLING AND BENTHIC MACROINVERTEBRATES *Proceedings of the 14th International Conference on Environmental Science and Technology Athens, Greece, 3-5 September 2015. 15p.*

Toft, A.R., Pethick, J.S., Burd, F., Gray, A.J., Doody, J.P. & Penning-Rowsell, E. (1995). A guide to the understanding and management of salt marshes. *National Rivers Authority, R&D Note 324*. NRA, Bristol.

Turner, R.E. & Streever, B. (2002). *Approaches to Coastal Wetland Restoration: Northern Gulf of Mexico.* SPB Academic Publishing: The Hague. ISBN 90-5103-141-6.

Velicogna, I., (2009) Increasing rates of ice mass loss from the Greenland and Antarctic ice sheets revealed by GRACE. *Geophysical Research Letters* 36, L19503.

Wolanski, E., Chicharo, L., Chicharo, M.A., Morais, P., 2006. An ecohydrology model of the Guadiana estuary (South Portugal). Estuarine, Coastal and Shelf Science 70, 132–143.

Wolanski, E., Chicharo, L. & Chicharo, M.A. (2008). Estuarine Ecohydrology. In: *Ecological Engineering*. Jørgensen, S.E., Fath, B.D. (Eds). Vol. 2 of Encyclopedia of Ecology, Elsevier, Oxford, ISBN 13: 978-0-44-452033-3

Chapter 8
General conclusions

To complement observational investigations that have described geomorphological history and sea-level change over the last 13,000 years in the Guadiana Estuary, in the present study a new hybrid approach was formulated to simulate the long-term morphological evolution of the Guadiana estuary during the Holocene period and in response to the projected sea-level rise and sediment deficiency scenarios for the 21st century. In this hybrid approach, a simple idealized model was based on analytical solutions to the simplified one-dimensional equation of axial momentum propagation of tidal waves in shallow waters and the continuity equation. Empirical information was used to define the local hydrodynamic and morphodynamic parameters.

The model written by means of MATLAB tool takes into account the processes of sea-level rise, depth dependent deposition of sediment supplied by marine and fluvial sources and erosion due to tidal currents. It represents a substantial improvement of previously used Estuarine Sedimentation Model, as it takes into account the important local controls of morphological evolution of an estuary like the variation in river discharge, current velocities, time series of suspended sediment concentration, tidal heights, sediment size, bed friction, erodibility of sediment and porosity of sediment. The new approach was further improved by

including formulations to calculate settling velocity for both sands and fine fluvial sediment and the phase difference between tides and currents was also introduced.

The new hybrid approach was validated by simulating the sediment infilling of the Guadiana estuary due to eustatic sea-level rise during the Holocene. The simulated model corresponding to the present day estuarine bathometry reasonably agrees with the observed bathymetry in the year 2000. The chronostratigraphic best-fit model was established using 16 radiocarbon ages obtained from five boreholes in the estuary. The decadal scale sub model was validated by successfully simulating the bathymetry for the year 2014 May. The results were compatible with the corresponding observed bathymetry. In particular the model was able to simulate the erosional and depositional areas with a satisfactory accuracy. Thus, the present approach can be applied for simulating the morphological evolution in response to environmental forcing acts over centennial/millennial and decadal time scale.

According to the results, the power of the current velocity in the erosion rate function and the bed friction coefficient are mutually related in determining the elevation change in response to sea-level rise and sediment supply changes. The difference between average elevation change with and without sea-level rise relative to increasing rate of the accommodation space converges to near zero value with the increase of sea-level rise rate above the present global mean sea-level rise rate. That suggests the estuary cannot keep pace with sea-level rise like the observed during the Holocene. This study further shows that there is a normal probability distribution in elevation change over a period of time and that can be simulated using the hybrid model. Furthermore, a new approach was introduced to estimate the sediment retention by dams, using the sediment budget approach and ^{10}Be isotope method.

The model proved to be very useful to estimate the environmental flow required for minimizing the negative impacts of the accelerating sea-level rise and strong flow regulations

by dams on saltmarsh habitats. A multi-dimensional approach has to be adopted to mitigate the consequences of sea-level rise and strong flow regulations on the ecosystem of the estuary.

Though this new model is in its infancy, it combines the deterministic rigour of process-based models with the observational frames encapsulated in rule-based geomorphological or behaviour-oriented models. Although there is much work to be carried out to improve the general applicability of the model to simulate morphological evolution of estuarine systems with different characteristics including tidal regimes, sediment supply conditions, sea-level rise, the results, conclusions and recommendations presented in this thesis can provide new insights for a better understanding of the long-term behaviour of any estuary.